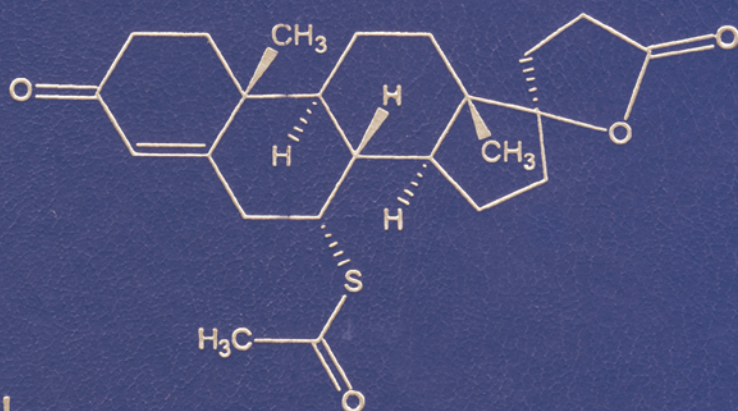


# Analytical Profiles of Drug Substances and Excipients

VOLUME 29



Edited by  
Harry G. Brittain

**Analytical Profiles  
of  
Drug Substances  
and  
Excipients**

# **EDITORIAL BOARD**

**Abdullah A. Al-Badr**

**Gunawan Indrayanto**

**Alekha K. Dash**

**David J. Mazzo**

**Klaus Florey**

**Leroy Shervington**

# **Analytical Profiles of Drug Substances and Excipients**

**Volume 29**

*edited by*

**Harry G. Brittain**

Center for Pharmaceutical Physics  
10 Charles Road  
Milford, New Jersey 08848

*Founding Editor:*

**Klaus Florey**



**ACADEMIC PRESS**

---

An imprint of Elsevier Science

Amsterdam · Boston · London · New York · Oxford · Paris  
San Diego · San Francisco · Singapore · Sydney · Tokyo



This book is printed on acid-free paper. ☺

© 2002 Elsevier Science (USA)

All rights reserved.

No part of this publication may be reproduced or transmitted in any form or by any means, electronic or mechanical, including photocopy, recording, or any information storage and retrieval system, without permission in writing from the Publisher.

The appearance of the code at the bottom of the first page of a chapter in this book indicates the Publisher's consent that copies of the chapter may be made for personal or internal use of specific clients. This consent is given on the condition, however, that the copier pay the stated per copy fee through the Copyright Clearance Center, Inc. (222 Rosewood Drive, Danvers, Massachusetts 01923), for copying beyond that permitted by Sections 107 or 108 of the U.S. Copyright Law. This consent does not extend to other kinds of copying, such as copying for general distribution, for advertising or promotional purposes, for creating new collective works, or for resale. Copy fees for pre-2002 chapters are as shown on the title pages. If no fee code appears on the title page, the copy fee is the same as for current chapters. 1075-6280/02 \$35.00

Explicit permission from Academic Press is not required to reproduce a maximum of two figures or tables from an Academic Press chapter in another scientific or research publication provided that the material has not been credited to another source and that full credit to the Academic Press chapter is given.

Academic Press

*An Elsevier Science Imprint*

525 B Street, Suite 1900, San Diego, California 92101-4495, USA

<http://www.academicpress.com>

International Standard Book Number: 0-12-260829-1

PRINTED IN THE UNITED STATES OF AMERICA

02 03 04 05 06 07      9 8 7 6 5 4 3 2 1

# CONTENTS

	<i>Affiliations of Editors and Contributors</i>	vii
1.	<b>Profiles of Drug Substances, Excipients, and Related Methodology</b> <i>Harry G. Brittain</i>	1
2.	<b>Aspartame</b> <i>Richard J. Pranker</i>	7
3.	<b>Edetic Acid (EDTA)</b> <i>F. Belal and Abdullah A. Al-Badr</i>	57
4.	<b>Etodolac</b> <i>Ketan P. Shah, Kavita Gumbhir-Shah, and Harry G. Brittain</i>	105
5.	<b>Eugenol</b> <i>Mohammad Yuwono, Siswandono, Achmad Fuad Hafid, Achmad Toto Poernomo, Mangestuti Agil, Gunawan Indrayanto, and Siegfried Ebel</i>	149
6.	<b>Mandelic Acid</b> <i>Harry G. Brittain</i>	179
7.	<b>Pantoprazole</b> <i>Adnan A. Badwan, Lina N. Nabulsi, M.M. Al Omari, Nidal H. Daraghme, Mahmoud K. Ashour, Ahmad M. Abdoh, and A. M. Y. Jaber</i>	213
8.	<b>Spironolactone</b> <i>Badraddin M.H. Al-Hadiya, Fathalla Belal, Yousif A. Asiri, and Othman A. Gubara</i>	261
	<b>Cumulative Index</b>	321

This Page Intentionally Left Blank

## AFFILIATIONS OF EDITORS AND CONTRIBUTORS

**Ahmad M. Abdoh:** The Jordanian Pharmaceutical Manufacturing Company Ltd., Na'or, Jordan

**Mangestuti Agil:** Faculty of Pharmacy, Airlangga University, Jl. Dharmawansa dalam, Surabaya 60286, Indonesia

**Abdullah A. Al-Badr:** Department of Pharmaceutical Chemistry, College of Pharmacy, King Saud University, P.O. Box 2457, Riyadh-11451, Saudi Arabia

**Badraddin M.H. Al-Hadiya:** Department of Clinical Pharmacy, College of Pharmacy, King Saud University, P.O.Box 2457, Riyadh 11451, Kingdom of Saudi Arabia

**M.M. Al Omari:** The Jordanian Pharmaceutical Manufacturing Company Ltd., Na'or, Jordan

**Mahmoud K. Ashour:** The Jordanian Pharmaceutical Manufacturing Company Ltd., Na'or, Jordan

**Yousif A. Asiri:** Department of Clinical Pharmacy, College of Pharmacy, King Saud University, P.O.Box 2457, Riyadh 11451, Kingdom of Saudi Arabia

**Adnan A. Badwan:** The Jordanian Pharmaceutical Manufacturing Company Ltd., Na'or, Jordan

**Fathalla. Belal:** Department of Pharmaceutical Chemistry, College of Pharmacy, King Saud University, P.O. Box 2457, Riyadh-11451, Saudi Arabia

**Harry G. Brittain:** Center for Pharmaceutical Physics, 10 Charles Road, Milford, NJ 08848-1930, USA

**Nidal H. Daraghme:** The Jordanian Pharmaceutical Manufacturing Company Ltd., Na'or, Jordan

**Alekha K. Dash:** Department of Pharmaceutical & Administrative Sciences, School of Pharmacy and Allied Health Professions, Creighton University, Omaha, NE 68178, USA

**Siegfried Ebel:** Department of Pharmacy, University of Würzburg, Am Hubland, D-97074 Würzburg, Germany

**Klaus Florey:** 151 Loomis Court, Princeton, NJ 08540, USA

**Othman A. Gubara:** Department of Clinical Pharmacy, College of Pharmacy, King Saud University, P.O.Box 2457, Riyadh 11451, Kingdom of Saudi Arabia

**Achmad Fuad Hafid:** Faculty of Pharmacy, Airlangga University, Jl. Dharmawangsa dalam, Surabaya 60286, Indonesia

**Gunawan Indrayanto:** Faculty of Pharmacy, Airlangga University, Jl. Dharmawangsa dalam, Surabaya 60286, Indonesia

**A.M.Y. Jaber:** Chemistry Department, King Fahd University of Petroleum and Minerals, Dhahran 31261, Saudi Arabia

**David J. Mazzo:** Preclinical Development, Hoechst Marion Roussel, Inc., Route 202-206, P.O. Box 6800, Bridgewater, NJ 08807, USA

**Lina N. Nabulsi:** The Jordanian Pharmaceutical Manufacturing Company Ltd., Na'or, Jordan

**Achmad Toto Poernomo:** Faculty of Pharmacy, Airlangga University, Jl. Dharmawangsa dalam, Surabaya 60286, Indonesia

**Richard J. Pranker:** Victorian College of Pharmacy, Monash University, Parkville, VIC 3052, Australia

**Ketan P. Shah:** Schering-Plough Corporation, NJ Quality Laboratories, 1011 Morris Avenue, Union, NJ 07083

**Kavita Gumbhir-Shah:** PharmaConsult, Inc., 23 Honeyman Road, Basking Ridge, NJ 07920

**Leroy Shervington:** Pharmacy Faculty, Applied Science University, Amman 11931, Jordan

**Siswandono:** Faculty of Pharmacy, Airlangga University, Jl. Dharmawangsa dalam, Surabaya 60286, Indonesia

**Mochammad Yuwono:** Faculty of Pharmacy, Airlangga University, Jl. Dharmawangsa dalam, Surabaya 60286, Indonesia

# **Profiles of Drug Substances, Excipients, and Related Methodology**

Harry G. Brittain

Center for Pharmaceutical Physics  
10 Charles Road  
Milford, NJ 08848 U.S.A.

In 1970, scientists from the Pharmaceutical Analysis Section of the Academy of Pharmaceutical Sciences began to plan a cooperative venture to compile and publish a series of volumes entitled the *Analytical Profiles of Drug Substances*. The aim of the series was to provide information not available in the official compendial monograph of a drug substance, such as physical or chemical data, methods of synthesis, and pathways of physical or biological degradation and metabolism. Klaus Florey became the first editor of the series, and between 1972 and 1991 he edited the first 20 volumes in the *Analytical Profiles* series.

In 1992, I assumed the role of editor for the *Analytical Profiles*, and expanded the scope of the series to include profiles of additional materials. Consequently the series title changed slightly to that presently used, *Analytical Profiles of Drug Substances and Excipients*. Although the content of individual profiles differed from substance to substance, the basic content of most profile chapters contained six main sections:

1. Description
2. Methods of Preparation
3. Physical Properties
4. Methods of Analysis
5. Stability
6. Drug Metabolism and Pharmacokinetics

This format has characterized all of the volumes I have edited (21 –29), which were published over the time period of 1992 to 2002.

I have been considering another expansion of the scope of the series for some time, and with the acquisition of Academic Press by the Elsevier



Publishing Company it is now appropriate to set these designs into action. Beginning with volume 30, the name of the series will be changed to *Profiles of Drug Substances, Excipients, and Related Methodology*. The traditional profile chapters will, of course, still be acceptable for publication, but it is envisioned these contributions will be augmented by publication of critical review chapters that summarize information related to the characterization of drug substances and excipients.

Contributions to the *Profiles* series will generally fall within one of the following six categories of review articles:

- A. Physical profiles of drug substances and excipients
- B. Analytical profiles of drug substances and excipients
- C. Drug metabolism and pharmacokinetic profiles of drug substances and excipients
- D. Methodology related to the characterization of drug substances and excipients
- E. Methods of chemical synthesis
- F. Reviews of the uses and applications for individual drug substances, classes of drug substances, or excipients

More detailed descriptions of the chapter content anticipated for each category are summarized in the following sections. The scope of described topics is illustrative in nature, since it is fully realized that the actual content of any given chapter will vary somewhat according to the compound or methodology being reviewed.

#### **A. Physical Profiles of Drug Substances and Excipients**

##### **1. General Information**

- 1.1 Nomenclature
  - 1.1.1 Systematic Chemical Name
  - 1.1.2 Nonproprietary Names
  - 1.1.3 Proprietary Names
- 1.2 Formulae
  - 1.2.1 Empirical Formula, Molecular Weight, CAS Number
  - 1.2.2 Structural Formula
- 1.3 Elemental Analysis
- 1.4 Appearance

**2. Physical Characteristics**

- 2.1 Ionization Constants
- 2.2 Solubility Characteristics
- 2.3 Partition Coefficients
- 2.4 Optical Activity
- 2.5 Particle Morphology
- 2.6 Crystallographic Properties
  - 2.6.1 Single Crystal Structure
  - 2.6.2 X-Ray Powder Diffraction Pattern
- 2.7 Hygroscopicity
- 2.8 Thermal Methods of analysis
  - 2.8.1 Melting Behavior
  - 2.8.2 Differential Scanning Calorimetry
  - 2.8.3 Thermogravimetric Analysis
- 2.9 Spectroscopy
  - 2.9.1 UV/VIS Spectroscopy
  - 2.9.2 Vibrational Spectroscopy
  - 2.9.3 Nuclear Magnetic Resonance Spectrometry
    - 2.9.3.1  $^1\text{H}$ -NMR Spectrum
    - 2.9.3.2  $^{13}\text{C}$ -NMR Spectrum
- 2.10 Mass Spectrometry

**3. Stability**

- 3.1 Solid-State Stability
- 3.2 Solution-Phase Stability
- 3.3 Stability in Biological Fluids
- 3.4 Incompatibilities with Functional Groups

**B. Analytical Profiles of Drug Substances and Excipients**

**1. Compendial Methods of Analysis**

- 1.1 Identification
- 1.2 Physical Methods of Analysis
- 1.3 Impurity Analyses
- 1.4 Assay Methods

**2. Titrimetric Methods of Analysis**

- 2.1 Aqueous Titration Methods
- 2.2 Non-Aqueous Titration Methods

- 2.3 Potentiometric Titration
- 2.4 Miscellaneous Titration Methods

### **3 Electrochemical Methods of Analysis**

- 3.1 Voltammetry
- 3.2 Amperometry
- 3.3 Coulometry
- 3.4 Polarography

### **4 Spectroscopic Methods of Analysis**

- 4.1 Spectrophotometry
- 4.2 Colorimetry
- 4.3 Fluorimetry

### **5 Chromatographic Methods of Analysis**

- 5.1 Paper Chromatography
- 5.2 Thin Layer Chromatography
- 5.3 Gas Chromatography
- 5.4 High Performance Liquid Chromatography
- 5.5 Ion-Exchange Chromatography
- 5.6 Supercritical Fluid Chromatography
- 5.7 Capillary Electrophoresis

### **6 Determination in Body Fluids and Tissues**

- 6.1 Radio-immunoassay Methods
- 6.2 Enzyme-immunoassay Methods
- 6.3 Chromatographic Methods

## **C. Drug Metabolism and Pharmacokinetic Profiles of Drug Substances and Excipients**

- 1. Uses, Applications, and Pertinent History
- 2. Adsorption
- 3. Distribution
- 4. Metabolism
- 5. Elimination
- 6. Pharmacological Effects

**D. Methodology Related to the Characterization of Drug Substances and Excipients**

1. Introduction
2. Apparatus and Instrumentation
3. Principles of Operation
4. Illustrative Examples of the Methodology
5. Summary and Indications for Future Work

**E. Methods of Chemical Synthesis**

1. Historical Overview
2. Preparative Chemical Methods
3. Preparative Microbiological Methods

**F. Uses and Applications for Individual drug substances, classes of drug substances, or excipients**

1. Historical Overview
2. Uses and Applications – format largely dependent on the nature of the substance(s) being reviewed

The change in series scope and title is not being effected merely for the sake of change, but to allow the series to better meet the needs of the pharmaceutical community. The time for publication of simple data compilations seems to be passing, and it is equally clear that the need is growing for publication of more critical evaluations of data, information, and methodology. The revised series title *Profiles of Drug Substances, Excipients, and Related Methodology* reflects this emerging trend, and future volumes in the series will attempt to better meet the information needs of the drug development community.

This Page Intentionally Left Blank

# ASPARTAME

Richard J. Prankerd

Victorian College of Pharmacy  
Monash University  
Parkville, VIC 3052  
AUSTRALIA



## **Contents**

### **1. Description**

- 1.1 Nomenclature
  - 1.1.1 Systematic Chemical Names
  - 1.1.2 Non-proprietary Names
  - 1.1.3 Proprietary Names
- 1.2 Formulae
  - 1.2.1 Empirical Formula, Molecular Weight, CAS Number
  - 1.2.2 Structural Formula
  - 1.2.3 Stereochemical Description
- 1.3 Elemental Analysis
- 1.4 Appearance
- 1.5 Uses and Applications

### **2. Methods of Preparation**

- 2.1 Chemical Methods
- 2.2 Enzymatic Methods
- 2.3 Impurities

### **3. Physical Properties**

- 3.1 Ionization Constants
- 3.2 Solubility Characteristics
- 3.3 Partition Coefficient
- 3.4 Optical Activity
- 3.5 Particle Morphology
- 3.6 Crystallographic Properties
  - 3.6.1 Single Crystal Structure
  - 3.6.2 X-Ray Powder Diffraction Pattern
  - 3.6.3 Polymorphism
- 3.7 Thermal Methods of analysis
  - 3.7.1 Melting Behavior
  - 3.7.2 Differential Scanning Calorimetry
  - 3.7.3 Thermogravimetric Analysis
- 3.8 Micromeritics
- 3.9 Spectroscopy
  - 3.9.1 UV/VIS Spectroscopy
  - 3.9.2 Vibrational Spectroscopy
  - 3.9.3 Nuclear Magnetic Resonance Spectrometry
- 3.10 Mass Spectrometry

**4. Methods of Analysis**

- 4.1 Compendial Tests
  - 4.1.1 Identification
  - 4.1.2 Transmittance
  - 4.1.3 Specific Rotation
  - 4.1.4 Loss on Drying
  - 4.1.5 Residue on Ignition
  - 4.1.6 Heavy Metals
  - 4.1.7 Limit of 5-Benzyl-3,6-Dioxo-2-Piperazineacetic Acid
  - 4.1.8 Chromatographic Purity
  - 4.1.9 Organic Volatile Impurities
  - 4.1.10 Assay
- 4.2 Electrochemical Analysis
- 4.3 Spectroscopic Analysis
- 4.4 Chromatographic Methods of Analysis
  - 4.4.1 High Performance Liquid Chromatography
  - 4.4.2 Capillary zone electrophoresis (CZE) methods

**5. Stability**

- 5.1 Solution stability
- 5.2 Solid state stability
- 5.3 Stabilization
- 5.4 Chemical interactions
- 5.5 Complexation

**6. Biological Properties**

- 6.1 Activity
- 6.2 Toxicity and safety

**7. Acknowledgements****8. References**

## 1. **Description**

### 1.1 **Nomenclature**

#### 1.1.1 **Systematic Chemical Names**

*N*-(*L*)- $\alpha$ -Aspartyl-L-phenylalanine 1-methyl ester

3-amino-*N*-( $\alpha$ -carboxyphenethyl)succinamic acid *N*-methyl ester

3-amino-*N*-( $\alpha$ -methoxycarbonylphenethyl)succinamic acid

aspartyl phenylalanine methyl ester

methyl *N*- $\alpha$ -(*L*)-aspartyl-L-phenylalaninate

*N*- $\alpha$ -aspartylphenylalanine 1-methyl ester, 9CI

#### 1.1.2 **Non-proprietary Names**

Aspartame, APM

#### 1.1.3 **Proprietary Names**

Aspartil, Canderel, Dietacil, Diyet-Tat, Equal, Finn, Goldswite, Hermesetas Gold, Milisucré, Nozucar, NutraSweet, Nutra-tat, Sanecta, Sanpa, SC 18862, Slap, Start, Sucret, Tri-Sweet, Usal

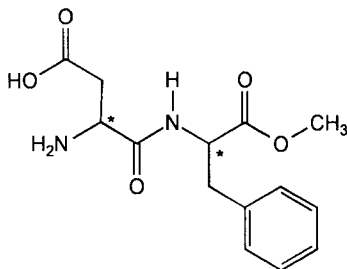
## 1.2 **Formulae**

### 1.2.1 **Empirical Formula, Molecular Weight, CAS Number**

$C_{14}H_{18}N_2O_5$  [MW = 294.31]

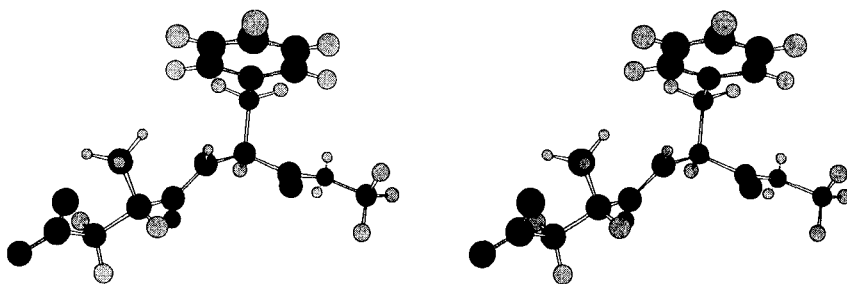
CAS number: 22839-47-0

### 1.2.2 **Structural Formula**



### 1.2.3 Stereochemical Description

Aspartame is a diastereomeric dipeptide ester, with the two asymmetric carbons (\*) being derived from (*L*)-amino acids. The other three diastereomers of aspartame (the *D,D*-, *D,L*- and *L,D*- diastereomers) are not sweet. The three dimensional structure of aspartame in the zwitterionic form can be depicted in the following stereoscopic figure:



The model was constructed using enhanced force-field energy minimization (CS Chem3D Ultra version 4.0) to a final RMS gradient of 0.001 kcal/mol/Å<sup>2</sup>. Other conformations of similar energy are also known [6]. This energy-minimized model is closely similar to the single crystal X-ray structure described in a following section.

### 1.3 Elemental Analysis

The calculated elemental composition is as follows:

carbon:	57.14%
hydrogen:	6.16%
oxygen:	27.18%
nitrogen:	9.52%

### 1.4 Appearance

Aspartame exists as colorless needles (recrystallized from water) [7]. It is an off-white, almost odorless crystalline powder with an intensely sweet taste [5].

## 1.5 Uses and Applications

Aspartame is a non-cariogenic, low energy sweetening agent with 160-200 times the sweetness of sucrose, but without the bitter or metallic aftertaste of other artificial sweeteners. It was accidentally discovered during the late 1960's by J.M. Schlatter at the research laboratories of G.D. Searle while conducting syntheses of oligopeptides related to gastrin [1]. The properties of aspartame have been reviewed in general [2-5]

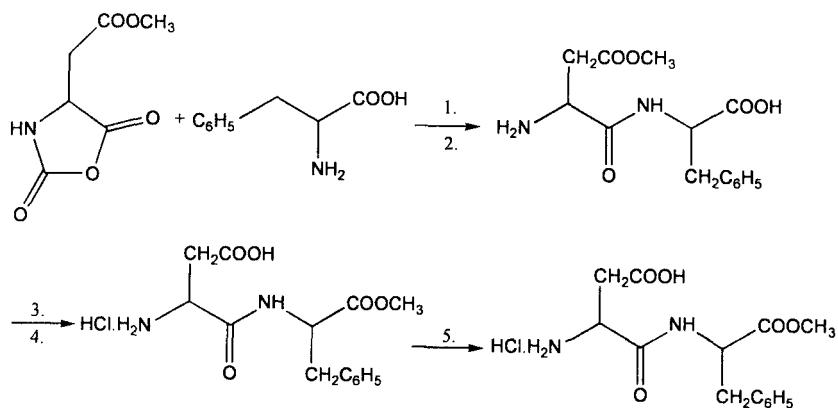
## 2. Methods of Preparation

The synthesis of aspartame can be achieved by numerous chemical and enzymatic methods of amide bond formation between (*L*)-aspartic acid and either (*L*)-phenylalanine or (*L*)-phenylalanine methyl ester. Both approaches have been thoroughly reviewed [10]. The chief difficulty with chemical methods is formation of the non-sweet  $\beta$ -isomer as a by-product.

### 2.1 Chemical Methods

Two chemical methods have been devised to avoid formation of the non-sweet (*L*)- $\beta$ -aspartyl compound. The first of these entails the use of an activated precursor in which the  $\beta$ -carboxyl group is protected [11]. In this method, the approach described in Scheme 1 is used. This route gives an overall aspartame yield of about 55%. The rate of formation of the product depends on the degree of hydrolysis of the intermediate aspartyl  $\beta$ -methyl ester to the diacid (not shown), before entering the esterification medium (steps 3 and 4).

In the second method, dehydroaspartame is used as an intermediate, which was devised to deal with the issue of the higher cost of (*L*)-phenylalanine as compared to (*L*)-aspartic acid [12]. The route involves synthesis of an *N*-protected dehydroaspartame from (*L*)-aspartic acid, benzaldehyde, and glycine. This intermediate is asymmetrically hydrogenated over a chiral rhodium catalyst to yield >90% of an (*L,L*)-intermediate, which is then deprotected and separated from the < 10% of corresponding (*L,D*)-diastereomer by recrystallization. The yield is about 65% of product that is 99.5% pure by HPLC.



1. aq. NaOH, pH 10.1, 0-2°C

2. aq. HCl, pH 3.7

3. aq. HCl

4. MeOH

5. aq. NaOH, 0-2°C

Scheme 1. Synthesis of aspartame using an activated *N*-protected aspartic acid derivative.



## 2.2 Enzymatic Methods

The enzymatic approach for the synthesis of aspartame has the advantage of producing only the (*L*)- $\alpha$ -aspartyl compound (the sweet diastereomer). The less expensive racemic (*DL*)-phenylalanine can be used as the starting material. The unreacted (*D*)-phenylalanine can be recovered and racemized for further reaction. By contrast, the chemical methods used industrially also produce the (*L*)- $\beta$ -aspartyl compound (non-sweet) in 10-40% yield, for which a purification step is needed. In 1999, the world market for enzymatically synthesized aspartame was reported to be 800 million \$US [13].

Enzymatic methods are now preferred for the commercial production of aspartame from aspartate and phenylalanine. Typically, these use thermolysin (EC 3.4.24.4; derived from *Bacillus spp.*) to couple benzyloxycarbonyl-protected aspartate (Z-asp) with phenylalanine methyl ester. The resulting Z-APM is then deprotected using standard methods [14-18]. Numerous enzymatic methods have been reported [10].

## 2.3 Impurities

The impurities found in aspartame are typically those arising from degradation. These include 3-methylenecarboxyl-6-benzyl-2,5-diketopiperazine, phenylalanyl aspartic acid,  $\alpha$ -aspartylphenylalanine, aspartic acid, phenylalanine, (*L*)- $\beta$ -aspartyl-(*L*)-phenylalanine methyl ester). (*L*)- $\beta$ -aspartyl-(*L*)-phenylalanine methyl ester may also be formed as a byproduct when aspartame is chemically synthesized.

The content of the principal degradation impurity, 3-methylenecarboxyl-6-benzyl-2,5-diketopiperazine (also called 5-benzyl-3,6-dioxo-2-piperazine-acetic acid), is controlled at not more than 1.5% [19, 20]. Other controlled impurities are moisture (*i.e.*, loss on drying,  $\leq 4.5\%$ ), residue on ignition ( $\leq 0.2\%$ ), arsenic ( $\leq 3$  ppm), heavy metals ( $\leq 0.001\%$ ), and related substances ( $\leq 2\%$ ) [19].

## 3. Physical Properties

### 3.1 Ionization Constants

pK<sub>a</sub> values of  $3.19 \pm 0.01$  ( $\beta$ -carboxyl group) and  $7.87 \pm 0.02$  (amino group) have been obtained using the potentiometric method [42] at 25°C and an ionic strength of 0.100M (NaCl) [28].

The pH of aspartame in aqueous solutions has been reported to be 4.0 to 6.5 (0.8% w/v solution in water) [19]. The isoelectric pH has been reported to be 5.2 [5]. However, the pKa values from Skwierczynski and Connors [28] predict a pI value of 5.5 at an ionic strength of 0.100M and 25°C.

### 3.2 Solubility Characteristics

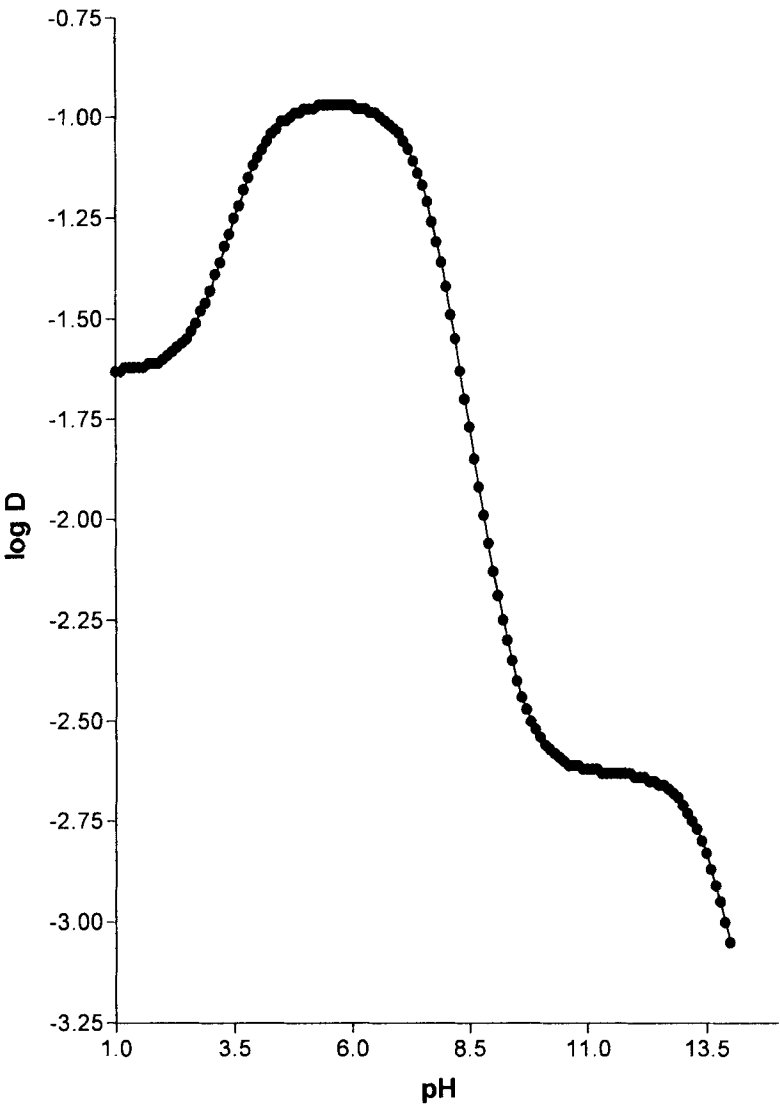
Aspartame is slightly soluble in 95% ethanol, sparingly soluble in cold water (1% w/v at the isoelectric point of pH 5.2 and at 20° C), and is soluble at higher temperatures and at pH values other than the isoelectric pH [5]. The low solubility in water appears to be a consequence of details of the aspartame crystal structure (see section 3.6.1 for details of the aspartame crystal structure).

The intrinsic dissolution profiles in water for both hemihydrate forms and the monohydrate form of aspartame were determined using 1 cm diameter compacts [23]. The compacts were mounted so that only one face was exposed to the medium, which was stirred at 50 rpm by a paddle near the solid surface. The three forms gave essentially identical profiles, corresponding to an intrinsic dissolution rate of about  $7.3 \times 10^{-4}$  mg/mL/min/cm<sup>2</sup>. X-ray powder patterns for the solid recovered from the measurements showed that the two hemihydrate forms had converted *in situ* to the monohydrate. As all intrinsic dissolution profiles were quite linear, the conversion to the monohydrate appears to be so rapid as to preclude assessment of the dissolution rates for the unaltered hemihydrates.

### 3.3 Partition Coefficient

Using the ACD PhysChem program (Advanced Chemistry Development, Toronto CA), the pH dependence of the distribution coefficient of aspartame acid was calculated. The values are plotted in Figure 1, which demonstrate the hydrophilic nature of the compound.

Figure 1.      pH dependence of the calculated distribution coefficient of aspartame.



### 3.4 Optical Activity

The sign and magnitude for the specific rotation of aspartame are sensitive to both temperature and solvent, as demonstrated by the reported values:

$$[\alpha]_D^{22} = -2.3^\circ \text{ (1N HCl) [7]}$$

$$[\alpha]_D^{22} = +14.5^\circ \text{ to } +16.5^\circ \text{ (40 mg/mL in 15N formic acid, with the measurement to be made within 30 minutes of solution preparation, using the dried material or material of known moisture content) [19]}$$

$$[\alpha]_D^{22} = +32^\circ \text{ (c, 1 in acetic acid) [21]}$$

$$[\alpha]_D^{22} = +0^\circ \text{ (water) [21]}$$

### 3.5 Particle Morphology

Aspartame is obtained as colorless needles when crystallized from water. Optical photomicrographs of aspartame monohydrate crystals have been published previously [5, 22, 23], showing changes that occur upon heating or milling.

### 3.6 Crystallographic Properties

#### 3.6.1 Single Crystal Structure

The crystal structure of aspartame hemihydrate in its zwitterionic form has been reported [9], and is illustrated in Figure 2. The substance crystallized in the tetragonal space group  $P4_1$ , with the unit cell dimensions of  $a = b = 17.685(5) \text{ \AA}$  and  $c = 4.919(2) \text{ \AA}$ . The unit cell was characterized by an occupancy of  $z = 4$ , and the calculated density was  $1.310 \text{ g/cm}^3$ . The tetragonal space group resulted from crystallization in four-fold infinite columns, with the aspartyl  $\beta$ -carboxylate and protonated amine groups being extensively hydrogen-bonded to the water molecules (50% unit cell occupancy) forming cores that are located at the corners of each unit cell. The columns are then stacked together with the hydrophobic phenyl rings (and the methyl ester groups) protruding from the columns. Each phenyl ring interacts laterally with three others in the middle of the unit cell and vertically with the corresponding phenyl rings in adjacent unit cells. The hydrophobic surfaces of each column are claimed to be responsible for the relatively low water solubility of aspartame. The four-fold infinite

columns result in the strong tendency of aspartame to crystallize in very thin needles.

Leung and Grant [22] state that the reported single crystal hemihydrate structure [9] does not correspond to the commercial form of aspartame (Form II, also a hemihydrate), but corresponds instead to their Form I. A crystal structure has not been determined for the anhydrous form of aspartame, which has so far resisted all attempts at isolation.

The single crystal X-ray diffraction structure for aspartame hydrochloride dihydrate has also been reported at 120 K [51]. The substance crystallized in the orthorhombic space group  $P2_12_12_1$  with unit cell dimensions  $a = 6.768(1)$ ,  $b = 9.796(1)$ ,  $c = 26.520(3)$  Å. The unit cell was characterized by  $z = 4$  molecules per unit cell, and the calculated density was  $1.386 \text{ g/cm}^3$ . The conformation and hydrogen bonding of the aspartame molecule were found to have similarities with those of the zwitterionic form of aspartame, above, but there were also some significant differences, especially in the orientation of the aspartate carboxylate group. This finding is reasonable, considering the changed electronic environment of this group.

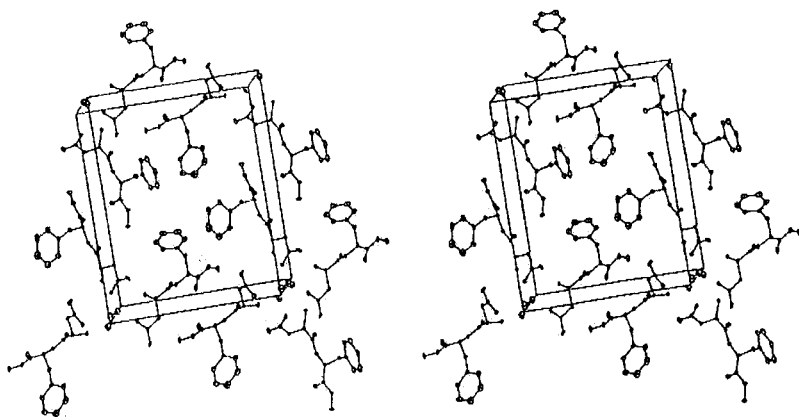
### 3.6.2 X-Ray Powder Diffraction Pattern

Aspartame is known to exist in a variety of polymorphs and solvatomorphs, and the x-ray powder patterns for several forms are shown in Figure 3.

The theoretical powder diffraction pattern based on the single crystal x-ray structure is very similar to that observed experimentally for Form I. X-ray powder diffraction has been used to demonstrate the transformation from aspartame to the 2,5-diketopiperazine derivative [22].

X-ray powder diffractometry has also been used to characterize fused mixtures of aspartame and mannitol [50].

(a)



(b)

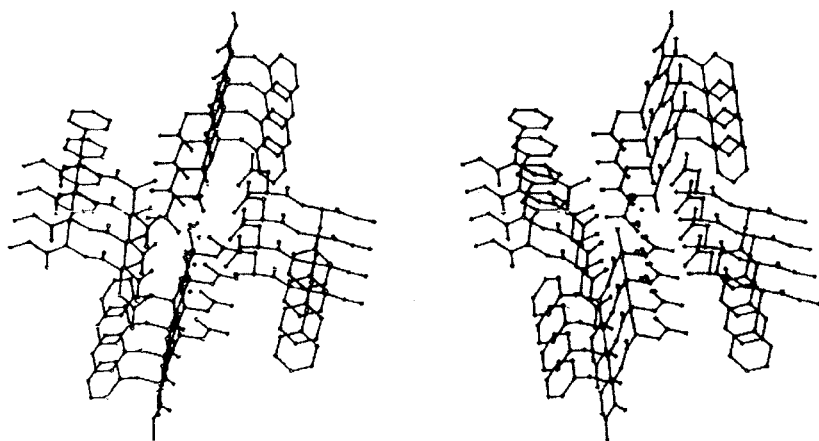


Figure 2. Stereoscopic representations of the crystal structure for aspartame (Form I). (a) unit cell, showing phenyl rings interacting in the center of each cell and hydrogen-bonded water molecules at the edges; (b) columnar representation, showing hydrogen-bonded stacks of water molecules and zwitterionic aspartyl amino and carboxylate groups in center with stacked phenyl rings at edges. Reproduced from [9].



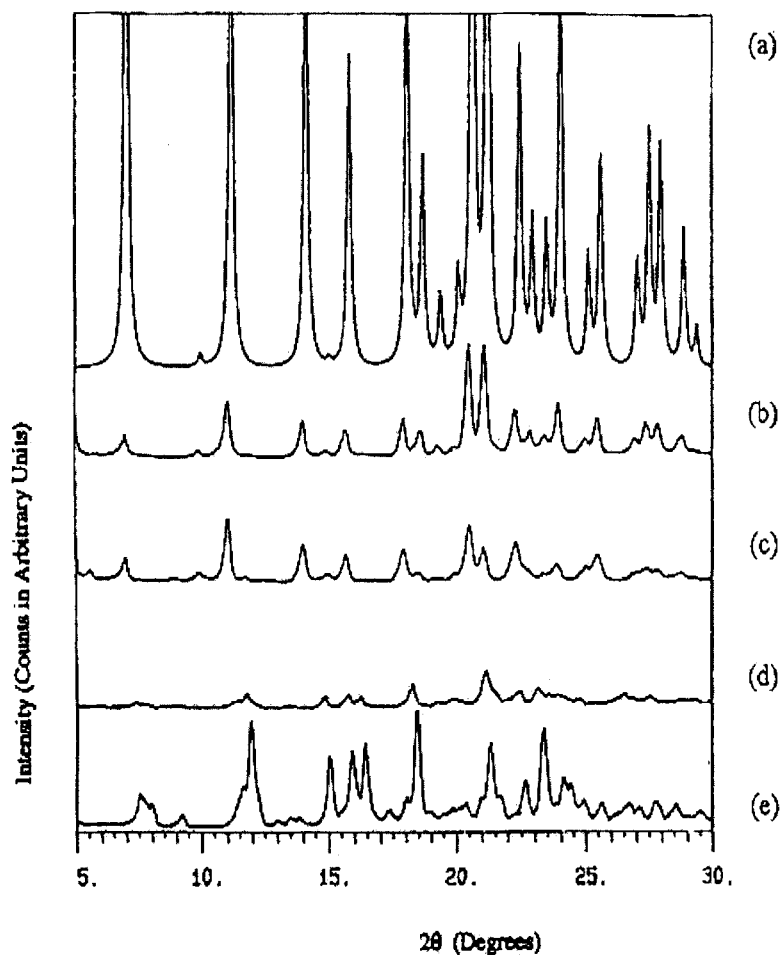


Figure 3. XRPD diffraction patterns for aspartame hemihydrate. Shown are (a) theoretical pattern calculated from the single crystal structure; (b) Form I (ball-milled); (c) Form I (heated in steam); (d) Form II (after compression at 250 MPa); and (e) Form II (commercial). Reproduced from [23].

### 3.6.3 Polymorphism

Aspartame has been reported in a variety of solvatomorphic forms, namely one anhydrous form, two hemihydrate forms (Forms I and II) and a di-hemihydrate [8]. The structural details of the crystal properties have been discussed earlier, and will also be addressed in the discussion on thermal analysis. The room temperature transition between the hemihydrate and di-hemihydrate forms occurs between relative humidities of 40% and 60%.

The commercially available hemihydrate Form II can be converted into Form I by recrystallization from a quaternary mixture containing distilled water, ethanol, acetone and dimethyl sulfoxide [9], ball milling, or by heating to 160°C for 30 minutes in the presence of steam.

The anhydrous form can be obtained from any of the other forms by heating to 150°C, but it has not yet actually been isolated

## 3.7 Thermal Methods of analysis

### 3.7.1 Melting Behavior

Aspartame (and its (*D,D*), (*D,L*), and (*L,D*) diastereomers) display double melting points. When recrystallized from aqueous ethanol or water, aspartame melts initially at 190°C, and then solidifies and re-melts at 246-247° C [21]. Other sources give only the 246-7°C value [5]. The explanation for this behavior is that intramolecular self-aminolysis and simultaneous demethanolation of aspartame takes place on initial melting, to yield 3-methylenecarboxyl-6-benzyl-2,5-diketopiperazine (DKP) ( $C_{12}H_{14}N_2O_4 = 262.26$  g/mole). The latter compound has been reported to melt at  $259 \pm 1.1^\circ \text{C}$  [22].

### 3.7.2 Differential Scanning Calorimetry

The unusual double melting point behavior of aspartame has been confirmed by differential scanning calorimetry (DSC) [22, 52]. This behavior was interpreted [52] in terms of initial conversion of the methyl ester to *L*- $\alpha$ -aspartyl-*L*-phenylalanine, followed by formation of the substituted 2,5-diketopiperazine, although no clear evidence was produced to support this view. However, the alternative explanation that the 2,5-diketopiperazine was produced in a concerted manner from simultaneous self-aminolysis and demethanolation of aspartame seemed more likely to

this reviewer. This was confirmed independently by Leung and Grant [22].

DSC has been used in studies of the thermal properties of aspartame in solid state combination with several other substances with which it may be formulated, such as mannitol [50, 52], caffeine [53], ampicillin [54], and cephalexin [55].

The aspartame hydrates have been studied by DSC [22, 23], giving the results (obtained using crimped pans) summarized in the following table:

<b>Form</b>	<b>First Endotherm Onset Temperature (°C)</b>	<b>Second Endotherm Onset Temperature (°C)</b>	<b>Third Endotherm Onset Temperature (°C)</b>
Hemihydrate (Form I)	100.7	184.5	248
Hemihydrate (Form II)	129.4	188.6	248
Dihemihydrate	92.5	188.1	248

Very similar results were found in open pans, although the dihemihydrate and the hemihydrate Form II yielded an additional exotherm at 133°C, which was attributed to recrystallization of the anhydrous form.

### **3.7.3 Thermogravimetric Analysis**

Leung et al [8] reported that the thermogravimetric analysis (TGA) of aspartame hemihydrate (Forms I and II) and aspartame dihemihydrate displayed mass losses for water (first mass loss) and methanol (second mass loss). This information is summarized in the following table:

TGA data for three hydrated forms of Aspartame

Form	Hemihydrate (Form I)	Hemihydrate (Form II)	Dihemihydrate
Temperature of First Mass Loss (°C)	58	113	27.5 (110)
Percent of First Mass Loss	2.21	2.02	10.3 (1.51)
Temperature of Second Mass Loss (°C)	189	196	200
Percent of Second Mass Loss	11.7	11.7	10.5

The dihemihydrate was found to lose water in two steps, the first being near room temperature, and corresponding to the loss of 2 mole equivalents. The second loss took place near the temperature for dehydration of hemihydrate Form II. The reported mass losses were in good agreement with the theoretical losses, and the transition temperatures were consistent with the DSC data.

### 3.8 Micromeritics

The bulk density of commercial material has been reported to be 0.4–0.5 g/cm<sup>3</sup> for the granular form, and 0.3–0.4 g/cm<sup>3</sup> for the powdered form [5].

The theoretical value for the true density (from a single crystal X-ray study of the hemihydrate Form I) is 1.310 g/cm<sup>3</sup> [9]. The measured true density has been reported to have values of  $1.46 \pm 0.03$  g/cm<sup>3</sup> (Form I) and  $1.49 \pm 0.04$  g/cm<sup>3</sup> (Form II) [22].

The true density has also been reported to be  $1.347 \text{ g/cm}^3$  [5], but no details of the sample origin or method were given. It is presumed that this value referred to a sample of the commercial hemihydrate, Form II, although it is clearly at variance with the other values [22].

The following powder properties for the commercial hemihydrate were reported by Leung and Grant [22]:

Specific surface area	$2.29 \pm 0.07 \text{ m}^2/\text{g}$
Particle size	$8.3 \pm 0.6 \text{ }\mu\text{m}$
Water content (room temperature)	$3.76 \pm 0.05 \text{ \%w/w}$
Water content (after heating to $140^\circ\text{C}$ )	$0.33 \pm 0.05 \text{ \%w/w}$

### 3.9 Spectroscopy

#### 3.9.1 UV/VIS Spectroscopy

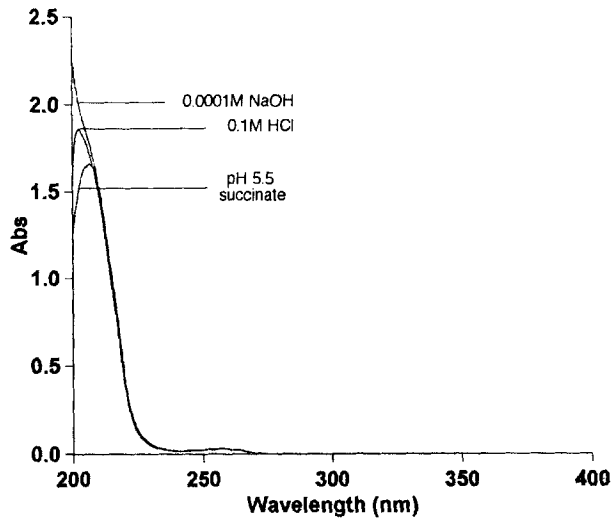
The ultraviolet spectra of aspartame, obtained under various conditions, are shown in Figure 4. The spectral features up to about 225 nm are attributed to end absorption, primarily from the amide and carboxylate carbonyl groups. The benzenoid group is responsible for absorption in the range of 245 – 270 nm, exhibiting maxima at 252.2, 257.6 ( $\epsilon = 752$ , anion;  $\epsilon = 727$ , zwitterion and cation) and 263.0 nm, as well as shoulders at about 247 and 267 nm. There is minimal dependence of absorption on pH, as would be expected for a primary unconjugated amine, except in the end absorption region below 210 nm.

#### 3.9.2 Vibrational Spectroscopy

The infrared spectrum of commercial aspartame (Form II hemihydrate) is shown in Figure 5. 4. The spectrum was obtained using a 1:100 w/w dispersion in KBr on a Shimadzu 8201 FT-IR spectrometer (resolution of  $4 \text{ cm}^{-1}$ ) using Happ-Genzel apodization. Assignments for the principal absorption bands are reported in Table 1.

The infrared absorption spectrum of aspartame is also recorded in the Aldrich IR Library [47], and by Grant and coworkers [8, 23].

(a)



(b)

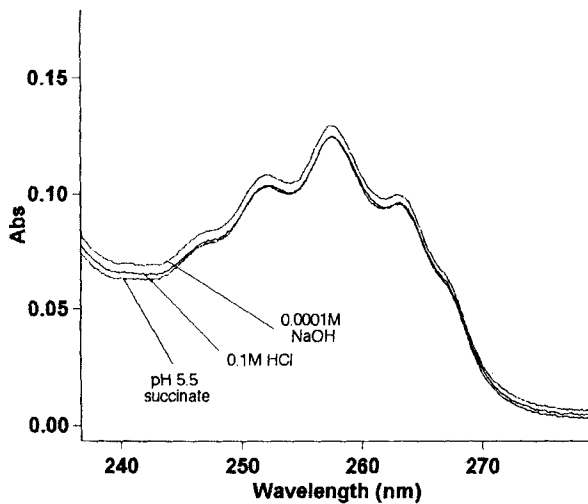


Figure 4. UV spectra of aspartame: (a) 0.050 mg/mL = 0.170 mM; and (b) 0.200 mg/mL = 0.680 mM in aqueous solutions at pH values of 1 (monocation), 5.5 (zwitterion) and 10 (monoanion).

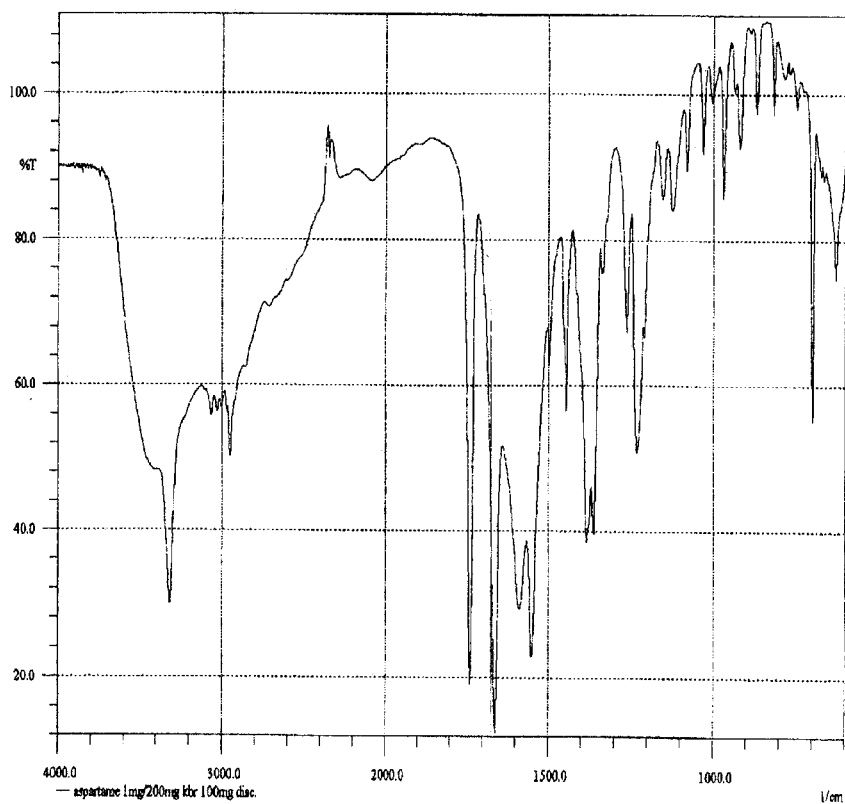


Figure 5. Infrared absorption spectrum of aspartame.

Table 1

## Principal Infrared Absorption Bands of Aspartame

Frequency ( $\text{cm}^{-1}$ )	Relative Intensity	Assignment
3333	m; sharp	amide NH str (H-bonded)
1718	s	C=O str (ester)
1645	s	C=O str (amide I)
1610	s	$^-\text{O}-\text{C}=\text{O}$ str ( $\text{COO}^-$ ) (asym)
1563	s	$>\text{NH}$ deformation (amide II)
1531	s	$^+\text{NH}_3$ deformation
1362	s	$^-\text{O}-\text{C}=\text{O}$ str ( $\text{COO}^-$ ) (sym)
1247	m	fingerprint
1217	s	fingerprint
1196	m	NH in plane vibration?
695	s	NH out of plane vibration



### 3.9.3 Nuclear Magnetic Resonance Spectrometry

The  $^1\text{H}$  and  $^{13}\text{C}$  nuclear magnetic resonance spectra of aspartame are shown in Figures 6 and 7, respectively. These spectra were obtained from a  $d_6$ -DMSO solution (7.5 mg/mL) using a Bruker Avance DRX-500 spectrometer. All spectra were referenced to tetramethylsilane, and assignments for the  $^1\text{H}$ -NMR and  $^{13}\text{C}$ -NMR spectra are found in Tables 2 and 3, respectively.

High resolution NMR studies, in combination with molecular mechanics, were performed to unequivocally assign the prochiral  $\beta$ -protons for the phenylalanine sidechain and to define the shape of the sweet receptor [49]. The previous assignment [48] of the NMR signals for the  $\beta$ -protons of phenylalanine was shown to be in error.

The  $^{13}\text{C}$ -NMR spectrum of aspartame was also determined for the solid state of both hemihydrate Forms I and II [23]. Form I gave single peaks for each carbon atom, indicating that only one crystallographically nonequivalent site was present in the unit cell. Conversely, the spectrum for Form II displayed multiple signals for each carbon in the aspartyl and phenylalanyl sidechains, indicating that there were two or three crystallographically nonequivalent sites. The reduced symmetry of Form II, compared to Form I suggests that it is of higher energy. Theoretical studies indicated that packing in the crystal structure received an important contribution from the hydrophobic phenyl sidechains.

### 3.10 Mass Spectrometry

The electrospray mass spectra for aspartame were collected in both negative and positive ion modes using a Waters Micromass ZQ single quadrupole instrument (Waters, Milford, MA, USA). Solution samples were infused at 25  $\mu\text{L}/\text{min}$ . The spectra thus obtained are shown in Figures 8 and 9.

The mass spectra display signals corresponding to the deprotonated and protonated  $M-1$  (negative mode) and  $M+1$  (positive mode) molecular ions, respectively. Other ions identified are those for the dehydrated species (cyclic imide),  $(M+1)-18$ , and phenylalanine methyl ester (des-aspartyl),  $(M+1)-115$  (positive ion mode only). Also identified were the demethanolated 2,5-diketopiperazine degradation product,  $(M-1)-32$  and  $(M+1)-32$  (both modes).

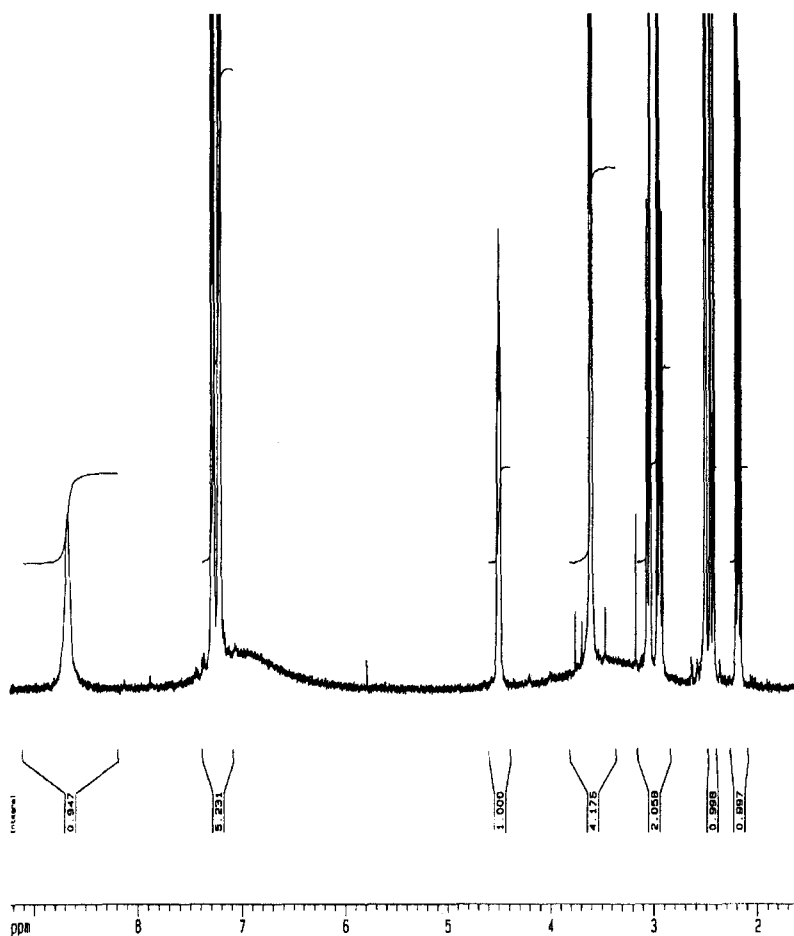


Figure 6.  $^1\text{H}$  nuclear magnetic resonance spectra of aspartame, obtained in deuterated dimethyl sulfoxide solution.

Table 2

500 MHz  $^1\text{H}$  Nuclear Magnetic Resonance Spectral  
Assignments for Aspartame

Chemical Shift (ppm)	Integral	Multiplicity	Coupling constant (J, Hz) <sup>a</sup>	Assignment
2.18, 2.44	2H	split AB quartet (ABX system)	$J_{AB}$ , $17.1 \pm 0.1$ ; $J_{AX}$ , $8.3 \pm 0.2$ ; $J_{BX}$ , $4.9 \pm 0.3$	asp -CH <sub>2</sub> -
2.94, 3.04	2H	split AB quartet (ABX system)	$J_{AB}$ , $14.0 \pm 0.4$ ; $J_{AX}$ , $8.8 \pm 0.9$ ; $J_{BX}$ , $5.4 \pm 0.6$	phe -CH <sub>2</sub> - (decoupled by irradiating at 4.50 ppm)
3.60	1H	triplet	4.5	asp >CH- (coupled to 2.18, 2.44)
3.61	3H	singlet	—	-O-methyl
4.50	1H	multiplet (obscured)	7.0	phe >CH- (coupled to 2.94, 3.04)
~7.0	~3H	very broad singlet	—	<sup>+</sup> NH <sub>3</sub>
7.26	(3+2)H	multiplet		aromatic protons
8.67	1H	broad singlet	—	peptide (amide) proton

(a) from studies in D<sub>2</sub>O: there is a small pD dependency for these coupling constants [48]

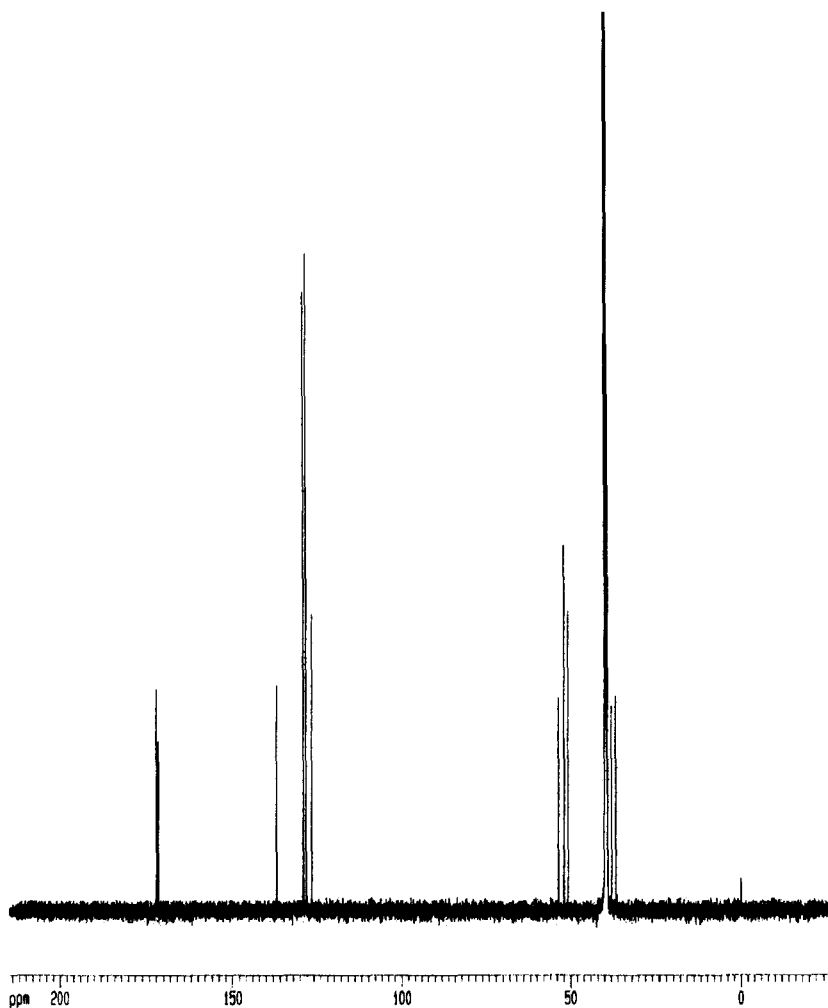


Figure 7.  $^{13}\text{C}$  nuclear magnetic resonance spectra of aspartame, obtained in deuterated dimethyl sulfoxide solution.

Table 3

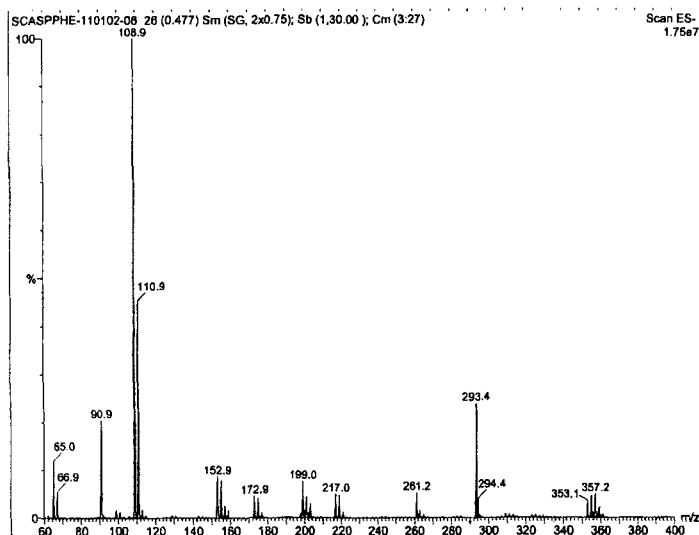
125.7 MHz  $^{13}\text{C}$  Nuclear Magnetic Resonance Spectral  
Assignments for Aspartame

Chemical Shift (ppm)	Assignment	Comments
36.5	-CH <sub>2</sub> - (asp)	-ve DEPT signal
37.8	-CH <sub>2</sub> - (phe)	-ve DEPT signal
50.7	>CH- (asp)	+ve DEPT signal
51.8	-O-methyl	+ve DEPT signal
53.4	>CH- (phe)	+ve DEPT signal
126.5	Para aromatic carbon <sup>a</sup>	
128.2	Meta aromatic carbon <sup>a</sup>	
129.0	ortho aromatic carbon <sup>a</sup>	
136.8	substituted aromatic carbon <sup>a</sup>	
171.5	>C=O (amide) <sup>a</sup>	
171.7	>C=O (ester) <sup>a</sup>	
172.0	>C=O (carboxylate) <sup>a</sup>	

(a) assignment made by the author from consideration of partial electronic charges in a semi-empirical molecular orbital model (PM3).

Figure 8. Mass spectra of aspartame (0.1 mg/mL) in negative ion mode (capillary 2.6 kV; cone 26V). The data were obtained under the conditions indicated for each spectrum.

**(A) in acetonitrile:0.1% formic acid (50:50 v/v)**



**(B) in acetonitrile:0.01M ammonium acetate (50:50 v/v)**

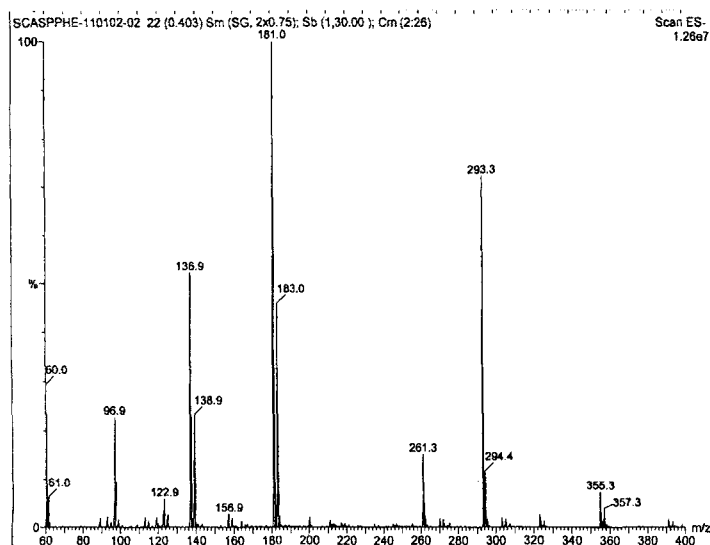


Figure 8 (continued)

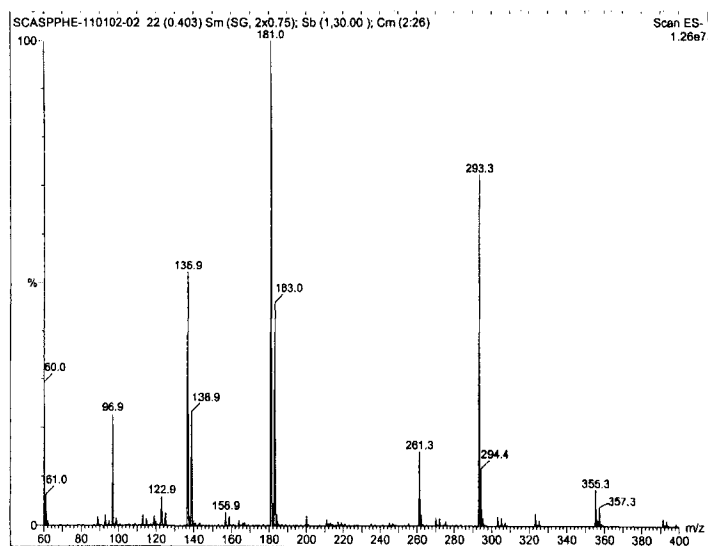
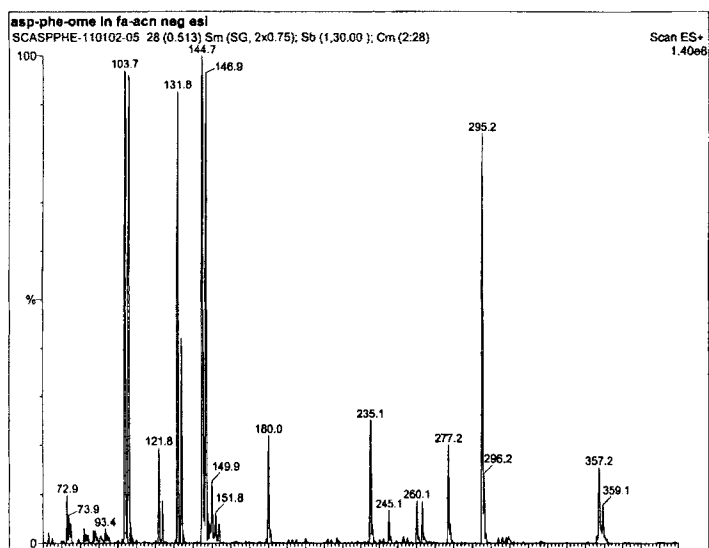
**(C) in acetonitrile:1% ammonia (50:50 v/v)**

Figure 9. Mass spectra of aspartame (0.1 mg/mL) in positive ion mode (capillary, 3.2 kV; cone 18V). The data were obtained under the conditions indicated for each spectrum.

**(A) in acetonitrile:0.1% formic acid (50:50 v/v)**



**(B) in acetonitrile:0.01M ammonium acetate (50:50 v/v)**

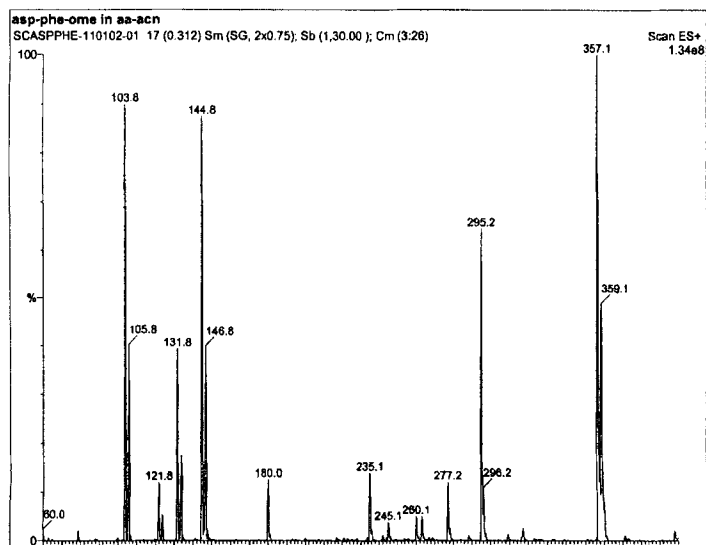
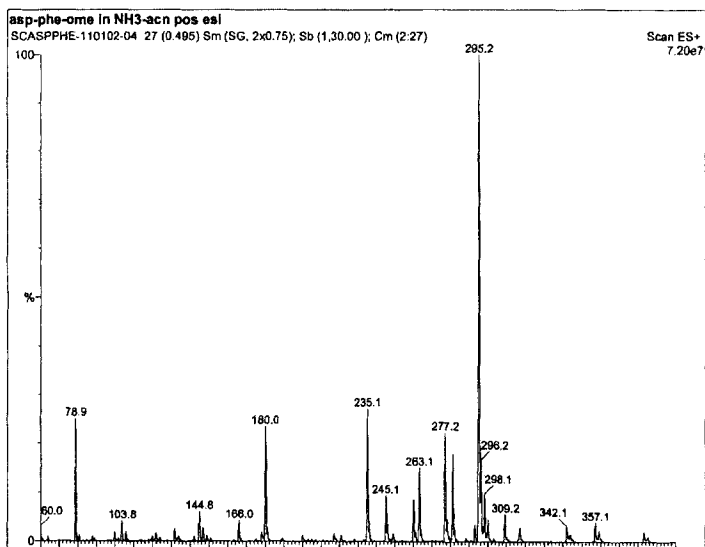




Figure 9 (continued)

**(C) in acetonitrile:1% ammonia (50:50 v/v)**

## **4. Methods of Analysis**

### **4.1 Compendial Tests**

Aspartame is a compendial article, whose specifications and test methods are listed in the National Formulary of the United States Pharmacopeia [19]. The described program of testing and qualification is described in the following sections.

#### **4.1.1 Identification**

The identification is performed by comparing the infrared absorption spectrum of the test article with that the reference standard according to General Test <197M>. The monograph contains a specific instruction not to dry the test specimen.

#### **4.1.2 Transmittance**

The transmittance of a 1 in 100 solution of the test article dissolved in 2 N HCl, and determined in a 1-cm cell at 430 nm with a suitable spectrophotometer, is not less than 0.95 (corresponding to an absorbance of not more than about 0.022). The test solution is prepared by means of sonication.

#### **4.1.3 Specific Rotation**

A test solution having a concentration of 40 mg/mL in 15 N formic acid is prepared, and the optical rotation determined according to General Test <781S>. The specific rotation is to be between +14.5° and +16.5°, determined at 20°C within 30 minutes after preparation of the solution.

#### **4.1.4 Loss on Drying**

The LOD procedure is conducted according to General Test <731>. After the test article is dried at 105°C for 4 hours, it loses not more than 4.5% of its weight.

#### **4.1.5 Residue on Ignition**

When analyzed according to General Test <281>, the test article does not yield more than 0.2% of residue.

#### **4.1.6 Heavy Metals**

When analyzed according to General Test <231>, Method II, the test article does not contain more than 0.001%.

#### 4.1.7 Limit of 5-Benzyl-3,6-Dioxo-2-Piperazineacetic Acid

This compound is determined using HPLC analysis. A Diluent reagent is prepared as a 9:1 mixture of water and methanol. The Mobile Phase is prepared as a filtered and degassed solution by dissolving 5.6 g of monobasic potassium phosphate in 820 mL of water in a 1-liter volumetric flask, adjusting with phosphoric acid to a pH of 4.3, diluting with methanol to volume, and mixing. Adjustments in the composition may be made if required by the System Suitability requirements.

A Standard Solution is prepared by dissolving an accurately weighed quantity of USP Aspartame Related Compound A RS in Diluent, and then diluting quantitatively with Diluent to obtain a solution having a known concentration of about 75 µg/mL. The Test Solution is prepared by transferring 50 mg of the test article (accurately weighed) to a 10-mL volumetric flask, dissolving in and diluting with Diluent to volume, and mixing. The method directs to avoid heat and excessive holding times.

The liquid chromatograph is equipped with a 210-nm detector and a 4.6-mm × 25-cm column containing packing L1 (octadecyl silane chemically bonded to porous silica or ceramic 3-10 µm microparticles). The flow rate is about 2 mL/min, and the column temperature is maintained at 40°C. The suitability of the system is determined by chromatographing the Standard solution, and recording the peak responses as directed under Procedure. The tailing factor is not more than 2.0, and the relative standard deviation for replicate injections is not more than 4.0%.

Procedure: The assay is performed by separately injecting equal volumes (about 20 µL) of the Standard Solution and the Test Solution into the chromatograph, recording the chromatograms, and measuring the responses for the major peaks. The percentage of aspartame related compound A in the test article is calculated using:

$$(C / W)(r_U / r_S),$$

where C is the concentration (µg/mL) of 5-benzyl-3,6-dioxo-2-piperazineacetic acid in the Standard Solution, W is the weight (mg) of the test article, and  $r_U$  and  $r_S$  are the peak responses of aspartame related compound A obtained from the Test Solution and the Standard Solution, respectively. Not more than 1.5% of 5-benzyl-3,6-dioxo-2-piperazineacetic acid is found.

#### 4.1.8 Chromatographic Purity

The Diluent, Mobile Phase, Test Solution, and Chromatographic system used for this test method are the same as those described for the Limit determination of 5-benzyl-3, 6-dioxo-2-piperazineacetic acid. The procedure requires a Diluted Test Solution, which is prepared by pipetting 2.0 mL of the Test Solution into a 100-mL volumetric flask, diluting to volume with Diluent, and mixing.

Procedure: The assay is performed by injecting equal volumes (about 20  $\mu$ L) of the Test Solution and the Diluted Test Solution into the HPLC system, recording the chromatograms, and measuring the peak responses. The method contains a directive that the elution of the Test solution is to be continued for twice the retention time of the aspartame peak. The sum of the responses of all the peaks in the chromatogram of the Test Solution, excluding the 5-benzyl-3,6-dioxo-2-piperazineacetic acid and aspartame peak responses, is not greater than the aspartame peak response obtained from the Diluted Test Solution. This corresponds to not more than 2.0% of chromatographic impurities.

#### 4.1.9 Organic Volatile Impurities

The OVI content of the test article is determined according to General Test <467>, Method IV, and the substance is to meet the requirements.

#### 4.1.10 Assay

The assay method is based on potentiometric titration, and uses 0.1 N  $\text{HClO}_4$  (0.1 N in glacial acetic acid) as the titrant. In the standardization of the titrant, one titrates to the crystal violet green endpoint.

Procedure: Transfer about 300 mg of the test article (accurately weighed) to a 150-mL beaker, dissolve in 1.5 mL of anhydrous formic acid, and add 60 mL of glacial acetic acid. Add crystal violet Test Solution, and immediately titrate with 0.1 N  $\text{HClO}_4$  to a green endpoint. Perform a blank determination, and make any necessary correction. Each milliliter of 0.1 N  $\text{HClO}_4$  is equivalent to 29.43 mg of aspartame. The method description cautions that a blank titration exceeding 0.1 mL may be due to excessive water content, and may cause loss of visual endpoint sensitivity.

Aspartame NF contains not less than 98.0 percent and not more than 102.0 percent of  $\text{C}_{14}\text{H}_{18}\text{N}_2\text{O}_5$ , calculated on the dried basis.

Aspartame is GRAS listed, and is accepted as a food additive in Europe and is in the FDA Inactive Ingredients Guide. It is included in non-parenteral medicines licensed in the UK, and is listed in the USP-NF, BP, JP, and EP. Aspartame is the subject of a monograph in the Food Chemicals Codex issued by the National Academy of Sciences. This document is very similar to the corresponding USP-NF monograph.

#### **4.2 Electrochemical Analysis**

Aspartame has been assayed by a flow injection analysis biosensor employing an immobilized enzyme (pronase) which cleaves the peptide bond. The resulting phenylalanine methyl ester is then detected by an *L*-amino acid oxidase electrode. This method was applied to analysis of aspartame in foods [82].

#### **4.3 Spectroscopic Analysis**

A number of spectrometric methods have been proposed for the quantitative analysis of aspartame. These include colorimetric [56-60], UV absorption [61-66], and fluorescence methods [67, 68].

In view of the inherent solution stability problems that will be discussed in a later section, it is strongly recommended that chromatographic or electrophoretic methods be used for quantitation of aspartame, especially where contact with moisture may occur.

#### **4.4 Chromatographic Methods of Analysis**

##### **4.4.1 High Performance Liquid Chromatography**

The most popular method used for the assay of aspartame is that of high performance liquid chromatography. A large number of methods and studies have been reported, and the reported conditions used for these analyses since 1980 are summarized in Table 4.

##### **4.4.2 Capillary zone electrophoresis (CZE) methods**

Although methods based on capillary zone electrophoresis have not achieved the popularity of HPLC methods, a few studies have been reported. The defining characteristics of these are summarized in Table 5.

Table 4  
Conditions for the High Performance Liquid Chromatographic  
Analysis of Aspartame

Column type	Mobile phase	Flow rate (mL/min)	Sample type	Detection	Reference
Waters $\mu$ Bondapak C18, 300 x 4.6 mm	ACN 15%  Triethylammonium phosphate buffer, pH adjusted with NaOH to 4.3	2.0	Drinks	214 nm	69
Separon SI C18	MeOH 15%  NaH <sub>2</sub> PO <sub>4</sub> 0.5M, pH adjusted to 2.1		Drinks		70
Waters $\mu$ Bondapak C18, 10 $\mu$ m, 300 x 3.9 mm	MeOH 5%  Acetate buffer (pH 3) 95%	2.0	Foods and drinks	254 nm	71
Supelcosil LC-18, 5 $\mu$ m, 150 x 4.6 mm	ACN 3-20%  KH <sub>2</sub> PO <sub>4</sub> 0.02M (pH 5 to pH 3.5) 97-80%  gradient elution	1.0	Diet foods	200/210 nm	72
ACHT-CSP $\alpha$ - chymotrypsin bonded to silica, 5 $\mu$ m, 250 x 4.6 mm  or  ACHT-CSP $\alpha$ - chymotrypsin bonded to silica, 15 $\mu$ m, 100 x 4.6 mm	acetate (1 mM, pH 5.5), containing NaCl 0.07M  or  phosphate, 0.07 M, pH 5.5  or  acetate, 0.082 M, pH 5.5  or  acetate, 1 mM, pH 5.5, containing Na <sub>2</sub> SO <sub>4</sub> , 0.023 M	0.6     or     0.3	Pure optical isomers of APM	254 nm	73

Table 4 (continued)

Column type	Mobile phase	Flow rate (mL/min)	Sample type	Detection	Reference
Bonded chiral crown ether	Propan-2-ol 1.5%  Aqueous $\text{HClO}_4$ , pH adjusted to 2.8  Temperature gradient		Drinks containing added aspartame		74
Waters $\mu$ Bondapak Phenyl	ACN 5% v/v  $\text{KH}_2\text{PO}_4$ 0.01M, pH 2.5	1.5	Aqueous reaction solutions  (Internal standard: guaiphenesin)		39
Beckman Ultrasphere ODS C18; 4.6 x 150 mm; 5 $\mu$ m	40% MeOH;  60% citrate (0.05M, pH 4.7)	1.5	Aqueous reaction solutions	252 nm	37
LiChrosorb C18, 5 $\mu$ m, 250 x 4 mm	ACN, 15%  phosphate buffer, pH 4.5, I = 0.1M, 85%	not stated	Drinks	215 nm	75
Waters $\mu$ Bondapak C18; 3.9 x 300 mm	MeOH 15%  $\text{NaH}_2\text{PO}_4$ 0.5M, pH adjusted to 2.1 with $\text{H}_3\text{PO}_4$ , 85%  Separates aspartame from 6 degradation products	2.0 for first 15.1 min, then 3.0 from 15.1 to 20 min	Aqueous acidic reaction solutions  (Int. std., tyrosine)	200 nm	25
Keystone octylsilyl C8; 4.6 x 150 mm; 5 $\mu$ m	(i) 12.5% v/v ACN  (ii) 87.5% v/v phosphate (0.18M $\text{NaH}_2\text{PO}_4$ adj. to pH 2.1 with $\text{H}_3\text{PO}_4$ ; also contains 0.02M sodium heptanesulphonate and 0.114 M KCl	1.2	Aqueous reaction solutions  Separates aspartame from 6 degradation products (DKP, $\alpha$ -AP, PA, PM, $\beta$ -APM, unknown)	210 nm	26

Table 4 (continued)

Column type	Mobile phase	Flow rate (mL/min)	Sample type	Detection	Reference
Divinylbenzene-polystyrene resins; modified chemically, milled and screened to 30-45 micron and then packed by the authors; 200 x 22 mm	Aqueous disodium hydrogen phosphate, monopotassium dihydrogen phosphate and sodium chloride; pH 2.8; temperature at 20, 30 or 40° C.	0.5, 1.0, or 1.5	Aspartic acid, asparagine, phenylalanine, aspartame (theoretical adsorption study)		76
Waters $\mu$ Bondapak C18, 10 $\mu$ m, 300 x 3.9 mm	ACN 2% or 15%  KH <sub>2</sub> PO <sub>4</sub> 0.0125M, pH adjusted to 3.5 98% or 85%	0.8	Foods, drinks, tabletop sweetener	214 nm	77
Waters NovaPak C18; 4.6 x 150 mm; 5 $\mu$ m	ACN 15% v/v  Phosphate buffer, pH 3.9, ionic strength 0.1 (Adapted from Moors et al, <i>Anal. Chim. Acta</i> , <b>255</b> , 177 (1991))	1.0	Commercial sweeteners and soft drinks		78
Polsil ODS C18; 4 x 250 mm; 7 $\mu$ m	ACN 85% v/v  KH <sub>2</sub> PO <sub>4</sub> 20 mM, pH adjusted to 3.5 with 0.1M KOH and containing 2 mM d,l-[4,4'-(1-methyl-2-propylethane-1,2-diylidimino)bis(pent-3-en-2-onato)]nickel(II) 15% v/v	0.8	Commercial powdered sweeteners  (Internal standard: 0.1 mg/mL m-hydroxybenzoic acid)	210 nm	79
Econosphere octylsilyl C8; 4.6 x 250 mm; 5 $\mu$ m	ACN 20% v/v  Phosphate buffer 0.04 M, pH 2.23, containing sodium hexanesulphonate 0.01M, 80% v/v	2.0	Aqueous reaction solutions	254 nm	28
Waters $\mu$ Bondapak C18  8 x 100 mm Radial-Pak	ACN 10% v/v  K <sub>2</sub> HPO <sub>4</sub> 10 mM, pH adjusted to 4.0 with H <sub>3</sub> PO <sub>4</sub>	2.0	Commercial low joule soft drinks, cordials, tomato sauce, marmalade jam, powder sweeteners	220 nm	80



Table 5  
Conditions for the Capillary Zone Electrophoresis  
Analysis of Aspartame

Column	Mobile phase	Potential	Sample type	Detection	Reference
Waters Accu-Sep fused silica capillary 60 cm x 75 $\mu$ m  Distance to detector: 52 cm	Sodium phosphate buffer at pH 11 and ionic strength 0.025.	15 kV	Commercial sweetener powders and soft drinks	214 nm	78
Polymicro Technologies uncoated fused-silica capillary 75 cm x 75 $\mu$ m;  Distance to detector: 50 cm	0.05 M sodium deoxycholate, 0.01 M potassium dihydrogen-orthophosphate, 0.01 M sodium borate, pH 8.6	20 kV  27°C	Commercial low joule soft drinks, cordials, tomato sauce, marmalade jam, powder sweeteners  (Internal standard: dehydroacetic acid)	220 nm	80
Written in Czech {no details available}					81

Two studies have compared HPLC and CZE methods for aspartame [78, 80]. Although the CZE method was found to be faster than the HPLC method and had better resolution, it was also found to be ten to twenty fold less sensitive. While this may not be important when raw materials are assayed, it may be of concern in the analysis of biological samples.

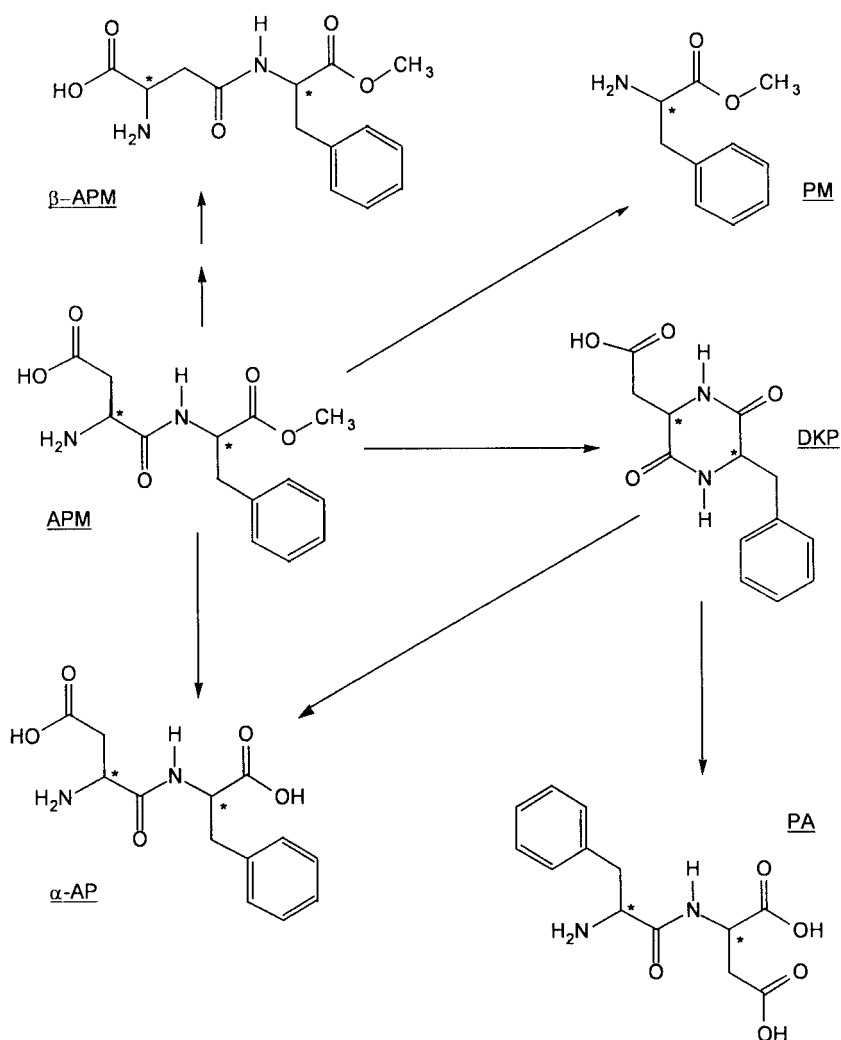
## 5. Stability

### 5.1 Solution stability

Several kinetic studies have been performed on aspartame, which is relatively unstable in solution [24-30]. The half-life at pH 4.3 (the pH of maximum stability) is about 260 days at 25°C [30]. The shelf life ( $t_{90}$ ) at this temperature and pH 4.0 is about 53 days [28]. Degradation is more rapid at other pH values: *e.g.* shelf-life 12 days at pH 1, and 1 day at pH 7 [30].

As outlined in Scheme 2, aspartame can degrade through multiple pathways. These involve:

- (i) Formation of 3-methylenecarboxyl-6-benzyl-2,5-diketopiperazine (5-benzyl-3,6-dioxo-2-piperazineacetic acid) via nucleophilic attack of the free base *N*-terminal amino group on the phenylalanine carboxyl group (intramolecular self-aminolysis) at pH values exceeding 2 [24]. This pathway is precluded at lower pH values, owing to protonation of the aspartame *N*-terminal amino group which then cannot take part in nucleophilic attack on the carbonyl group. The 2,5-diketopiperazine further hydrolyzes to *L*-aspartyl-*L*-phenylalanine and to *L*-phenylalanyl-*L*-aspartate.
- (ii) Acid-catalyzed hydrolysis of the methyl ester to form *L*- $\alpha$ -aspartyl-*L*-phenylalanine and methanol at pH values less than 2.
- (iii) Hydrolysis of the peptide bond to aspartate and phenylalanine methyl ester.
- (iv) Isomerization to *L*- $\beta$ -aspartyl-*L*-phenylalanine methyl, probably through an intermediary succinimide, as has been described for other peptides [31-33].



Scheme 2: Degradation pathways for aspartame

APM = aspartame

 $\beta$ -APM =  $\beta$ -aspartame

PM = phenylalanine methyl ester

DKP = 3-benzyl-6-carboxymethyl-2,5-diketopiperazine

 $\alpha$ -AP =  $\alpha$ -L-aspartyl-L-phenylalanine

PA = L-phenylalanyl-L-aspartic acid)

In addition to the degradation pathways shown in Scheme 2, very slow epimerization of all species is also feasible [24]. The end products of degradation are aspartate, phenylalanine, and methanol.

Chromatograms of degraded aspartame solutions also showed irregular, low intensity, strongly retained peaks which were more prominent in solutions with higher initial aspartame concentrations [26]. These may be due to polymerization products from pseudo-second order intermolecular self-aminolysis of aspartame.

A careful detailed study separated the contributions to the pH-rate profile (pH range 0.27 to 11.5 at 25°C) from intramolecular self-aminolysis and ester hydrolysis [28]. The results were used as a baseline for further studies of degradation in binary solvent mixtures [29].

The stability of aspartame in food products has been studied [34], with the main degradation product being the substituted 2,5-diketopiperazine. Stability in syrup medication vehicles has also been examined [35].

## 5.2 Solid state stability

The solid state properties of aspartame have been extensively investigated by Grant and coworkers [8, 22, 23]. In the dry powder form, anhydrous aspartame is stable at up to its melting temperature [22], although degradation occurs in the presence of moisture. Heating to 150°C (*i.e.*, to higher temperatures than are needed for dehydration at 129°C) gives a product with identical HPLC retention characteristics as aspartame. When heated to 210°C, samples gave HPLC peaks that corresponded to the 2,5-diketopiperazine. This interpretation was confirmed by TGA, which showed near-stoichiometric mass losses at 129°C (water) and 188°C (methanol). The solid state reaction kinetics corresponded to a nucleation control mechanism (Prout-Tompkins kinetics). The activation energies determined by various methods for 2,5-diketopiperazine formation were closely similar: 63.3 kcal/mol (DSC) and 64.1 kcal/mol (isothermal TGA).

Hydration and dehydration of the aspartame hydrates has been studied by Grant and coworkers [8]. The anhydrous form is very susceptible to moisture uptake and could not be isolated, being only detected *in situ* during variable temperature x-ray powder diffraction, DSC, or TGA studies. Equilibration of either of the hemihydrates (Forms I and II) with

water vapor (relative humidities exceeding 58% at 25°C) or with liquid water gave the dihemihydrate,  $\text{APM} \cdot 2.5\text{H}_2\text{O}$ .

In principle, solid state degradation should also take place slowly in surface moisture films at ambient temperatures and humidities. Similar products are to be expected as for solution degradation, but no studies were found that examined this phenomenon. Given the high concentrations of substrate that are present in surface moisture films, there is also the possibility that intermolecular self-aminolysis and polymerization could occur, in addition to the intramolecular reaction reported under anhydrous conditions by Grant and coworkers.

### 5.3 Stabilization

Aspartame has been stabilized in aqueous solution to some extent by the addition of cyclodextrins or modified cyclodextrins [24, 36, 37], and by formulation with PEG 400 [38]. Hydroxylic solvents, including methanol, ethanol, and glycerol, were not found to stabilize significantly aqueous solutions of aspartame in the pH range for typical carbonated drinks [39].

### 5.4 Chemical interactions

Ascorbic acid (0.8% w/v) in aqueous solution degraded according to apparent first order kinetics, with a rate constant of  $2.34 \times 10^{-2}$ /hour, when irradiated by artificial sunlight [40]. The presence of 5% aspartame in the solution decreased the rate constant to  $1.48 \times 10^{-2}$ /hour, thus stabilizing ascorbic acid to photochemical degradation by about 37%. Similar effects were also seen with some carbohydrate sweeteners.

Aspartame contains a free *N*-terminal amino group. In its deprotonated form, this could be expected to react with carbonyl compounds, forming Schiff base compounds. Some evidence has been obtained for this type of reaction, involving aspartame and flavoring agents [41]. A similar explanation might also apply to the interactions with ascorbic acid and carbohydrate sweeteners described in the previous paragraph.

### 5.5 Complexation

In aqueous solution, aspartame has been shown to be stabilized by the presence of certain cyclodextrins, presumably through the formation of

inclusion complexes. Complexation of aspartame by cyclodextrins has been studied by NMR [43, 44] and by flow microcalorimetry [45]. The microcalorimetric equilibrium binding constants in aqueous buffer at 25°C for the aspartame complexes with  $\beta$ -cyclodextrin and 2-hydroxypropyl- $\beta$ -cyclodextrin were  $128 \pm 22 \text{ M}^{-1}$  and  $46 \pm 9 \text{ M}^{-1}$ , respectively [45]. The value for the aspartame complex with  $\beta$ -cyclodextrin was similar to a value of  $90 \text{ M}^{-1}$  obtained in  $\text{D}_2\text{O}$  using NMR [43]. The interaction enthalpies determined by microcalorimetry were determined to be  $-11,700 \pm 700 \text{ J/mol}$  and  $-2,200 \pm 200 \text{ J/mol}$ , respectively. These values indicate that binding between aspartame and cyclodextrins is relatively weak.

Aspartame in aqueous solution has recently been reported to interact with calf thymus DNA [46]. This study was an attempt to suggest a biochemical mechanism that might provide evidence for a supposed link to the increased incidence and severity of brain tumors observed since the commercial introduction of aspartame in 1981. Aspartame interacted with DNA, which displayed 40-65% of the extent of interaction shown by doxorubicin (a known DNA intercalator), while aspartate (39%) and phenylalanine (31%) interacted to a lesser extent. Control experiments suggested that much of the binding was attributed to electrostatic reactions with the DNA phosphate anions. Alanine gave only a weak interaction (12%), that was also attributed to ionic interactions. It was suggested that the observed interactions provided support for the opinion that aspartame might promote DNA replication errors. These observations need to be confirmed by independent methods, such as isothermal titration microcalorimetry or spectroscopy, as well as a demonstration, so far lacking, that intact aspartame can access the brain ventricles after oral administration.

## **6. Biological Properties**

### **6.1 Activity**

The low energy sweetening properties of aspartame have been discussed on the basis of structural relationships [1, 83] within the context of the three point contact model of the sweet taste receptor. This model involves a hydrogen bond donor, a hydrogen bond acceptor, and a hydrophobic region with specific geometric relationships. The model accounts for the fact that only one of the four diastereomers of aspartylphenylalanyl methyl ester is sweet.

## **6.2 Toxicity and safety**

The toxicity and safety of aspartame, especially a reputed causal connection with an increased incidence of brain tumors about the time that aspartame was approved (1981], has received much attention in the popular press. A FDA discussion paper (T96-75, November 1996) on the topic can be found at <http://vm.cfsan.fda.gov/~lrd/tpaspart.html>. This discussion paper refutes the association, chiefly on the grounds that the incidence of brain and CNS tumors began its rise in 1973, well before the introduction of aspartame. Since 1985, the incidence of brain tumors has in fact been increasing at a slower rate. The incidence peaked in about 1991 and has declined slightly since then.

Other safety concerns are covered by documents found on searching the website of the International Food Information Council Foundation (<http://www.ific.org/>), a non-profit organization supported by the food and beverage industry. These include issues such as allergy, hyperactivity, weight loss, and asthma.

## **7. Acknowledgements**

The author is grateful to Dr. Francis Chiu (VCP, Monash University) (electrospray mass spectra), Dr. Agnes Taillardat (VCP, Monash University) (UV spectra), Ms Stacey Collie (School of Pharmacy, University of Queensland) (IR spectra), and Dr Ian Brereton (CMR, University of Queensland) (NMR spectra) for technical assistance.

## 8. References

1. R.H. Mazur, J.M. Schlatter, and A.H. Goldkamp, *J. Am. Chem. Soc.*, **91**, 2684-2691 (1969).
2. M. Neuman, *Drugs of Today*, **16**, 63-67 (1980).
3. T.A. Gossel, *US Pharmacist*, **26**, 9(Jan), 28-30 (1984).
4. L.A. Pagliaro and R.A. Locock, *Can. Pharm. J.*, **119**, 121-125 (1986).
5. H. Kibbe, Ed., *Handbook of Pharmaceutical Excipients*, 3<sup>rd</sup> edn., American Pharmaceutical Association, Washington DC, pp. 27-29 (2000).
6. Y.K. Kang, *Int. J. Peptide Protein Res.*, **38**, 79-83 (1991).
7. S. Budavari, ed., *The Merck Index*, 12<sup>th</sup> edn., Merck and Co., Whitehouse Station, NJ pp. 141-142 (1996).
8. S.S. Leung, B.E. Padden, E.J. Munson, and D.J.W. Grant, *J. Pharm. Sci.*, **87**, 508-513 (1998).
9. M. Hatada, J. Jancarik, B. Graves, and S.-H. Kim, *J. Am. Chem. Soc.*, **107**, 4279-4282 (1985).
10. P. Kuhl, *Die Pharmazie*, **45**, 881-887 (1990). A translation of this paper is available from the author, and should be consulted for the array of chemical and enzymatic methods reported up to 1990.
11. J.S. Tou and B.D. Vineyard, *J. Org. Chem.*, **50**, 4982-4984 (1985).
12. C. Fuganti, P. Grasselli, and L. Malpezzi, *J. Org. Chem.*, **51**, 1126-1128 (1986).
13. J.D. Rozzell, *Bioorg. Med. Chem.*, **7**, 2253-2261 (1999).
14. K. Oyama et al., *J. Chem. Soc.*, **11**, 356-360, (1981).
15. G.A. Iacobucci, "Enzymatic method for the synthesis and separation of peptides," U.S. Patent 5,002,871 (1991).
16. M. Miyanaga, T. Tanaka, T. Sakiyama, and K. Nakanishi, *Biotech. Bioeng.*, **46**, 631-635 (1995).



17. E.V. Kudryashova, V.V. Mozhaev, and C. Balny, *Biochim. Biophys. Acta*, **1386**, 199-210 (1998).
18. A.S. Bommarius, M. Schwarm, and K. Drauz, *J. Mol. Catalysis B: Enzymatic*, **5**, 1-11 (1998).
19. *United States Pharmacopeia, National Formulary XVIII*, United States Pharmacopoeial Convention, Inc., Rockville, MD, pp. 2215-2216 (1995).
20. *Food Chemicals Codex*, National Academy of Sciences, Washington DC.
21. J. Elks and C.R. Ganellin, eds., *Dictionary of Drugs*, Chapman and Hall, London UK, A-00460 (1990).
22. S.S. Leung and D.J.W. Grant, *J. Pharm. Sci.*, **86**, 64-71 (1997).
23. S.S. Leung, B.E. Padden, E.J. Munsen, and D.J.W. Grant, *J. Pharm. Sci.*, **87**, 501-507 (1998).
24. S.M. Gaines and J.L. Bada, *J. Org. Chem.*, **53**, 2757-2764 (1988).
25. P. Langguth, R. Alder, and H.P. Merkle, *Pharmazie*, **46**, 188-192, (1991).
26. R.J. Prankerd, H.W. Stone, K.B. Sloan, and J.H. Perrin, *Int. J. Pharm.*, **88**, 189-199 (1992).
27. T. Loftsson, and J. Baldvinsdottir, *Acta Pharm. Nord.*, **4**, 329-330, (1992).
28. R.D. Skwierzynski and K.A. Connors, *Pharm. Res.*, **10**, 1174-1180 (1993).
29. R.D. Skwierzynski and K.A. Connors, *J. Pharm. Sci.*, **83**, 1690-1696 (1994).
30. R.H. Mazur, *J. Tox. Environ. Health*, **2**, 243-249 (1976).
31. L.E. Kirsch, R.M. Molloy, M. Debono, P. Baker, and K.Z. Farid, *Pharm. Res.*, **6**, 387-393 (1989).
32. N. Bhatt, K. Patel, and R.T. Borchardt, *Pharm. Res.*, **7**, 593-599 (1990).
33. K. Patel and R.T. Borchardt, *Pharm. Res.*, **7**, 703-711 (1990).

34. T. Tuncel and A. Araman, *Acta Pharmaceutica Turcica*, **31**, 61-66 (1989).
35. T. Ozol, *Acta Pharm. Turcica*,; **28**, 125-130 (1986).
36. T. Ojima, N. Nagashima, and T. Ozawa, Eur. Patent 0,097,950-B1 (1983).
37. M. Brewster, T. Loftsson, J. Baldvinsdottir, and N. Bodor, *Int. J. Pharm.*, **75**, R5-R8 (1991).
38. S.H. Yalkowsky, E. Davis, and T. Clark, *J. Pharm. Sci.*, **82**, 978 (1993).
39. S. Sanyude, R.A. Locock, and L.A. Pagliaro, *J. Pharm. Sci.*, **80**, 674-676 (1991).
40. A.H.L. Ho, A. Puri, and J.K. Sugden, *Int. J. Pharm.*, **107**, 199-203 (1994).
41. F. Tateo, L. Triangeli, E. Ciserchia, R. Nicoletti, and F. Berte, *Boll. Chim. Farm.*, **125**, 404-409 (1986).
42. K.A. Connors, *A textbook of Pharmaceutical Analysis*, 3<sup>rd</sup> edn., Wiley-Interscience, New York, PP. 147-150 (1982).
43. S. Takahashi, E. Suzuki, and N. Nagashima, *Bull. Chem. Soc. Jap.*, **59**, 1129-1132 (1986).
44. M.M. Maheswaran and S. Divakar, *Indian J. Chem.*, **30A**, 30-34 (1991).
45. D. Moelands, N.A. Karnik, R.J. Prankerd, K.B. Sloan, H.W. Stone, and J.H. Perrin, *Int. J. Pharm.*, **86**, 263-265 (1992).
46. G.A. Karikas, K.H. Schulpis, G. Reclos, and G. Kokotos, *Clin Biochem.*, **31**, 405-407(1998).
47. C.J. Pouchert, ed., *The Aldrich Library of Infrared Spectra*, 3<sup>rd</sup> edn., Aldrich Chemical Co., Milwaukee, p.1005H (1981).
48. F. Lelj, T. Tancredi, P.A. Temussi, and C.Toniolo, *J. Am. Chem. Soc.*, **98**, 6669-6675 (1976).
49. M.A. Castiglione-Morelli, F. Lelj, F. Naider, M. Tallon, T. Tancredi, and P.A. Temussi, *J. Med. Chem.*, **33**, 514-520 (1990).

50. H.H. El-Shattawy, D.O. Kildsig, and G.E. Peck, *Drug Dev. Ind. Pharm.*, **10**, 1-17 (1984).
51. C.H. Görbitz, *Acta Chem. Scand.*, **B41**, 87-92 (1987).
52. H.H. El-Shattawy, D.O. Kildsig, and G.E. Peck, *Drug Dev. Ind. Pharm.*, **8**, 429-443 (1982).
53. H.H. El-Shattawy, D.O. Kildsig, and G.E. Peck, *Drug Dev. Ind. Pharm.*, **8**, 651-662 (1982).
54. H.H. El-Shattawy, D.O. Kildsig, and G.E. Peck, *Drug Dev. Ind. Pharm.*, **8**, 857-868 (1982).
55. H.H. El-Shattawy, D.O. Kildsig, and G.E. Peck, *Drug Dev. Ind. Pharm.*, **8**, 923-935 (1982).
56. J. Vachek, *Ceska-a-Slovenska-Farmacie*, **33**, 217-219 (1984).
57. J. de A. Nobrega, O. Fatibello-Filho, and I. da C. Vieira, *Analyst*, **119**, 2101-2104 (1994).
58. E. Majewska, *Zywnosc*, **7(3, Supl.)**, 133-137 (2000).
59. G. Iskender, A.O. Sagirli, and A. Olcay, *Acta Pharm. Turc.*, **42**, 1-5 (2000).
60. T. Hamano, Y. Mitsuhashi, N. Aoki, S. Yamamoto, S. Tsuji, Y. Ito, and Y. Oji, *Analyst*, **115**, 435-438 (1990).
61. K.C. Guven and T. Ozol, *Acta Pharm. Turcica*, **26**, 28-30 (1984).
62. T. Ozol, *Acta Pharm. Turcica*, **26**, 59-62 (1984).
63. E. Hassan, I. Hewala, A.A. Wahbi, and Y. Hassan, *Farmaco*, **48**, 1137-1151 (1993).
64. X. Meng, Q. Liu, and Q. Jiao, *Shipin Gongye Keji*, (6), 77-79 (1997).
65. I.I. Hewala, A. Wahbi, M. El-Aziz, E.H. Hassan, and Y.H. Hussein, Yousria H. *Alexandria J. Pharm. Sci.*, **10**, 59-64 (1996).
66. D. Bertini and V. Nuti, *Boll. Chim. Ig., Parte Sci.* **43(S1)**, 11-18 (1992).

67. S. Atmaca, G. Iskender, and E. Bayer, *Acta Pharm. Turcica*, **31**, 37-40 (1989).
68. M. Poctova and B. Kakac, *Ceska-a-Slovenska-Farmacie*, **31**, 113-115 (1982).
69. T.A. Tyler, *J. Assoc. Off. Anal. Chem.*, **67**, 745-747 (1984).
70. M. Prudel and E. Davidkova, *Nahrung.*, **29**, 381-389 (1985).
71. M. Veerabhadrrao, M.S. Narayan, O. Kapur, and C.S. Sastry, *J. Assoc. Off. Anal. Chem.*, **70**, 578-82 (1987).
72. J.F. Lawrence and C.F. Charbonneau, *J. Assoc. Off. Anal. Chem.*, **71**, 934-937 (1988).
73. P. Jadaud and I.W. Wainer, *Chirality*, **2**, 32-37 (1990).
74. S. Motellier and I.W. Wainer, *J. Chromatogr.*, **516**, 365-373 (1990).
75. M. Moors, C.R.R.R. Teixiera, M. Jimidar, and D.L. Massart, *Anal. Chim. Acta*, **255**, 177-186 (1991).
76. J.L. Casillas, F. Addo-Yobo, C.N. Kenney, J. Aracil, and M. Martinez, *J. Chem. Tech. Biotech.*, **55**, 163-169 (1992).
77. J. Prodolliet and M. Bruehlhart, *J. Assoc. Off. Anal. Chem.*, **76**, 275-282 (1993).
78. M. Jimidar, T.P. Hamoir, A. Foriers, and D.L. Massart, *J. Chromatogr.*, **636**, 179-186 (1993).
79. G. Bazylak, *J. Chromatogr.*, **A668**, 519-27 (1994).
80. C.O. Thompson, V.C. Trenerry, and B. Kemmery, *J. Chromatogr.*, **A694**, 507-514 (1995).
81. I. Zelensky, V. Madajova, E. Simunicova, V. Zelenska, and J. Novak, *Cesk. Farm.*, **38**, 248-256 (1989).
82. K.B. Male, J.H. Luong, B. Gibbs, and Y. Konishi, *Appl. Biochem. Biotech.*, **38**, 189-201 (1993).
83. M.R. Cloninger and R.E. Baldwin, *Science*, **170**, 81-82 (1970).

This Page Intentionally Left Blank

**EDETIC ACID**  
**[ETHYLENEDIAMINE TETRAACETIC ACID, EDTA]**

F. Belal and Abdullah A. Al-Badr

Department of Pharmaceutical Chemistry  
College of Pharmacy  
King Saud University  
P.O. Box 2457  
Riyadh-11451  
Kingdom of Saudi Arabia

## **Contents**

### **1. Description**

- 1.1 Nomenclature
  - 1.1.1 Systematic Chemical Name
  - 1.1.2 Nonproprietary Names
  - 1.1.3 Proprietary Names
- 1.2 Formulae
  - 1.2.1 Empirical Formula, Molecular Weight, CAS Number
  - 1.2.2 Structural Formula
- 1.3 Elemental Analysis
- 1.4 Appearance
- 1.5 Uses and Applications

### **2. Methods of Preparation**

### **3. Physical Properties**

- 3.1 Ionization Constants
- 3.2 Solubility Characteristics
- 3.3 Crystallographic Properties
  - 3.3.1 X-Ray Powder Diffraction Pattern
  - 3.3.2 Polymorphism
- 3.4 Thermal Methods of analysis
  - 3.4.1 Melting Behavior
  - 3.4.2 Differential Scanning Calorimetry
- 3.5 Spectroscopy
  - 3.5.1 UV/VIS Spectroscopy
  - 3.5.2 Vibrational Spectroscopy
  - 3.5.3 Nuclear Magnetic Resonance Spectrometry
    - 3.5.3.1  $^1\text{H}$ -NMR Spectrum
    - 3.5.3.2  $^{13}\text{C}$ -NMR Spectrum
- 3.6 Mass Spectrometry

#### **4. Methods of Analysis**

- 4.1 Identification
  - 4.1.1 British Pharmacopoeia
  - 4.1.2 United States Pharmacopoeia
- 4.2 Compendial Methods of Analysis
  - 4.2.1 Edetic Acid
  - 4.2.2 Edetate Disodium
  - 4.2.3 Edetate Calcium Disodium
- 4.3 Electrochemical Methods of Analysis
  - 4.3.1 Polarography
  - 4.3.2 Amperometry
  - 4.3.3 Potentiometry
  - 4.3.4 Voltammetry
- 4.4 Spectroscopic Methods of Analysis
  - 4.4.1 Spectrophotometry
  - 4.4.2 Fluorimetry
  - 4.4.3 Atomic Absorption Spectroscopy
- 4.5 Chromatographic Methods of Analysis
  - 4.5.1 Thin Layer Chromatography
  - 4.5.2 Gas Chromatography – Mass Spectrometry
  - 4.5.3 Gas Chromatography
  - 4.5.4 High Performance Liquid Chromatography
  - 4.5.5 Electrophoresis

#### **5. Stability**

#### **6. Acknowledgement**

#### **7. References**



## 1. Description

### 1.1 Nomenclature

#### 1.1.1 Systematic Chemical Name [1]

*N,N'*-1,2-Ethanediyibis-[*N*-(carboxymethyl)glycine]

Ethylenedinitrilotetraacetic acid

Ethylenediamine tetraacetic acid

#### 1.1.2 Nonproprietary Names [1]

Edetic acid; Edetate sodium; Edetate disodium; Edetate trisodium;  
Edetate calcium disodium

#### 1.1.3 Proprietary Names [1]

Edathamil; EDTA; Havidote, Versene acid. Titriplex II

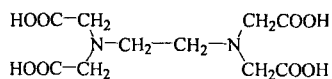
### 1.2 Formulae

#### 1.2.1 Empirical Formula, Molecular Weight, CAS Number [1-3]

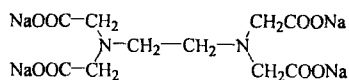
Edetic acid	$C_{10}H_{16}N_2O_8$	292.25	60-00-4
Edetate sodium	$C_{10}H_{12}N_2Na_4O_8$	380.17	64-02-8
Edetate disodium	$C_{10}H_{14}N_2Na_2O_8$	336.21	139-33-3
Edetate trisodium	$C_{10}H_{13}N_2Na_3O$	358.19	150-38-9
Edetate calcium disodium	$C_{10}H_{12}CaN_2Na_2O_8$	374.27	62-33-9

#### 1.2.2 Structural Formula

Edetic acid

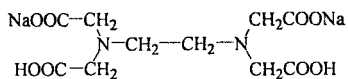


Edetate sodium

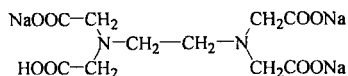


### 1.2.2 Structural Formula (continued)

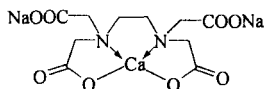
Edetate disodium



Edetate trisodium



Edetate calcium  
disodium



### 1.3 Elemental Analysis

The theoretical element composition of EDTA and its salts are as follows:

	C%	H%	O%	N%	Na%	Ca%
EDTA	41.1	5.52	43.8	9.59	—	—
Edetate sodium	34.59	3.18	33.67	7.37	24.19	—
Edetate disodium	35.72	4.2	38.07	8.33	13.68	—
Edetate trisodium	33.53	3.66	35.73	7.82	19.25	—
Edetate calcium disodium	32.09	3.23	34.2	7.48	12.29	10.71

### 1.4 Appearance [1]

Edetic acid is obtained as crystals from water; Edetate sodium is a powder; Edetate disodium is composed of dihydrate crystals; Edetate trisodium is obtained as monohydrate crystals from water; Edetate calcium disodium is a tetrahydrate powder. All materials are white in color, and odorless.

### 1.5 Uses and Applications

EDTA is considered as a pharmaceutical aid (metal complexing agent). The acid, rather than any salt, is the form most potent in removing metals from solutions. It may be added to drawn blood to prevent clotting, and is also used in pharmaceutical analysis and for the removal or inactivation of unwanted ions in solution [4]. EDTA was most effective in preventing the oxidation of thiol group in drugs, such as captopril [5]. The edetate calcium disodium salt is primarily used in the diagnosis and treatment of lead poisoning. It is administered in the form of infusion containing 1.0 g in 250 or 500 mL of water over a period of 1-2 hours for 3-5 days [4]. The edetate disodium salt is used to remove calcium from solutions, and thus it may be used as an anticoagulant [4].

EDTA is also used to sequester polyvalent cations which may cause the cross linking of some suspending agents, thus leading to increased viscosity of gelatin [6].

The  $\alpha$ -amino acids have been reported to form stable complexes with transition metals. The derivatives of acetic acid are particularly noteworthy for their chelating ability. The most remarkable for the acetic acid derivatives, however, is ethylenediamine tetraacetic acid (often abbreviated EDTA or  $H_4Y$ ). The complexes of EDTA are remarkably stable, and have been investigated extensively from the industrial point of view. The substance has been used in water softening, electroplating, controlling of metal content of dye paths, in removing lead and other heavy metals from the human systems, and in the treatment of chlorosis in plants [7].

EDTA is also used as a synergist to increase the activity of antioxidants, and to complex small amounts of heavy metal ions. EDTA has been frequently used to stabilize preparations of penicillins, ascorbic acid, epinephrine and prednisolone [4]. Over the past 35 years, EDTA has been used to induce hypocalcaemia in cows and other species, primarily for the induction of hypocalcaemia as a model for milk fever [8].

## 2. Methods of Preparation

Two methods have been reported for the synthesis of EDTA. The first method involves condensation of ethylenediamine with sodium monochloroacetate with the aid of sodium carbonate. An aqueous solution of the reactants is

heated to about 90°C for 10 hours, and is then cooled and acidified with HCl to precipitate the free acid [4]. This method is described in Scheme 1.

The second method makes use of the modified Streckter synthesis [9]. First, hydrogen cyanide is reacted with formaldehyde to produce cyanohydrine. The latter compound is condensed with ethylenediamine to produce ethylenediamine tetracyanomethylene. Hydrolysis of the this compound produces the free acid. These reactions are schematically represented by Scheme 2.

### 3. Physical Properties

#### 3.1 Ionization Constants

EDTA is a weak acid, for which four ionization constants ( $pK_1 = 2$ ;  $pK_2 = 2.67$ ;  $pK_3 = 6.16$ ;  $pK_4 = 10.26$ ) are known. These values indicate that the first two protons are lost much more readily than are the remaining two. In addition to the four acidic hydrogens, each nitrogen atom has an unshared pair of electrons, and thus the molecule has six potential sites for binding with metal ions. As such, it is ordinarily considered to be a hexadentate ligand. The abbreviations  $H_4Y$ ,  $H_3Y^-$ ,  $H_2Y^{2-}$ ,  $HY^{3-}$ , and  $Y^{4-}$  are often used for EDTA and its salts [10,11].

#### 3.2 Solubility Characteristics

The following solubility information has been reported [1-3]:

Edetic acid	very slightly soluble in water (0.5 g/L at 25°C)
Edetate sodium	very soluble in water (103 g/100 mL)
Edetate disodium	soluble in water
Edetate trisodium	more soluble in water than the corresponding acid or disodium salt
Edetate calcium disodium	soluble in water; a 0.1 M solution (~ 37 g/L) can be prepared at 30°C. Practically insoluble in organic solvents.



The solubility product constant ( $K_{sp}$ ) of EDTA was determined by adjusting the pH of an aqueous solution to a low value using nitric acid, and leaving the system to reach equilibrium overnight at room temperature. The precipitate was filtered off, dried at 105°C, and weighed to determine the amount of solubilized material. Alternatively, the precipitate was analyzed by complexometric titration, using standardized 0.05 M Zn(II) solution and xylenol orange as indicator [12]. The estimated value of the solubility product is  $10^{-24.66}$  ( $pK_{sp} = 24.66$ ).

The pH values of 1% aqueous solutions of EDTA and its salts are reported [1-3] to be as follows:

Edetic acid	1.35
Edetate sodium	11.3
Edetate disodium	5.3
Edetate trisodium	9.3
Edetate calcium disodium	~ 7

### 3.3 Crystallographic Properties

#### 3.3.1 X-Ray Powder Diffraction Pattern

The x-ray powder diffraction pattern of EDTA was obtained using on a Philips PW 1710 diffractometer with a single crystal monochromator and copper  $K\alpha$  radiation, and is shown in Figure 1. The values of the scattering angles (degrees  $2\theta$ ), d-spacings, and intensities were automatically obtained on a Philips digital printer, and are collected in Table 1.

#### 3.3.2 Polymorphism

There are two known forms of EDTA. The  $\alpha$ -form is precipitated upon addition of acid to one of its sodium salts at room temperature. Precipitation of the free acid at a temperature near the boiling point of water produces the high temperature  $\beta$ -form. The x-ray powder patterns of the  $\alpha$  and  $\beta$  forms have been reported, and were obtained using iron  $K\alpha$  radiation [13].

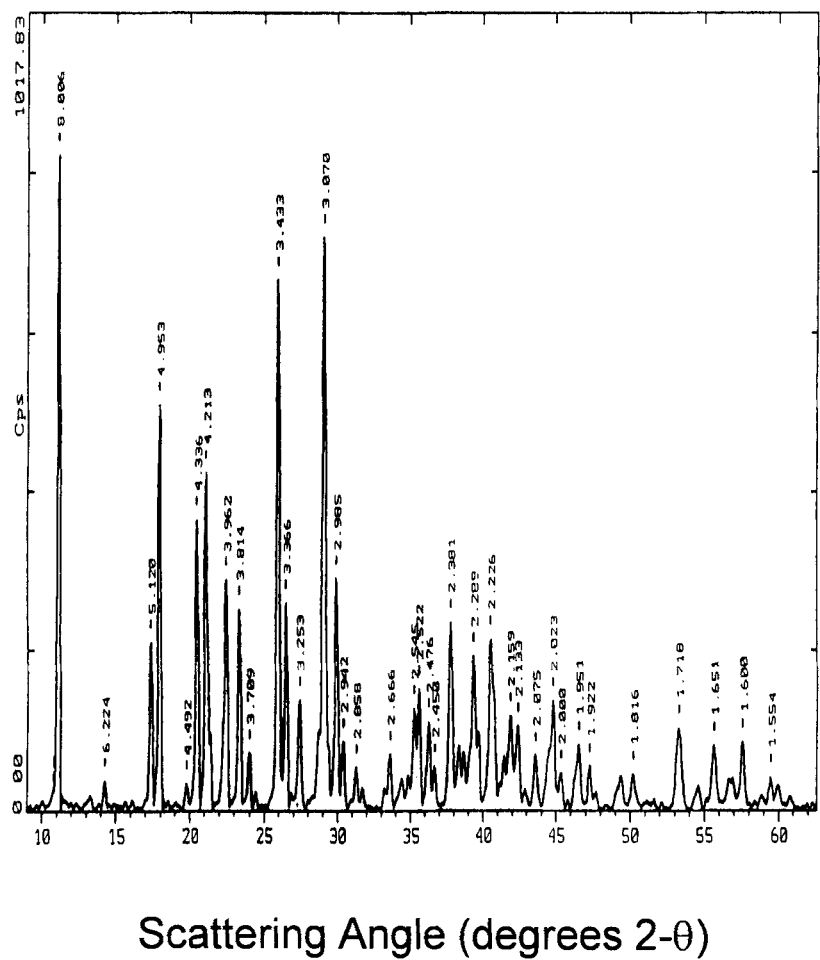


Figure 1. X-ray powder diffraction pattern of EDTA.

Table 1  
X-Ray Powder Diffraction Data of  
Ethylenediaminetetraacetic Acid

Scattering Angle (degrees 2- $\theta$ )	d-Spacing (Å)	Intensity (Cps)	Relative Intensity (I/I max $\times$ 100)
11.042	8.0063	834.67	100.00
29.062	3.070	729.86	87.44
25.934	3.4328	676.33	81.03
17.895	4.9525	516.58	61.89
21.070	4.2130	429.37	51.44
20.463	4.3365	369.62	44.28
29.906	2.9852	293.84	35.20
22.419	3.9624	291.66	34.94
26.460	3.3657	262.73	31.48
23.303	3.8141	254.47	30.49
37.747	2.3812	238.25	28.54
40.493	2.2258	217.00	26.00
17.306	5.1197	213.10	25.53
39.333	2.2888	195.17	23.38
35.562	2.5224	128.76	18.39
27.396	3.2528	139.86	16.76
35.231	2.5453	138.76	15.43
41.814	2.1586	118.78	14.23
36.248	2.4762	111.54	13.36
42.340	2.1329	106.60	12.77
30.357	2.9419	86.91	10.41
46.506	1.9511	87.40	9.87
23.975	3.7087	72.00	8.63
43.577	2.0752	68.79	8.24
36.650	2.4500	55.20	6.61
47.257	1.9218	54.54	6.53
50.198	1.8159	45.00	5.39
14.219	6.2237	36.02	4.31
19.745	4.4925	32.65	3.91



The refractive indices of the two forms were measured by microscopy [13], the values are (1.53-1.54) and (1.576-1.620) for the  $\alpha$  and  $\beta$  forms, respectively.

### 3.4 Thermal Methods of analysis

#### 3.4.1 Melting Behavior

EDTA and its salts all melt with decomposition, and the reported melting points are as follows [1-3]:

Edetic acid	220°C (dec.)
Edetate sodium	>300°C (dec.)
Edetate disodium	252°C (dec.)
Edetate trisodium	220°C (dec.)

#### 3.4.2 Differential Scanning Calorimetry

A DuPont TA-9900 thermal analyzer system, attached to a DuPont Data Unit, was used to obtain the DSC thermogram of EDTA over a range of 50 to 350°C. The thermogram shown in Figure 2 is fairly complicated, showing possible water loss at low temperature. The melting endotherm exhibited a maximum at 250.9°C, and the noise in the baseline following the endothermic transition is indicative of the thermal decomposition of the compound.

### 3.5 Spectroscopy

#### 3.5.1 UV/VIS Spectroscopy

Owing to its lack of chromophores, EDTA does not exhibit any absorption maxima in the ultraviolet or visible region.

#### 3.5.2 Vibrational Spectroscopy

The infrared absorption spectrum of EDTA shown in Figure 3 was obtained using the KBr pellet method on a Perkin-Elmer infrared spectrophotometer. The principal peaks observed were at 3480, 3380, 2998, 1603  $\text{cm}^{-1}$ .

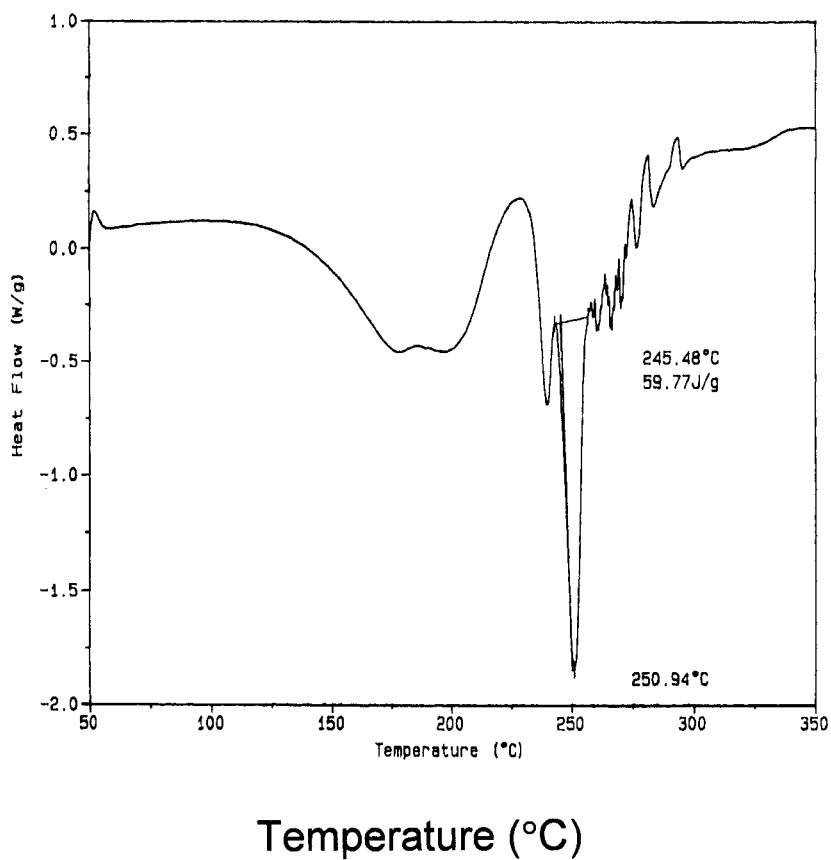


Figure 2. Differential scanning calorimetry thermogram of EDTA.

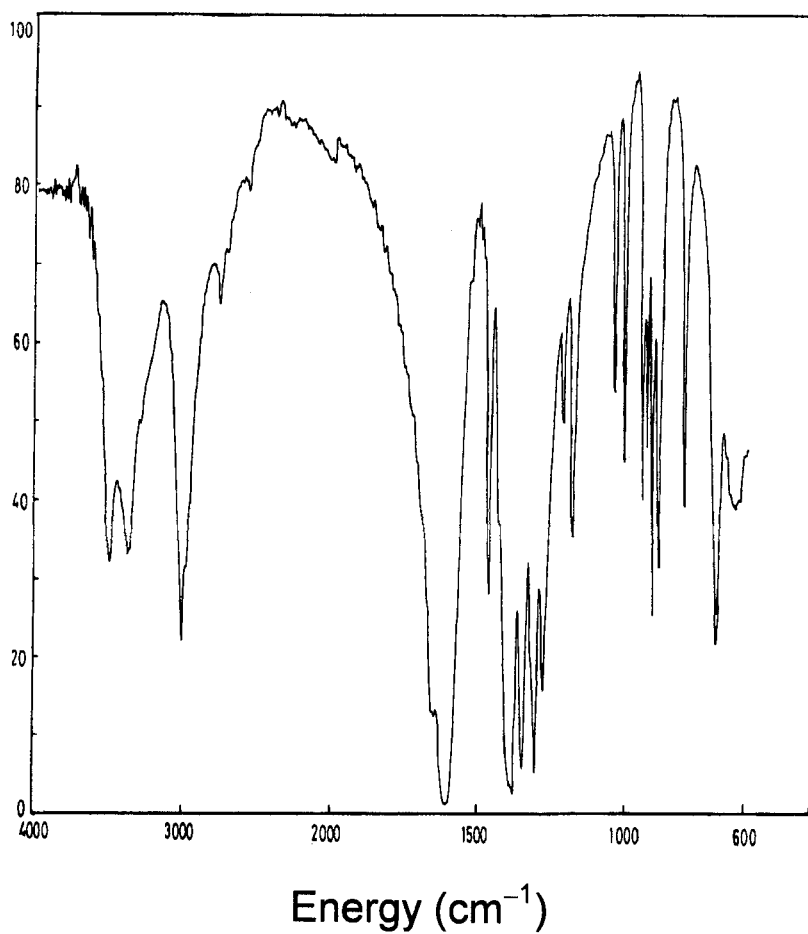


Figure 3. Infrared absorption spectrum of EDTA.

### 3.5.3 Nuclear Magnetic Resonance Spectrometry

#### 3.5.3.1 $^1\text{H}$ -NMR Spectrum

The proton NMR spectrum of EDTA was obtained using a Bruker system operating at 300, 400, or 500 MHz. Standard Bruker Software was used to execute recording of DEPT, COSY, and HETCOR spectra. The sample was dissolved in  $\text{D}_2\text{O}$  or in  $\text{CDCl}_3$ , and all resonance bands were referenced to the tetramethylsilane internal standard.

The  $^1\text{H}$ -NMR spectrum of EDTA in  $\text{D}_2\text{O}$  (shown in Figure 4) showed one singlet at 3.61 ppm that integrated for four protons, and was assigned to the protons of the two ethylenediamine  $\text{CH}_2$  groups. Also observed was a singlet at 3.84 ppm that integrated for eight protons, and was assigned to the protons of four acetic acid  $\text{CH}_2$  groups. Figures 5 through 7 show the expanded  $^1\text{H}$ -NMR spectra of EDTA.

#### 3.5.3.2 $^{13}\text{C}$ -NMR Spectrum

The carbon-13 NMR spectrum of EDTA was obtained using a Bruker system operating at 75, 100, or 125 MHz. The sample was dissolved in  $\text{D}_2\text{O}$ , and all resonance bands were referenced to the tetramethylsilane internal standard.

The noise modulated broad band decoupled  $^{13}\text{C}$ -NMR spectrum of EDTA in  $\text{D}_2\text{O}$  (Figure 8) showed two methylene carbon atoms resonating at 52.02 ppm and at 58.48 ppm. These were assigned to the methylene carbons of the ethylenediamine backbone, and the four acetic acid carbons, respectively. The four carbonyl carbon atoms were found to resonate at 171.22 ppm.

### 3.6 Mass Spectrometry

The mass spectrum of EDTA was obtained utilizing a Shimadzu PQ 5000 mass spectrometer. Figure 9 shows the detailed mass fragmentation, and Table 2 shows the proposed mass fragmentation pattern.

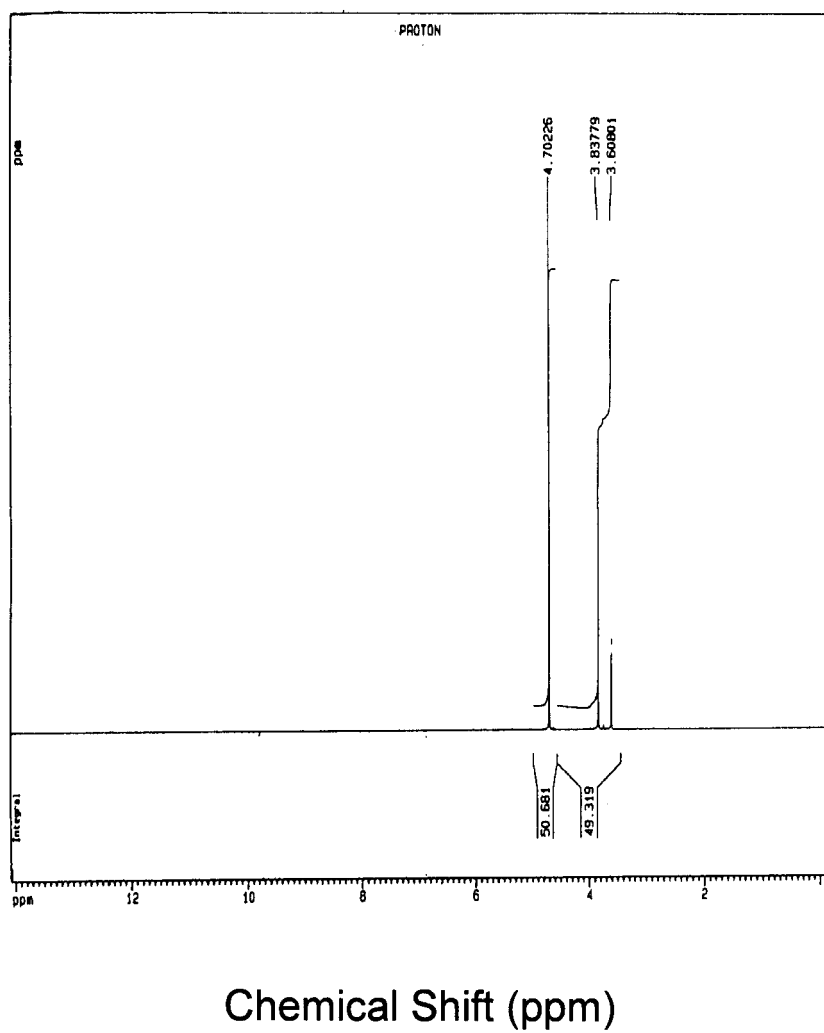


Figure 4.  $^1\text{H}$ -NMR spectrum of EDTA in  $\text{D}_2\text{O}$ .

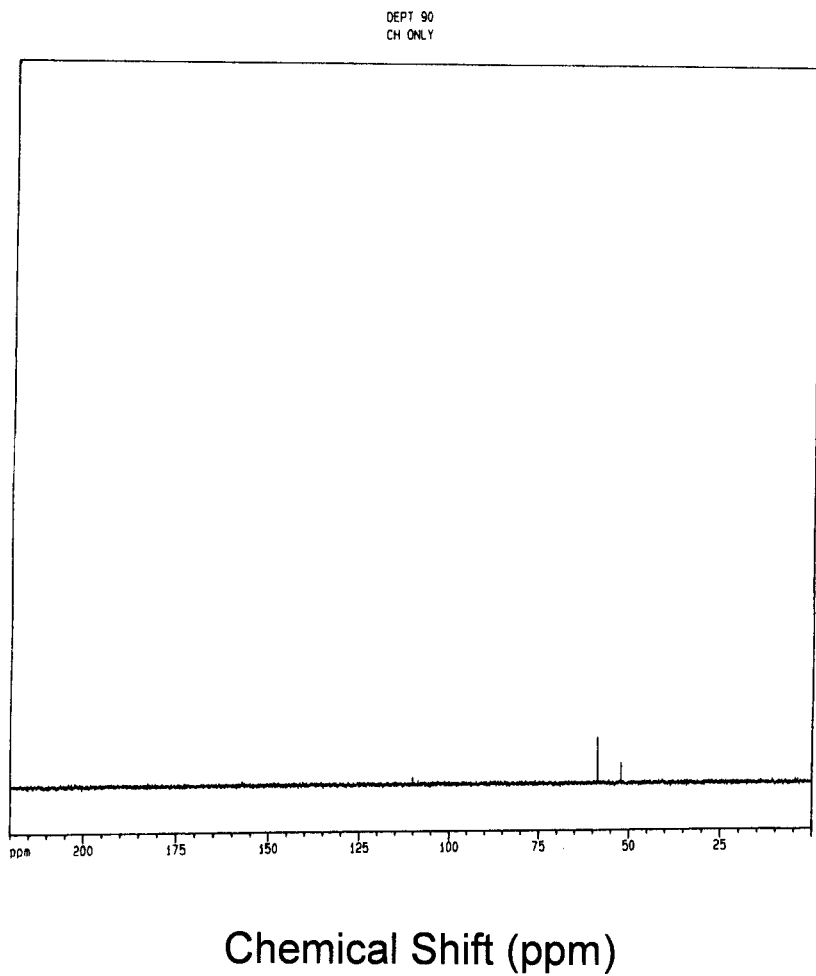


Figure 5. DEPT 90 <sup>1</sup>H-NMR spectrum of EDTA in D<sub>2</sub>O.

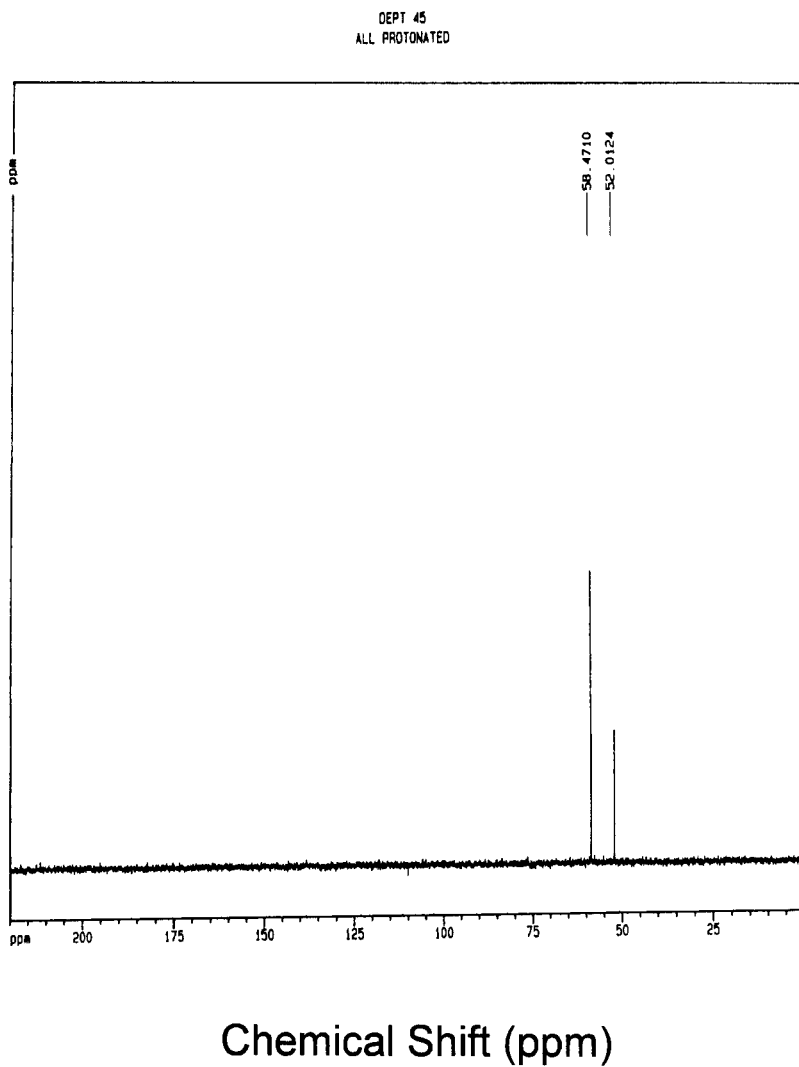


Figure 6. DEPT 45  $^1\text{H}$ -NMR spectrum of EDTA in  $\text{CDCl}_3$ .

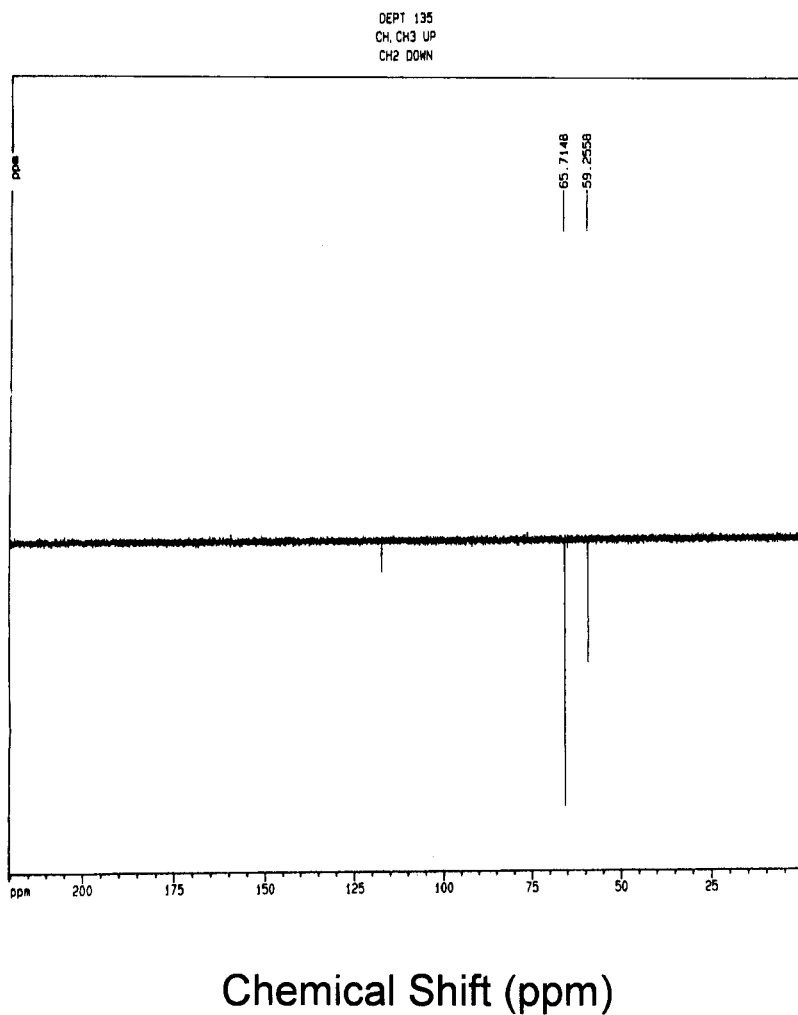


Figure 7. DEPT 135  $^1\text{H}$ -NMR spectrum of EDTA in  $\text{CDCl}_3$ .



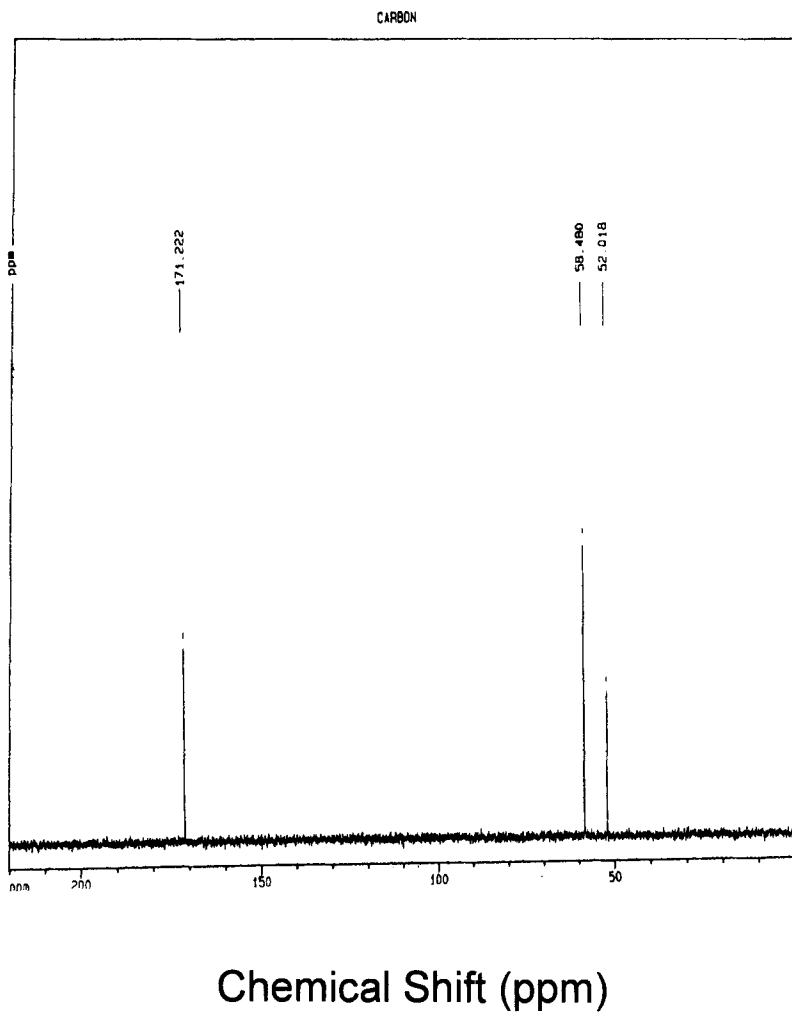


Figure 8.  $^{13}\text{C}$ -NMR spectrum of EDTA in  $\text{D}_2\text{O}$ .

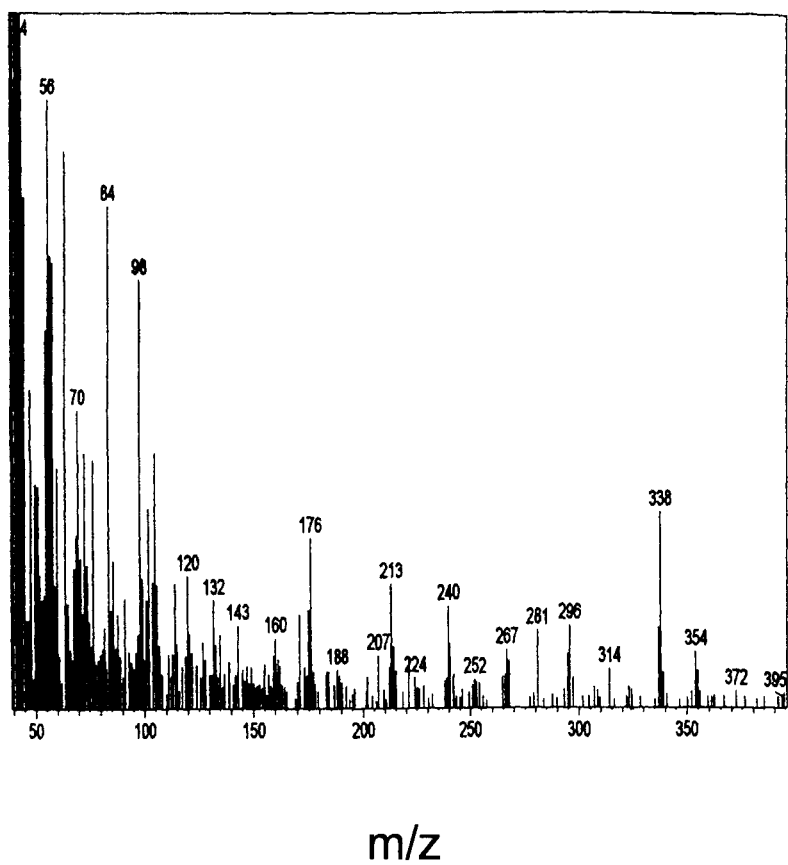
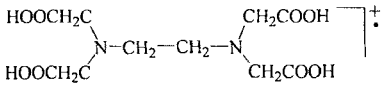
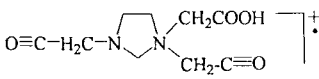
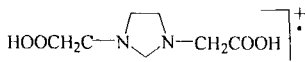
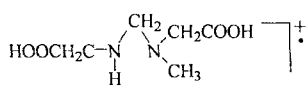
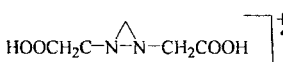
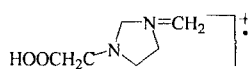
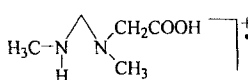
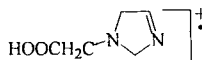
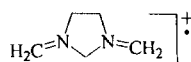
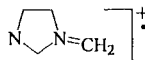
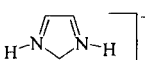
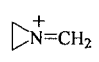
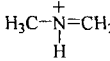


Figure 9. Mass spectrum of EDTA.

Table 2  
Mass Fragmentation Pattern of EDTA

M/z	Relative intensity	Fragment
292	3%	
213	18%	
188	6%	
176	25%	
160	10%	
143	12%	
132	16%	
128	10%	
98	64%	
84	74%	
70	44%	
56	90%	
44	100%	

#### **4. Methods of Analysis**

Many of the methods that are used for the analysis of EDTA have been comprehensively reviewed by Sillanpaa and Sihovonin [14].

##### **4.1 Identification**

###### **4.1.1 British Pharmacopoeia**

The BP [3] recommends the following four identification tests for edetate disodium:

Test 1. The infrared absorption spectrum is in concordant with the spectrum of the edetate disodium EP-CRS.

Test 2. Dissolve 2 g of the substance in 25 mL of water, add 6 mL of lead nitrate solution, shake, and add 3 mL of potassium iodide solution. No yellow precipitate is produced. Make the solution alkaline (red litmus paper indicator) with 2 M ammonia and add 3 mL of ammonium oxalate solution. No precipitate is produced.

Test 3. Dissolve 0.5 g of the substance in 10 mL of water, add 0.5 mL of a 10% w/v solution of calcium chloride, make alkaline (red litmus paper indicator) with 2 M ammonia and add 3 mL of ammonium oxalate solution. No precipitate is produced.

Test 4. Yields the reactions characteristic of sodium salts.

###### **4.1.2 United States Pharmacopoeia**

The USP [2] describes the following identification tests for edetic acid, edetate disodium and edetate calcium disodium.

###### **Edetic Acid**

Test: The infrared absorption spectrum compares with that of Reference Standard sample.

###### **Edetate Disodium**

Test 1. The infrared absorption spectrum compares with that of the Reference Standard sample.

Test 2. To 5 mL of water in a test tube add 2 drops of ammonium thiocyanate TS and 2 drops of ferric chloride TS. Upon mixing, the red color is discharged, leaving a yellowish solution.

Test 3. It responds to the flame test for sodium.

### **Edetate Calcium Disodium**

Test 1. The infrared absorption spectrum compares with that of Reference Standard sample.

Test 2. A 1 in 20 solution responds to the oxalate test for calcium, and to the flame test of sodium.

Test 3. To 5 mL of water add 2 drops of ammonium thiocyanate TS and 2 drops of ferric chloride TS. To the deep red solution add about 50 mg of edetate calcium disodium. Upon mixing the deep red color disappears.

## **4.2 Compendial Methods of Analysis**

Edetic acid (EDTA), edetate disodium, and edetate calcium disodium are the subjects of three monographs in the United States Pharmacopoeia (USP) [2]. Only disodium edetate is official in the British Pharmacopoeia (BP) [3].

### **4.2.1 Edetic Acid**

The USP [2] recommends a titrimetric method for the determination of EDTA using chelometric standard calcium carbonate previously dried at 110°C for 2 hours, and hydroxy naphthol blue as the indicator. The weight of EDTA (in mg) is calculated by the formula:

$$\frac{292.25}{100.09} \times 0.1 \text{ w/v}$$

where **w** is the weight (in mg) of calcium carbonate, and **v** is the volume (in mL) of EDTA solution used in the titration.

#### 4.2.2 Edetate Disodium

The USP [2] describes a method for the titration of EDTA, using a weighed amount of chelometric standard calcium carbonate previously dried. The weight of edetate disodium (in mg) is calculated using the following formula:

$$839.8 (w/v)$$

where **w** is the weight (in mg) of calcium carbonate, and **v** is the volume (in mL) of EDTA solution used in the titration.

The same procedure is used to determine the content injection solutions. Here, the weight is calculated using the formula:

$$335.9 (w/v)$$

The BP [3] described a similar titrimetric method for the determination of edetate disodium. Here, the titration is performed in hexamine / HCl buffer using 0.1 M lead nitrate as the titrant and xylenol orange as the indicator. Each milliliter of 0.1 M lead nitrate solution is equivalent to 37.22 mg of  $C_{10}H_{14}N_2Na_2O_8 \cdot 2H_2O$ .

#### 4.2.3 Edetate Calcium Disodium

For the pure substance and its injection solutions, the USP [2] recommends a titration procedure that uses 0.1 M mercuric nitrate as the titrant and diphenylcarbazone as the indicator. Each milliliter of 0.1 M mercuric nitrate is equivalent to 37.43 mg of  $C_{10}H_{12}CaN_2Na_2O_8$ .

### 4.3 Electrochemical Methods of Analysis

#### 4.3.1 Polarography

Belal *et al* [15] developed a polarographic method for the determination of EDTA in pharmaceutical dosage forms based on chelation with Eu(III) at pH 4, and followed by measuring the cathodic current. The current-concentration range was found to be linear over the ranges 8-160  $\mu\text{g/mL}$  and over 2-120  $\mu\text{g/mL}$  using direct current ( $DC_I$ ) and differential pulse (DPP) modes of detection, respectively, with minimum detectability of 0.1  $\mu\text{g/mL}$ .

An indirect polarographic method for the determination of EDTA in eyewash and ophthalmic solutions has been reported [16]. The method is based on the decrease of the polarographic wave of Cd(II) or Zn(II). A similar method involving the use of Bi(III) was also reported [17].

#### 4.3.2 Amperometry

EDTA was determined using an amperometric flow injection method conducted in 0.1 M H<sub>2</sub>SO<sub>4</sub>, and which used a glassy carbon electrode held at 1.25 V vs. a saturated calomel electrode. Calibration curves were found to be linear over the range of 0.01-10 µg/mL EDTA [18].

#### 4.3.3 Potentiometry

A potentiometric method for the determination of EDTA that involves the use of a urease-based inhibition biosensor was described [19].

#### 4.3.4 Voltammetry

EDTA was determined in waste water by Fayyad *et al*, who used potentiometric stripping analysis after adding Bi(III) and K<sub>2</sub>Cr<sub>2</sub>O<sub>7</sub> to the test solution. Uncomplexed Bi(III) was electrodeposited on a mercury film electrode (at -0.4 V vs. SCE) for 50 seconds. The working range was 4.5-95 ppb of EDTA [20].

Ciszkowska and Stojek reported the determination of traces of EDTA by absorptive accumulation of their Hg(II) complexes, and followed by cathodic stripping [21]. During the pre-electrolysis at a hanging mercury drop electrode, EDTA is absorbed on the electrode surface, and the complex with Hg(II) can be determined by a cathodic stripping procedure under linear scan voltammetric condition. Hg (II) forms a complex with the ligands during the electrodeposition stage or before deposition. The addition of Hg(II) to the test solution allows differentiation between the free and the bound form of the complexans in solution. In the former instance, only free complexans were deposited on the electrode, whereas, in the latter instance the added Hg(II) displaces other ions bound to the complexans permitting the total complexan concentration to be determined.

Voulgaropoulos *et al* used a differential pulse anodic-stripping voltammetric method for the indirect trace determination of EDTA and nitrilotriacetic acid in natural waters [22]. To the sample (50 mL, adjusted

to pH 2 with  $\text{HNO}_3$  when collected), ascorbic acid was added, and the pH was adjusted to pH 2 with  $\text{HNO}_3$ . A solution of Bi(III) was then added to yield a content of Bi(III) more than twice that of nitriloacetic acid or EDTA in the sample. From the deaerated and stirred solution, uncomplexed Bi(III) was deposited at a hanging-mercury-drop electrode by electrolysis at  $-0.15$  V vs. SCE for 2 minutes. Stirring was discontinued for 30 seconds, and the Bi(III) was stripped anodically in the differential pulse mode, whereupon the peak current of the uncomplexed Bi(III) was recorded. This procedure was repeated twice after adding a standard Bi(III) solution. The difference between the concentration of Bi(III) added and that determined corresponds to the concentration of nitriloacetic acid or EDTA in the sample.

Voulgaropoulos and Tzivanakis used ion exchangers for the voltammetric determination of nitrilotriacetic acid and EDTA in natural waters [23]. The interference caused by chloride ion, Fe(III), and Cu(II) in the determination of nitriloacetic acid and EDTA in natural waters was removed by pre-treating samples ( $\text{pH} > 4$ ) with cation exchangers. Some samples required additional treatment with an anion exchanger ( $\text{pH} 1$ ). The analytes were complexed with Bi (III) before being determined by differential pulse anodic stripping voltammetry at the hanging mercury drop electrode (vs. Ag/AgCl. The detection limit was  $0.1 \mu\text{g/L}$  for EDTA.

#### **4.4 Spectroscopic Methods of Analysis**

##### **4.4.1 Spectrophotometry**

These methods are based on the formation of a metal chelate complex, and then either directly or indirectly measuring its amount. Most of these methods do not differentiate between complexing agents, and are subject to interferences, and are not sufficiently sensitive for trace analysis. On the other hand, their rapidity and simplicity are unquestionable advantages.

Edetic acid was determined in urine and detergents through its reaction with Co(II) and phosphomolybdic acid at pH 0.5-2 [24]. The absorbance was measured at 750 nm, and Beer's law was valid over the range of 0.3 to  $1.9 \mu\text{g/mL}$ .



Parkash and Bansal reported the detection and determination of microgram quantities of ethylenediaminetetraacetic acid with molybdophosphoric acid by a spectrophotometric method [25]. For the detection of EDTA, 5 to 10 Amberlite IRA-400 resin beads (hydroxide form) were placed on a white spot-plate and blotted dry. One drop of sample solution was added, followed by one drop of 4% molybdophosphoric acid solution. A blue color develops if EDTA is present. For the determination, the sample solution (2 mL, containing 18.6 to 186  $\mu\text{g}$  of EDTA) and 4% molybdophosphoric acid solution (3 mL) are mixed for 5 minutes and diluted to 10 mL with water or sodium acetate-acetic acid buffer solution of pH 2. The absorbance is measured at room temperature at 690 nm against a reagent blank.

A kinetic-photometric method for the determination of EDTA, zinc, and bismuth by interchange reactions of azomethine groups, was reported by Rios and Valcarcel [26]. The method involves the *in situ* formation of the Ni(II) complex with 6-methylpicolinaldehyde thiosemicarbazone when Ni(II), 6-methylpicolinaldazine, and thiosemicarbazide are mixed at pH 4.5. The reaction was monitored spectrophotometrically at 396 nm. EDTA was determined indirectly by its interference effect, since the Ni(II) complex with EDTA is more stable than the Ni(II) complex of 6-methylpicolinaldehyde thiosemicarbazone. Since the addition of EDTA decreases both the initial reaction rate and the final absorbance, it can be determined kinetically within the range 5 to 25  $\mu\text{M}$  or photometrically in the range of 5 to 35  $\mu\text{M}$ .

EDTA could also be determined through its reaction with Ti(IV),  $\text{H}_2\text{O}_2$  and mixed surfactants (composed of Triton N-101 and Amphitol 24B) in phosphate/citrate buffer of pH 5.5 by heating at 60°C for 25 minutes and measuring the color produced at 615 nm [27]. The calibration graph was found to be linear from 1-6  $\mu\text{M}$  EDTA, with a relative standard deviation of 1.8% [27].

EDTA has been assayed in foods through its reaction with Fe(III) [28]. Excess Fe(III) is removed by chloroform and N-benzoyl-N-phenylhydroxylamine. The calibration graph was linear over the range of 0.5 - 40  $\mu\text{g/mL}$  [28]. A similar method for EDTA in food involving reaction with Cu(II) in Tris-HCl buffer at pH 8.5 has been reported [29]. The excess Cu(II) was determined at 477 nm using 2,9-dimethyl-4,7-diphenyl-1,9-phenanthroline. This calibration curve was found to be linear over the range of 4-12  $\mu\text{M}$  EDTA.

EDTA was determined in the urine of patients treated with  $\text{Na}_2\text{CaEDTA}$  upon formation of its Fe(II) complex with 2,4,6-tripyridyl-*s*-triazine at pH 4.5 [30]. Concentrations ranging from 0.1-15.7  $\mu\text{M}$  of EDTA in urine could be accurately determined. EDTA can be standardized by spectrophotometric titration with electrolytically pure Cu(II) at pH 5 without an indicator [31]. The break of the titration curve obtained at 700 nm is used as the end-point of the titration.

A colorimetric method based on the inhibitory effect of EDTA on the Mn(II) catalyzed oxidation of malachite green by periodate was reported [32]. An alternative method based on using Fe(III) instead of Mn(II) was proposed [33]. The reduction of the absorbance of Bi(III) bromo-pyrogallol red tenside ternary complex upon the addition of EDTA has been exploited for its determination. Calibration curves obtained at 650 nm were linear over the range of 0.2-6  $\mu\text{g/mL}$  of EDTA [34]. EDTA in ophthalmic solutions could be assayed by spectrophotometric titration using Mg(II) as the titrant and Arsenazo I as the indicator. The working range was 0.05-2  $\mu\text{g/mL}$  [35].

An indirect spectrophotometric method using flow injection analysis, and based on the redox reaction of Cu(II) with Fe(II), was described by Itabashi *et al* for the determination of EDTA and other complexing agents [36]. This method depends on acceleration by the complexing agents (EDTA-type complexans, citrate, or pyrophosphate) of the reaction of Cu(II) with Fe(II) in the presence of neocuproine (2,9-dimethyl-1,10-phenanthroline). The test solution was injected into a carrier stream of water, which was then merged with a pre-mixed stream of (a) 0.1 mM-Cu(II), 0.5 mM 2,9-dimethyl-1,10-phenanthroline, 50mM pH 5.6 acetate buffer, and (b) 0.1 mM Fe(II). After passing the solution through a 1-m reaction coil at room temperature, its absorbance was monitored at 454 nm. Selective determination of EDTA was then performed at pH 3 with the use of a 10-cm reaction coil.

#### 4.4.2 Fluorimetry

The ternary complex formed by the reaction of lanthanide ions (La(III) and Y(III)) with 7-(1-naphthylamineazo)-8-hydroxyquinoline-5-sulfonic acid has been exploited for the fluorimetric determination of EDTA over the range of 2-20  $\mu\text{M}$ . The fluorescence is measured at 525/350 nm [37]. A similar method based on the reaction of Ca(II) with Fluo-3 and EDTA

in the presence of *N*-cyclohexyl-3-aminopropane sulfonic acid (at pH 10) was described for the fluorimetric determination of EDTA. The fluorescence is measured at 485/535 nm, and the detection limit is 0.21  $\mu\text{M}$  EDTA [38].

Another flow injection method coupled with catalytic fluorimetric detection was described for EDTA [39]. The method is based on the catalytic inhibition effect of EDTA on the catalytic action of Cu(II) on the oxidation of di-2-pyridyl ketone hydrazone by  $\text{H}_2\text{O}_2$ . Concentrations of 0.4-2  $\mu\text{g/mL}$  of EDTA could be determined.

#### **4.4.3 Atomic Absorption Spectroscopy**

Belal *et al* [40] reported on the use of flame atomic absorption spectroscopy (FAAS), coupled with ion-exchange, to determine EDTA in dosage forms. EDTA is complexed with either Ca(II) or Mg(II) at pH 10, and the excess cations retained on an ion-exchange resin. At the same time, the Ca(II) or Mg(III) EDTA complexes are eluted and determined by AAS. Calibration curves were found to be linear over the range of 4-160 and 2-32  $\mu\text{g/mL}$  EDTA when using Ca(II) or Mg(II), respectively. The method could be applied to eye drops and ampoules containing pharmaceuticals. Another combined AAS flow injection system was proposed for the determination of EDTA based on its reaction with Cu(II). The calibration curve was linear over the range of 5-50  $\mu\text{g/mL}$ , with a limit of detection of 0.1  $\mu\text{g/mL}$  [41].

An indirect AAS method was described for EDTA in the antibiotic streptomycin [42]. The method involved formation of the Ni(II) complex with EDTA, release of complexed Ni(II) by pH adjustment, and subsequent determination of Ni(II) by AAS. EDTA was also determined through its masking effect on the extraction of copper oxinate into methylisobutyl ketone at pH 6.5. The decrease in AAS signal of Cu(II) was linearly proportional to the EDTA concentration [43].

### **4.5 Chromatographic Methods of Analysis**

#### **4.5.1 Thin Layer Chromatography**

Fitzgerald [44] developed a TLC method for EDTA using cellulose 300 DEAE anion-exchange thin layer sheets, and formic acid of different concentrations as the mobile phases. The visualization was effected using

0.01%  $\text{NiSO}_4$  solution, exposing the spots to ammonia vapor, and then spraying with 0.1% dimethylglyoxime to obtain white spots on a pink background. The following retention times were noted:

Mobile Phase	$R_f$
0.3 M formic acid	0.00
1.5 M formic acid	0.45
Formic acid + 0.3 M HCl	0.54

Another TLC method was reported that involved the use of silica gel as the stationary phase and iodine vapor for visualization [45]. Several mobile phases were attempted and the  $R_f$  values are tabulated as follows:

Mobile Phase	$R_f$
Propanol- $\text{NH}_3$ -HOAc (70:30:2)	0.16
Propanol- $\text{NH}_3$ (70:30)	0.15
Ethanol- $\text{NH}_3$ -HOAc (70:30:2)	0.30
Ethanol- $\text{NH}_3$ (70:30)	0.33
Methanol-ethanol- $\text{NH}_3$ -HOAc (30:30:40:2)	0.56
Ethanol-HOAc- $\text{H}_2\text{O}$ (70:20:20)	0.15

The TLC method reported by Fitzgerald [44] was further improved by using  $\text{Cu(II)}$  sarcosine cresol red for the detection of the spots. This reagent is 1 or 2 orders of magnitude more sensitive than  $\text{Ni(II)}$  dimethylglyoxime [46]. The following retention time values were reported:

Mobile Phase	$R_f$
0.3 M formic acid	0.2
1.5 M formic acid	0.6

#### 4.5.2 Gas Chromatography – Mass Spectrometry

Nguyen *et al* reported on the development of a high-resolution capillary gas chromatography-mass spectrometric (GC-MS) method for EDTA and other low molecular weight organic compounds in municipal waste water [47]. A multistage extraction procedure was used to isolate a wide range of compounds from the municipal waste waters. Volatile organic compounds were extracted using a purge and trap concentrator connected directly to a wide pore capillary column (70 m  $\times$  0.53 mm i.d.) of DB-624, with temperature programming from 30-200°C (held for 5 minutes) at 5°C/min. Volatile and semi-volatile basic/neutral compounds and acids were extracted with CH<sub>2</sub>Cl<sub>2</sub> at pH 11 and pH 2, respectively. Acidic compounds were subsequently derivatized with diazomethane. Both fractions were separated on a column (30 m  $\times$  0.25 mm i.d.) of DB-5 ms with temperature programming from 50-310°C (held for 5 min) at 5°C/min. Specific ionic substances such as EDTA and linear alkylbenzenesulphonates and nitrilotriacetic acid were isolated by solid phase extraction followed by derivatization.

Nishikawa and Okumura reported on the determination of EDTA and nitrilotriacetic acid (as their methyl ester derivatives) in environmental samples by GC-MS [48]. The sediment for homogenized fish tissues plus EDTA as a surrogate standard in H<sub>2</sub>O at pH 9-12 was extracted ultrasonically for 10 minutes, centrifuged at 1600 g for 10 minutes, and the supernatant adjusted to pH 2.5 with 4 M formic acid. The sediment was re-centrifuged at 1600 g for 10 minutes, the aqueous phase (the fish extract or water plus EDTA adjusted to pH 2.5) was rotary evaporated to dryness, and the residue methylated with BF<sub>3</sub>/methanol. The esters were extracted with CH<sub>2</sub>Cl<sub>2</sub>, the extract concentrated, and a portion was analyzed by GC-MS. The method used a column (25 m  $\times$  0.32 mm id) coated with 5% phenylmethylsilicone (0.52  $\mu$ m), operated with temperature programming from 70°C (held for 4 min) to 300°C (held for 10 min) at 15°C/min with helium (7.5 psi) as the carrier gas. The detection limit was 6.2 ng/mL for EDTA.

The conditions used in other GC-MS methods [49,50] are shown in Table 3.

### 4.5.3 Gas Chromatography

Gas chromatography requires volatility of the compound to be determined, so EDTA is most commonly converted into its methyl, ethyl, propyl, or butyl ester. Methyl esterification is most commonly used method of derivitization. Silylation has also reported, but salts (as in case of sea water) can interfere.

A gas chromatographic (GC) method was used by Wanke and Eberle for the determination of EDTA in surface water [51]. The sample was filtered, stabilized by the addition of 37% formaldehyde, adjusted to pH 2.5 with concentrated formic acid, and passed at 2 to 3 mL/min through a column (10 cm  $\times$  0.7 mm) of BIORAD AG 1-X2 (50-100 mesh) preconditioned with H<sub>2</sub>O. Elution was effected with 16 M formic acid, and the eluent was evaporated to dryness under nitrogen. The EDTA was taken up in hexane, and the resulting solution was analyzed by GC on a capillary column (20 m long) coated with DB-5 (0.25  $\mu$ m). The column was operated with temperature programming from 160 to 280° (held for 11 min) at 8°C/min. Nitrogen was used as the carrier gas, and nitrogen selective detection was used for quantification.

Sillanpaa *et al* described a gas chromatographic method for the determination of low levels of EDTA in natural water [52]. 10 mL of water was adjusted to pH 2 with formic acid, and the solution evaporated to dryness at 110°C. The residue was esterified with 1.5 mL of a solution containing 2.5 mL of concentrated H<sub>2</sub>SO<sub>4</sub>, 25  $\mu$ L acetic acid, and 2.5 mL of 10 mg/L heptadecanoic acid nitrile (internal standard) in 50 mL ethanol at 100°C for four hours. The sample was extracted into 1.5 mL of toluene and neutralized with 20 mL of 1 M potassium carbonate. The organic phase was dried, and a 10 mL portion was analyzed by GC on a column (30 m  $\times$  0.25 mm i.d.) coated with HP-5 (0.25  $\mu$ m). The system was operated with temperature programming from 100°C (held for 1 min) to 200°C (held for 5 min) at 60°C/min, then to 250°C (held for 8 min) at 50°C/min, with nitrogen as carrier gas (3.5 mL/min) and N-P detection. The detection limit for EDTA was 3  $\mu$ g/L.

The conditions used in other gas chromatographic methods are shown in Table 3 [53-56].

Table 3

## Gas Chromatography Methods for EDTA in Different Matrices

Material	Ester	Method	Carrier gas	Detector	Detection limit	Ref.
Blood	Methyl, propyl butyl	GC	Nitrogen	MS	10 ng/mL	[49]
River water	Propyl	GC	Nitrogen	MS	1 µg/mL	[50]
Natural water	Ethyl	GLC	Nitrogen	FID	15 µg/mL	[53]
Waste water	Methyl	GLC	Helium	FID	10 µg/mL	[54]
Pickled vegetables	Methyl	GLC	Nitrogen	FID	—	[55]
Tinned bean	Methyl	GC	Nitrogen	FID	5 mg/kg	[56]

#### 4.5.4 High Performance Liquid Chromatography

EDTA has been determined in a wide variety of sample matrices by HPLC. These matrices include waste waters, natural waters, sediments, fertilizers, chemical cleaning solutions, radioactive waste solutions, and pharmaceutical preparations. Chinnick reported the separation and identification of EDTA and other aminopolycarboxylic acid sequestrants by a high performance liquid chromatographic (HPLC) method [57].

A reversed-phase HPLC method was used by Yamaguchi *et al* for the determination of EDTA and other aminopolycarboxylic acids as their Fe(III) complexes [58]. The conditions used in other HPLC methods [58-83] are listed in Table 4.

#### 4.5.5 Electrophoresis

Ballou *et al* reported the determination of EDTA and other chelating agents in Hanford tank waste stimulant using a capillary zone electrophoresis method [84]. Simulated waste water (25 mL) was treated with representative amounts of solid ethylenediaminediacetic acid, hydroxyethylidiaminetriacetic acid, EDTA, nitrilotriacetic acid, and diethylenetriaminepentaacetic acid, stirred until solution was complete, and then diluted to 100 mL. A 1 mL portion of this solution was mixed with an excess of  $\text{CuCl}_2$ , diluted to 10 mL with 5 mM pH 11.5 phosphate buffer, and filtered. This solution was diluted further (1:40 dilution) with the buffer to give a range of dilutions ranging up to 1:2562 for the calibration series. Portions of these solutions were injected by pressure for one second into the capillary (80 cm  $\times$  52  $\mu\text{m}$  i.d.), fitted with a 3  $\times$  bubble cell for increased path length. Electrophoresis was carried out at 600 V/cm and 25°C in 10 mM pH 11.5 phosphate buffer. Detection of the Cu(II) complexes was effected at their absorbing wavelength of 254 nm. EDTA and the other four complexes were separated in 9 minutes.

EDTA was determined in human plasma and urine by capillary electrophoresis/MS [85]. Using a BC stable labile isotope, the detection and quantitation limits were found to be 7.3 and 14.6 ng/mL, respectively. The running buffer was pH 3.5 ammonium formate/formic acid buffer, at an inlet pressure 50 mb and a separation potential of -30 KV. The same authors [86] utilized this technique for the determination of EDTA as the nickel chelate in environmental water.



Table 4  
HPLC Methods for EDTA in Different Matrices

Column	Mobile phase and flow rate	Detection	Remarks	Ref.
25 cm $\times$ 4.6 mm of Zobrax-ODS	20 mM phosphate buffer (pH 2.5) containing 0.175-mM tetrabutyl-ammonium bromide and 5% of acetonitrile.	255 nm	Analysis of EDTA in its iron (III) complex.	[58]
Co: Pell ODS	16.2 mM-tetrabutyl-ammonium bromide in 50 mM-acetate buffer (pH 4.5), containing 4% of methanol.	254 nm	Analysis in boiled water without interference with metal ions.	[59]
3 $\mu$ m C <sub>18</sub> column	1.5 mM phthalate, Tris buffer solution and 7% acetonitrile	Indirect UV	Fixed-site ion exchangers of a LC determination of EDTA	[60]
LiChrosorb RP-8 (7 $\mu$ m)	50 mM-KH <sub>2</sub> PO <sub>4</sub> with 4 mM-tetrabutyl-ammonium hydroxide at pH 6.5 (1 mL/min)	260 nm	Quantitative determination of EDTA and its behavior in radioactive waste solutions.	[61]
25 cm $\times$ 4.6 or 4.1 mm of Biophase ODS (5 $\mu$ m) or: Hamilton PRP-1 (10 $\mu$ m)	Aqueous trichloroacetic acid pH $\leq$ 2 (1 mL/min)	Amperometric at 1.1 to 1.3 V	Reversed phase HPLC	[62]

Table 5 (continued)  
HPLC Methods for EDTA in Different Matrices.

Column	Mobile phase and flow rate	Detection	Remarks	Ref.
20 cm × 4.6 mm of Zorbax BP C8 (7 μm)	4-mL of methanol + 96 mL of 0.05 M sodium acetate – 16.2 mM tetrabutyl-ammonium bromide (1.5 mL/min)	254 nm	Low level analysis of EDTA in complex matrices	[63]
25 cm × 4.6 mm of Ultrasphere ODS (5 μm)	100% 0.1 M acetate buffer (pH 4.5)-methanolic 25% tetrabutyl-ammonium hydroxide (1000:17) (1.5 mL/min).	260 nm	Analysis of EDTA in vancomycin vials with absorbance ratioing for peak identification	[64]
25 cm × 4 mm in series of Dionex CarboPac Pa 1	20 mM nitric acid (0.8 mL/min)	290 nm	Analysis of EDTA in water and waste water.	[65]
10 cm × 4.6 mm of Shandon Hypercarb (10 μm)	2% ethanediol and 0.1 mM-ferric sulfate in a buffer of 0.1 H <sub>2</sub> SO <sub>4</sub> at pH 1.5 (1 mL/min)	270 nm	Analysis of EDTA as metal complexes on a porous graphitic carbon column	[66]
25 cm × 4.6 mm of Nucleosil 5-C <sub>18</sub> (5 μm)	0.03 M Acetate/ acetic acid buffer of pH 4. (1.5 mL/min).	254 nm	Analysis of EDTA in water	[67]

Table 5 (continued)  
HPLC Methods for EDTA in Different Matrices.

Column	Mobile phase and flow rate	Detection	Remarks	Ref.
25 cm $\times$ 4.1 mm of Anion/R anion-exchange column (10 $\mu$ m)	2 mM Cu(II) nitrate, 11 mM-nitric acid of pH 3 containing 25% acetonitrile (1 mL/min)	250 nm	Analysis of EDTA in a cataract inhibiting ophthalmic drug	[68]
10 cm $\times$ 4.6 mm of Hypersil ODS (5 $\mu$ m)	Aqueous 50% methanol containing 10 mM-cetrimide buffer pH 4.5 and 50 mM $\text{KH}_2\text{PO}_4$ buffer pH 4.5 (0.8 mL/min).	260 nm	Analysis of EDTA in pulp and paper mill process and waste waters.	[69]
15 cm $\times$ 3.9 mm of Delta-pak $\text{C}_{18}$ (5 $\mu$ m)	0.6 mM- $\text{KH}_2\text{PO}_4$ of pH 7.3 in 6 mM $\text{K}_2\text{SO}_4$ (1 mL/min).	500 nm (excit. at 360 nm)	Analysis of metal EDTA complex with post column detection using fluorescent ternary complexes.	[70]
25 cm $\times$ 4 mm of LiChrocart RP 18 with a Lichrocart 4-4 pre-column	1 mM tetrabutyl-ammonium bromide in formate buffer containing 8% acetonitrile (1 mL/min).	258 nm	Analysis of dissolved and absorbed EDTA species in water and sediments	[71]

Table 5 (continued)  
HPLC Methods for EDTA in Different Matrices.

Column	Mobile phase and flow rate	Detection	Remarks	Ref.
15 cm × 4.6 mm of Adsorbosphere HS C <sub>18</sub> (3 μm)	50 mM-Tetrabutylammonium hydrogen sulfate (1 mL/min)	254 nm	Analysis of EDTA in ophthalmic cleanser.	[72]
15 cm × 4.6 mm of Phenomenex Prodigy 5 ODS-2 (5 μm)	3 mM-Tetrapropylammonium bromide in 1 mM-K <sub>2</sub> SO <sub>4</sub> for 4 min then gradient to 3 mM K <sub>2</sub> SO <sub>4</sub> in 4% acetonitrile (1 mL/min).	500 nm (excitation at 360 nm)	Analysis of chelating ligands based on the post-column formation of ternary fluorescent complexes.	[73]
(25 cm × 4 mm id) of C <sub>18</sub> Bischoff column (5 μm)	0.2 M acetate buffer of pH 4 containing tetrabutylammonium hydroxide (1.2 mL/min)	254 nm	Analysis of sewage treatment plant effluents	[74]
PRP X-100 ion chromatographic column	3 mM H <sub>2</sub> SO <sub>4</sub> /methanol (19:1). (2 mL/min)	243 nm	Analysis of blood stains	[75]
(15 cm × 4.6 mm) of LiChrosorb 5-RP-18	0.03 M sodium acetate of pH 4 containing 20 mM tetrabutylammonium hydroxide in methanol (1 mL/min)	300 nm	Analysis of canned mushrooms	[76]

Table 5 (continued)  
HPLC Methods for EDTA in Different Matrices

Column	Mobile phase and flow rate	Detection	Remarks	Ref.
(25 cm × 4.6 mm) of Partisil-10 SAX	3% NaCl containing 3 mL/L acetic acid pH (3.1). (1 mL/min)	258 nm	Analysis of waters	[77]
(25 cm × 4 mm) (5 µm) of Lichrospher 100 column	pH 3.3 Acetate buffer/methanol (49:1) (1 mL/min)	258 nm	Analysis of natural waters	[78]
(125 cm × 4 mm i.d.) of Hypersil ODS, 5 µm.	H <sub>2</sub> O methanol (4:1) containing 0.0 M tetrabutylammonium bromide and 0.03 M acetate buffer pH 4 (0.8 mL/min)	254 nm	Analysis of canned food	[79]
(15 cm × 4.6 mm) of DuPont Zorbex C <sub>8</sub> .	10% Methanol/ 90% water, 0.01 M tetrabutylammonium hydroxide pH 7.5 (2 mL/min)	254 nm	Analysis of Pharmaceuticals and food	[80]
(15 cm × 4.5 mm) of Resolve C <sub>18</sub> , 5 µm.	0.006 M aqueous tetrabutylammonium phosphate of pH 6.5/acetonitrile (80:20) (1.5 mL/min)	254 nm	Analysis of ophthalmic and contact lens care solutions	[81]

Table 5 (continued)

HPLC Methods for EDTA in Different Matrices

Column	Mobile phase and flow rate	Detection	Remarks	Ref.
(30 cm × 4 mm) of $\mu$ Bondapak C <sub>18</sub> column.	0.01 M tetrabutyl-ammonium hydroxide of pH 7.5 adjusted with H <sub>3</sub> PO <sub>4</sub> /methanol (100:8).	254 nm	Analysis of ophthalmic preparations, blood serum and human feces	[82]
(300 × 4 mm) of $\mu$ Bondapak C <sub>18</sub> .	18% methanol: 82%, 0.0175 M tetrabutyl-ammonium hydroxide in 0.05 M acetate buffer pH 4.5 (1.2 mL/min)	280 nm	Analysis of carbmeat and mayonnaise	[83]
	5% methanol: 95% 0.02 M tetrabutyl-ammonium hydroxide in 0.04 M acetate buffer pH 4.7. (1.6 mL/min)	254 nm		

A radiochemical displacement method was reported for EDTA [87]. The method depends on shaking pH 5.5 borate buffer containing EDTA with  $^{65}\text{Zn}$ -labeled Zn-1-(2-pyridylazo)-2-naphthol complex in  $\text{CHCl}_3$ . The displaced  $^{65}\text{Zn}$  in the aqueous layer is measured. The working range of the method was 50-150  $\mu\text{g}$  of EDTA.

A capillary electrophoresis method was described for EDTA in spent fixing solutions [88]. After complexation with Ni(II), separation is effected using a fused silica capillary (57 cm  $\times$  75  $\mu\text{m}$  i.d) filled with borate buffer containing 0.1 mM pH 8.5 tetradecyltrimethylammonium hydroxide. The applied voltage was -30 kV, and detection was effected at 214 nm.

Another CE method was reported for EDTA in nutrient media, with the analyte being detected as its metal complex with Ca(II), Co(II), Ni(II), Cu(II), Zn(II), Cd(II), Pb(II), or Fe(III). The calibration curves were linear over the range 10-1000  $\mu\text{M}$  [89].

## **5. Stability**

The free acid (EDTA) is less stable than its salts, and tends to undergo a decarboxylation reaction when heated to temperature of 150°C. The substance is stable on storage and on boiling in aqueous solutions [1].

## **6. Acknowledgement**

The authors wish to thank Mr. Tanvir A. Butt, Department of Pharmaceutical Chemistry, College of Pharmacy, King Saud University, Riyadh, Saudi Arabia for the typing of the profile manuscript.

## 7. **References**

1. ***The Merck Index***, 12<sup>th</sup> edn., S. Budavari, ed., Merck and Co., NJ (1996) p. 3559.
2. ***The United States Pharmacopoeia XXIII***, United States Pharmacopoeial Convention, Rockville, MD (1995) p. 570.
3. ***The British Pharmacopoeia***, Her Majesty's Stationary Office, London (1993) p. 234.
4. A.R. Gennaro, in ***Remington, The Science and Practice of Pharmacy***, 19<sup>th</sup> edn., Mack Publishing Co., Easton, Pennsylvania (1995) p. 935.
5. K.E. Avis, H.A. Lieberman, and L. Lachman, ***Pharmaceutical Dosage Forms***, volume 1, Marcel Dekker, Inc., New York (1992) p. 307.
6. H.A. Lieberman, M.M. Rieger, and G.S. Banker, ***Pharmaceutical Dosage Forms***, volume 2, Marcel Dekker, Inc., New York (1989) p. 217.
7. J.C. Bailar, Jr. and D.H. Busch, eds., ***The Chemistry of Coordination Compounds***, Reinhold Publishing Co., NY (1956) p. 39.
8. R.J. Jorgensen, N.R. Nyengaard, R.C.W. Daniel, L.S.B. Mellan, and J.M.D. Ehemark, *J. Vet. Med.*, **A46**, 389 (1999).
9. R. Smith, J.L. Bullock, F.C. Bersworth, and A.E. Martell, *J. Org. Chem.* **14**, 355 (1949).
10. D.A. Skoog and D.M. West, ***Fundamentals of Analytical Chemistry*** 3<sup>rd</sup> edn., Reinhart and Winston, NY (1983) p. 272.
11. K.A. Connors, ***A Textbook of Pharmaceutical Analysis***, 3<sup>rd</sup> edn., John Wiley and Sons, NY (1982).
12. J. Karhu, L. Harju, and A. Ivaska, *Anal. Chim. Acta*, **380**, 105 (1999).
13. R.B. LeBlanc and H.L. Spell, *J. Phys. Chem.*, **64**, 949 (1960).



14. M. Sillanpaa and M.L. Sihovonen, *Talanta*, **44**, 1487 (1997).
15. F. Belal, F.A. Aly, M.I. Walash, and A.O. Mesbah, *J. Pharm. Biomed. Anal.*, **17**, 1249 (1998).
16. M. Carlson and L.E. Habeger, *J. Pharm. Sci.*, **69**, 826 (1980).
17. C. Schramm, S. Maier, O. Bobleter, and P. Plankenhorn, *GIT. Fachz. Lab.*, **38**, 184 (1994); through *Anal. Abstr.* **56** (1994) 11 E104.
18. A.G. Fogg, M.A. Fernandez-Arciniega, and R.M. Alonso, *Analyst*, **110**, 1201 (1985).
19. V. Volotovskiy and N. Kim, *Electroanal.*, **10**, 61 (1998).
20. M. Fayyad, M. Tutunji, and Z. Taha, *Anal. Lett.*, **21**, 1425 (1988).
21. M. Ciszowska and Z. Stojek, *Talanta*, **33**, 817 (1986)
22. A. Voulgaropoulos, P. Valenta, and H.W. Nuernberg, *Fresenius Z. Anal. Chem.*, **317**, 367 (1984).
23. A. Voulgaropoulos and N. Tzivanakis, *Electroanal.*, **4**, 647 (1992).
24. R. Parkash, R. Bansal, S.K. Rehani, and S. Dixit, *Talanta*, **46**, 1573 (1998).
25. R. Parkash and R. Bansal, *Anal. Lett.*, **23**, 1159 (1990).
26. A. Rios and M. Valcarcel, *Analyst*, **109**, 1147 (1984).
27. Y. Fujita, I. Mori, and T. Matsuo, *Anal. Sci.*, **14**, 1157 (1998).
28. T. Hamano, Y. Mitsuhashi, N. Kojima, N. Aoki, M. Shibata, Y. Ito, and Y. Oji, *Analyst*, **118**, 909 (1993).
29. T. Hamano, Y. Mitsuhashi, K. Tanaka, Y. Matsuki, Y. Oji, and S. Okamoto, *Lebensm. Unters. Forsch.*, **180**, 280 (1985).
30. B. Kratochvil and M.C. White, *Anal. Chem.*, **37**, 111 (1965).
31. S.G. Hulden and L. Hariu, *Talanta*, **27**, 815 (1980).

32. H.A. Mottola and H. Freiser, *Anal. Chem.*, **39**, 1294 (1967).
33. S.N. Bhattacharyya and K.P. Kundu, *Talanta*, **18**, 446 (1971).
34. I. Nemcova, H. Pesinova, and V. Suk, *Microchem. J.*, **30**, 27 (1984).
35. E.E. Kaminski and D.M. Pacenti, *J. Pharm. Sci.*, **63**, 1133 (1974).
36. H. Itabashi, K. Umetsu, N. Teshima, K. Satoh, and T. Kawashima, *Anal. Chim. Acta*, **261**, 213 (1992).
37. G.Y. Zhu, R.X. Zhu, C.G. Duan, and R.X. Wang, *Spectrochim. Acta*, **55**, 955 (1999).
38. N. Kawasaki, Y.C. Lee, O. Hashimoto, M. Yamamoto, T. Kawanishi, and T. Hayakawa, *Anal. Biochem.*, **270**, 329 (1999).
39. F. Lazaro, M.D. Luque-de-Castro, and M. Valcarcel, *Fresenius'Z. Anal. Chem.*, **321**, 467 (1985).
40. F. Belal, F.A. Aly, M.I. Walash, I.M. Kenawy, and A.M. Osman, *IL Farmaco*, **53**, 365 (1998).
41. E.B. Milosavljevic, L. Solujic, J.L. Hendrix, and J.H. Nelson, *Analyst*, **114**, 805 (1989).
42. R.J. Hurtubise, *J. Pharm. Sci.*, **63**, 1131 (1974).
43. G.D. Christian and F.J. Feldman, *Anal. Chim. Acta*, **40**, 173 (1968).
44. E.A. Fitzgerald, *Anal. Chem.*, **47**, 356 (1975).
45. J.L. Swain and J.L. Sudmeier, *Anal. Chem.*, **40**, 418 (1968).
46. K. Momoki and H. Katano, *Anal. Chem.*, **56**, 1035 (1984).
47. D.K. Nguyen, A. Bruchet, and P. Arpino, *J. High Resolut. Chromatogr.*, **17**, 153 (1994).
48. Y. Nishikawa and T. Okumura, *J. Chromatogr.*, **690**, 109 (1995).

49. R.L. Sheppard and J. Henion, *Anal. Chem.*, **69**, 2901 (1997).
50. V.T. Wanke and S.H. Eberle, *Acta Hydrochim. Hydrobiol.*, **20**, 192 (1992).
51. V.T. Wanke and S.H. Eberle, *Z Wasser Abwasser Forsch.*, **25**, 192 (1992).
52. M. Sillanpaa, J. Sorvari, and M.L. Sihvonen, *Chromatographia*, **42**, 578 (1996).
53. J. Gardiner, *Analyst*, **102**, 120 (1977).
54. L. Rudling, *Water Res.*, **6**, 871 (1972).
55. A.P. Toste and T.J. Lechner-Fish, *Waste Management*, **13**, 237 (1993).
56. D.T. Williams, *J. Assoc. Off. Anal. Chem.*, **57**, 1388 (1974).
57. C.C.T. Chinnick, *Analyst*, **106**, 1203 (1981).
58. A. Yamaguchi, A.R. Rajput, K. Ohzeki, and T. Kambara, *Bull. Chem. Soc. Japan*, **56**, 2621 (1983).
59. D.L. Venezky and W.E. Rudzinski, *Anal. Chem.*, **56**, 315 (1984).
60. R.M. Cassidy and S. Elchuk, *Anal. Chem.*, **57**, 615 (1985).
61. M. Unger, E. Mainka, and W. Koenig, *Fresenius' Z. Anal. Chem.*, **329**, 50 (1987).
62. J. Dai and G.R. Helz, *Anal. Chem.*, **60**, 301 (1988).
63. G. Retho and L. Diep, *Z. Lebensm Unters Forsch*, **188**, 223 (1989).
64. E.L. Inman, R.L. Clemens, and B.A. Olsen, *J. Pharm. Biomed. Anal.*, **8**, 513 (1990).
65. C. Randt, R. Wittlinger, and W. Merz, *Fresenius' J. Anal. Chem.*, **346**, 728 (1993).
66. O. Stalberg and T. Arvidsson, *J. Chromatogr.*, **684**, 213 (1994).

67. P.J.M. Bergers and A.C. De-Groot, *Water Res.*, **28**, 639 (1994).
68. A.S. Kord, I. Tumanova, and W.L. Matier, *J. Pharm. Biomed. Anal.*, **13**, 575 (1995).
69. M. Sillanpaa, R. Kokkonen, and M.L. Sihvonen, *Anal. Chim Acta*, **303**, 187 (1995).
70. L.W. Ye and C.A. Lucy, *Anal. Chem.*, **67**, 2534 (1995).
71. B. Nowack, F.G. Kari, S.U. Hilger, and L. Sigg, *Anal. Chem.*, **68**, 561 (1996).
72. G.A. Tran, C.A. Chen, and R.B. Miller, *J. Liq. Chromatogr. Relat. Technol.*, **19**, 1499 (1996).
73. L. Ye and C.A. Lucy, *J. Chromatogr.*, **739**, 307 (1996).
74. P.M. Nirel, P.E. Pardo, J.C. Landry, and R. Revaclier, *Water Res.*, **32**, 3615 (1998).
75. M.L. Miller, B.R. McCord, R. Martz, and B. Budowle, *J. Anal. Toxicol.*, **21**, 521 (1997).
76. J. De Jong, A. Van Polanen, and J.J.M. Driessen, *J. Chromatogr.*, **553**, 243 (1991).
77. J. Harmsen and A. Van den Toorn, *J. Chromatogr.*, **249**, 379 (1982).
78. S. Loyaux-Lawniczak, J. Douch, and P. Behra, *Fresenius' J. Anal. Chem.*, **364**, 727 (1999).
79. X.X. Shi and X.M. Shen, *Sepu.*, **18**, 445 (2000).
80. D.G. Parkes, M.G. Caruso, and J.E. Spardling, *Anal. Chem.*, **53**, 2154 (1981).
81. L. Hall and L. Takahashi, *J. Pharm. Sci.*, **77**, 247 (1988).
82. J. Bauer, D. Heathcote, and S. Krogh, *J. Chromatogr.*, **369**, 422 (1986).

83. G.A. Perfetti and C.R. Warner, *J. Assoc. Off. Anal. Chem.*, **62**, 1092 (1979).
84. N.E. Ballou, G.R. Ducatte, C. Quang, and V.T. Remcho, *J. High Resolut. Chromatogr.*, **19**, 183 (1996).
85. R.L. Sheppard and J. Henion, *Anal. Chem.*, **69**, 477A (1997).
86. R.L. Sheppard and J. Henion, *Electrophoresis*, **18**, 287 (1997).
87. V. Sivamoorthy, K.V. Varma, K.V. Muralikrishna, and B. Rangamannar, *J. Radioanal. Nucl. Chem.*, **108**, 169 (1987).
88. V. Pauliulionyte and A. Pararaskas, *Chromatographia*, **51**, 491 (2000).
89. G. Owens, V.K. Ferguson, M.J. McLaughlin, I. Singleton, R.J. Reid, and F.A. Smith, *Environ. Sci. Technol.*, **34**, 885 (2000).

# ETODOLAC

Ketan P. Shah<sup>1</sup>, Kavita Gumbhir-Shah<sup>2</sup>, and Harry G. Brittain<sup>3</sup>

(1) Schering-Plough Corporation  
NJ Quality Laboratories  
1011 Morris Avenue  
Union, NJ 07083

(2) PharmaConsult, Inc.  
23 Honeyman Road  
Basking Ridge, NJ 07920

(3) Center for Pharmaceutical Physics  
10 Charles Road  
Milford, NJ 08848

## **Contents**

### **1. Description**

- 1.1 Nomenclature
  - 1.1.1 Systematic Chemical Name
  - 1.1.2 Nonproprietary Names
  - 1.1.3 Proprietary Names
- 1.2 Formulae
  - 1.2.1 Empirical Formula, Molecular Weight, CAS Number
  - 1.2.2 Structural Formula
- 1.3 Elemental Analysis
- 1.4 Appearance
- 1.5 Uses and Applications

### **2. Methods of Preparation**

### **3. Physical Properties**

- 3.1 Ionization Constants
- 3.2 Solubility Characteristics
- 3.3 Partition Coefficients
- 3.4 Optical Activity
- 3.5 Crystallographic Properties
  - 3.5.1 Single Crystal Structure
  - 3.5.2 X-Ray Powder Diffraction Pattern
- 3.6 Hygroscopicity
- 3.7 Thermal Methods of analysis
  - 3.7.1 Melting Behavior
  - 3.7.2 Differential Scanning Calorimetry
- 3.8 Spectroscopy
  - 3.8.1 UV/VIS Spectroscopy
  - 3.8.2 Vibrational Spectroscopy
  - 3.8.3 Nuclear Magnetic Resonance Spectrometry
- 3.9 Mass Spectrometry

**4. Methods of Analysis**

- 4.1 Spectroscopic Analysis
  - 4.1.1 Colorimetry and Spectrophotometry
  - 4.1.2 Fluorimetry
- 4.2 Chromatographic Methods of Analysis
  - 4.2.1 Thin Layer Chromatography
  - 4.2.2 High Performance Liquid Chromatography
  - 4.2.3 Capillary Chromatography
- 4.3 Determination in Biological Fluids
  - 4.3.1 Non-Enantiomeric Separation Methods
  - 4.3.2 Enantiomeric Separation Methods

**5. Stability**

- 5.1 Solution-Phase Stability
- 5.2 Stability in Biological Fluids

**6. Drug Metabolism and Pharmacokinetics**

- 6.1 Adsorption
- 6.2 Distribution
- 6.3 Metabolism
- 6.4 Elimination

**7. References**



## 1. Description

### 1.1 Nomenclature

#### 1.1.1 Systematic Chemical Name

1,8-diethyl-1,3,4,9-tetrahydropyrano-[3,4-b]indole-1-acetic acid

#### 1.1.2 Nonproprietary Names

Etodolac; Etodolic acid

#### 1.1.3 Proprietary Names

Lodine<sup>®</sup>; Ramodar<sup>®</sup>; Ultradol<sup>®</sup>; Zedolac<sup>®</sup>; Edolan<sup>®</sup>

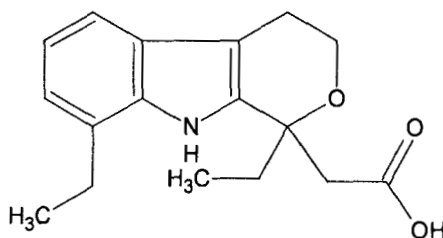
### 1.2 Formulae

#### 1.2.1 Empirical Formula, Molecular Weight, CAS Number

C<sub>17</sub>H<sub>21</sub>NO<sub>3</sub> [MW = 287.354]

CAS number = 41340-25-4

#### 1.2.2 Structural Formula



### 1.3 Elemental Analysis

The calculated elemental composition is as follows:

carbon:	71.06%
hydrogen:	7.37%
oxygen:	16.70%
nitrogen:	4.87%

## 1.4 Appearance

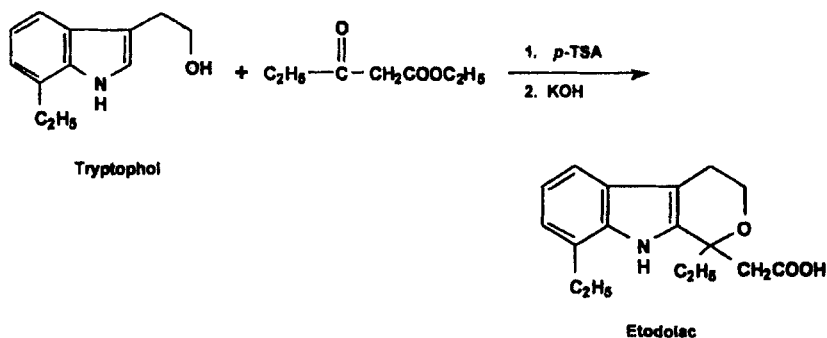
Etodolac is a crystalline white powder.

## 1.5 Uses and Applications

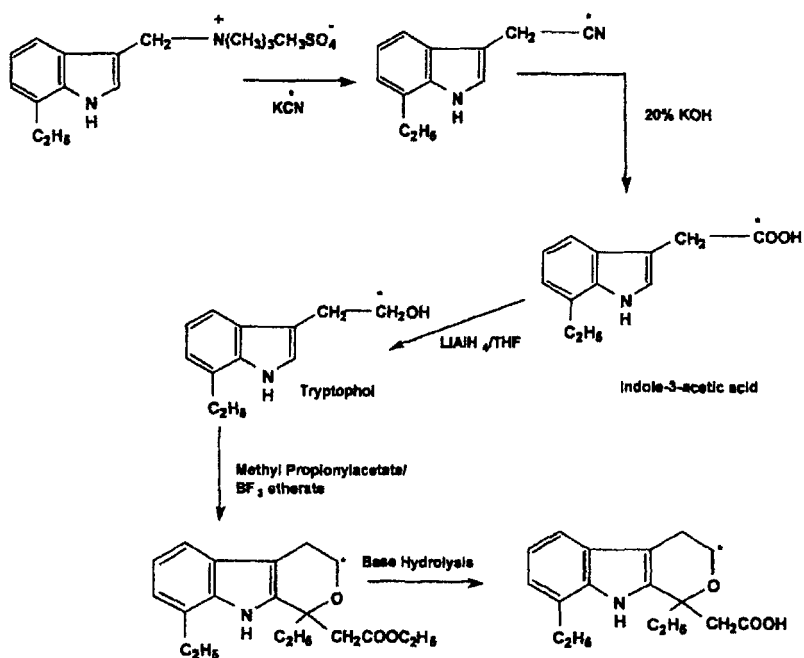
Etodolac belongs to the non-steroidal anti-inflammatory class of drugs (NSAIDs) that have anti-inflammatory, analgesic, and anti-pyretic properties [1]. NSAIDs provide analgesic properties at lower doses, whereas, higher doses are required to produce anti-inflammatory action. Etodolac has been marketed in United States since 1991 and is used in management of rheumatoid arthritis [2] and osteoarthritis [3]. Etodolac has also found application in treatment of ankylosing spondylitis, post-operative pain (dental, obstetric, or orthopedic surgery), and non surgical pain (lower back pain, tendonitis, sports injury, or gout) [4].

## 2. Methods of Preparation

As shown in the following scheme, one synthetic route to etodolac involves acid catalyzed (*p*-TSA or P<sub>2</sub>O<sub>5</sub>) condensation of an indole starting material, tryptophol, with a keto ester, such as, ethyl propionylacetate. This is followed by alkaline hydrolysis to yield etodolac [5, 6], which was recrystallized from hexane and chloroform. The yield was 93% from the tryptophol starting material.



In another synthetic route,  $^{14}\text{C}$ -labeled etodolac was synthesized from a radiolabeled tryptophol intermediate [7].



The radiolabel was introduced by displacement of a quaternary amine with potassium  $^{14}\text{C}$ -cyanide to give a nitrile. The nitrile was readily converted to indole-3-acetic acid by hydrolysis with 20% aqueous potassium hydroxide. Reduction of the indole-3-acetic acid derivative with lithium aluminum hydride in tetrahydrofuran gave a tryptophol with 95% yield. The tryptophol was condensed with methyl propionylacetate using boron trifluoride etherate as the catalyst to produce tetrahydropyranoindole. Basic hydrolysis of the ester gave  $[3\text{-}^{14}\text{C}]$ etodolic acid (overall yield 26% from the labeled starting material). The compound was recrystallized in presence of an antioxidant to prevent formation of peroxides and stored at  $-10^\circ\text{C}$ . The radiochemical purity was determined to be 99%.

Several metabolites of etodolac have been synthesized to confirm their identity during drug metabolism studies including 6-hydroxyetodolac, *N*-methyletodolac, 4-ureidoetodolac, 8-(1'-hydroxy) etodolac, and 4-oxoetodolac [8].

### **3. Physical Properties**

#### **3.1 Ionization Constants**

Etodolac contains a single ionizable group, characterized by a pKa of 4.65.

#### **3.2 Solubility Characteristics**

Etodolac is insoluble in water, but soluble in alcohols, chloroform, dimethyl sulfoxide, and aqueous polyethylene glycol.

The pH dependence of the aqueous solubility was calculated using the ACD Solubility Suite 6.0 program (Advanced Chemistry Development, Toronto Canada), and is shown in Figure 1. It is predicted that although the drug exhibits very low solubility at low pH, its solubility dramatically increases at high pH.

#### **3.3 Partition Coefficients**

The partition coefficient of etodolac was determined in the 1-octanol/water system, where the aqueous phase was buffered to pH 7.4. A logP value of 11.4 was obtained under these conditions.

However, when using the ACD program for calculating partition coefficients, a octanol water logP value of  $3.59 \pm 0.41$  was calculated. Using the ACD program that calculated the pH distribution of distribution coefficients, the data plotted in Figure 2 were obtained.

#### **3.4 Optical Activity**

Etodolac contains one chiral center and is resolved into two enantiomers. The pharmacologic and biochemical results generated with racemic etodolac and its optically pure enantiomers showed that most of the anti-inflammatory activity is due to the (+) enantiomer [10].

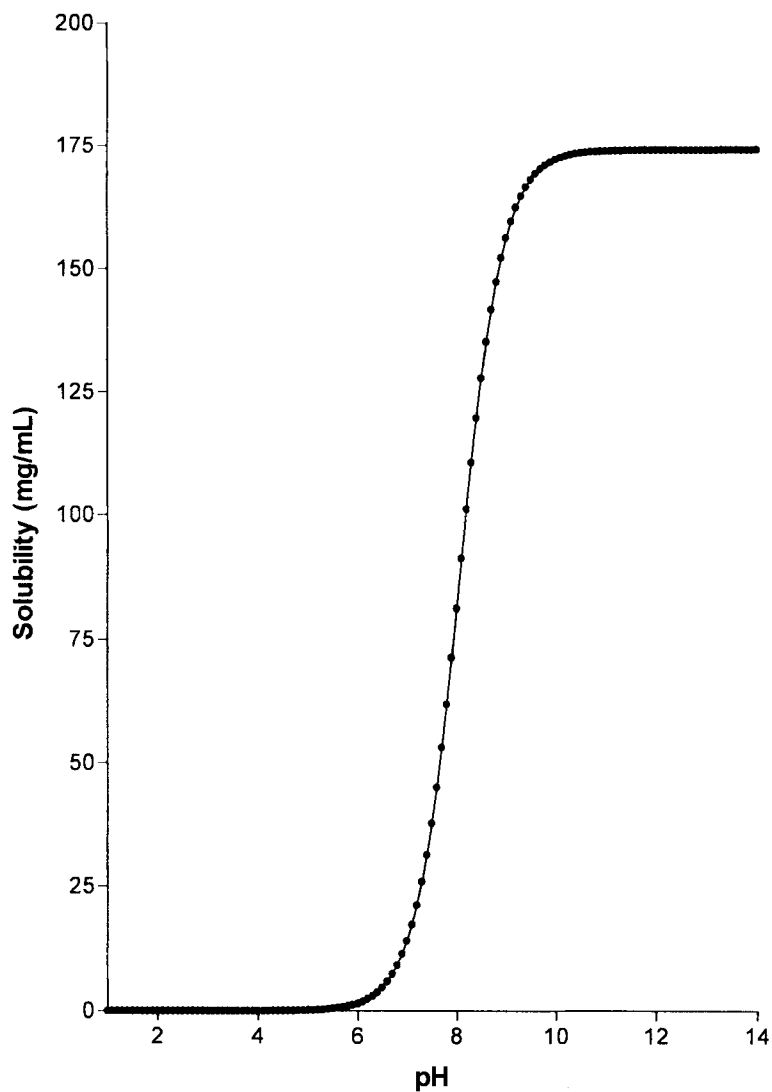


Figure 1. pH dependence of the aqueous solubility of etodolac, as calculated using the ACD Solubility Suite 6.0 program (Advanced Chemistry Development, Toronto Canada).

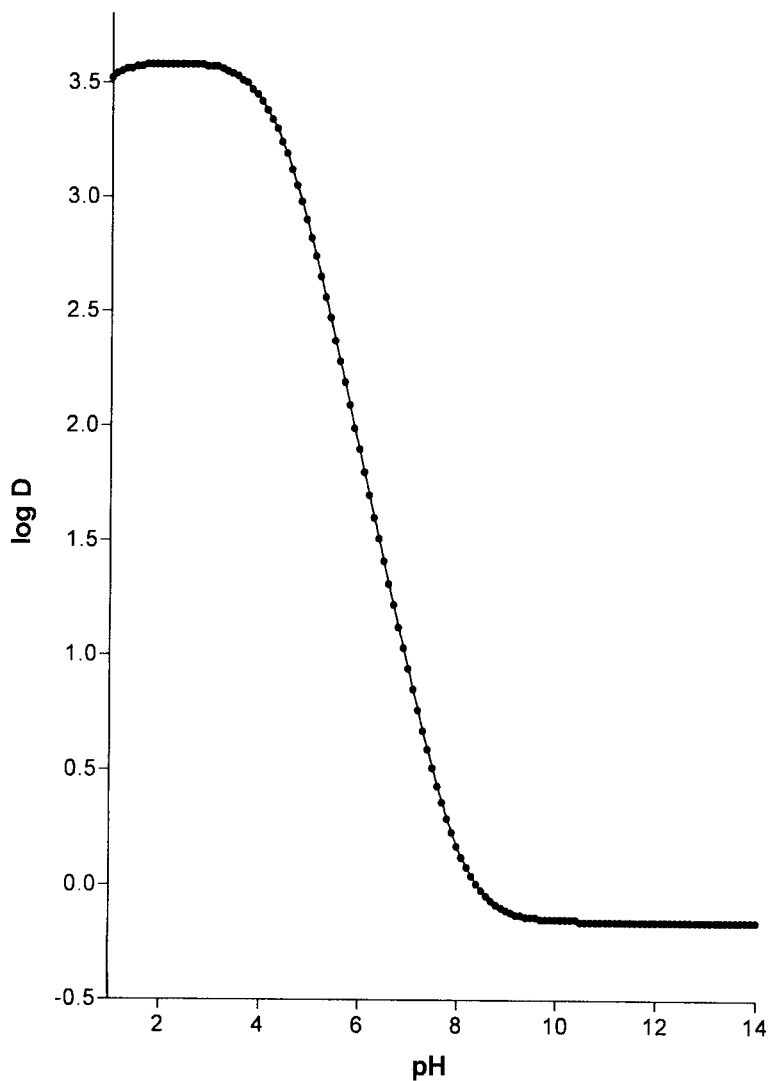


Figure 2. pH dependence of the distribution coefficient of etodolac, as calculated using the ACD logD program (Advanced Chemistry Development, Toronto Canada).

Racemic etodolac has been resolved into its individual enantiomers following formation of its diastereomeric ester derivatives with (-)-borneol as the chiral discriminating agent [10]. The (+)-diastereomer was crystallized from hexane, and characterized by a melting point range of 142-143°C and an  $[\alpha]_D$  equal to + 47.4° (c=1, ethanol). The (-)-diastereomer was characterized by a melting point range of mp 93-96°C and  $[\alpha]_D$  of - 61.4° (c=1, ethanol). Hydrolysis of each diastereomer with methanolic potassium hydroxide yielded the (+)- and (-)-etodolac enantiomers. (+)-etodolac was obtained from the (-)-diastereomer, and was characterized by a melting point range of 138-140 °C and  $[\alpha]_D$  of +25.2° (c=3, ethanol). (-)-etodolac was obtained from the (+)-diastereomer, had was characterized by a melting point range of 139-141°C and  $[\alpha]_D$  of -25.6° (c=3, ethanol). The enantiomeric purity of both isomers was in excess of 99.9%.

A method for preparative scale separation of the enantiomers of etodolac involved crystallization of racemic etodolac with optically active 1-phenethylamine [13]. Racemic etodolac was allowed to crystallize with either S(-)- or R(+)-phenethylamine in anhydrous 2-propanol for 12 hours at 4°C. Pure diastereomeric salts were decomposed with sulfuric acid (10% v/v), and extracted with ethyl acetate. The enantiomeric purity of both enantiomers was at least 98%.

### 3.5 Crystallographic Properties

#### 3.5.1 Single Crystal Structure

The structure of etodolac has been established by single crystal X-ray diffraction analysis [9]. Crystals of racemic etodolac were obtained by recrystallization from benzene-petroleum ether. A small brick shaped sample having approximate dimensions 0.2 x 0.2 x 0.3 mm was used for collecting three dimensional intensity data on a computer-controlled Picker FACS-I four circle diffractometer with a graphite monochromator.

The space group of the racemic compound was found to be  $P_{bca}$ , with cell constants of  $a = 8.60 \text{ \AA}$ ,  $b = 18.59 \text{ \AA}$ , and  $c = 19.06 \text{ \AA}$ . The stereoview of ( $\pm$ )-etodolac indicates that the oxygen of the pyrano ring and the acetic acid chain lie above the plane of the indole ring, and that the torsion angle about the acetic acid side chain is 297.6°. The carbon atom of the carboxyl group is situated at 5.53 Å from the center of the benzene ring, and lies in

a plane 2.21 Å above that of the indole ring. This conformer, as well as energy-minimized conformations obtained by molecular mechanics calculations, did not enable the identification of a probable receptor-site conformation.

The absolute configuration of (+)-etodolac (the biologically active enantiomer), has been determined from a single-crystal study of the borneol-ester derivative of racemic etodolac [9, 10]. A single-crystal X-ray analysis was performed on the (–)-etodolac (*S*)-(–)-borneol ester, since this derivative formed superior thin plate like crystals from hexane. A crystal with dimensions of 0.15 x 0.05 x 0.20 mm was used for the x-ray diffraction analysis. The space group was found to be  $P2_12_12_1$ , with cell constants of  $a = 22.75$  Å,  $b = 10.66$  Å, and  $c = 9.77$  Å. Since (–)-etodolac has the (*R*) absolute configuration (based on the single-crystal x-ray diffraction analysis), the active (+) enantiomer of etodolac was assigned an absolute (*S*) configuration.

The X-ray diffraction pattern of solid dispersions of etodolac in propylene glycol was obtained using a PW 1730 diffractometer with Cu K $\alpha$  radiation, collimated by a 0.08° divergence slit and a 0.2° receiving slit and scanned at a rate of 2.4°/min over 2 $\theta$  range of 5–45° [11]. Characteristic peaks of etodolac appeared at scattering angles at 9.51, 14.55, 16.69, 27.55 degrees 2- $\theta$ .

An x-ray powder diffraction study performed on the sodium salts of (±)- and (+)-etodolac showed these salts to be mixtures of amorphous and crystalline materials [12]. Scanning electron microscope studies showed that the amorphous form of (±)-etodolac sodium salt transformed into various crystal forms when exposed to 75% relative humidity conditions for 7 days. The crystalline form of (+)-etodolac sodium salt transformed into swollen rod-like crystals under the same exposure conditions.

### 3.5.2 X-Ray Powder Diffraction Pattern

The x-ray powder diffraction pattern of etodolac was obtained using a Rigaku MiniFlex powder diffraction system, equipped with a horizontal goniometer in the  $\theta/2-\theta$  mode. The x-ray source was nickel-filtered K- $\alpha$  emission of copper (1.544056 Å). A 10-mg sample was packed into an aluminum holder using a back-fill procedure, and was scanned over the range of 5 to 6 degrees 2- $\theta$ , at a scan rate of 0.5 degrees 2- $\theta$ /min.



Calibration of the powder pattern was effected using the characteristic scattering peaks of aluminum at 44.738 and 38.472 degrees 2- $\theta$ .

The powder pattern of etodolac is shown in Figure 3, and a summary of the observed scattering angles, d-spacings, and relative intensities is shown in Table 1. Since the unit cell parameters of etodolac are known [9], it was possible to index the observed lines to the  $P_{bca}$  and these assignments are also found in Table 1.

### 3.6 Hygroscopicity

The hygroscopicity of the sodium salts of etodolac has been studied [12]. Samples of ( $\pm$ )- and (+)-etodolac sodium were exposed to various relative humidity (RH) conditions at room temperature, and the percent weight change after 7 days was recorded. As seen in Table 2, ( $\pm$ )-etodolac sodium lost weight at 0% and 75% RH, but gained weight at other RH conditions. In contrast, the (+)-enantiomer lost weight at 0% RH, but showed increasing weight gain as the %RH values were increased. The abnormal hygroscopic behavior observed with racemic etodolac sodium salt at 75% RH after 7 days was attributed to nucleation of small crystals of the product in the presence of water vapor.

### 3.7 Thermal Methods of analysis

#### 3.7.1 Melting Behavior

The melting point range of etodolac, crystallized from mixed hexane and chloroform, has been reported as 145 – 148°C.

#### 3.7.2 Differential Scanning Calorimetry

Measurements of differential scanning calorimetry were obtained on a TA Instruments 2910 thermal analysis system. Samples of approximately 2-4 mg were accurately weighed into an aluminum DSC pan, and covered with an aluminum lid that was crimped in place. The DSC thermogram is shown in Figure 4, and consisted of a single melting endothermic transition. In good agreement with the known melting behavior, the endothermic transition was characterized by an onset temperature of 147.1°C, a temperature maximum of 148.6°C, and an enthalpy of fusion of 118.6 J/g.

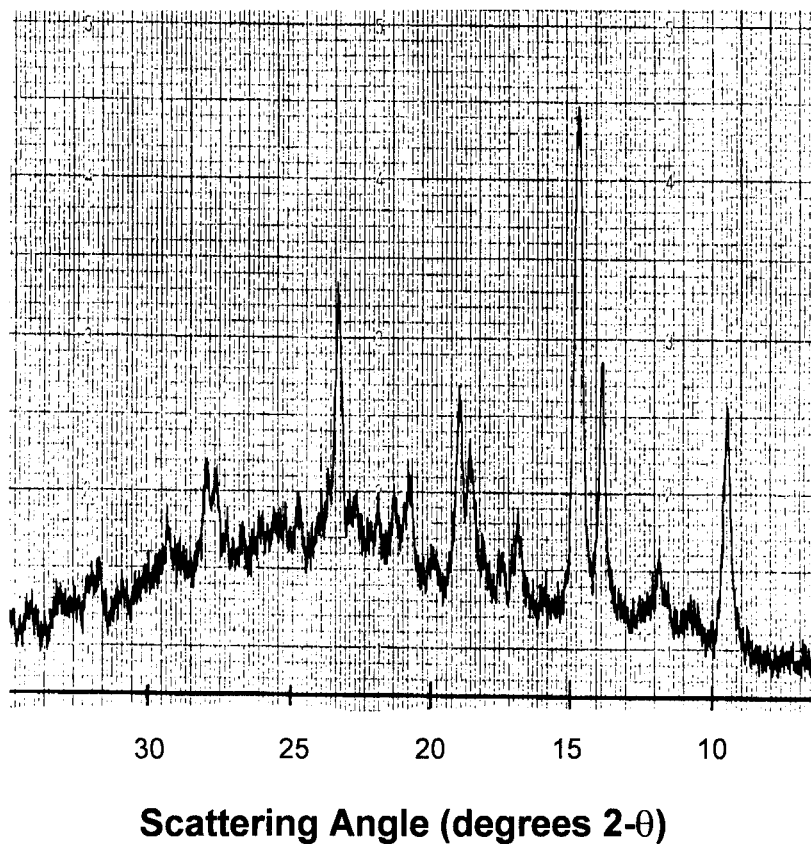


Figure 3. X-ray powder diffraction pattern of etodolac.

Table 1

Scattering Angles, Interplanar d-Spacings, and Relative Intensities in the X-Ray Powder Diffraction of Etodolac

Scattering Angle (degrees 2- $\theta$ )	d-Spacing (Å)	Relative Intensity (%)	Assignment
9.437	9.385	49.38	(002),(020)
10.767	8.228	4.94	(021)
11.893	7.452	14.81	(111)
13.887	6.386	50.62	(102)
14.655	6.053	100.00	(112)
16.854	5.268	18.52	(0 -2 3)
17.468	5.084	8.64	(113)
18.082	4.913	12.35	(131)
18.542	4.792	30.86	(004)
18.931	4.695	40.74	(040)
19.872	4.474	6.17	(132)
20.691	4.299	19.75	(200)
21.253	4.187	16.05	(042)
21.816	4.080	13.58	(114)
22.634	3.934	13.58	(133)
23.248	3.832	55.56	(213)
24.680	3.612	13.58	(222)
25.499	3.498	8.64	(231)
26.010	3.431	8.64	(143)
26.658	3.349	7.41	(223)
27.187	3.285	9.88	(232)
27.647	3.231	19.75	(204)
27.954	3.196	22.22	(240)
29.284	3.054	14.81	(224)

Table 2

Hygroscopicity of Etodolac Sodium at Various Humidity Conditions after 7 Days of Storage at Room Temperature

Relative Humidity (%)	Percent Weight Change after 7 Days	
	(±)-Etodolac, Sodium Salt	(+)-Etodolac, Sodium Salt
0.0	– 5.45	– 0.83
22.5	+ 0.34	+ 1.64
54.0	+ 1.08	+ 7.71
75.0	– 5.16	+ 22.70

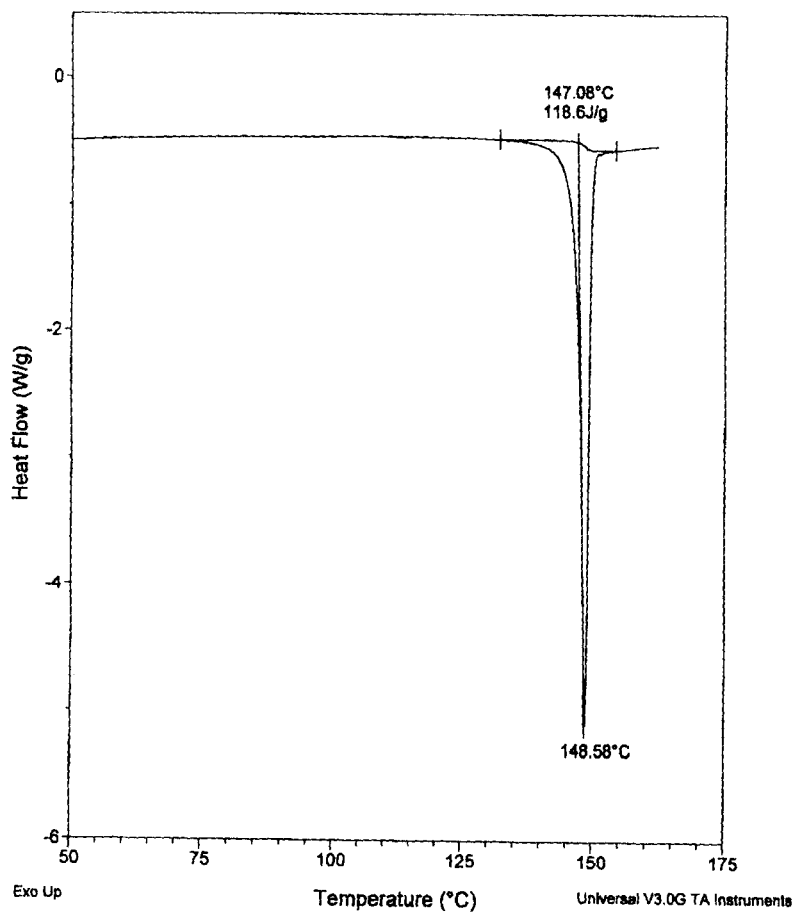


Figure 4. Differential scanning calorimetry thermogram of etodolac.

The DSC of etodolac and its solid dispersions in propylene glycol were performed by heating the samples in a hermetically sealed aluminum pan at a heating rate of 10°C/min over the range of 20-300°C [11]. The thermograms of etodolac and PEG 6000 solid dispersions, and physical mixtures were similar, indicating the absence of chemical or physical interactions between the components.

Differential thermal analysis (DTA) thermograms of (±)-etodolac sodium salt exhibited endothermic transitions around 80, 120, and 297°C and an exothermic transition around 83°C [12]. The exothermic phase change was observed after exposure of the sample to moisture, indicating conversion of the amorphous form of (±)-etodolac sodium salt to a crystalline phase. In contrast, the thermogram of (+)-etodolac sodium salt, after exposure to moisture, showed endotherms at 60, 80, 120, and 297°C, indicating that the salt contained methanol, acetonitrile, and water. There was no sign of degradation product formation.

### **3.8 Spectroscopy**

#### **3.8.1 UV/VIS Spectroscopy**

Ultraviolet absorption spectra of etodolac at concentrations of 20 µg/mL were obtained using a Varian DMS-200 spectrophotometer, scanning over the wavelength range 200-400 nm. The spectrum of the protonated form of etodolac was obtained in neat ethanol, and the spectrum of the deprotonated form was obtained in 0.5 N NaOH. The spectra shown in Figures 5 and 6, respectively.

In both solvents, two absorption bands were observed. The various absorbance parameters calculated for each band system are collected in Table 3.

#### **3.8.2 Vibrational Spectroscopy**

The infrared absorption spectrum of etodolac was obtained using a Buck Scientific model M500 single-beam infrared absorption spectrophotometer, and a Pike single-reflection attenuated total reflectance accessory. The full infrared spectrum is shown in Figure 7, and the fingerprint region is expanded in Figure 8. Assignments for the observed bands are found in Table 4.

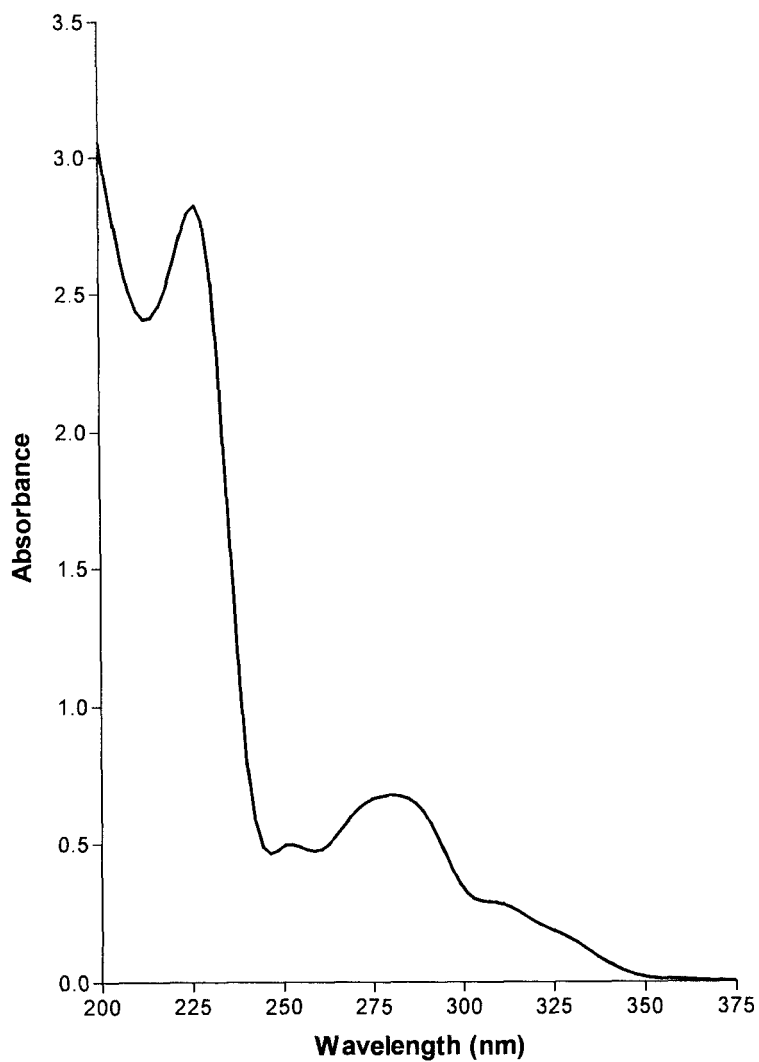


Figure 5. Ultraviolet absorption spectrum of a 20 µg/mL solution of etodolac in ethanol.

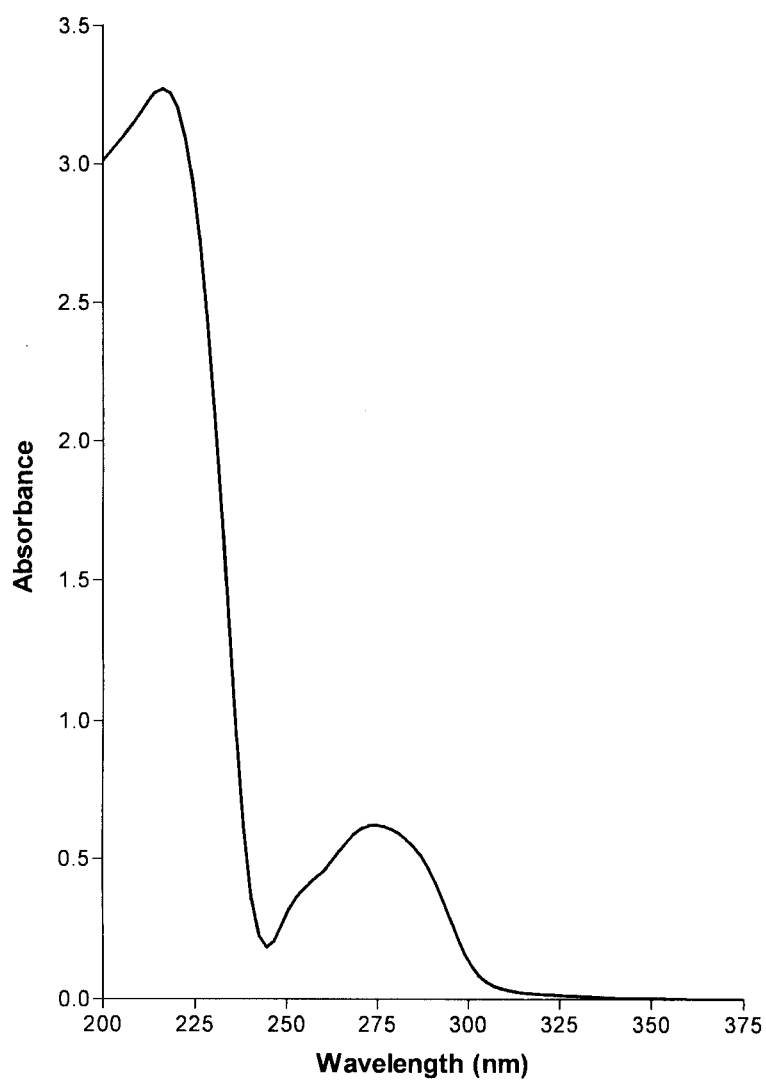


Figure 6. Ultraviolet absorption spectrum of a 20  $\mu\text{g/mL}$  solution of etodolac in 0.1 N NaOH.



Table 3

Absorbance Parameters for the Two Absorption Bands of  
Etodolac in Various Solvent Systems

	<b>Ethanol</b>	<b>0.5 N NaOH</b>
<b>Band 1</b>		
Maximum wavelength (nm)	280	274
Molar Absorptivity (L/cm•mole)	9,729	8951
<b>Band 2</b>		
Maximum wavelength (nm)	226	216
Molar Absorptivity (L/cm•mole)	40,530	47,010

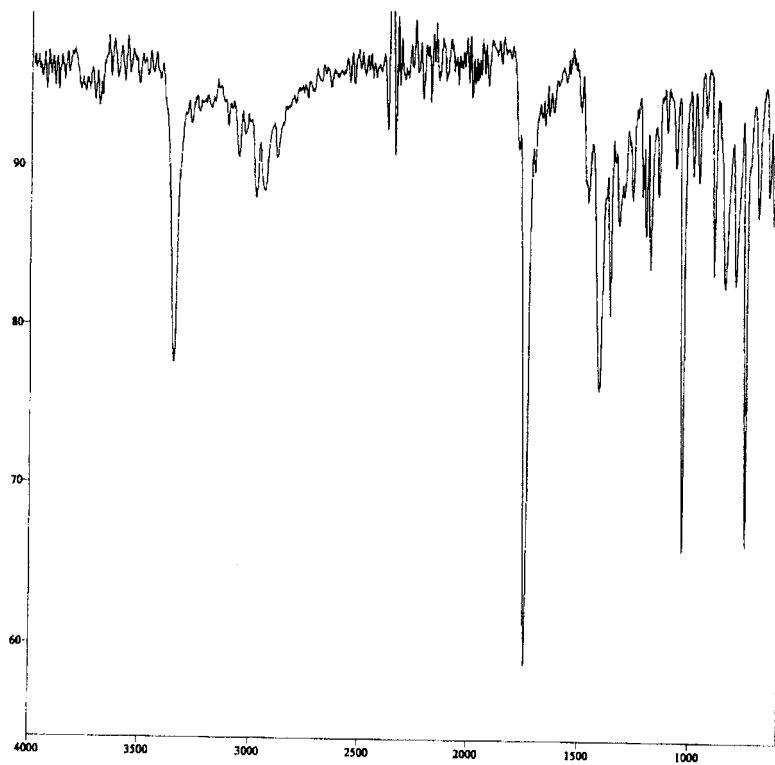


Figure 7. Full attenuated total reflectance infrared spectrum of etodolac.

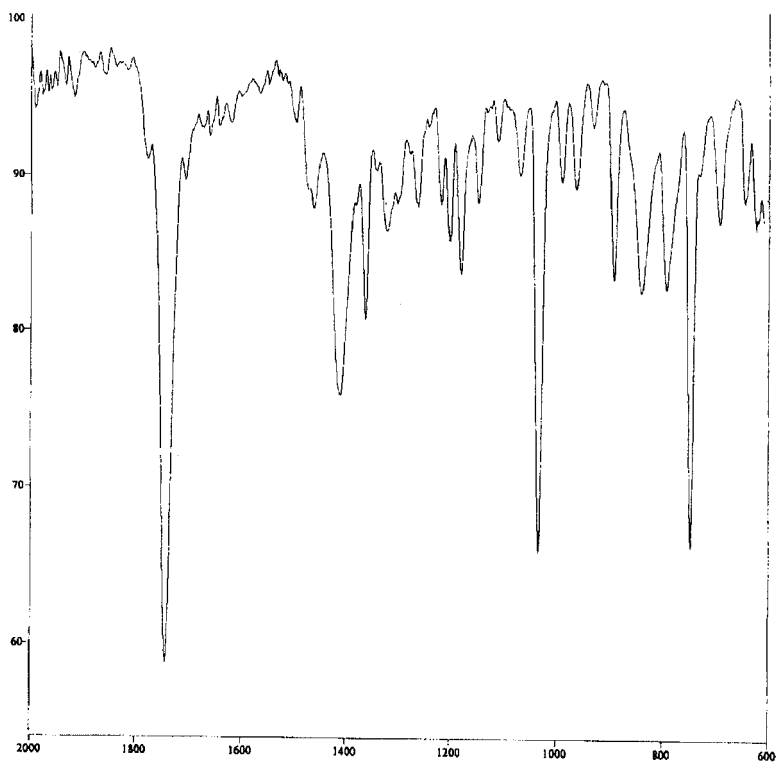


Figure 8. Fingerprint region of the attenuated total reflectance infrared spectrum of etodolac.

Table 4

Energies and Assignments for the Major Infrared Absorption Bands of Etodolac

Energy (cm <sup>-1</sup> )	Assignment
644	
693	
747	-NH wagging mode
792	Aromatic hydrogen out-of-plane vibrations
839	
891	
930	
962	
989	
1033	-CO stretching mode
1067	
1146	
1180	
1201	
1263	
1321	
1364	-CH <sub>2</sub> scissors deformation mode;
1413	-CH <sub>3</sub> asymmetric deformation mode
1464	
1499	
1743	Carbonyl group of carboxylate stretching mode
2884	Aromatic -CH modes
2939	
2977	
3059	
3108	
3348	Hydroxyl group of carboxylate mode

### 3.8.3 Nuclear Magnetic Resonance Spectrometry

The one-dimensional  $^1\text{H}$ -NMR spectrum of the methylated derivative of etodolac has been reported [15].

The  $^{13}\text{C}$ -NMR spectrum of etodolac has also been determined, and assignments for the observed resonance bands were determined using spin-decoupling experiments. The assignments for observed resonance bands are provided in Table 5.

### 3.9 Mass Spectrometry

The mass spectrum of etodolac methyl ester was obtained using a Hewlett-Packard quadrupole mass spectrometer, operating in the GC-MS positive electron impact (EI+) mode [15, 16]. The monitored ions were at  $m/z$  154, 168, 198, 213, 228, 272, and 301, and assignments for these are summarized in Table 6.

The fragmentation occurring on electron impact was cleavage at the C-1 substituents. Loss of the methylene methyl acetate group ( $M^+ - 73$ ) gave rise to the ion at  $m/z = 228$  (70%), while an ion at  $m/z = 198$  (36%) was formed by further loss of an ethyl group. Alternatively, the fragmentation pattern may start with the loss of an ethyl group ( $M^+ - 29$ ,  $m/z = 272$ , 29%), followed by those of a methyl acetate ( $m/z = 213$ , 10%) and a methylene ( $m/z = 198$ , 36%). Loss of the second ethyl group, resulting in a pyrano indole unsubstituted ring, explains the ion at  $m/z = 168$  (24%). The ion at  $m/z = 154$  (28%) probably is derived from cleavage of the pyranosyl ring side (loss of methylene unit to give a  $\text{C}_{10}\text{H}_4\text{NO}$  structure).

## 4. Methods of Analysis

### 4.1 Spectroscopic Analysis

#### 4.1.1 Colorimetry and Spectrophotometry

The UV spectrum of etodolac in methanol is characterized by maxima at  $224 \pm 1$  nm ( $a = 37970$ ) and  $279 \pm 1$  nm ( $a = 8440$ ), and a minimum at  $246 \pm 1$  nm. The absorbance of the 278 nm or 279 nm peak was used to quantitate the amount of drug dissolved from etodolac capsules and sustained release tablets in pH 7.5 phosphate buffer [17, 18].

Table 5

Assignments of the Resonance Bands Observed in the  
 $^{13}\text{C}$ -NMR Spectrum of Etodolac

[insert structure]

Position of Carbon Atom	Chemical Shift (ppm)
C-1	75.1
C-1a	134.4
C-3	60.8
C-4	23.9
C-4a	108.5
C-5	115.9
C-5a	126.0
C-6	119.7
C-7	120.6
C-8	126.5
C-8a	134.5
C-9	22.1
C-10	13.6
C-11	30.9
C-12	7.6
C-13	42.6
C-14	175.7

Table 6

Interpretation of the Electron Impact  
Mass Spectrum of Etodolac

<b>m/z</b>	<b>Relative Intensity</b>	<b>Fragment</b>
301	-	M
272	29	M - C <sub>2</sub> H <sub>5</sub>
228	70	M - C <sub>3</sub> H <sub>5</sub> O <sub>2</sub>
213	10	M - C <sub>4</sub> H <sub>8</sub> O <sub>2</sub>
198	36	M - C <sub>5</sub> H <sub>11</sub> O <sub>2</sub>
168	24	M - C <sub>7</sub> H <sub>17</sub> O <sub>2</sub>
154	28	C <sub>10</sub> H <sub>4</sub> NO

A colorimetric method for the analysis of etodolac has been reported which is based on the formation of colored complexes with *p*-dimethyl-aminobenzaldehyde in the presence of sulfuric acid and ferric chloride [19]. Absorbance measurements were made at 591.5 nm, and the method was found to be linear over the concentration range of 10 to 80 µg/mL. This method was used to determine etodolac in bulk powder and other dosage forms.

#### 4.1.2 Fluorimetry

A simple, sensitive, and reproducible fluorimetric method for the determination of etodolac in bulk powder or dosage forms has been reported [19]. The method involves measurement of the native fluorescence at a wavelength of 345 nm, when ethanolic solutions of the drug were excited at 235 nm. The calibration was found to be linear over the concentration range of 96 to 640 ng/mL.

A fluorimetric method developed for prodolic acid can also be used to quantitate etodolac in serum [20]. This method involved using a 1:1 mixture of isoamyl alcohol and *n*-heptane to extract the drug from serum. An aliquot of the organic phase was then mixed with a 1:1 mixture of dimethyl sulfoxide and isoamyl alcohol, and the fluorescence of the clear solution was determined by excitation at 280 nm and scanning the emission spectra from 240-370 nm. The limit of detection of this method was about 2 µg/mL.

### 4.2 Chromatographic Methods of Analysis

#### 4.2.1 Thin Layer Chromatography

A TLC method has been developed to determine etodolac and its metabolites (6-OH-etodolac and 7-OH-etodolac) in biological fluids and extracts (before and after enzyme hydrolysis) [15]. The method used silica gel plates and hexane-ethyl acetate-acetic acid (60:40:2, v/v) and hexane-ethyl acetate (70:30, v/v) solvent systems to separate the free carboxylic acid and methyl esters of etodolac and the two metabolites. The relative retention ( $R_f$ ) values obtained under these conditions were 0.29, 0.20 and 0.24 for etodolac, 6-OH-etodolac, and 7-OH-etodolac respectively. An  $R_f$  value of 0.45 was obtained for methyl ester of etodolac.



Another TLC method has been reported, which uses 0.25 or 2 mm silica gel plates as the stationary phase, and ethyl acetate/methanol (95:5, v/v) or toluene/ethyl acetate (7:3, v/v) as the developing agent [21]. The method was used to separate etodolac and its metabolites in urine and bile.

#### 4.2.2 High Performance Liquid Chromatography

A sensitive reverse-phase HPLC method has been developed for the analysis of etodolac in tablet formulation [22]. The chromatographic separation was achieved using a reverse-phase C<sub>18</sub> column, having dimensions of 3.3 cm x 0.46 cm i.d. (3 µm particles) and which was maintained at 30°C. The mobile phase consisted of pH 6.0 phosphate buffer / methanol (60:40 v/v), and was eluted at 1 mL/min. Analyte detection was effected on the basis of UV detection at 230 nm. Diazepam was used as an internal standard. The sample preparation entailed grinding the etodolac tablets, followed by extraction with methanol (using sonication). A retention time of 1.46 min was obtained for etodolac under these conditions, and the method was found to be linear, precise, and accurate over the concentration range of 0.01 to 0.1 mg/mL.

A simple, accurate, and reproducible HPLC method has been developed to determine etodolac in presence of impurities (1-methyl and 8-methyl-etodolac) and in pharmaceutical formulations [14]. A Viospher ODS-2 (15 cm x 4.6 mm i.d., 5 µm particle size) HPLC column was used as stationary phase, and acetonitrile/0.05 M phosphate buffer (pH 4.75) (60:40 v/v) eluted at 0.8 mL/min was used as mobile phase. The system was thermostatted to 25 °C, and acetaminophen was used as an internal standard. Detection was achieved by measurement of the UV absorbance at 229 nm. The method was found to be linear over the concentration range of 2-20 µg/mL. The relative retention times for etodolac and acetaminophen were 2.2 and 2.9 min respectively. The retention times for the two impurities, 1-methyl-etodolac and 8-methyl-etodolac, were 1.4 and 3.8 min respectively.

A stability indicating HPLC method has been developed to measure etodolac in presence of three main degradants, 7-ethyl-2-(1-methylene-propyl)-1-*H*-indole-3-ethanol, the decarboxylated product of etodolac, and 7-ethyltryptophol [23]. A reverse phase ODS column (15 cm x 0.41 cm i.d., 5 µm particles) was used to achieve separation. The mobile phase

(phosphate buffer / acetonitrile (55:45) was pumped at 2.0 mL/min and the UV detector was set at 230 nm.

Separation of enantiomers of etodolac using two different derivitization agents and three chiral stationary phases has been studied [24]. Etodolac was converted to its anilide derivative with either 1,3-dicyclohexylcarbodiimide or 1-(3-dimethylaminopropyl)-3-ethylcarbodiimide hydrochloride. Etodolac, derivatizing agent, aniline, and dichloromethane were allowed to incubate for 30 minutes, which was followed by addition of 1 M HCl. The organic layer was removed, washed, dried, and then injected into normal phase or reverse phase HPLC. The HPLC system consisted of a 250 x 4.6 mm (5  $\mu$ m particle size) column packed with chiral stationary phases, and detection was effected by the UV absorbances at 254 and 280 nm. Separation of etodolac enantiomers was achieved on only one of the stationary phases when using 20% 2-propanol in hexane as the mobile phase at a flow rate of 2.0 mL/min.

A simple, isocratic chromatographic method for the separation, identification, and measurement of etodolac enantiomers without derivitization using chiral stationary phase columns has been reported [25]. A chiral stationary phase column packed with Chiracel OD (cellulose tris-3,5-dimethylphenylcarbamate coated on 10  $\mu$ m silica gel) was used as the stationary phase. The mobile phase (85:15 v/v, n-hexane/2-propanol (containing 0.1% trifluoroacetic acid)) was pumped at 0.7 mL/min and the UV detection was set at 230 nm. The (–)-(*R*)-etodolac enantiomer eluted first, indicating its stronger interaction between the stationary phase relative to the (+)-(*S*)-etodolac enantiomer.

#### 4.2.3 Capillary Chromatography

The use of capillary electro-chromatography for the separation of etodolac and its metabolites has recently been reported [26, 27]. Separation of etodolac was achieved using 3 different methods: capillary HPLC, capillary electro-chromatography (CEC), and pressure assisted CEC. Fused-silica capillaries of 100  $\mu$ m i.d. were packed with 5  $\mu$ m octadecyl silica (C<sub>18</sub>) under 400 bar pressure. The length of the packed capillaries was 24.5 cm.

In one report, a LCQ<sup>®</sup> ion trap mass spectrometer equipped with a sheath flow electrospray interface was used for on-line coupling with CEC [26].

The buffer (10 mM pH 3.0 ammonium formate /acetonitrile, 50/50 v/v) served both as mobile phase and sheath liquid, and was delivered at a flow rate of 3  $\mu$ L/min using a syringe pump. A voltage of 20 kV was applied. The  $m/z$  =286 mass response of etodolac was detected at 18.3 min after injection, and detailed elution patterns of etodolac and its hydroxy metabolites were provided.

In another report, separation of etodolac and its metabolites was studied using three different capillary techniques, capillary HPLC, CEC, and pressure assisted CEC, with either UV detection or ion trap mass spectrometer [27]. Baseline separation of all compounds was achieved in different modes and conditions.

### **4.3 Determination in Biological Fluids**

#### **4.3.1 Non-Enantiomeric Separation Methods**

A specific and sensitive HPLC method has been developed for the determination of etodolac in biological fluids [28]. The serum (or plasma) sample was extracted with 4 mL of 1 N HCl and 5 mL of isopentyl alcohol-hexane (1:19 v/v). After agitation for 15 minutes, the two phases were separated by low-speed centrifugation. A 4-mL aliquot of the upper phase was mixed with 1 mL of pH 11.0 glycine buffer, and then agitated for 15 minutes. Prior to injection onto the HPLC column, 20  $\mu$ L of 2.5 M phosphoric acid was added to an aliquot of the aqueous phase to partially neutralize the glycine buffer. Two 250 x 4.6 mm columns were employed: Chromosorb LC-7 ODS 10  $\mu$ m column and Spherisorb ODS 5  $\mu$ m column. Chromatographic separation was achieved under following conditions: sample injection volume, 50-150  $\mu$ L; temperature, 50°C; flow rate, 1.8 mL/min; mobile phase, acetonitrile (30% or 38%)-0.1 M pH 6 phosphate buffer; UV detection at 226 nm. The retention time of etodolac was 5.0 min with both the columns. The method was linear in the 1-10  $\mu$ g/mL (low) and 5-50  $\mu$ g/mL (high) concentration ranges, and the limit of detection was 0.2  $\mu$ g/mL. The specificity of the method was demonstrated by a lack of response with control sera, sera spiked with etodolac congeners, and sera from rats treated with other drugs that may be administered concurrently.

The method of Cosyns *et al* [28] was modified with fluorescence detection to increase sensitivity [18]. The plasma extraction procedure and HPLC

conditions were the same, with the exception of fluorescence detection with excitation at 280 nm and emission at 350 nm. This method was linear over 0.018 to 1.11  $\mu\text{g/mL}$  range. Method precision ranged from 1.7% to 5.8 %, and the mean recovery of the method was 103.1%.

An isocratic HPLC method for screening plasma samples for sixteen different non-steroidal anti-inflammatory drugs (including etodolac) has been developed [29]. The extraction efficiency from plasma was 98%. Plasma samples (100-500  $\mu\text{L}$ ) were spiked with internal standard {(benzoyl-4-phenyl)-2-butyric acid} and 1 M HCl and were extracted with diethyl ether. The organic phase was separated, evaporated, the dry residue reconstituted in mobile phase (acetonitrile-0.3% acetic acid-tetrahydrofuran, in a 36:63.1:0.9 v/v ratio), and injected on a reverse-phase ODS 300 x 3.9 mm i.d. column heated to 40°C. A flow rate of 1 mL/min was used, and UV detection at 254 nm was used for quantitation. The retention time of etodolac was 30.0 minutes. The assay was found to be linear over the range of 0.2 to 100  $\mu\text{g/mL}$ , with a limit of detection of 0.1  $\mu\text{g/mL}$ . The coefficients of variation for precision and reproducibility were 2.9% and 6.0%, respectively. Less than 1% variability for intra-day, and less than 5% for inter-day, in retention times was obtained. The effect of various factors, such as, different organic solvents for extraction, pH of mobile phase, proportion of acetonitrile and THF in mobile phase, column temperature, and different detection wavelengths on the extraction and separation of analytes was studied.

A reverse-phase microbore HPLC method with photodiode-array detection and UV spectral library was developed for toxicological screening of various drugs in plasma including etodolac and its methyl ester [30]. Sample preparation involved addition of prazepam (internal standard) to 500  $\mu\text{L}$  of plasma followed by addition of 30  $\mu\text{L}$  of 1M sodium hydroxide and 5 mL of dichloromethane. After shaking the sample for 1 minute and centrifuging, the upper aqueous layer was discarded. The organic phase was evaporated and reconstituted with 50  $\mu\text{L}$  methanol and 20  $\mu\text{L}$  water; 10  $\mu\text{L}$  was injected into the HPLC system. The HPLC system consisted of 20-mm precolumn, 100-mm column containing Hypersil ODS (2.1 mm i.d.), thermostatted to 40°C. The analysis was performed using a mixture of 20 mM phosphate buffer containing 500  $\mu\text{L}$  of triethylamine per liter of (Solvent A) and acetonitrile (Solvent B) maintained at a flow rate of 0.4 mL/min. Gradient elution with acetonitrile varying from 15% to 80% over 16 min was used. Absorbance was recorded at 210, 230, and 254 nm.

Etodolac and etodolac methyl ester were found to have retention times of 7.4 and 14.2 minutes, respectively. However, no information on the quantitation of the drug was presented.

An HPLC method to determine etodolac during *in vitro* studies was developed [31]. Plasma was precipitated with acetonitrile, evaporated to dryness, and reconstitution in 25% acetonitrile. The HPLC consisted of a guard column, a 4 x 150 mm (5  $\mu$ m particles) C<sub>18</sub> column, and UV detection at 280 nm. The mobile phase was methanol / 0.01 M trifluoroacetic acid (25:75, v/v) at 1 mL/min. Etodolac was located at a retention time of 15.2 minutes.

An HPLC method to determine racemic etodolac and its major metabolites in urine using a reverse-phase column has been developed [13]. Determination of etodolac in urine involved acidifying the diluted urine before extraction with cyclohexane-ethyl acetate (95:5, v/v). The organic layer was separated, evaporated, and reconstituted in solution of ibuprofen in acetonitrile (internal standard). The samples were injected onto a LiChrosper 100 RP-18 25 cm x 4 mm i.d., (5  $\mu$ m particle size) column. The mobile phase was 0.05 M pH 4 phosphate buffer / acetonitrile (55:45, v/v) at a flow rate of 1.3 mL/min. Detection was carried out at 220 nm with a UV detector. The retention times were 12.5 and 16.9 minutes for etodolac and ibuprofen, respectively. The method was linear over a concentration range of 0.125 to 10.0  $\mu$ g/mL. The recovery of etodolac was 93.9 % ( $\pm$  5.3 %). Detailed methods for the analysis of metabolites of etodolac were also provided.

An HPLC method for the analysis of etodolac and its metabolites in equine serum and urine was developed [32]. Serum (1 mL) or urine (0.5 mL) samples were extracted with iso-octane/isopropanol (95:5, v/v) after addition of ibuprofen as internal standard, diluting with 1 or 2 mL of distilled water, and adjusting the pH to 1 with 1 M HCl. The organic layer was evaporated under a stream of nitrogen, the residue dissolved in 100  $\mu$ L of mobile phase, and a 20  $\mu$ L aliquot injected on to the HPLC system. The HPLC system consisted of a pre-column, a 250 x 4 mm (7  $\mu$ m particles) LiChrosorb RP-18 column at 25°C, isocratic elution with 1% acetic acid/acetonitrile (50:50, v/v) at a flow rate of 1.3 mL/min, and UV detector at 227 nm. The retention time of etodolac was 8.5 minutes. The method was linear over the range of 0.1-20  $\mu$ g/mL in serum, and in 0.5-800  $\mu$ g/mL range in urine. The limits of quantitation were 40 ng/mL in

serum and 0.4  $\mu\text{g/mL}$  in urine. The recovery of etodolac from serum ranged from 89% to 108%, and from 96% to 108% from urine. The method was judged to be precise and accurate for the quantitation of etodolac in serum and urine.

The same article just cited [32] also presented an LC-MS method for the analysis of etodolac metabolites in urine. The LC-MS system consisted of a pre-column, a 125 x 4 mm (5- $\mu\text{m}$  particle size) LiChrosorb RP-18 column at ambient temperature, isocratic elution with 1% acetic acid/acetonitrile (50:50, v/v) at a flow rate of 1 mL/min, and a triple quadrupole mass spectrometer system using atmospheric pressure chemical ionization (heated nebulizer) interface. The pressure of the nebulizing gas (nitrogen), and the temperature of the heated nebulizer interface, were 80 psi and 500  $^{\circ}\text{C}$ , respectively. The auxiliary nitrogen gas was delivered at 2 L/min, and the curtain gas was delivered at flow rate of 0.8 mL/min. Other MS parameters included an orifice potential of -50 V, negative ionization at -3  $\mu\text{A}$ , and MS-MS using collision-induced dissociation (CID) at -20 V. The MS was operated either in Q1 scan or CID mode. The LC-MS analysis in Q1 scan mode over a  $m/z$  50-400 range showed an intense ion at  $m/z$  at 286. The CID showed a strong ion at  $m/z$  at 286, and two intense fragments having  $m/z$  242 and 212.

A GS-MS method for the analysis of etodolac in human plasma has been developed [16]. Plasma samples were spiked with meclofenamic acid (the internal standard), acidified with 5N HCl, and extracted twice with chloroform / dichloromethane / hexane (50:25:25, v/v). The organic phase was evaporated, the residue methylated with ethereal diazomethane, dried again, and reconstituted in hexane. Analytical separation was performed on a 15 m x 0.24 mm i.d., 0.25  $\mu\text{m}$  film thickness, fused silica capillary column. The oven temperature was variable (150 to 260 $^{\circ}\text{C}$ ) and the injector was at 260 $^{\circ}\text{C}$ . The carrier gas was helium at 1 mL/min. Mass spectra were obtained using positive electron impact ionization (70 eV) at  $m/z$  228 for etodolac. The method was linear in the 1-10 ng/mL (low) and 10-100 ng/mL (high) concentration range. The detection limit was 0.5 ng/mL in plasma, and recovery of etodolac from plasma sample exceeded 92%.

The capillary chromatography method previously described [26, 27], has also been used for the analysis in the etodolac and its metabolites in urine.

The urine samples were extracted with ethyl acetate, and analyzed using different capillary chromatographic procedures.

#### 4.3.2 Enantiomeric Separation Methods

An HPLC method to determine etodolac enantiomers and their major metabolites in urine, using a bovine serum albumin stationary phase, has been developed [13]. After extraction of etodolac from acidified urine with cyclohexane / ethyl acetate (95:5, v/v), the organic layer was separated, evaporated, and reconstituted in 2-propanol. The samples were injected onto a 125 x 4 mm i.d. (10  $\mu$ m particles) column. The mobile phase used was 0.05 M pH 4 phosphate buffer / 2-propanol (98:2, v/v) at a flow rate of 1.2 mL/min. Detection was effected at 230 nm using a UV detector. The (*S*)-(+)-etodolac enantiomer eluted before the (*R*)-(-)-enantiomer. The enantiomeric analysis of various metabolites of etodolac was also described.

A stereospecific HPLC assay for the pharmacokinetic analysis of etodolac enantiomers in human plasma has been developed [33]. Sample preparation involved addition of an internal standard, ( $\pm$ )-2-(4-benzoylphenyl)butyric acid, to 0.5 mL of plasma, followed by extraction with isooctane / isopropanol (95:5). The organic layer was evaporated, and etodolac and internal standard derivatized with ethyl chloroformate and (*L*)- $\alpha$ -phenylethylamine. The diastereomers were then extracted and chromatographed on a normal phase Partisil 5 Silica (25 cm x 4.6 mm; 5- $\mu$ m particles) column, with a mobile phase consisting of hexane / ethyl acetate / isopropanol (85:15:0.2) at a flow rate of 2 mL/min. The etodolac diastereomers were separated with a resolution factor of 6.4, and detected using a UV detector at a wavelength of 280 nm. The method was linear over the range of 0.2-20 mg/L, with intra- and inter-day variations being less than 10%. The extraction efficiency for the etodolac enantiomers exceeded 90%. Application of this method for conjugated etodolac esters in plasma and urine was described.

The potential contamination from either stereochemical impurities or stereochemical inversion of NSAID'S (such as etodolac) that might take place when using ethyl chloroformate as the derivatizing agent in the sample preparation described above [33] was investigated in a separate study [34]. The study concluded that the extent of stereochemical conversion induced by assay procedures was small (approximately 1%) for

etodolac, and that it would not significantly contribute to analytical error in the absence of large differences in concentrations of the enantiomers.

A stereoselective GC method for determination of etodolac enantiomers in human plasma and urine was first reported as a preliminary method [35], and then as a validated method [36]. Sample preparation involved addition of (*S*)-(+)-naproxen (internal standard) and sodium hydroxide to diluted plasma or urine. The samples were washed with diethyl ether, acidified with hydrochloric acid, and extracted with toluene. (*S*)-(+)-naproxen was used as a derivatizing agent to form diastereomeric derivatives of etodolac. The gas chromatograph system used in this work was equipped with fused-silica capillary column (12 m x 0.2 mm i.d.) coated with high-performance cross-linked methylsilicone film (thickness 0.33  $\mu\text{m}$ ) and a nitrogen-phosphorous detector. The operating conditions were: injector 250°C; detector 300°C; column 100-260°C (32 °C/min). The gas flow rates were: helium 2 mL/min; hydrogen 3 mL/min; air 50 mL/min. The column head pressure was maintained at 0.85 bar. GC peaks representing diastereomers of (+)- and (–)-etodolac eluted at 17.5 and 19.8 min, respectively. The derivatized internal standard had a retention time of 12.5 min. The calibration curves for each enantiomer were linear over the concentration range of 0.25 - 20  $\mu\text{g/mL}$ . The minimum quantifiable concentration of each enantiomer was 50 ng/mL, with observed coefficients of variation being within 8%. The recoveries from plasma for (+)- and (–)-etodolac at concentrations of 2.5  $\mu\text{g/mL}$  were  $66.50 \pm 0.04\%$  and  $65.83 \pm 0.03\%$ , respectively.

## 5. Stability

### 5.1 Solution-Phase Stability

The extent and mechanism of degradation of etodolac, as a function of pH and temperature, has been studied [23]. The three main degradation products of etodolac were 7-ethyl-2-(1-methylenepropyl)-1H-indole-3-ethanol, 1,8-diethyl-1-methyl-1,3,4,9-tetrahydropyrano-[3,4-*b*]indole, and 7-ethyltryptophol. No appreciable effect on the degradation of etodolac was observed in several buffer systems. The log  $k_{\text{app}}$ -pH profiles for degradation of etodolac at various temperatures are shown in Figure 9.



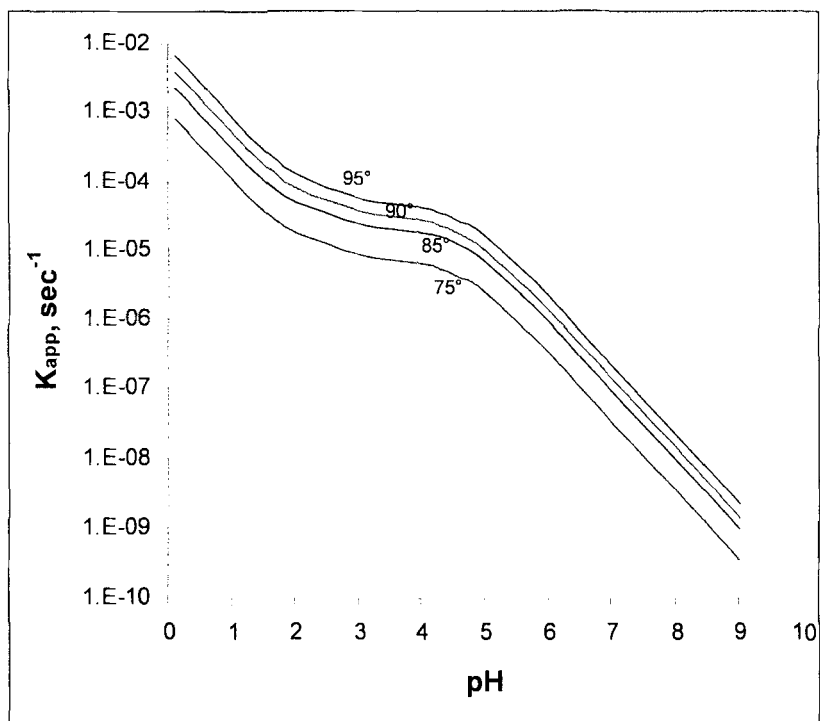


Figure 9. The pH-rate profiles for degradation of etodolac at various temperatures.

The profiles show that the apparent first-order rate constant ( $k_{app}$ ) for the degradation of etodolac rapidly decreases linearly with increasing pH from 0 to 2, then slowly decreases from 2.5 to 5.0, and finally rapidly decreases linearly with increasing pH above 5.0. Since the slopes of the straight line portions are close to unity, these two regions are associated with specific acid catalysis. The inflection in the pH range of 3 to 5 indicates that ionization of the carboxylic group ( $pK_a = 4.65$ ) exerted an effect on the rate of degradation. The log  $k_{app}$ -pH profile can be expressed by the following rate law:

$$k_{app} = (k_H \alpha_H^2 + k'_H K_a \alpha_H) / (K_a + \alpha_H)$$

where  $k_H$  and  $k'_H$  are second-order rate constants for the hydrogen ion-catalyzed degradation of undissociated and dissociated fractions of etodolac and  $K_a$  is the ionization constant ( $2.24 \times 10^{-5}$ ). Using Arrhenius plots, the activation energies for  $k_H$  and  $k'_H$  were found to be 26 and 24 kcal/mol, respectively. The mechanisms for the acid catalyzed degradation of etodolac have been postulated.

## 5.2 Stability in Biological Fluids

When added to pooled serum and kept for up to 7 days at room temperature (20°C) or under refrigerated conditions (4°C), etodolac showed no significant loss of drug [28]. The stability of test-tube standards and extracted spiked control serum standards was also investigated in this work. The peak height response of the test tube standard declined from 100.0 to 91.5% in 1 hour, while the extracts from spiked control serum remained unchanged.

The stability of etodolac in equine serum and urine was studied under various temperatures (freezing, refrigerated, and room temperatures) for up to 45 days [32]. Etodolac was stable in urine and serum under frozen condition for 45 days, at refrigerated temperature for 30 days (7 days for urine). At room temperature, etodolac was stable in serum for up to 7 days, whereas it was stable in urine for 2 days. Etodolac serum and urine samples also showed stability through 5 freeze-thaw cycles.

## 6. Drug Metabolism and Pharmacokinetics

The pharmacokinetics of etodolac have been extensively studied [4, 37-38]. Etodolac possesses a chiral center, and it has been established that the (*S*)-(+)-etodolac enantiomer possesses almost all of the anti-inflammatory property. Pharmacokinetic properties of the non-stereospecific and stereospecific etodolac are described in the following sections

### 6.1 Adsorption

Etodolac is rapidly absorbed after oral administration. The maximal plasma concentrations ( $C_{\max}$ ) of etodolac are achieved within 1 to 2 hours of administration of tablets or capsules in healthy subjects [38]. The time to maximal plasma concentration ( $t_{\max}$ ) increases to approximately 8 hours with the sustained release formulation [18]. Absorption of an oral solution proceeds rapidly with a  $t_{\max}$  of 0.5 hour [18, 39]. The two enantiomers of etodolac show similar  $t_{\max}$  values [40].

Etodolac achieves a  $C_{\max}$  of 15 to 20  $\mu\text{g/mL}$  following a 200-mg oral dose [38]. With sustained release products, mean  $C_{\max}$  values of 4.6, 7.5, and 11.9  $\mu\text{g/mL}$  were observed following administration of doses of 200, 400, and 600 mg, respectively [18]. The  $C_{\max}$  after rectal administration of a 200-mg dose was 13.6  $\mu\text{g/mL}$  [41, 42]. The  $C_{\max}$  of (*R*)-etodolac is significantly higher than that of (*S*)-etodolac following a single oral dose of racemic etodolac [40]. The exposure to (*R*)-etodolac was also greater than 10-fold as compared to (*S*)-etodolac.

The bioavailability of sustained released formulation of etodolac is about 80% of that of an oral solution in healthy male subjects [18]. Etodolac from tablets and capsules is 100% bioavailable relative to oral solution [39], and is 100% bioavailable from suppositories as compared to tablets [42]. Etodolac does not show accumulation after repeated 200 mg doses in young subjects [39]. The pharmacokinetics of etodolac exhibit dose proportionality over the 100-300 mg dose range for immediate release formulations [18]. Single doses of etodolac ranging from 400 mg to 1600 mg showed dose-dependent increases in area under the concentration time curve (AUC) of etodolac in serum [21]. The sustained release formulation was found to yield dose proportionality in the 200-600 mg range [18].

## 6.2 Distribution

The mean apparent volume of distribution (Vd/F) of etodolac after oral administration is about 0.3 to 0.5 L/kg [38]. The Vd/F values for (*S*)-etodolac are 7.5-fold greater than those of R-etodolac [33, 40].

Etodolac is highly protein bound (greater than 95%) [38]. At low concentrations, the (*R*)-etodolac enantiomer shows higher protein binding than does the (*S*)-etodolac enantiomer. Interestingly, the opposite is true at higher concentrations [43].

Etodolac distributes well into synovial fluid, the proposed primary site of action of NSAID's. Following multiple doses of 200 mg twice daily for 7 days, the  $C_{\max}$  in synovial fluid was 2.6  $\mu\text{g/mL}$  and the  $t_{\max}$  was 3.2 hours [44]. The synovial fluid AUC of total etodolac was about 67% of the serum values [44]. The AUC of the unbound etodolac was 172% of the serum values. After a single 200 mg dose of etodolac, the ratio of (*S*)-etodolac to (*R*)-etodolac in six subjects with rheumatoid arthritis was 0.074 in plasma and 0.17 in synovial fluid [45].

## 6.3 Metabolism

In humans, etodolac is extensively metabolized, with almost no intact drug being recovered in urine [15]. Etodolac does not undergo significant first pass metabolism following oral administration. In humans, etodolac is metabolized mainly to 5 metabolites: acyl glucuronide; 6-hydroxyetodolac; 7-hydroxyetodolac; 8-(1'-hydroxyethyl)-etodolac; 4-ureido-etodolac [15, 46]. The metabolites further form glucuronide conjugates.

In serum, 90% of radiolabeled drug was found as unconjugated etodolac, of which 70% to 80% was present as unchanged etodolac, 10% as 7-hydroxy-etodolac, and 1% to 2% as 6-hydroxy-etodolac [15]. In urine, less than 5% of the dose is unconjugated etodolac, and 20% is the conjugated etodolac glucuronide. The hydroxy metabolites (6-, 7-, 8-(hydroxyethyl)-) of etodolac together account for about 46% of the dose [15]. The 4-ureido- metabolite accounts for 8% of the dose in urine.

No significant stereoselectivity in etodolac enantiomeric metabolism was noted in a 24 hour urine recovery study [40]. Analytical methods for the

determination of metabolites of etodolac in human plasma and urine are available [13, 26-27, 47].

The rate of metabolism of the (*S*)-enantiomer was higher than that of the (*R*)-enantiomer as indicated by its higher oral clearance [40].

#### 6.4 Elimination

Etodolac shows a terminal elimination half-life of 6 to 8 hours following administration of capsules, tablets, sustained-release formulation, and suppositories [38]. The elimination of etodolac is not dose dependent. The AUC increases in a dose dependent manner for 200 to 1600 mg single doses [21]. Individual enantiomers show similar half-lives [40]. Following radiolabeled etodolac administration, 69% to 76% of the dose was recovered in urine over 7 days. Urine and feces together accounted for 80% to 92% of dose [15]. Biliary excretion is a minor route for the elimination of etodolac [40].

#### 7. References

1. L.G. Humber, *Medicinal Res. Rev.*, **7**, 1-28 (1987).
2. G. Spencer-Green, *J Rheumatol.*, **24** (Suppl. 47), 3-9 (1997).
3. T.J. Schnitzer and G. Constantine, *J Rheumatol.*, **24** (Suppl. 47), 23-31 (1997).
4. L. Humber, *Drugs of Today*, **29**, 265-293 (1993).
5. C.A. Demerson, L.G. Humber, T.A. Dobson, and R.R. Martel, *J. Med. Chem.*, **18**, 189-191 (1975).
6. C.A. Demerson, L.G. Humber, A.H. Philipp, and R.R. Martel, *J. Med. Chem.*, **19**, 391-395 (1976).
7. E.S. Ferdinandi, D.R. Hicks, W. Verbestal, and R. Raman, *J. Label Comp. Radiopharm.*, **14**, 411-425 (1978).

8. L.G. Humber, E. Ferdinandi, C.A. Demerson, S. Ahmed, U. Shah, D. Mobilio, J. Sabatucci, B. DeLange, F. Labbadia, P. Hughes, J. DeVirgilio, G. Neuman, T.T.Chau, and B.M. Weichman, *J. Med. Chem.*, **31**, 1712-1719 (1988).
9. L.G. Humber, C.A. Demerson, P. Swaminathan, and P.H. Bird, *J. Med. Chem.*, **29**, 871-874 (1986).
10. C.A. Demerson, L.A. Humber, N.A. Abraham, G. Schilling, R.R. Martel, and C. Pace-Asciak, *J. Med. Chem.*, **26**, 1778-1780 (1983).
11. Y. Özkan, N. Doğanay, N. Dikmen, and A. Işkin, *Il Farmaco.*, **55**, 433-438 (2000).
12. J. Zawadzki, H.-K. Lee, R. DeNeale, and R. Enever, *J. Pharm. Sci.*, **80**, 559-563 (1991).
13. U. Becker-Scharfenkamp and G. Blaschke, *J. Chromatogr.*, **621**, 199-207 (1993).
14. D. Marini, G. Pollino, and F. Balestrieri, *Boll. Chim. Farm.*, **127**, 182-187 (1988).
15. E.S. Ferdinandi, S.N. Sehgal, C.A. Demerson, J. Dubuc, J. Zilber, D. Dvornik, and M.N. Cayen, *Xenobiotica*, **16**, 153-166 (1986).
16. C. Giachetti, A. Assandri, G. Zanolio, and E. Brembilla, *Biomed. Chromatogr.*, **8**, 180-183 (1994).
17. M. Dey, R. Enever, M. KramL, D. G. Prue, D. Smith, and R. Weierstall, *Pharm. Res.*, **10**, 1295-1300 (1993).
18. M. Dey, R. Enever, M. Marino, J. Michelucci, D. Smith, R. Warner, and R. Weierstall, *Int. J. Pharm.*, **49**, 121-128 (1989).
19. N.M. El Kousy, *J. Pharm. Biomed. Anal.*, **20**, 185-194 (1999).
20. W.T. Robinson, M. KramL, E. Greselin, and D. Dvornik, *Xenobiotica*, **7**, 329-337 (1977).
21. M.N. Cayen, M. KramL, E.S. Ferdinandi, E. Greselin, and D. Dvornik, *Drug Metab. Reviews*, **12**, 339-362 (1981).

22. R. Ficarra, P. Ficarra, M.L. Calabro, and D. Costantino, *II Farmaco.*, **46**, 403-407 (1991).
23. Y.J. Lee, J. Padula, and H.-K. Lee, *J. Pharm. Sci.*, **77**, 81-86 (1988).
24. W. H. Pirkle and P.G. Murray, *J. Liquid Chromatogr.*, **13**, 2123-2134 (1990).
25. S. Caccamese, *Chirality*, **5**, 164-167 (1993).
26. D.B. Strickman and G. Blaschke, *J. Chromatogr. B*, **748**, 213-219 (2000).
27. D.B. Strickman, B. Chankvetadze, G. Blaschke G.C. Desiderio, and S. Fanali, *J. Chromatogr. A*, **887**, 393-407 (2000).
28. L. Cosyns, M. Spain, and M. KramL, *J. Pharm. Sci.*, **72**, 275-277 (1983).
29. F. Lapique, P. Netter, B. Bannwarth, P. Trechot, P. Gillet, H. Lambert, and R.J. Royer, *J. Chromatogr.*, **496**, 301-320 (1989).
30. T. Turcant, A. Premel-Cabic, A. Cailleux, and P. Allain, *Clin. Chem.*, **37**, 1210-1215 (1991).
31. P.C. Smith, W.Q. Song, and R.J. Rodriguez, *Drug Metab. Dispos.*, **20**, 962-965 (1992).
32. M.R. Koupai-Abyazani, B. Esaw, and B. Laviolette, *J. Anal. Toxicol.*, **23**, 200-209 (1999).
33. F. Jamali, R. Mehver, C. Lemko, and O. Eradiri, *J. Pharm. Sci.*, **77**, 963-966 (1988).
34. M.R. Wright and J. Fakhreddin, *J. Chromatogr.*, **616**, 59-65 (1993).
35. N.N. Singh, F.M. Pasutto, R.T. Coutts, and F. Jamali, *J. Chromatogr.*, **378**, 125-135 (1986).

36. N.N. Singh, F. Jamali, F.M. Pasutto, and R.T. Coutts, *J. Chromatogr.*, **382**, 331-337 (1986).
37. D.C. Brater, and K. Lasseter, *Clin. Rheumat. Suppl.*, **1**, 25-35 (1989).
38. D.R. Brocks and F. Jamali, *Clin. Pharmacokinet.*, **26**, 259-274 (1994).
39. M. KramL, L. Coysns, D.R. Hicks, J. Simon, J.F. Mullane, and D. Dvornik, *Biopharm. Drug Dispos.*, **5**, 63-74 (1984).
40. D.R. Brocks, F. Jamali, A. S. Russell, and K. J. Skeith, *J. Clin. Pharmacol.*, **32**, 982-989 (1992).
41. R. Cadorniga, R. Herrero, E. Barcia, I.T. Molina, J.A. Guitierrez, J.L. Fabregas, and A. Martineztobed, *Eur. J. Drug Metab. Pharmacokinetics Suppl.*, **16**, 389-96 (1991).
42. T. Molina-Martinez, R. Herrero, J.A. Gutierrez, J.M. Iglesias, J.L. Fabregas, A. Martinez-Tobed, and R. Cadorniga, *J. Pharm. Sci.*, **82**, 211-213 (1993).
43. N. Muller, F. Lapique, C. Monot, E. Payan, R. Dropsy, and P. Netter, *Chirality*, **4**, 240-246 (1992).
44. M. KramL, D.R. Hicks, M. McKean, J. Panagides, and J. Furst, *Clin. Pharmacol. Therap.*, **43**, 571-576 (1988).
45. D.R. Brocks, F. Jamali, and A.S. Russell, *J. Clin. Pharmacol.*, **31**, 741-746 (1991).
46. E.S. Ferndinandi, D. Cochran, and R. Gedamke, *Drug Metab. Dispos.*, **15**, 921-924 (1987).
47. U. Berendes and G. Blaschke, *Enantiomer*, **1**, 415-422 (1996).



This Page Intentionally Left Blank

# EUGENOL

Mochammad Yuwono<sup>1</sup>, Siswandono<sup>1</sup>, Achmad Fuad Hafid<sup>1</sup>,

Achmad Toto Poernomo<sup>1</sup>, Mangestuti Agil<sup>1</sup>,

Gunawan Indrayanto<sup>1</sup>, and Siegfried Ebel<sup>2</sup>

(1) Faculty of Pharmacy  
Airlangga University  
Jl. Dharmawangsa dalam  
Surabaya 60286  
Indonesia

(2) Department of Pharmacy  
University of Würzburg  
Am Hubland,  
D-97074 Würzburg  
Germany

## **Contents**

### **1. Description**

- 1.1 Nomenclature
  - 1.1.1 Systematic Chemical Names
  - 1.1.2 Nonproprietary Names
- 1.2 Formulae
  - 1.2.1 Empirical Formula, Molecular Weight, CAS Number
  - 1.2.2 Structural Formula
- 1.3 Elemental Analysis
- 1.4 Appearance
- 1.5 Uses and Applications

### **2. Methods of Preparation**

- 2.1 Isolation from Natural Sources
- 2.2 Biosynthesis
- 2.3. Chemistry
  - 2.3.1 Isomerization
  - 23.2 Methylation

### **3. Physical Properties**

- 3.1 Ionization Constant
- 3.2 Solubility Characteristics
- 3.3 Phenol Coefficient
- 3.4 Density and Specific Gravity
- 3.5 Refractive Index
- 3.6 Thermal Properties
  - 3.6.1 Melting Behavior
  - 3.6.2 Boiling Point
  - 3.6.3 Volatility
  - 3.6.4 Flammability
- 3.7 Spectroscopy
  - 3.7.1 UV/VIS Spectroscopy
  - 3.7.2 Vibrational Spectroscopy
  - 3.7.3 Nuclear Magnetic Resonance Spectrometry
    - 3.7.3.1  $^1\text{H}$ -NMR Spectrum
    - 3.7.3.2  $^{13}\text{C}$ -NMR Spectrum
- 3.8 Mass Spectrometry

**4. Methods of Analysis****4.1 Compendial Tests**

4.1.1 Specific Gravity

4.1.2 Distilling Range

4.1.3 Refractive Index

4.1.4 Heavy Metals

4.1.5 Hydrocarbons

4.1.6 Limit of Phenol

**4.2 Chromatographic Methods of Analysis**

4.2.1 Thin Layer Chromatography

4.2.2 High Performance Liquid Chromatography

4.2.3 Gas Chromatography

**4.3 Supercritical Fluid Methods****5. Stability****6. Absorption, Distribution, and Excretion****7. Pharmacological Action****8. Toxicity****9. References**

## 1. Description

### 1.1 Nomenclature

#### 1.1.1 Systematic Chemical Names

4-Allyl-2-methoxyphenol [1-4]

Phenol, 2-methoxy-4-(2-propenyl) [5]

#### 1.1.2 Nonproprietary Names [1-4]

Eugenol; 4-Allylcatechol-2-methyl ether, 4-Allylguaiacol, 1-Allyl-4-hydroxy-3-methoxybenzene, 4-Allyl-1-hydroxy-2-methoxybenzene, 4-Allyl-2-methoxyphenol, Caryophyllic acid, Eugenol, Eugenol, p-Eugenol, FEMA No. 2467, 1-Hydroxy-4-allyl-2-methoxybenzene, 1-Hydroxy-2-methoxy-4-allylbenzene, 1-Hydroxy-2-methoxy-4-propenylbenzene, 1-Hydroxy-2-methoxy-4-prop-2-enylbenzene, 4-Hydroxy-3-methoxyallylbenzene, 2-Methoxy-4-Allylphenol, 2-Methoxy-1-hydroxy-4-allylbenzene, 2-Methoxy-4-prop-2-enylphenol, 2-Methoxy-4-(2-propenyl)phenol, 2-Methoxy-4-(2-propen-1-yl)phenol, NCI-C50453, FA 100, Allylguaiacol, synthetic eugenol, 1-Allyl-4-hydroxy-3-methoxybenzene, 5-Allylguaiacol, 1-Hydroxy-2-methoxy-4-prop-2-enylbenzene and Phenol, 4-allyl-2-methoxy-

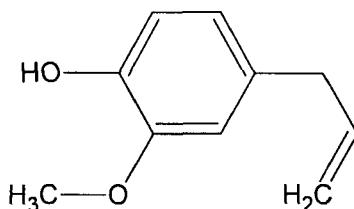
### 1.2 Formulae

#### 1.2.1 Empirical Formula, Molecular Weight, CAS Number

$C_{10}H_{12}O_2$  [MW = 164.201]

CAS number = 97-53-0

#### 1.2.2 Structural Formula



### 1.3 Elemental Analysis

The calculated elemental composition is as follows:

carbon:	73.15%
hydrogen:	7.37%
oxygen:	19.49%

### 1.4 Appearance

Eugenol is a clear, colorless, or pale yellow liquid. The substance has a strongly aromatic odor of clove, and a pungent, spicy taste. Upon exposure to air, it darkens and thickens [1, 3, 6].

### 1.5 Uses and Applications

Eugenol has been used since the nineteenth century as a flavoring agent in a variety of foods and pharmaceutical products. It has found use as a mild rubefacient in dentifrices, and as an obtundent for hypersensitive dentine, caries, or exposed pulp. Additional uses are in dental cement preparations, analgesics and anesthetics, and temporary dental filling when mixed with zinc oxide. The substance is also used in the perfumery or flavor industries, and also as insect attractant [1, 3, 4].

Eugenol has been used as a feedstock in the production of isoeugenol, which is needed in the manufacture of vanillin. Methylation of eugenol yields methyleugenol, which acts as a sex attractant for a certain type of fly (*Dacus dorsalis*) [7,8].

## 2. Methods of Preparation

### 2.1 Isolation from Natural Sources

Eugenol occurs in essential oils and is a major constituent of carnation, cinnamon, and clove oils. The substance is primarily obtained from the clove oil isolated from trees indigenous to the Molluca Islands, and which are also cultivated in other parts of Indonesia, Zanzibar, Madagascar, and Ceylon. Clove is rich in volatile oil (16-19% by weight), which can be obtained by distillation.

The main constituent of clove oil is eugenol (70-90%), acetyl eugenol (2-17%), and  $\beta$ -caryophyllen (5-12 %) [9-12]. Clove oil can be obtained from other parts of the tree, such as the buds, stem, or leaves. The eugenol content of clove oil depends upon the condition of the cloves and on the method of distillation [12].

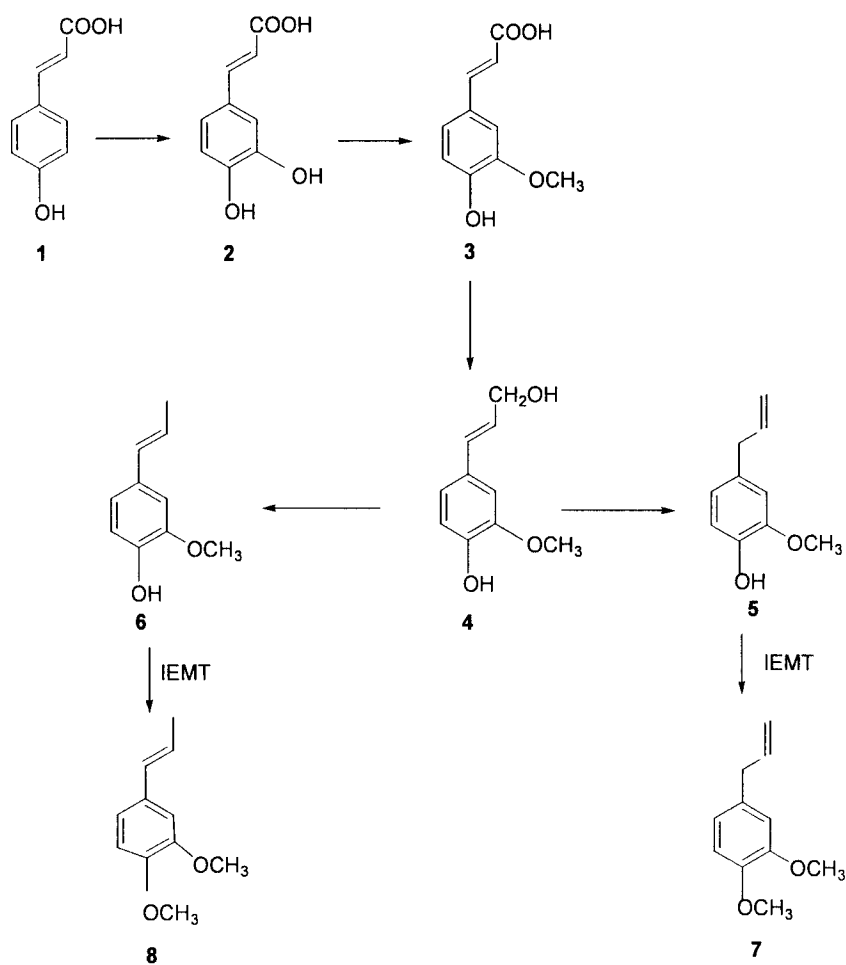
To obtain eugenol, clove oil is extracted further with alkali (10% NaOH). The alkaline extract is then separated by adding sulfuric acid, and further purification can be effected by distillation. The isolation procedure used to obtain eugenol from clove oil is as follows:

500 g distilled clove oil and 1.5 liter of 10% NaOH are stirred vigorously for 1 hour. The aqueous layer is then separated, and extracted three times with 200 mL petroleum ether (40:60, v/v). The extracts are then combined with the organic layer. Eugenol can be separated by acidification of the mixture to pH 3-4 with 10% sulfuric acid, and separation of the organic layer. The eugenol residual in the aqueous layer is recovered through extraction with 200 mL petroleum ether (40:60, v/v). The extract is combined with crude eugenol, and dried further over anhydrous  $\text{MgSO}_4$ . The yield is filtered and evaporated, and they subjected to vacuum distillation [12].

## 2.2 Biosynthesis

It was reported that the sweet fragrance of *Clarkia breweri* is, among others, caused by the presence of 4 phenyl propanoids, such as eugenol, isoeugenol, methyleugenol, and isomethyleugenol. Eugenol and isoeugenol are derived from the lignin precursors ferulic acid or coniferyl alcohol. The methylation of eugenol to methyleugenol, and isoeugenol to isomethyleugenol, is catalyzed by an *S*-adenosylmethionine dependent *O*-methyltransferase (IEMT) [18].

Scheme 1. Biosynthesis of eugenol and its derivatives.

1 = *p*-coumarate

2 = caffeinate

3 = ferrulate

4 = coniferyl alcohol

5 = eugenol

6 = isoeugenol

7 = Methyleugenol

8 = methylisoeugenol

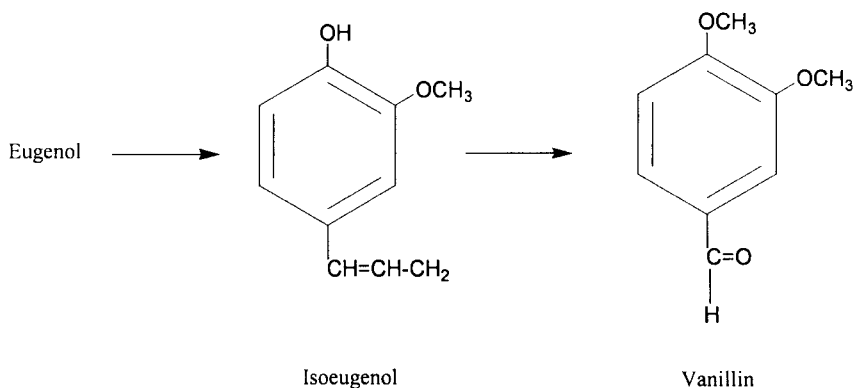
(modified from reference 13)



## 2.3. Chemistry

### 2.3.1 Isomerization

Since isoeugenol is the important intermediate in the vanillin production from eugenol, the isomerization of eugenol attracted a considerable amount of attention. The first report on the isomerization reaction appeared in 1891, in which Tiemann reported 50% conversion in 24 hours using an ethanolic KOH solution at 80°C [13].

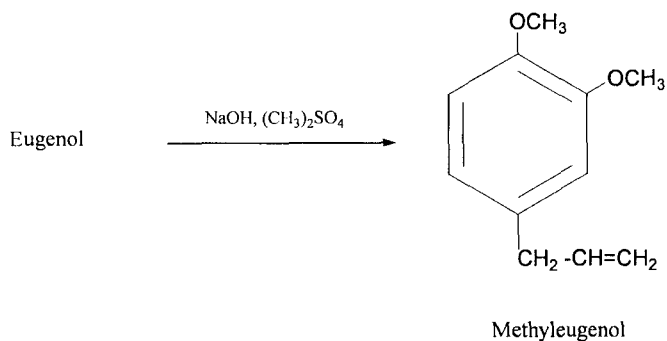


Peterson *et al* (1933) applied this method to study the kinetic of eugenol isomerization by chromatographic and spectroscopic techniques [14]. Lampman *et al* (1977) used the same alkaline solution method run in dimethyl sulfoxide, and obtained 80% conversion after 2 hours reaction at temperatures higher than 170°C [7]. Andrieux *et al* (1977) obtained 92% isoeugenol with 2 hours of reaction time using RhCl<sub>3</sub> as a catalyst run at 20 oC [15]. Isoeugenol could also be obtained by adding KOH and hexadecyl-tributylphosphonium bromide to clove oil at 150°C [16].

### 2.3.2 Methylation

Eugenol (82 g) is treated with NaOH solution (21 g in 200 mL water) with stirring in a 500 mL glass beaker. Dimethyl sulfate (83 g) solution was added slowly through a dropping funnel to achieve methylation. The organic layer was then separated, the water phase further extracted three times with ether, and then the organic layer was rendered anhydrous by adding anhydrous MgSO<sub>4</sub>. After the evaporation of the ether, the reaction

yielded crude methyleugenol (80.8 g = 90.5%). Pure methyleugenol was obtained by vacuum distillation [17].



### 3. Physical Properties

#### 3.1 Ionization Constant

Eugenol is characterized by a single ionizable group, for which the pKa has been reported to be 9.8 [6].

#### 3.2 Solubility Characteristics

The solubility of eugenol has been determined in a number of solvent systems, and the reported information is summarized in Table 1.

The filtrate of a 10% suspension in water has a pH of 4-7 [4].

#### 3.3 Phenol Coefficient

Eugenol has a phenol coefficient of 14.4 [19].

#### 3.4 Density and Specific Gravity

The density of eugenol has been reported to be 1.064 - 1.070 g/mL [3], as well as 1.064 - 1.068 g/mL [1,4]. The specific gravity has been reported as 1.0664 [1], as 1.0652 at 20/4°C [4], and as 1.067 at 25/25 °C [4].

Table 1

## Solubility Characteristics of Eugenol

Solvent System	Solubility
Water	practically insoluble [1]; Less than 1 mg/mL at 20°C [4]
70% Ethanol	1 mL in 2 mL [1,3]; Less than 1 mg/mL at 20°C [4]
95% Ethanol	More than 100 mg/mL at 21°C [4]
Dimethyl sulfoxide	More than 100 mg/mL at 21°C [4]
Acetone	More than 100 mg/mL at 21°C [4]
Benzene	More than 10% [4]
Alcohol, Chloroform, ether, oils	Miscible [1,4]
Volatile oils, glacial acetic acid, aqueous fixed alkali hydroxide solution and aqueous alkali	Soluble [1,4]

### 3.5 Refractive Index

The refractive index of eugenol has been variously reported as 1.540 - 1.542 at 20°C [3], 1.5416 [1], and 1.5410 [4].

### 3.6 Thermal Properties

#### 3.6.1 Melting Behavior

The melting point of eugenol has been reported as -9.2°C to 9.1°C [1, 4]

#### 3.6.2 Boiling Point

The boiling point of eugenol has been reported as 255°C at 760 torr, and 93 - 95°C at 10 torr [3]. The boiling point has also been reported as 254°C at 760 torr, and as 130.5°C at 10 torr [4, 5].

#### 3.6.3 Volatility

The vapor pressure of eugenol has been reported as 0.01 mmHg at 20°C; 0.03 mmHg at 25°C; 1 mmHg at 78.4 °C; 5 mmHg at 108.1 °C; 10 mmHg at 123.4 °C; 20 mmHg at 138.7 °C; 40 mmHg at 155.8 °C; 60 mm Hg at 167.3 °C; 100 mm Hg at 182.2 °C; 200 mmHg at 204.7 °C; 400 mmHg at 228.3 °C, and 760 mmHg at 253.5 °C [4]. These data have been plotted in Figure 1 on a logarithmic scale to illustrate the vapor pressure dependence upon temperature.

The vapor density of eugenol has been reported to exceed 1.0 [4].

#### 3.6.4 Flammability

Eugenol has a flash point of 104°C (219°F), and the substance is combustible. Fires involving eugenol can be controlled with a dry chemical, carbon dioxide, or Halon extinguisher, and a water spray may also be used [4].

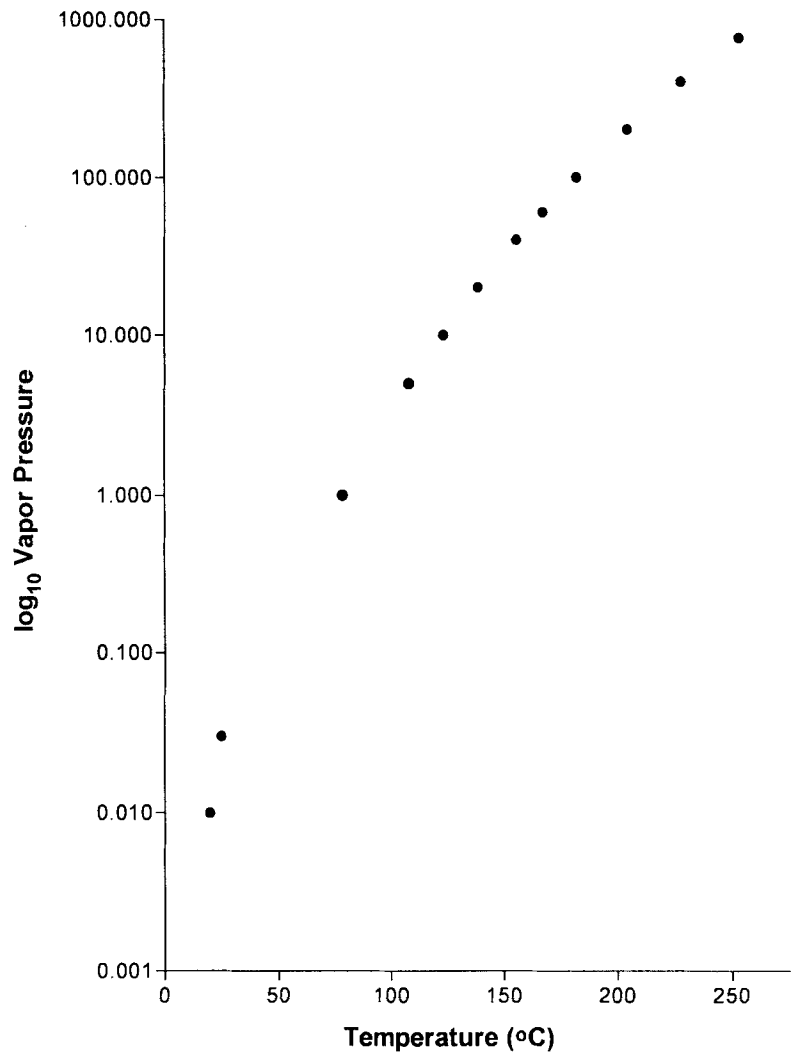


Figure 1. Vapor pressure of eugenol, plotted on a logarithmic scale.

### **3.7 Spectroscopy**

#### **3.7.1 UV/VIS Spectroscopy**

The ultraviolet absorption of eugenol was recorded on a HP 8452A diode array spectrophotometer. The spectrum obtained in alkaline solution (0.1 N NaOH) is shown in Figure 2, and was characterized by an absorption maximum at 296 nm. The E1%/1 cm parameters of alkaline aqueous solutions have been reported as 552 at 246 nm, and 262 at 296 nm in [6].

The spectrum obtained in ethanol is shown in Figure 3, and was characterized by absorption maxima at 232 and 282 nm. The E1%/1 cm parameters of ethanolic solutions have been reported as 406 at 232 nm, and 193 at 282 nm [6]. The absorption maxima of eugenol in 95% ethanol have also been reported as 281 nm and 230 nm [4].

#### **3.7.2 Vibrational Spectroscopy**

The infrared absorption spectrum of eugenol was recorded on a Jasco 5300 FTIR spectrophotometer, and is shown in Figure 4. Assignments for the diagnostic bands are given in Table 2.

#### **3.7.3 Nuclear Magnetic Resonance Spectrometry**

##### **3.7.3.1 <sup>1</sup>H-NMR Spectrum**

The <sup>1</sup>H-NMR spectrum of eugenol was obtained in deuterated chloroform, using a Hitachi R-1900 FT-NMR spectrometer, and with the chemical shifts being measured relative to tetramethylsilane. The spectrum is shown in Figure 5, and assignments for the observed band are given in Table 3.

##### **3.7.3.2 <sup>13</sup>C-NMR Spectrum**

The <sup>13</sup>C-NMR spectrum of eugenol was obtained in deuterated chloroform, using a Hitachi R-1900 FT-NMR spectrometer, and with the chemical shifts being measured relative to tetramethylsilane. The spectrum is shown in Figure 6, and assignments for the observed band are given in Table 4.

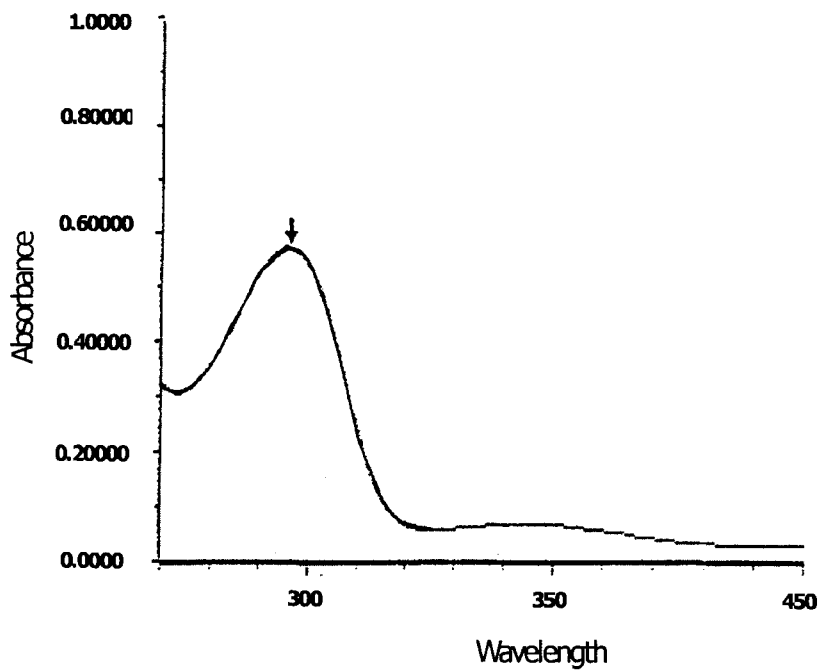


Figure 2. Ultraviolet absorption spectrum of eugenol in 0.1 N NaOH.

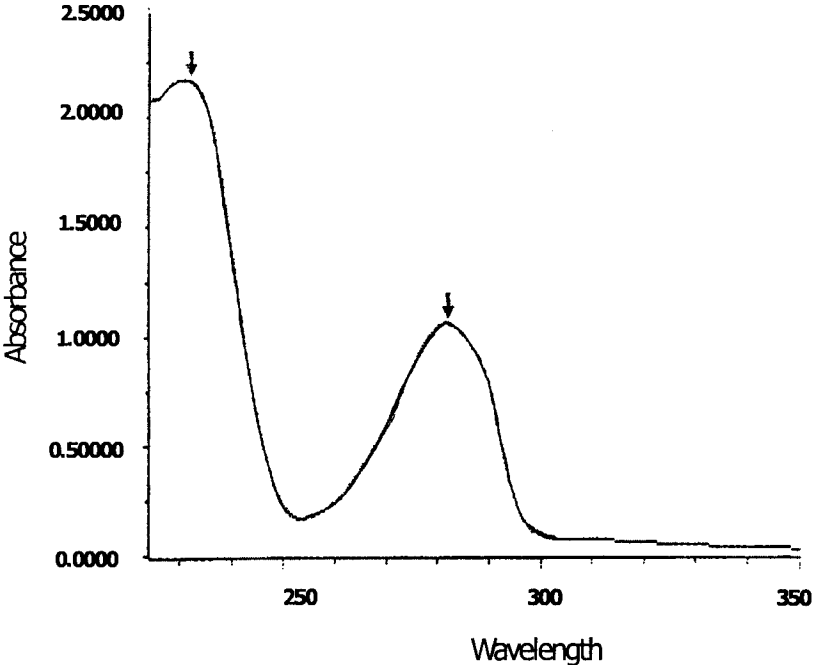
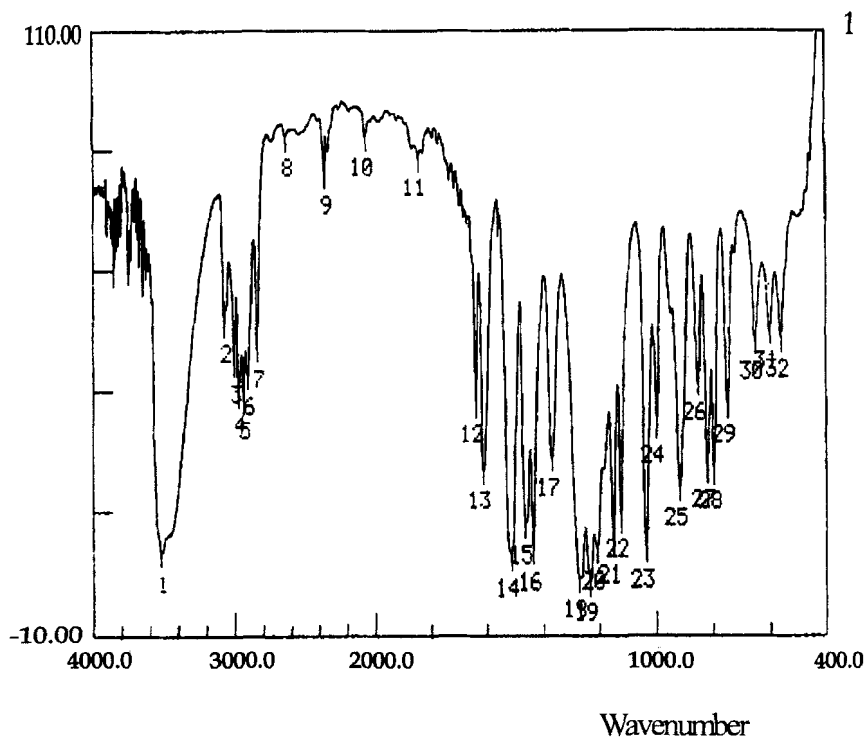


Figure 3. Ultraviolet absorption spectrum of eugenol in ethanol.

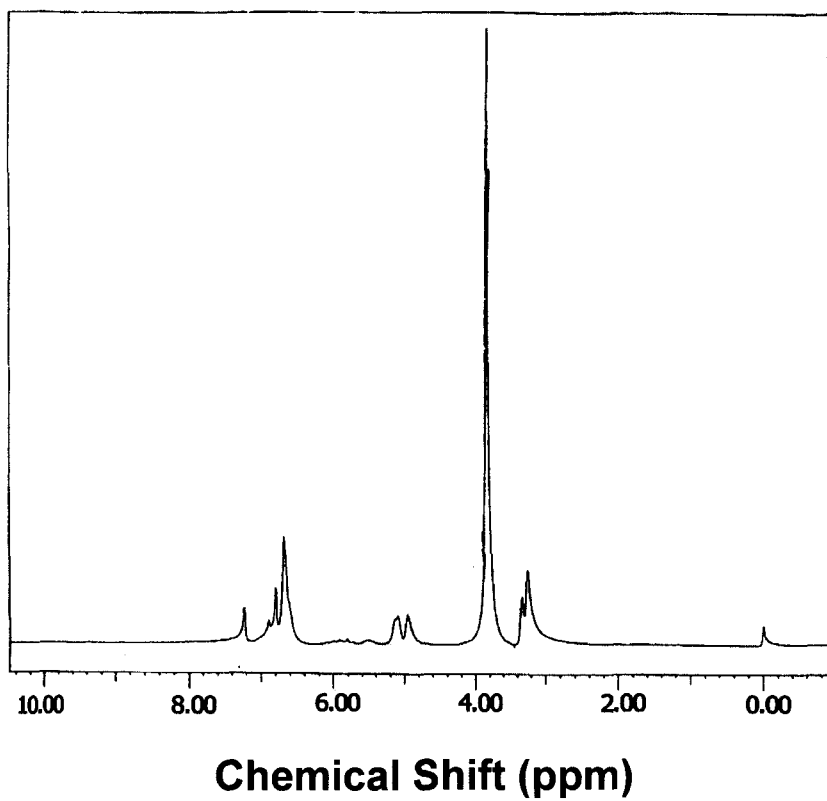


Figure 4. Infrared absorption spectrum, and band assignments, for eugenol.



Energy (cm <sup>-1</sup> )	Band Assignment
3600-3300	-OH
2900	-C-H, alkyl
1640	-C=C-, aromatic
1460	-OCH <sub>3</sub>
1000-900	-C=C-

Figure 5.  $^1\text{H}$ -NMR spectrum of eugenol in deuterio-chloroform.



Chemical Shift (ppm)	Multiplicity	Assignment
3.26-3.34	Doublet	$-\text{CH}_2$
3.85	Singlet	$-\text{OCH}_3-$
4.9-5.5	Multiplet	$=\text{CH}_2$
6.6-7.2	Multiplet	aromatic

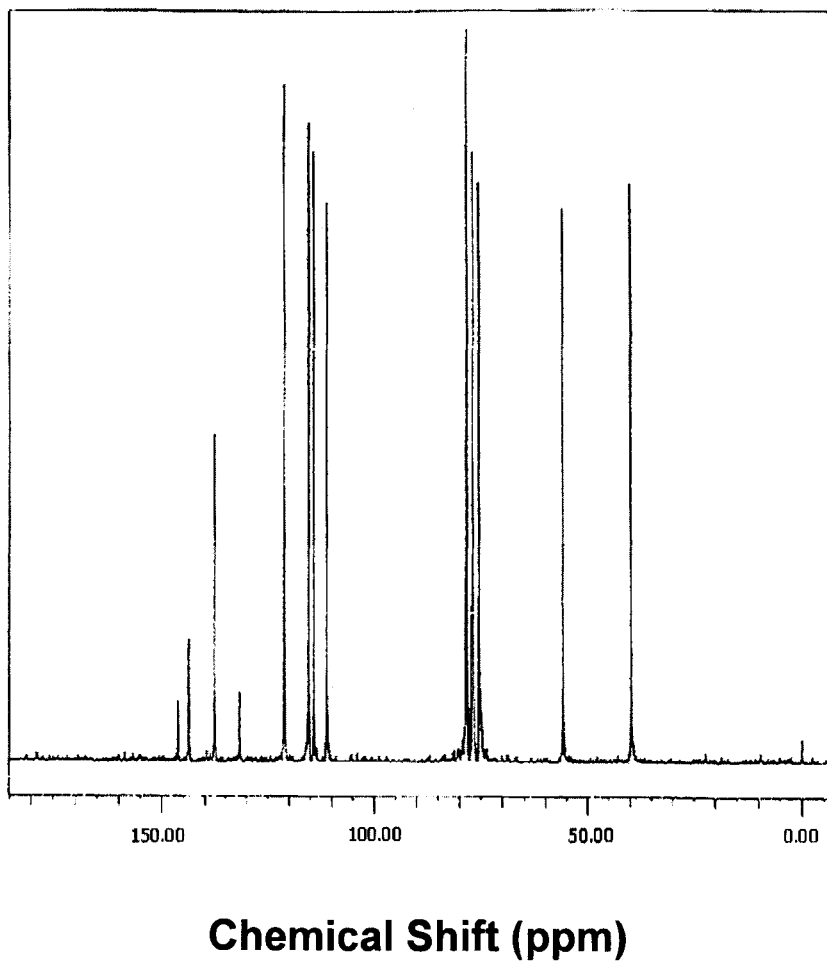
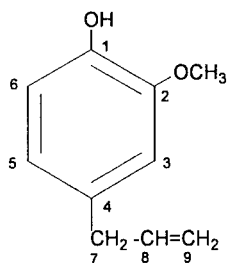


Figure 6.  $^{13}\text{C}$ -NMR spectrum of eugenol in deuterio-chloroform.

Table 2

Assignments for the  $^{13}\text{C}$ -NMR Resonances of Eugenol



Chemical shift (ppm)	Carbon number
39.8	7
55.87	Methoxy
111.1	9
114.2	3
115.4	6
121.1	5
131.8	4
137.7	8
143.8	1
146.8	2

### 3.8 Mass Spectrometry

The electron impact mass spectrum of eugenol was measured using a Jeol JMS-DX 303 system. The spectrum is presented in Figure 6, and assignments for the main observed fragments are provided in Table 3.

## 4. Methods of Analysis

### 4.1 Compendial Tests

Eugenol contains not less than 98 per cent by volume of phenols as  $C_{10}H_{12}O_2$  [5]. Eugenol USP is specified by the United States Pharmacopeia by the following sequence of tests and specifications [3].

#### 4.1.1 Specific Gravity

When determined according to General Test <841>, the specific gravity is between 1.064 and 1.070.

#### 4.1.2 Distilling Range

When determined according to General Test <721>, Method II, Not less than 95% distils between 250 and 255°C.

#### 4.1.3 Refractive Index

When determined according to General Test <831>, the refractive index is between 1.540 and 1.542 at 20°C.

#### 4.1.4 Heavy Metals

When determined according to General Test <231>, Method II, the heavy metal content does not exceed 0.004%.

#### 4.1.5 Hydrocarbons

Dissolve 1 mL of the test article in 20 mL of 0.5 N sodium hydroxide in a stoppered, 50-mL tube. Upon addition of 18 mL of water with mixing, a clear mixture results immediately. However, the solution may become turbid when exposed to air.

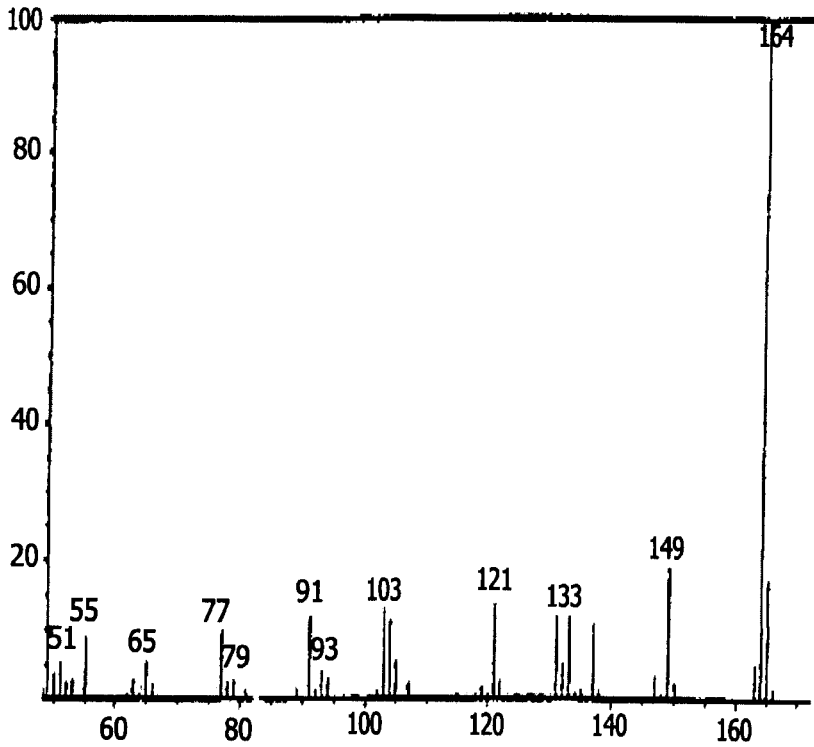


Figure 7. Electron impact mass spectrum of eugenol.

Table 3

## Electron Impact Mass Spectral Data for Eugenol

m/z Ratio (relative intensity)	Fragment assignment
164 (100)	$[M^+]$
149 (22)	$[M-(CH_3)]^+$
137(18)	$[M-(CH=CH_2)]^+$
133(20)	$[M-(OCH_3)]^+$
91(15)	$[M-(C_6H_5-CH_2)]^+$
77(14)	$(C_6H_5-CH_2)^+$

#### 4.1.6 Limit of Phenol

Shake 1 mL of the test article with 20 mL of water, filter, and add 1 drop of ferric chloride TS to 5 mL of the clear filtrate. The mixture exhibits a transient grayish green color, but not a blue or violet color.

### 4.2 Chromatographic Methods of Analysis

#### 4.2.1 Thin Layer Chromatography

Vollmann *et al* reported the TLC determination of eugenol in mixtures containing borneol, norphinon, and myrtenol as components of *Geum urbanum* [20]. The method uses silica gel as the stationary phase, and 3:1 pentane-ether as the mobile phase. Detection is effected on the basis of the UV absorbance at 366 nm, and by spraying with vanillin-sulfuric acid reagent and heating at 120°C for 10 minutes.

Cikalo *et al* used TLC to establish the origins of cinnamons of commerce. Six different solvent systems were used in conjunction with silica plates to separate eugenol, cinnamyl alcohol, cinnamyl acetate, *trans*-cinnamyl-aldehyde, 2-methoxy-cinnamylaldehyde, and coumarin [21]. Quantification was carried out by densitometry at 270 nm.

A silica gel plate, with chlorobenzene as the developing solvent, was used by Bary *et al* to optimize the separation of citral, citronellol, eugenol, cinnamon, menthol, and mentha by the OPLC technique [22]. Detection is obtained by spraying with vanillin-sulfuric reagent, and is carried out using densitometry at 600 nm.

Eugenol can be determined in mixtures with myristicin, apiol, allyltetramethoxybenzene, and elemicin using thin layer chromatography [23]. The method uses silica gel as the stationary phase, and 97:3 toluene-ethyl acetate as the mobile phase. Detection is effected on the basis of the UV absorbance at 254 nm, and by spraying with vanillin-sulfuric acid reagent.

Janssen *et al* carried out a comparison of TLC and HPLC methods to identify various cinnamons [24]. TLC methods were found to have a better retention time reproducibility relative to HPLC methods. In addition, solvent costs and time efforts were also less when using TLC.



#### **4.2.2 High Performance Liquid Chromatography**

Reversed phase isocratic HPLC with ultraviolet detection at 280 nm was used to separate and identify eugenol in the ethanolic extract of whole tobacco and clove cigarettes [25]. The samples were analyzed at 30°C on a RP 18 column using methanol-water (80:20) as the mobile phase. This method was also applied to determine the eugenol content within the total particulate matter of mainstream tobacco condensate [26].

#### **4.2.3 Gas Chromatography**

Eugenol is used as an internal standard in the gas chromatographic determination of thymol in biological samples [4].

A rapid method for the analysis of the essential oils (including eugenol) in Spearmint oil has been reported using gas chromatography combined with time of flight mass spectrometry (TOFMS) [27]. The analysis was performed using a DB-5 (4 m x 0.1 mm ID x 0.1  $\mu$ m phase film) column, and operated in a temperature-programmed oven. When using a program consisting of equilibration at 40°C for 0.5 minutes, ramping to 280°C at 75°C/min., and a final hold for 1 minute, the retention index of eugenol was reported as 91.83 seconds.

#### **4.3 Supercritical Fluid Methods**

A supercritical extraction procedure was developed to determine naled, methyleugenol, and cuelure in soil samples [28]. Recovery of methyleugenol was reported as 91-101% after spiking the sample with standard at concentrations of 0.25-45  $\mu$ g/g. The supercritical fluid was carbon dioxide (pressure of 27.6 Mpa), and the method worked for 5-30% soil moisture.

### **5. Stability**

Eugenol is compatible with strong oxidizers, such as ferric chloride, potassium permanganate, iron and zinc. It reacts with strong alkalis [4].

Eugenol darkens and thickens on exposure to air, and also darkens with age. The substance may decompose on exposure to light.

Stability screening using nuclear magnetic resonance shows that solutions of eugenol in dimethyl sulfoxide are stable for at least 24 hours [4].

## **6. Absorption, Distribution, and Excretion [29-33]**

It was reported that intraperitoneal injection of a single 450 mg/kg dose of  $^{14}\text{C}$ -methoxy labeled eugenol resulted in rapid distribution to all organs. Both ether- and water-soluble materials were recovered from most tissues and excretions. Only 0.2-1.0% of the dose was eliminated as expired  $^{14}\text{C}$ - $\text{CO}_2$ .

Over 70% of a lethal dose of eugenol was recovered from the urine of rabbits after death. The administration of single 200 mg doses to rats was also reported to increase urinary output of ethereal glucuronides of 33-35 mg/rat in 12 hours compared to the control value of 4 mg/rat. Ester glucuronide values were unchanged. Subcutaneous injection of 0.1 mL of purified eugenol in adult Walter Reed white rats caused necrosis and inflammation at the injection site [29-33].

## **7. Pharmacological Action**

Eugenol, like other phenolic compounds, is a structurally non-specific drug. The pharmacological action is not directly subordinated to chemical structure, except to the extent that structure affects physicochemical properties, as adsorption, solubility, pKa, and oxidation-reduction potential, factors which influence permeability, depolarization of the membrane and protein coagulation [34].

The antimicrobial activity of eugenol may be associated with structural damage and alteration of the permeability mechanism of microsome, lysosome, and cell walls. The substance acts primarily on cytoplasm membranes, causing alteration of its permeability, and thus allowing leakage of essential bacterial cell constituents with subsequent death of the bacteria.

The one common mechanism that might be used to explain the action of eugenol in its antibacterial and antifungal action is that of membrane perturbation. An extensive oxidative enzyme system is part of the membrane structure, and could easily turn off or diminish this vital system [35]. From the molecular structure of eugenol, the *para*-allyl and *ortho*-methoxy groups contribute to the antiseptic and anesthetic activity of the phenolic group [36]. When used as a dental analgesic, the dosage as high as 0.2 mL.

## 8. Toxicity

The toxicity of eugenol was tested in mice and rats by oral administration of a diet containing a high dose of eugenol. There was a significant increase in the incidence of liver tumors in female mice. The incidence increase in males was significant only for those receiving lower doses. There was no increase incidence of tumors observed in rats.

Other studies showed that acutely, high doses of eugenol were hepatotoxic to dogs and rats, but metabolic data is limited. Formation of small amounts of eugenol 2',3-epoxide from eugenol within *in vitro* systems has been reported. Mutagenicity tests using *Salmonella* strains with and without activation gave negative results for eugenol, although the 2',3-epoxide compound was active in these systems.

No studies on teratology or reproduction are available. The lifetime feeding study in the rat provides additional information for evaluating an acceptable daily intake for man. This data supports proposal of the previous temporary acceptable daily intake to an acceptable daily intake [29-33].

No case report or epidemiological study of the carcinogenicity of eugenol in humans is available [31]. The reported tumorigenic data of oral application in mus was 37080 mg/kg [4].

The LD<sub>50</sub> (mg/kg) of eugenol in various animals was reported as [4]: 500 (mus, ipr), 3000 (mus, oral), 1930 (rat, oral), 800 (rat, ipr), 5000 (rat, scu), 11 (rat, itr), 500 (dog, oral), 17 (ham, itr), and 2130 (gpg, oral).

## 9. **References**

1. S. Budnavi, ed., *The Merck Index*, 11<sup>th</sup> edn., Merck & Co Inc., Rahway (1989).
2. J.E.F. Reynolds, ed., *Martindale, The Extra Pharmacopoeia*, 30<sup>th</sup> edn., The Pharmaceutical Press, London (1993).
3. *The United States Pharmacopoeia*, 24<sup>th</sup> edn., United States Pharmacopeial Convention, Rockville, MD (1999).
4. [http://ntp-server.niehs.nih.gov/htdocs/Chem\\_H&S/NTP\\_Chem9/Radian97-53-0.html](http://ntp-server.niehs.nih.gov/htdocs/Chem_H&S/NTP_Chem9/Radian97-53-0.html) (4/4/2001).
5. Eugenol, IARC Summary and Evaluation, Vol. 36 (1982), Journal of Chromatographic Science 2 – files\v 44 aje 18.htm.
6. A.C. Moffat, J.V. Jackson, M.S. Moss, and B. Widopp, eds, *Clarke's Isolation and Identification of Drugs*, 2<sup>nd</sup> edn., The Pharmaceutical Press, London (1986).
7. G.M Lampman, J. Andrew, W. Bratz, O. Hanssen, K. Kelly, D. Perry, and A. Ridgeway, *J. Chem. Educ.*, 776-778 (1977).
8. H.H. Shorey and J.J. McKelvey, Jr., *Chemical Control of Insect Behavior*, John Wiley & Sons (1977), pp. 327-344.
9. E. Guenther, *The Essential Oils*, Volumes I & IV., Robert E. Krieger Publishing Co, Inc. (1972), pp. 292-293, 687-697.
10. G.E. Trease, *Pharmacognosy*, Bailliere Tindall, London (1978) pp. 440-446.
11. <http://edie.cprost.sfu.ca/~rhlogan/Chap6-4.html> (14/03/01).
12. <http://www.agric.ab.ca/crops/special/medconf/ibrahimd.html> (9/21/99).
13. <http://newcrop.hort.purdeel.edu/rhodch/hortbyoc/secprod/se0017.htm> (4/4/2001).
14. K.R. Payne, *The Industrial Chemist*, 523 (1961).

- 176 M. YUWONO, SISWANDONO, A.F. HAFID, A.T. POERNOMO,  
M. AGIL, G. INDRAYANTO, AND S. EBEL
15. T.H. Peterson, J.H. Bryan, and T.A. Weevil, *J. Chem. Educ.*, **70**, A96-A98 (1993).
16. J. Andrieux, D.H.R. Barton, and H. Patin, *J. Chem. Soc. Perkin I*, 359-363 (1977).
17. <http://rhodium.lycaeum.org/chemistry/isoeugenol.txt>. (4/3/2001).
18. B.S. Furniss, A.J. Hannaford, V. Rogers, P.W.G. Smith, A.R. Tatchell), *Vogel's Textbook of Practical Organic Chemistry, including Qualitative Organic Chemistry*, 4<sup>th</sup> edn., London, English Language Book Society/Longman (1978), pp. 755-756.
19. A.R., Martin, "Anti-infective agents", In *Wilson and Gisvold's Textbook of Organic Medicinal and Pharmaceutical Chemistry*, J.N. Degaldo and A.W. Remers, eds., 9<sup>th</sup> edn., J.B. Lippincott Company, Philadelphia (1991), pp. 133-134.
20. C. Vollmann, W. Schultze, *Deutsche Apotheker Zeitung*, **135**, 1238-1248 (1995).
21. M.J. Cikalo, S.K. Poole, and C.F. Poole, *J. Planar Chromatogr.* **5**, 135-138 (1992).
22. Z. Bary, M. Varadi, and E. Mincsovcics, *Proc. Intern. Symposium on TLC with special Emphasis on OPLC*, Szeged (1984), pp. 9-10.
23. H. Wagner and S. Bladt, *Plant drug Analysis: A Thin Layer Chromatography Atlas*, 2<sup>nd</sup> edn., Springer-Verlag Berlin (1996), pp. 166-175
24. A. Jannsen, A. Neitzel, and A. Lau, "Identifizierung von Zimstoffen mittels DC und HPLC", in Merck KgaA (Ed): *Chromatographie-Cronologie einer Analysentechnik*, GIT Verlag mbH, Darmstadt (1996), pp. 166-176
25. Health Canada - Official Method T-314.
26. Health Canada - Official Method, T-105.
27. Leco Separation Science Application Note, Pegasus II GC/TOFMS, Form No. 203-821-091.

28. J.P. Alcantara-Licudine, Q.X. Li, and M.K. Kawate, *J. Chromatogr. Sci.*, **34**, 238-244 (1966).
29. <http://ntp-server.niehs.nih.gov/htdocs/LT-studies/tr223.html> (4/4/2001).
30. <http://www.pulpdent.com/periodio/eugmsds.html> (4/4/2001).
31. **Eugenol**, WHO Food Additives Series 17, \Journal of Chromatographic Science\_files\17je10.htm (04/09/01).
32. **Eugenol**, WHO Food Additives Series 14, \Journal of Chromatographic Science\_files\17je11.htm (04/09/01).
33. <Http://193.51.164.11/htdocs/Monographs/v0136/Eugenol.html> (4/3/2001).
34. A. Korolkovas, **Essentials of Medical Chemistry**, 2<sup>nd</sup> edn., John Wiley & Sons, New York (1988), pp. 590-597, 692-697.
35. C. Hansch, and E.J. Lien, *J. Med. Chem.*, **14**, 653-659 (1971).

This Page Intentionally Left Blank

# MANDELIC ACID

Harry G. Brittain

Center for Pharmaceutical Physics

10 Charles Road

Milford, NJ 08848

U.S.A.



## **Contents**

### **1. Description**

- 1.1 Nomenclature
  - 1.1.1 Systematic Chemical Name
  - 1.1.2 Nonproprietary Names
  - 1.1.3 Proprietary Names
- 1.2 Formulae
  - 1.2.1 Empirical Formula, Molecular Weight, CAS Number
  - 1.2.2 Structural Formula
- 1.3 Elemental Analysis
- 1.4 Appearance
- 1.5 Uses and Applications

### **2. Methods of Preparation**

- 2.1 Racemic Mandelic Acid
- 2.2 Resolved Mandelic Acid

### **3. Physical Properties**

- 3.1 Ionic Equilibria
  - 3.1.1 Ionization Constant
  - 3.1.2 Metal Ion Binding Constants
- 3.2 Solubility Characteristics
- 3.3 Partition and Distribution Coefficient
- 3.4 Optical Activity
- 3.5 Crystallographic Properties
  - 3.5.1 Single Crystal Structure
  - 3.5.2 X-Ray Powder Diffraction Pattern
- 3.6 Thermal Methods of analysis
  - 3.6.1 Melting Behavior
  - 3.6.2 Differential Scanning Calorimetry
- 3.7 Spectroscopy
  - 3.7.1 UV/VIS Spectroscopy
  - 3.7.2 Vibrational Spectroscopy
  - 3.7.3 Nuclear Magnetic Resonance Spectrometry

**4. Compendial Methods of Analysis**

- 4.1 Identification
- 4.2 Melting Range
- 4.3 Turbidity
- 4.4 Water Content
- 4.5 Chloride Content
- 4.6 Residue on Ignition
- 4.7 Heavy Metals
- 4.8 Assay
- 4.9 Related Compounds

**5. References**

## 1. Description

### 1.1 Nomenclature

#### 1.1.1 Systematic Chemical Name

$\alpha$ -hydroxyphenylacetic acid

#### 1.1.2 Nonproprietary Names [1]

Mandelic acid; phenyl glycolic acid;  $\alpha$ -hydroxy- $\alpha$ -toluic acid; amygdalic acid; amygdalinic acid, uromaline

#### 1.1.3 Proprietary Names [2]

Used in multi-ingredient preparations sold as Intesticarbine, Mandocarbine, or Urodil N

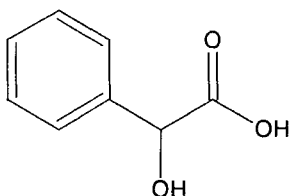
### 1.2 Formulae

#### 1.2.1 Empirical Formula, Molecular Weight, CAS Number

$C_8H_8O_3$  [MW = 152.147]

CAS number = 90-64-2

#### 1.2.2 Structural Formula



### 1.3 Elemental Analysis

The calculated elemental composition is as follows:

carbon:	63.15%
hydrogen:	5.30%
oxygen:	31.55%

### 1.4 Appearance

When precipitated from aqueous solutions, mandelic acid is obtained as orthorhombic plates. The calcium and sodium salts are obtained as white powders.

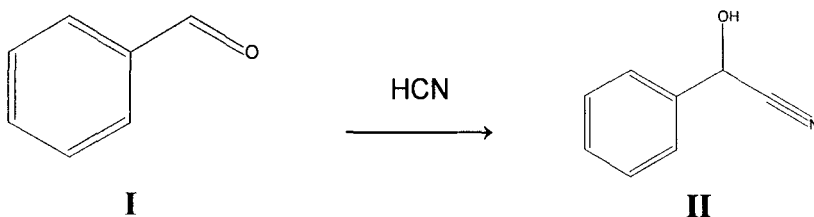
### 1.5 Uses and Applications [2]

Mandelic acid has bacteriostatic properties, and is given orally in the treatment of urinary tract infections. The usual form of the drug substance is either the ammonium or calcium salt. It has proven to be effective against simple infections due to Gram-negative bacteria, and a few Gram-positive species, provided that the pH is kept below 5.5. A 1% solution of mandelic acid is also used as a flushing solution for the maintenance of indwelling urinary catheters.

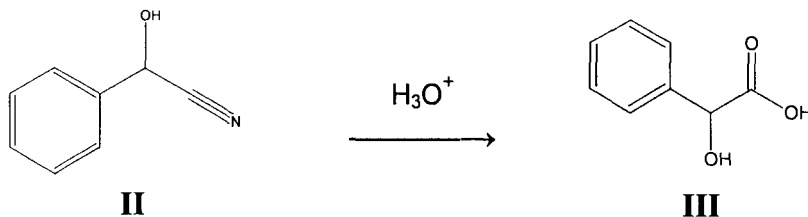
## 2. Methods of Preparation

### 2.1 Racemic Mandelic Acid

In the first step of one synthesis of (*D,L*)-mandelic acid, benzaldehyde (**I**) is converted to mandelonitrile (**II**, or benzaldehyde cyanohydrin):



In a safer route, the sodium bisulfite derivative of benzaldehyde is first prepared, whereupon compound **II** is obtained by reaction of that product with  $\text{KCN}$ . In the second step, mandelic acid (**III**) is obtained by the acid hydrolysis of compound **II**:

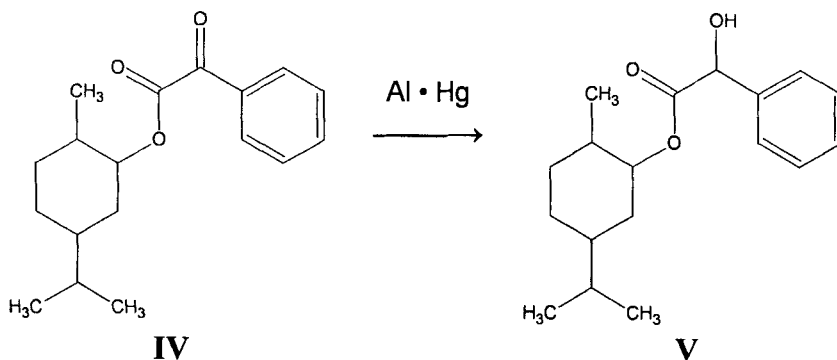


The method of preparation of (*D,L*)-mandelic acid has been described by Vogel in great detail [3]. 25 g of sodium cyanide is dissolved in 100 mL of water, and 53 g of purified benzylaldehyde is added. 335 mL of a saturated solution of sodium bisulfite is added to the benzylaldehyde/cyanide solution with stirring over a period of 10-15 minutes. During the first half of the addition, the temperature of the reaction mixture is kept low through the addition of 150 g of crushed ice. At the end of the reaction period, the solution is transferred to a separatory funnel, and the layer of crude mandelonitrile is separated.

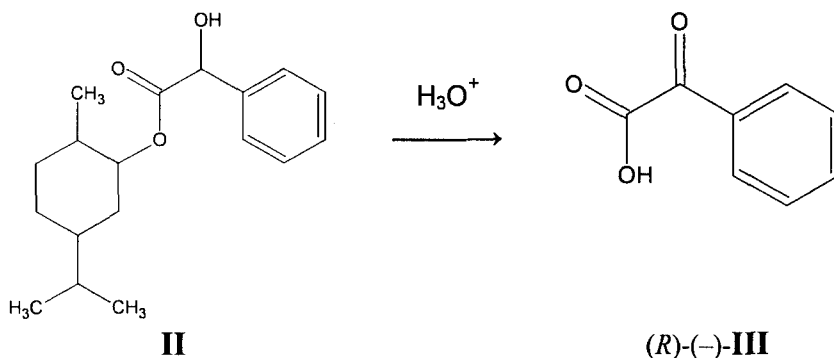
The mandelonitrile is immediately transferred to a large evaporating dish, and 75 mL of concentrated hydrochloric acid is added. The dish is covered, and allowed to stand refrigerated for 12 hours for the hydrolysis reaction. The solution is evaporated to dryness, the solids ground to a powder, and washed twice with 125 mL portions of cold toluene to remove colored products. The inorganic salts remaining from the first reaction are removed by extracting the residue in a Soxhlet apparatus (operated at a temperature of 100°C) with about 200 mL of toluene. Cooling the hot toluene solution causes crystallization of the product, which is filtered and dried.

## 2.2 Resolved Mandelic Acid

(*R*)-(-)-mandelic acid was prepared through one of the very first examples of an asymmetric synthesis [4]. The phenylglyoxylate ester of (-)-menthol (IV) was reduced with aluminum amalgam to the mandelate ester of (-)-menthol (V):



The enantiomerically enriched (*R*)-(-)-mandelic acid was obtained from compound (V) by acid hydrolysis:



Enantiomerically pure mandelic acid has also been prepared by resolution of the racemic substance through the formation of a dissociable diastereomer with ephedrine [5]. In a typical preparation, 12 g of (L)-ephedrine and 12 g of racemic mandelic acid are heated together in 40 mL of 90% ethanol. The diastereomer salt is obtained upon cooling of the solution, and may be purified by recrystallization from a small volume of alcohol. (R)-(-)-mandelic acid is obtained by acidification of the diastereomer salt, extraction with ether, and crystallization through the anti-solvent addition of acetone.

The enantiomers of racemic mandelic acid have since been obtained through the use of practically every known basic resolving agent, and the enantiomers are commercially available in any desired quantity.

### 3. Physical Properties

#### 3.1 Ionic Equilibria

##### 3.1.1 Ionization Constant

The single carboxylate group of mandelic acid is characterized by  $pK_a$  value of 3.20 at 25°C and an ionic strength of 0.1 [6]. Increasing the ionic strength to 1.0 only slightly shifts the  $pK_a$  to 3.18, but decreasing the ionic strength to 0 shifts the  $pK_a$  value to 3.40. The thermodynamics of the ionization process have been determined at 25°C and an ionic strength of 2.0, with  $\Delta H = 0.05$  and  $\Delta S = 15.3$  [6].

Using the ACD/PhysChem computational program (version 6.0, Advanced Chemistry Development, Toronto, Canada), the  $pK_a$  of the carboxylate

group was calculated to be  $3.41 \pm 0.20$ , in good agreement with the experimental results. In addition, the pK<sub>a</sub> of the hydroxyl group was predicated as  $15.65 \pm 0.25$ .

### 3.1.2 Metal Ion Binding Constants

Mandelic acid is an efficient chelating agent for transition metal ions, and the following binding constants have been reported [6]:

Metal Ion	Log K (25°C and $\mu = 1.0$ )
Co(II)	1.19
Ni(II)	1.31
Cu(II)	2.70
Zn(II)	1.36

Mandelic acid is known to bind with trivalent ions with greater efficiency, and log K values ranging from 2.3 to 2.8 have been reported for the various trivalent ions of the lanthanide series.

### 3.2 Solubility Characteristics

The solubility of racemic mandelic acid has been reported to be 158.7 mg/mL in water, 1000 mg/mL in ethanol, and freely soluble in ether or isopropyl alcohol [1]. The aqueous solubility of the resolved enantiomers of mandelic acid has been reported to be 72.6 mg/mL at 15°C, and 111.6 mg/mL at 25°C [7].

The racemic compound has been found to exhibit a lower degree of solubility in chloroform relative to the resolved enantiomer [7]:

Temperature (°C)	Solubility (+)-mandelic acid (mg/mL)	Solubility racemic mandelic acid (mg/mL)
15	9.52	8.77
25	13.28	1.07
35	19.50	1.60

Racemic mandelic acid exhibits appreciable solubility in alcoholic solvents, with a solubility (at 16.5°C) of 649 mg/mL being reported for methanol, 536 mg/mL for ethanol, and 430 mg/mL for propanol [7].

As would be anticipated for a carboxylic acid, mandelic acid is known to exhibit a pH strong dependence in its aqueous solubility. This pH dependence was calculated using the solubility module of the ACD/PhysChem computational program (version 6.0, Advanced Chemistry Development, Toronto, Canada), and these results are plotted in Figure 1. The results indicate that mandelic acid will be freely soluble in basic solution, which would be interpreted to imply that the sodium salt would be freely soluble as well.

### 3.3 Partition and Distribution Coefficient

When measured at a temperature of 25°C, the ethyl ether / water partition coefficient of mandelic acid was reported as  $\log P = 0.137$  [7]. The chloroform / water partition coefficient at the same temperature was reported as  $-1.32$ , demonstrating the hydrophilic nature of the compound.

The pH dependence of the octanol / water partition coefficient was calculated using the ACD/PhysChem computational program (version 6.0, Advanced Chemistry Development, Toronto, Canada), and these results are plotted in Figure 2. The plot demonstrates that the neutral compound is mildly hydrophobic, but that the ionized form is strongly hydrophilic. This finding is in accord with the solubility data.

### 3.4 Optical Activity

It has been established that the absolute configuration of (+)-mandelic acid is the (*S*)-configuration [8, 9]. In older literature, the compound is also known as (*L*)-mandelic acid.

The specific rotation of resolved mandelic has been determined at a wavelength of 589 nm (the sodium D line) and at a temperature of 20°C, with the following values being reported [10]:

$$(S)\text{-mandelic acid: } [\alpha]_D^{20} = +155.5^\circ$$

$$(R)\text{-mandelic acid: } [\alpha]_D^{20} = -157.4^\circ$$



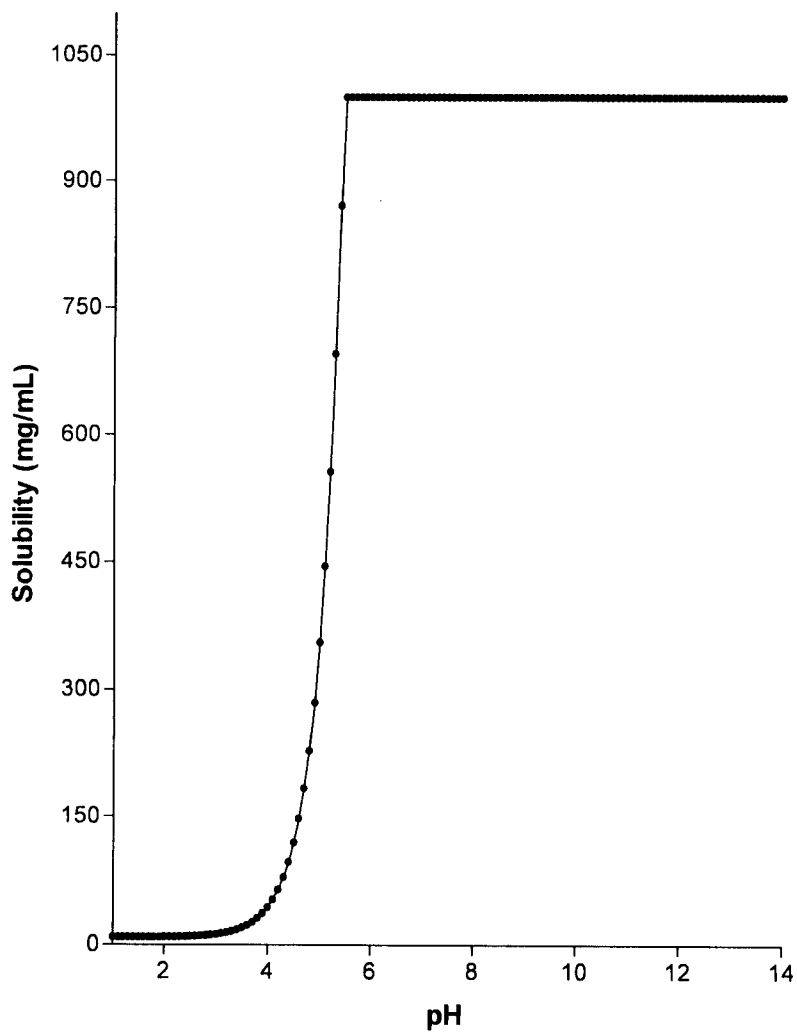


Figure 1. Calculated pH dependence of the aqueous solubility of mandelic acid.

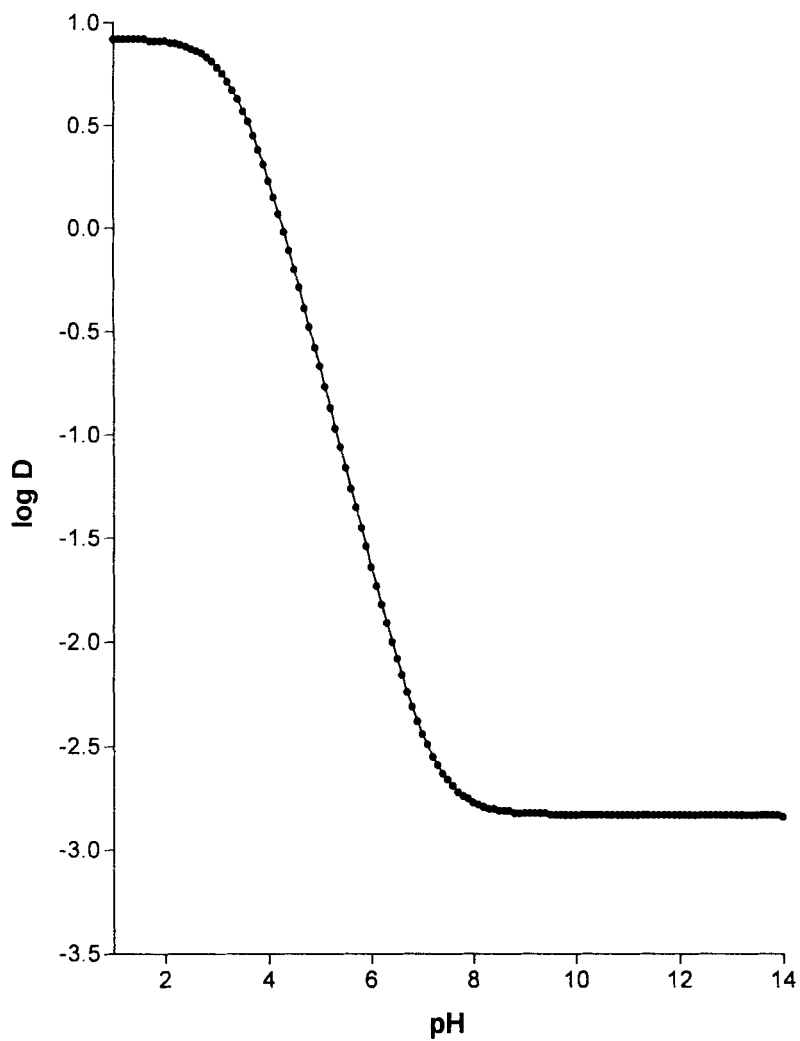


Figure 2. Calculated pH dependence of the distribution coefficient of mandelic acid.

### 3.5 Crystallographic Properties

#### 3.5.1 Single Crystal Structure

The single crystal structure of racemic mandelic acid was originally reported by Cameron and Duffin [11], and then re-determined by Wei and Ward [12]. The compound crystallizes in the orthorhombic *Pbca* space group, with the unit cell parameters being:

<i>a</i>	9.669 Å
<i>b</i>	16.183 Å
<i>b</i>	9.953 Å
<i>Z</i>	8
density (calc)	1.298 g/cm <sup>3</sup>

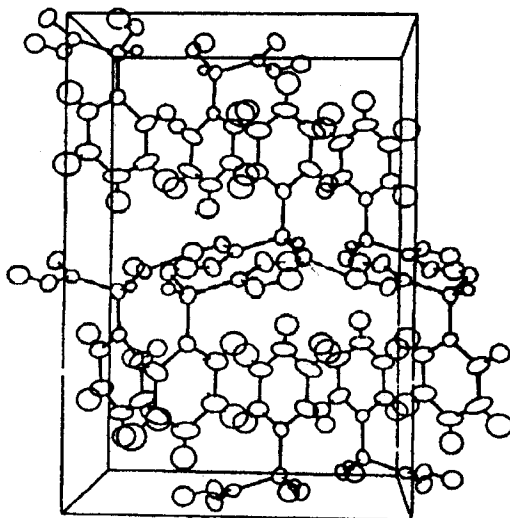
An overview of the structure is found in Figure 3a. The structure is characterized by an extensive hydrogen-bonding network parallel to the *ac* plane, involving the carboxyl and hydroxyl groups. The hydrogen-bonding effectively joins the molecules into sheets parallel to the *ac* plane, with the sheets being arranged in pairs with interpenetrating phenyl rings.

The single crystal structures of (*S*)-mandelic acid has been reported by Patil *et al* [13]. The compound crystallizes in the monoclinic *P2<sub>1</sub>* space group, with the unit cell parameters being:

<i>a</i>	8.629 Å
<i>b</i>	5.861 Å
<i>b</i>	15.185 Å
$\beta$	102.76°
<i>Z</i>	4
density (calc)	1.349 g/cm <sup>3</sup>

An overview of the structure is located in Figure 3b. The structure is assembled from chains of hydrogen-bonded molecules that stretch along the *b*-axis. The unit cell contains two types of non-equivalent molecules, each of which form their own chain structures and are inter-related only by a pseudocentering in the *a* and *b* directions.

(a)



(b)

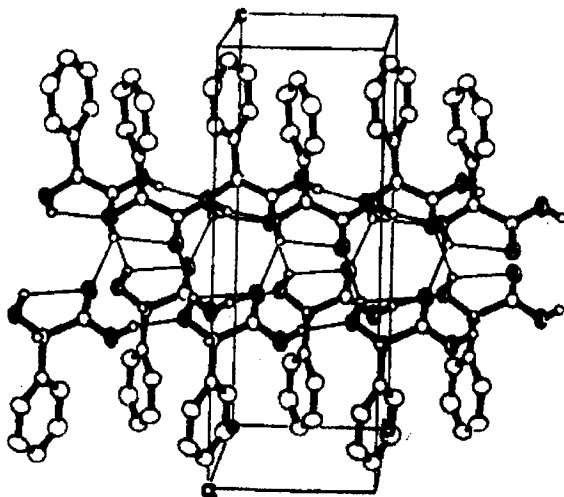


Figure 3. Single crystal structures of (a) racemic mandelic acid and (b) (*S*)-mandelic acid. The figures were adapted from references [12] and [13], respectively.

### 3.5.2 X-Ray Powder Diffraction Pattern

The x-ray powder diffraction patterns of racemic mandelic acid and (*S*)-mandelic acid were obtained using a Rigaku MiniFlex powder diffraction system, equipped with a horizontal goniometer in the  $\theta/2\theta$  mode. The x-ray source was nickel-filtered K- $\alpha$  emission of copper (1.544056 Å). A 10-mg sample was packed into an aluminum holder using a back-fill procedure, and was scanned over the range of 50 to 6 degrees  $2\theta$ , at a scan rate of 0.5 degrees  $2\theta$ /min. Calibration of the powder pattern was effected using the characteristic scattering peaks of aluminum at 44.738 and 38.472 degrees  $2\theta$ .

Samples of both racemic and enantiomerically pure mandelic acid were used as received from Aldrich Chemicals. The powder pattern of racemic mandelic acid is shown in Figure 4, and a summary of the observed scattering angles, d-spacings, and relative intensities is shown in Table 1. The powder pattern of (*S*)-mandelic acid is shown in Figure 5, and a summary of the observed scattering angles, d-spacings, and relative intensities is shown in Table 2.

## 3.6 Thermal Methods of analysis

### 3.6.1 Melting Behavior

The Merck Index lists the melting point of racemic mandelic acid as 119°C [1], while the Handbook of Chemistry and Physics gives the melting point range as 121-123°C [14]. The United States Pharmacopeia specifies the wider range of 118-121°C for the melting point range [15].

The melting points of the separated enantiomers have been reported as 133-135°C for (*R*)-(-)-mandelic acid, and 134-135°C for (*S*)-(+)-mandelic acid [14].

### 3.6.2 Differential Scanning Calorimetry

Measurements of differential scanning calorimetry were obtained on a TA Instruments 2910 thermal analysis system. Samples of approximately 2-4 mg were accurately weighed into an aluminum DSC pan, and covered with an aluminum lid that was crimped in place. Samples of both racemic and enantiomerically pure mandelic acid were used as received from Aldrich Chemicals.

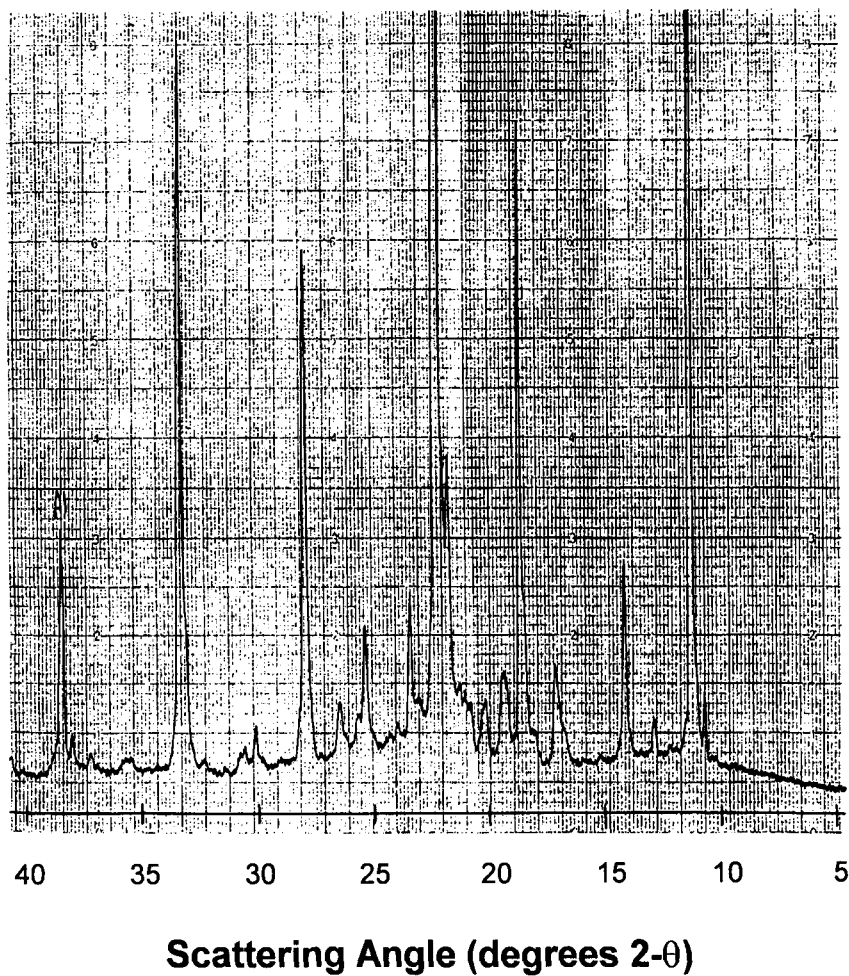


Figure 4. X-ray powder diffraction pattern of racemic mandelic acid (Aldrich lot KN07114MT). The aluminum calibration peak from the cell holder is marked.

Table 1

Scattering Angles, Interplanar d-Spacings,  
and Relative Intensities in the X-Ray Powder Diffraction of  
Racemic Mandelic Acid

Scattering Angle (degrees 2- $\theta$ )	d-Spacing (Å)	Relative Intensity (%)
10.912	8.1198	3.4
11.421	7.7588	61.4
13.102	6.7668	1.8
16.414	5.4084	10.4
16.974	5.2311	2.0
17.331	5.1242	5.0
18.451	4.8154	1.6
18.757	4.7376	32.4
19.521	4.5539	3.8
20.336	4.3732	2.8
20.948	4.2469	1.0
21.151	4.2065	1.0
21.457	4.1472	1.0
21.865	4.0708	11.0
22.323	3.9883	100.0
23.189	3.8412	1.8
23.495	3.7919	7.6
24.106	3.6972	1.2
25.502	3.4979	7.0
25.787	3.4598	1.6
26.602	3.3556	2.8
28.029	3.188	26.4
30.372	2.9472	2.2
30.627	2.9233	1.6

Table 1 (continued)

Scattering Angles, Interplanar d-Spacings,  
and Relative Intensities in the X-Ray Powder Diffraction of  
Racemic Mandelic Acid

Scattering Angle (degrees 2- $\theta$ )	d-Spacing (Å)	Relative Intensity (%)
32.359	2.7706	0.6
33.327	2.6924	37.2
35.619	2.5242	0.6
37.249	2.4174	0.8
38.064	2.3675	1.6
40.815	2.214	0.6
42.007	2.1539	6.0
43.495	2.0837	1.8
43.974	2.0621	1.0
46.623	1.9509	0.6



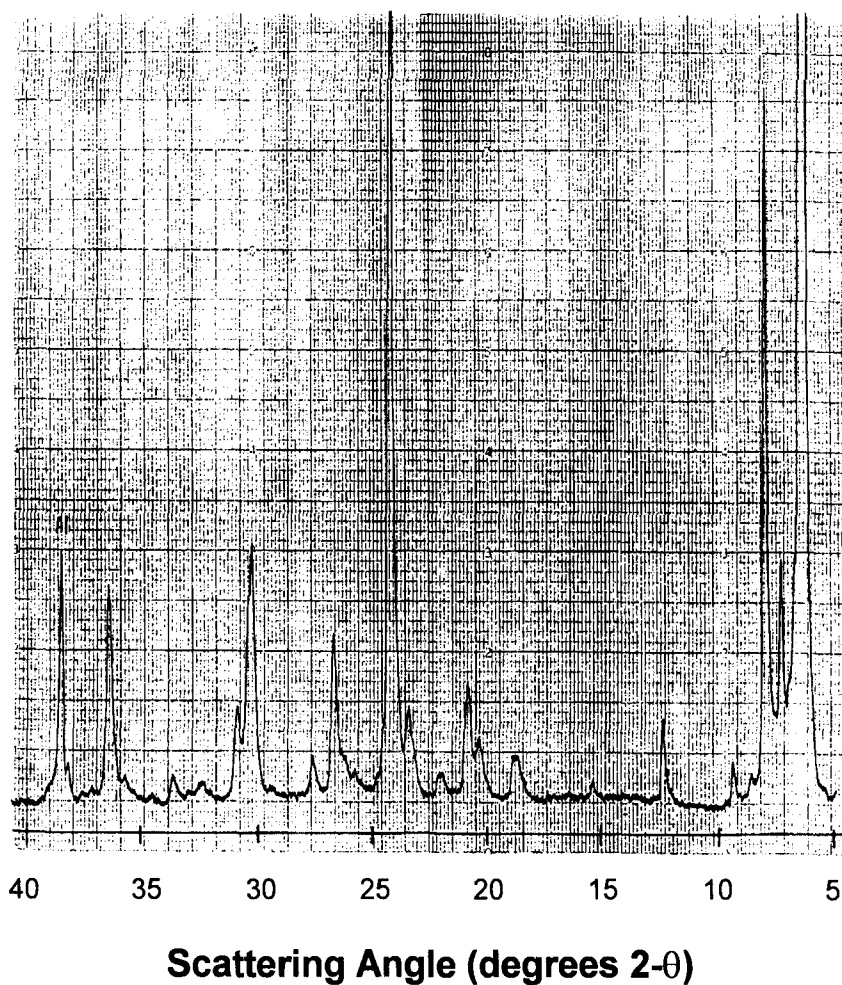


Figure 5. X-ray powder diffraction pattern of (*S*)-mandelic acid (Aldrich lot 11505DF). The aluminum calibration peak from the cell holder is marked.

Table 2

Scattering Angles, Interplanar d-Spacings,  
and Relative Intensities in the X-Ray Powder Diffraction of  
(*S*)-Mandelic Acid

Scattering Angle (degrees 2- $\theta$ )	d-Spacing ( $\text{\AA}$ )	Relative Intensity (%)
6.531	13.5538	100.0
6.836	12.9485	10.0
7.448	11.887	12.6
8.161	10.8497	36.0
8.772	10.0949	0.8
9.587	9.2384	2.4
12.542	7.0679	4.0
15.548	5.7076	0.8
18.91	4.6997	2.2
20.438	4.3516	3.2
20.948	4.2469	5.4
22.119	4.0245	1.0
23.495	3.7919	4.6
24.259	3.6742	43.8
26.755	3.3368	8.0
27.672	3.2283	2.2
30.168	2.9666	12.4
30.932	2.8951	4.6
32.359	2.7706	0.8
33.632	2.6686	1.6
35.67	2.5207	1.2
36.434	2.4695	10.6
38.115	2.3644	1.6
41.529	2.1776	1.0
42.547	2.1278	1.0
43.363	2.0897	0.6
43.974	2.0621	1.0
45.961	1.9775	1.6

The DSC thermogram of racemic mandelic acid is shown in Figure 6, and the DSC thermogram of (*S*)-mandelic acid is shown in Figure 7. Both thermograms consisted of a single melting endothermic transition, and were characterized by the following results:

	( <i>RS</i> )-mandelic acid	( <i>S</i> )-mandelic acid
Onset temperature	117°C	131°C
Endotherm maximum	121°C	134°C
Enthalpy of fusion	161.0 J/g	166.0 J/g

### 3.7 Spectroscopy

#### 3.7.1 UV/VIS Spectroscopy

Solution-phase ultraviolet absorption spectra of racemic mandelic acid were obtained using a Perkin-Elmer Lambda 3B spectrophotometer. Spectra (referenced against the corresponding solvent) of the protonated form were obtained in ethanol (Figure 8), and of the deprotonated form in 0.5N NaOH (Figure 9), both at concentrations of 0.1 and 0.01 mg/mL.

In both solvent systems, a weak band was observed at 260 nm, corresponding to absorbance by the phenyl ring. The following molar absorptivities were calculated:

Ethanol:  $a = 170 \text{ L/cm}\cdot\text{mole}$

0.5 N NaOH:  $a = 304 \text{ L/cm}\cdot\text{mole}$

#### 3.7.2 Vibrational Spectroscopy

The infrared absorption spectra of racemic and (*S*)-mandelic acid were obtained using a Buck Scientific model M500 single-beam infrared absorption spectrophotometer, and a Pike single-reflection attenuated total reflectance accessory. The fingerprint regions of these spectra are found in Figures 10 and 11, respectively, and assignments for the observed bands are found in Table 3.

Sample: (DL)-mandelic acid  
Size: 3.4500 mg  
Method: HXCA  
Comment: HB-21-073

DSC

File: C:\volume-29\mandelic\MAND01.001  
Operator: HGB  
Run Date: 3-JUL-02 14:09

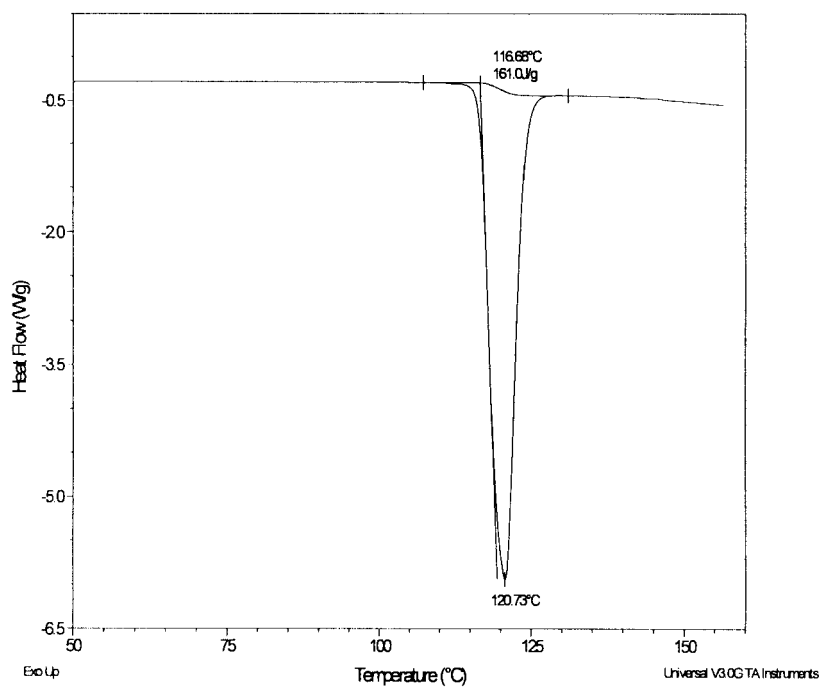


Figure 6. Differential scanning calorimetry thermogram of racemic mandelic acid (Aldrich lot KN07114MT).

Sample: (S)-mandelic acid  
Size: 1.8200 mg  
Method: H-PDA  
Comment: H-B-21-074 (ground)

DSC

File: C:\volume-29\mandelic\MAND04.001  
Operator: HGB  
Run Date: 9-Jul-02 10:00

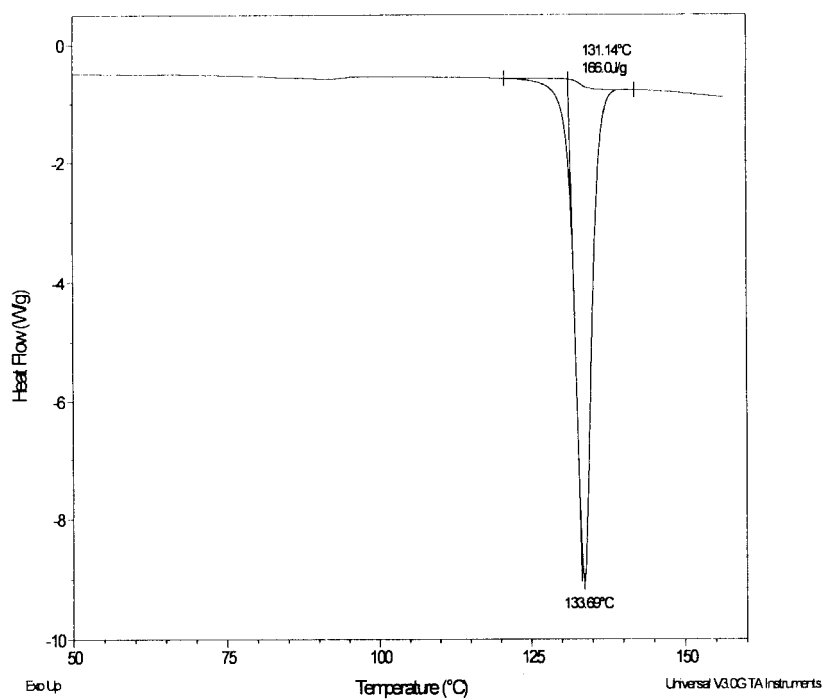


Figure 7. Differential scanning calorimetry thermogram of (*S*)-mandelic acid (Aldrich lot 11505DF).

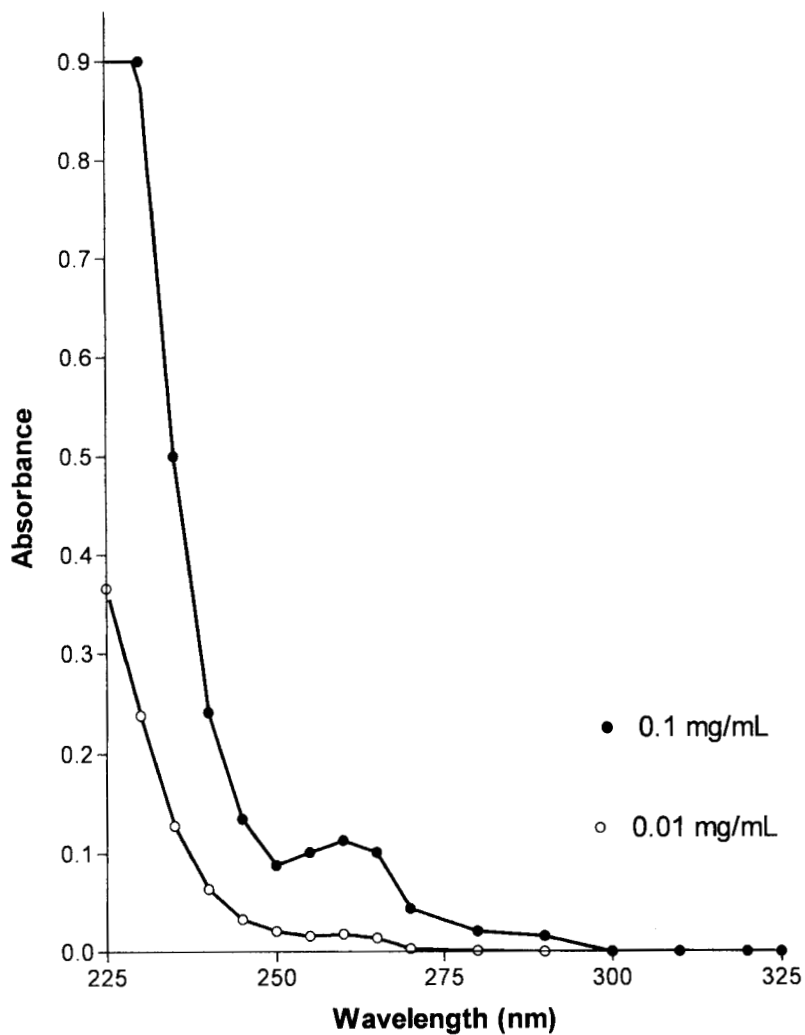


Figure 8. Ultraviolet absorption spectrum of 0.1 mg/mL and 0.01 mg/mL solutions of racemic mandelic acid in ethanol.

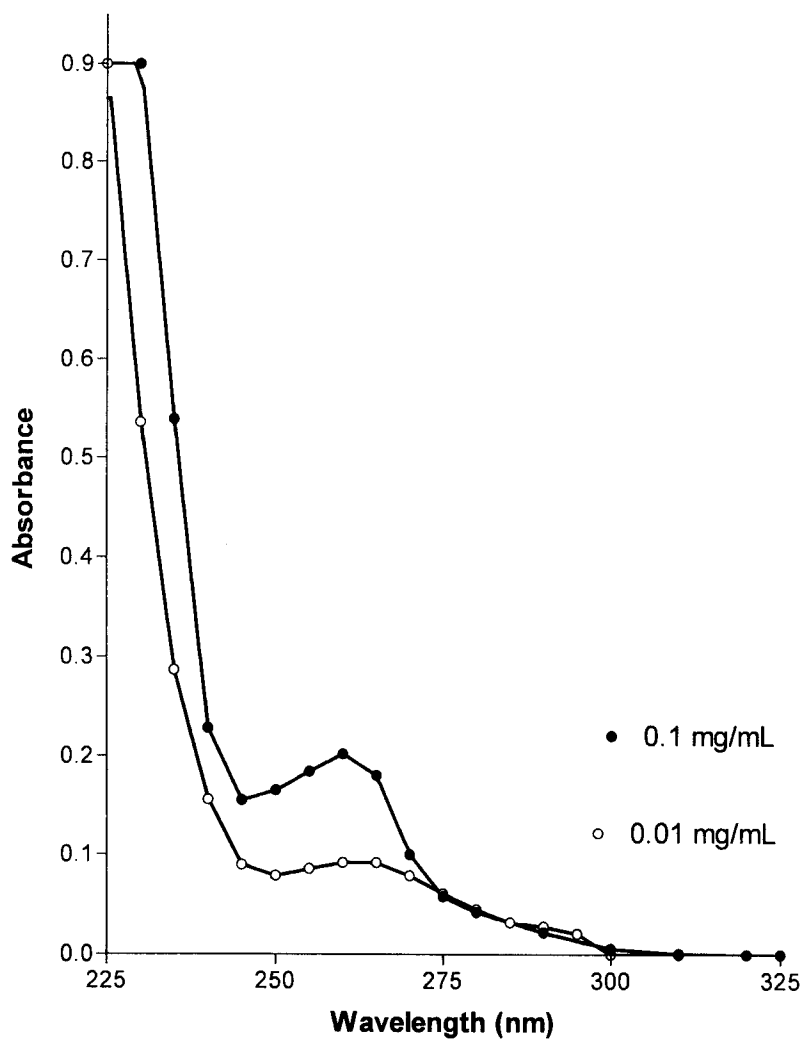


Figure 9. Ultraviolet absorption spectrum of 0.1 mg/mL and 0.01 mg/mL solutions of racemic mandelic acid in 0.1 N NaOH.

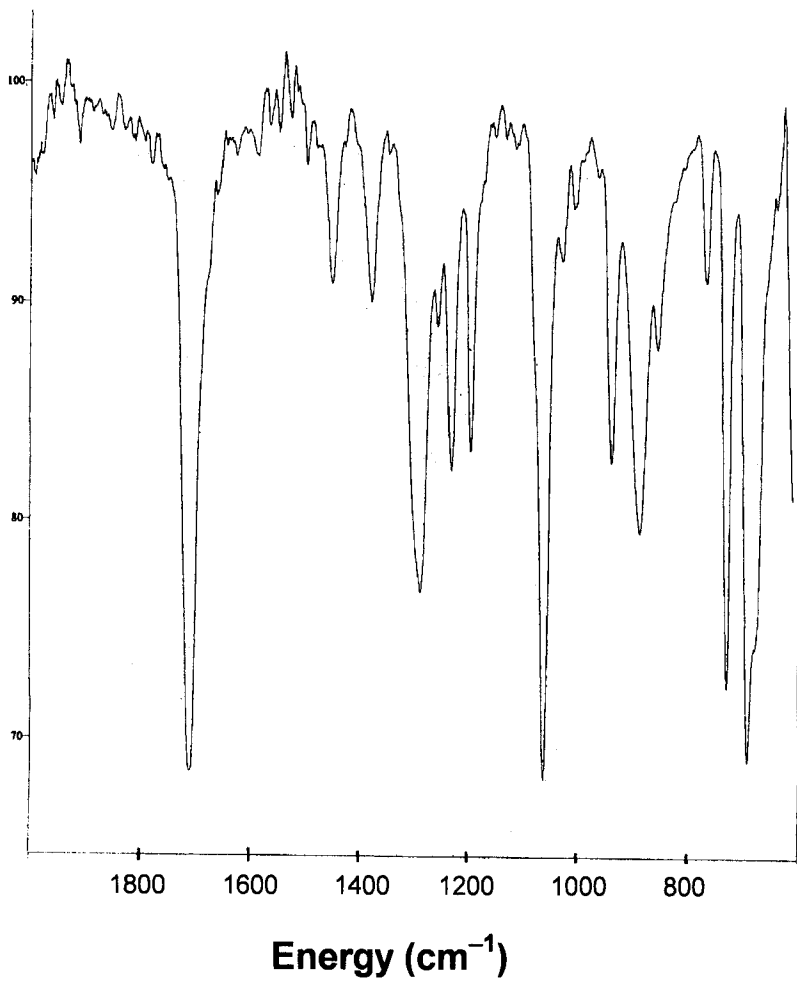


Figure 10. Fingerprint region of the attenuated total reflectance infrared spectrum of racemic mandelic acid.



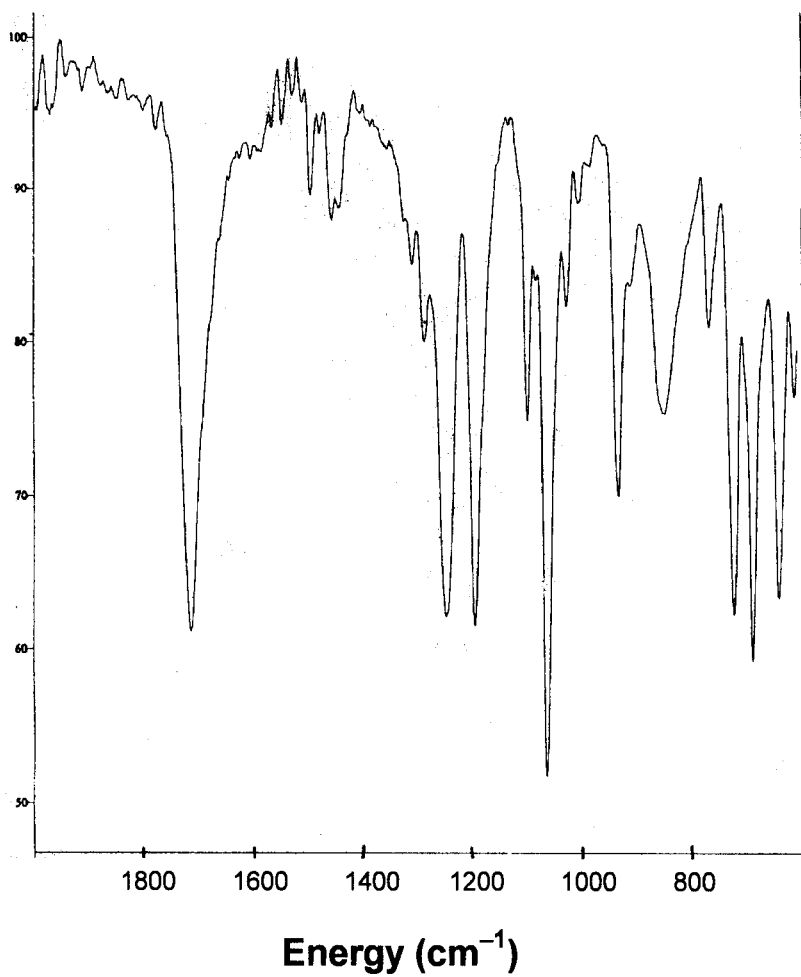


Figure 11. Fingerprint region of the attenuated total reflectance infrared spectrum of (*S*)-mandelic acid.

Table 4

Energies and Assignments for the Major Infrared Absorption Bands of Mandelic Acid

Energy, Racemic Mandelic Acid (cm <sup>-1</sup> )	Energy, (S)-Mandelic Acid (cm <sup>-1</sup> )	Assignment
691.6	688.8	
729.5	723.2	
766.8	769.0	
855.6	850.4	Aromatic hydrogen out-of-plane vibrations
888.5		
938.9	933.3	
1061.3	1061.8	–CO stretching mode
	1096.7	
1192.9	1192.6	
1228.7	1245.0	
1377.0		–CH <sub>2</sub> scissors deformation mode;
1450.0	1454.2	–CH <sub>3</sub> asymmetric deformation mode
1708.6	1712.8	Carbonyl group of carboxylate stretching mode
2900	2905	Aromatic –CH modes
3393	3448	Carboxylate mode

### 3.7.3 Nuclear Magnetic Resonance Spectrometry

The  $^1\text{H}$ -NMR spectrum of mandelic acid is fairly simple, and its resonance bands and assignments are summarized in Table 4. The  $^{13}\text{C}$ -NMR spectrum is also simple, and the analogous information is also summarized in Table 4. The information was calculated using the SpecManager Program (Advanced Chemistry Development, Toronto, Canada).

## 4. Compendial Methods of Analysis

The United States Pharmacopeia defines a number of test methods that define the USP grade of racemic mandelic acid [15]. The USP does not list any methods or specifications to differentiate the racemic substance from its resolved enantiomers.

### 4.1 Identification

Test A: When tested according to General Method <197K>, the infrared absorption spectrum of the test article is equivalent to that of the reference standard.

Test D: Dissolve about 200 mg of the test article in 2 mL of water, add 5 mL of sulfuric acid, and agitate gently. Then add an additional 10 mL of sulfuric acid, and heat gently. A positive reaction is indicated by the production of a purple color.

### 4.2 Melting Range

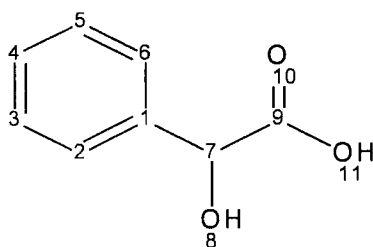
When tested according to General Method <741>, the melting range of the test article is between 118°C and 121°C.

### 4.3 Turbidity

Prepare a test solution of the test article in water at a concentration of 50 mg/mL (reserve a portion of the water used to prepare this solution for use as the blank). Measure the turbidity of the test solution according to General Method <851>) against the fixed reproducible standards defined in the Turbidity section under of General Method <381>. The turbidity is the difference between the values obtained for the blank and the test solution, expressed in Nephelos units. The test solution shows no more turbidity than the 10 Nephelos unit standard.

Table 4

Assignments for the Resonance Bands in the Nuclear Magnetic Resonance Spectra of Mandelic Acid



### $^1\text{H}$ -NMR Spectrum

Chemical Shift (ppm)	Resonance due to Proton at:
5.1	Carbon-7
8.5	Oxygen-8 and Oxygen-11
7.3	Carbon-4
7.6	Carbon-3 and Carbon-5
7.7	Carbon-2 and Carbon-6

### $^{13}\text{C}$ -NMR Spectrum

Chemical Shift (ppm)	Resonance due to Carbon at:
74.2	Carbon-7
126.6	Carbon-2 and Carbon-6
129.25	Carbon-3, Carbon-4, and Carbon-5
137.65	Carbon-1
176.5	Carbon-9

#### 4.4 Water Content

When tested according to General Method <921> (Method IA), not more than 0.5% of water is found.

#### 4.5 Chloride Content

When tested according to General Method <221>, a 1 gram portion shows no more chloride than corresponds to 0.15 mL of 0.020 N hydrochloric acid. This limit is equivalent to 0.01%.

#### 4.6 Residue on Ignition

When tested according to General Method <281>, the test article contains not more than 0.1%.

#### 4.7 Heavy Metals

When tested according to General Method <231> (Method I), the test article contains not more than 20 µg/g.

#### 4.8 Assay

The assay of mandelic acid is established using high performance liquid chromatography.

Mobile Phase: Prepare a 80:17:3 mixture of 0.01 M phosphoric acid, acetonitrile, and methanol. Adjustments in the composition may be made if necessary

Stock Solution: Dissolve accurately weighed quantities of acetophenone, benzoylformic acid, and benzaldehyde quantitatively in Mobile Phase to obtain a solution having known concentrations of about 0.2, 0.5, and 0.25 mg/mL, respectively.

Standard Stock Solution 1: Transfer about 25 mg of benzoic acid reference standard, accurately weighed, to a 250-mL volumetric flask, add 5.0 mL of Stock Solution, dilute with Mobile Phase to volume, and mix.

Standard Stock Solution 2: Dissolve an accurately weighed quantity of mandelic acid reference standard (previously dried in vacuum at 75°C for 4 hours) quantitatively in Mobile Phase to obtain a solution having a known concentration of about 5 mg/mL.

**Standard Preparation:** Transfer 5.0 mL of Standard Stock Solution 1 and 20.0 mL of Standard Stock Solution 2 to a 100-mL volumetric flask, dilute with Mobile Phase to volume, and mix. Each milliliter of this solution contains about 1 mg of mandelic acid, 0.2 µg of acetophenone, 0.5 µg of benzoylformic acid, 0.25 µg of benzaldehyde, and 5 µg of benzoic acid.

**Assay Preparation:** Transfer about 50 mg of the test article, accurately weighed, to a 50-mL volumetric flask, dissolve in and dilute with Mobile Phase to volume, and mix.

**Chromatographic System:** The HPLC system is equipped with a 240-nm detector and a 4.6-mm × 25-cm column that contains packing L1 (octadecyl silane bound to porous silica particles). The flow rate is about 0.8 mL/min.

**System Suitability:** Chromatograph the Standard Preparation, and record the peak responses as directed in the Procedure section. The relative retention times are about 0.8 for benzoylformic acid, 1.0 for mandelic acid, 2.5 for benzoic acid, 2.8 for benzaldehyde, and 3.7 for acetophenone. The tailing factor for each peak is not more than 2.0. The resolution between the benzoylformic acid peak and the mandelic acid peak, and between the benzoic acid peak and the benzaldehyde peak, is not less than 3.0. The relative standard deviation for replicate injections is not more than 1% for the mandelic acid peak.

**Procedure:** Separately inject equal volumes (about 20 µL) of the Standard Preparation and the Assay Preparation into the chromatograph, record the chromatograms, and measure the areas for the major peaks.

**Calculations:** Calculate the quantity, in mg, of mandelic acid in the amount of test article taken using:

$$\text{Mg(MAND)} = 50 C (R_U / R_S)$$

where C is the concentration (mg/mL), of mandelic acid in the Standard Preparation, and  $R_U$  and  $R_S$  are the mandelic acid peak responses obtained from the Standard Preparation and the Assay Preparation, respectively. The test article (previously dried in vacuum at 75°C for 4 hours) contains not less than 98.0% and not more than 102.0% of mandelic acid.

#### 4.9 Related Compounds

Using the chromatograms of the Standard Preparation and the Assay Preparation that were obtained during performance of the assay

determination, calculate the percentage of each related compound in the test article taken using the formula:

$$5 \{C_i/W\} \{R_i / R_{Si}\}$$

where  $C_i$  is the concentration ( $\mu\text{g/mL}$ ) of the relevant related compound in the Standard Preparation,  $W$  is the weight (mg) of test article taken to make up the Assay Preparation, and  $R_{Si}$  are the peak responses for the relevant related compound in the chromatograms of the Assay Preparation and the Standard Preparation, respectively.

The specification is that the test article contains not more than 0.1% of benzoylformic acid, 1.0% of benzoic acid, 0.05% of benzaldehyde, and 0.01% of acetophenone.

## 5. References

1. *The Merck Index*, 12<sup>th</sup> edn., S. Budavari, ed., Merck & Co., Whitehouse Station, NJ, 1996, p. 976.
2. *Martindale, the Extra Pharmacopeia*, 30<sup>th</sup> edn., J.E.F. Reynolds, ed., The Pharmaceutical Press, London, 1993, pp. 179-180.
3. A.I. Vogel, *Practical Organic Chemistry*, 3<sup>rd</sup> edn., Longmans, Green, and Co. Ltd., London (1956), p. 774.
4. A. McKenzie, *J. Chem. Soc.*, **85**, 1249 (1904).
5. R.H.F. Manske and T.B. Johnson, *J. Am. Chem. Soc.*, **51**, 1906 (1929).
6. R.M. Smith and A.E. Martell, *Critical Stability Constants*, volume 6, Plenum Press, New York (1989) pp. 314-315.
7. A. Seidell, *Solubilities of Organic Compounds*, D. van Nostrand Co., New York (1941) p. 593-596.
8. J. Jacques, C. Gros, and S. Bourcier, *Stereochemistry, Fundamentals and Methods*, volume 4, Georg Thieme Pub., Stuttgart (1977) p. 253a.

9. W. Klyne and J. Buckingham, *Atlas of Stereochemistry*, Oxford University Press, New York (1978) p. 25.
10. E.W. Washburn, *International Critical Tables*, McGraw-Hill, New York (1930) pp. 366-367.
11. T.S. Cameron and M. Duffin, *Cryst. Struct. Comm.*, **3**, 531 (1974).
12. K.-T. Wei and D.L. Ward, *Acta Cryst.*, **B33**, 797 (1977).
13. A.O. Patil, W.T. Pennington, I.C. Paul, D.Y. Curtin, and C.E. Dykstra, *J. Am. Chem. Soc.*, **109**, 1529 (1987).
14. *CRC Handbook of Chemistry and Physics*, 74<sup>th</sup> edn., D.R. Lide, ed., CRC Press, Boca Raton, 1993, p. 3-314.
15. *The United States Pharmacopeia*, 25<sup>th</sup> edn., United States Pharmacopoeial Convention, Rockville, MD, 2000, p. 1046.



This Page Intentionally Left Blank

# **PANTOPRAZOLE SODIUM**

Adnan A. Badwan<sup>1</sup>, Lina N. Nabulsi<sup>1</sup>, M.M. Al Omari<sup>1</sup>,  
Nidal H. Daraghme<sup>1</sup>, Mahmoud K. Ashour<sup>1</sup>, Ahmad M. Abdoh<sup>1</sup>,  
and A. M. Y. Jaber<sup>2</sup>

(1) The Jordanian Pharmaceutical Manufacturing Company Ltd.  
Na'or, Jordan

(2) Chemistry Department  
King Fahd University of Petroleum and Minerals  
Dhahran 31261  
Saudi Arabia

## **Contents**

### **1. Description**

- 1.1 Nomenclature
  - 1.1.1 Systematic Chemical Names
  - 1.1.2 Nonproprietary Names
  - 1.1.3 Proprietary Names
- 1.2 Formulae
  - 1.2.1 Empirical Formula, Molecular Weight, CAS Number
  - 1.2.2 Structural Formula
- 1.3 Elemental Analysis
- 1.4 Appearance
- 1.5 Uses and Applications

### **2. Methods of Preparation**

- 2.1 Synthesis Impurities
- 2.2 Degradation Products

### **3. Physical Properties**

- 3.1 Ionization Constants
- 3.2 Solubility Characteristics
- 3.3 Partition Coefficients
- 3.4 X-Ray Powder Diffraction Pattern
- 3.5 Thermal Methods of analysis
  - 3.5.1 Melting Behavior
  - 3.5.2 Differential Scanning Calorimetry
  - 3.5.3 Thermogravimetric Analysis
- 3.6 Spectroscopy
  - 3.6.1 UV/VIS Spectroscopy
  - 3.6.2 Vibrational Spectroscopy
  - 3.6.3 Nuclear Magnetic Resonance Spectrometry
    - 3.6.3.1  $^1\text{H}$ -NMR Spectrum
    - 3.6.3.2  $^{13}\text{C}$ -NMR Spectrum
- 3.7 Mass Spectrometry
- 3.8 Electrochemistry

**4. Methods of Analysis**

- 4.1 Identification
- 4.2 Titrimetric Analysis
  - 4.2.1 Aqueous Titration
  - 4.2.2 Non-aqueous Titration
- 4.3 Spectroscopic Analysis
  - 4.3.1 Spectrophotometry
  - 4.3.2 Colorimetry
- 4.4 Chromatographic Methods of Analysis
  - 4.4.1 Thin Layer Chromatography
  - 4.4.2 High Performance Liquid Chromatography
  - 4.4.3 Capillary Electrophoresis
- 4.5 Determination in Body Fluids and Tissues
  - 4.5.1 Determination of Pantoprazole and its Metabolite in Serum and Plasma
  - 4.5.2 Determination of Pantoprazole Enantiomers in Human Serum and Plasma

**5. Stability**

- 5.1 Solid-State Stability
- 5.2 pH Stability Profile
- 5.3 Drug-Excipient Interactions
- 5.4 Stability in the Presence of Various Salts

**6. Drug Metabolism and Pharmacokinetics**

- 6.1 Adsorption
- 6.2 Distribution
- 6.3 Metabolism
- 6.4 Elimination

**7. Pharmacology**

- 7.1 Mechanism of Action
- 7.2 Toxicity

**8. Acknowledgment****9. References**

**1. Description****1.1 Nomenclature [2, 3]****1.1.1 Systematic Chemical Names**

5-[difluoromethoxy]-2-[[[(3,4-dimethoxy-2-pyridinyl) methyl] sulfinyl]-1*H*-benzimidazole

5-Difluoromethoxybenzimidazol-2-yl-3,4-dimethoxy-2-pyridylmethyl sulfoxide

**1.1.2 Nonproprietary Names**

Pantoprazole (BAN, USAN, rINN)

**1.1.3 Proprietary Names**

Pantoprazole sodium is marketed as enteric coated tablets by Byk Gulden Lamberg Chemische Fabrik GmbH. under the proprietary name, "Pantoloc and Zurcal *Aust.*", "Somac Norw and *Austral*", "Pantozol, Zurcale *Belg*", "Eupantol and Inipomp *France*", "Pantozol and Rifun *Germany*", "Protium *Ireland*", "Pantecta, Pantopan and Peptazol *Italy*", "Pantozol *Neth.*", "Controloc and Pantoloc *S. Africa*", "Anagastra, Pantecta, Ulcotenal *Spain*", "Pantoloc *Swed.*", "Protium *UK*".

The finished product is also manufactured by the Jordanian Pharmaceutical Manufacturing Company (JPM)/Jordan under the proprietary name "Razon".

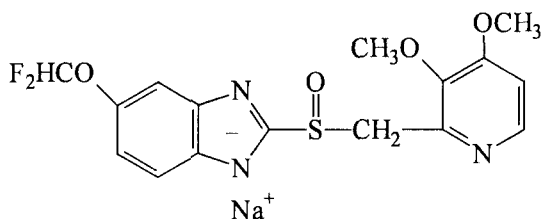
Pantoprazole has also been identified under the proprietary drug codes of BY-1023 and SKF-96022

**1.2 Formulae****1.2.1 Empirical Formula, Molecular Weight, CAS Number**

Pantoprazole free base	$C_{16}H_{15}F_2N_3O_4S$	383.371
Pantoprazole sodium anhydrate	$C_{16}H_{14}F_2N_3O_4SNa$	405.353
Pantoprazole sodium sesquihydrate	$C_{16}H_{14}F_2N_3O_4SNa \cdot 1.5H_2O$	432.375

The CAS number of the sodium salt is = 102625-70-7

### 1.2.2 Structural Formula



### 1.3 Elemental Analysis

The calculated elemental composition of the various forms is as follows:

	Free base	Sodium salt, anhydrate	Sodium salt, sesquihydrate
carbon:	50.13%	47.41%	44.45%
hydrogen:	3.94%	3.48%	3.96%
oxygen:	16.69%	15.79%	20.35%
nitrogen:	10.96%	10.37%	9.72%
fluorine	9.91%	9.37%	8.79%
sulfur:	8.36%	7.91%	7.42%
sodium:	—	5.67%	5.32%

The calculated water content of pantoprazole sodium sesquihydrate is 6.25%.

### 1.4 Appearance

The sodium salt of pantoprazole is obtained as an almost white to off-white, crystalline powder.

## 1.5 Uses and Applications

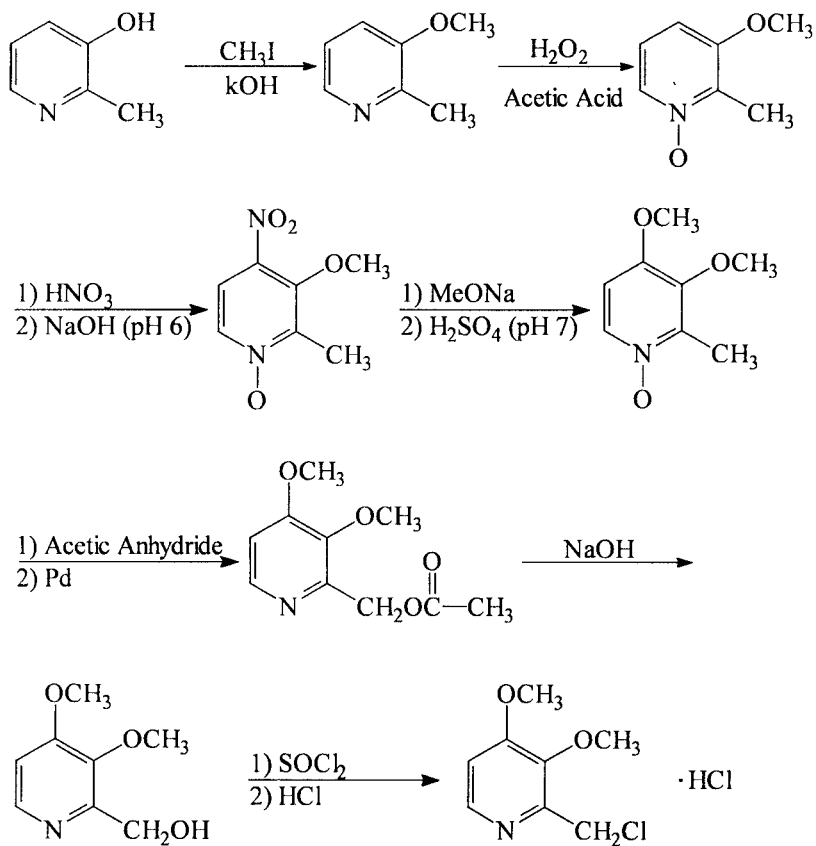
Pantoprazole sodium, a substituted benzimidazole derivative, is an irreversible proton pump inhibitor, and was developed for the treatment of acid-related gastrointestinal disorders. As with other drugs of its class (*e. g.* omeprazol or lansoprazole), pantoprazole reduces gastric acid secretion through inhibition of the portion on the gastric parietal cell. In combination with other drugs, pantoprazole can be used for the initial treatment of *H. Pylori* infection [1].

Pantoprazole sodium is patented by Byk Gulden Lamberg Chemische Fabrik GmbH (Kohl et al, US patent 4758579). In addition, the same company holds patents on enteric oral compositions containing pantoprazole (R. Rango and N. Hartmut, EP patent 519365, and US patent 4758579). The formulation was approved by the Food and Drug Administration on Feb 02, 2000, and is manufactured for Wyeth Ayerst (USA) under license from Byk Gulden Pharmaceuticals (Germany).

## 2. Methods of Preparation

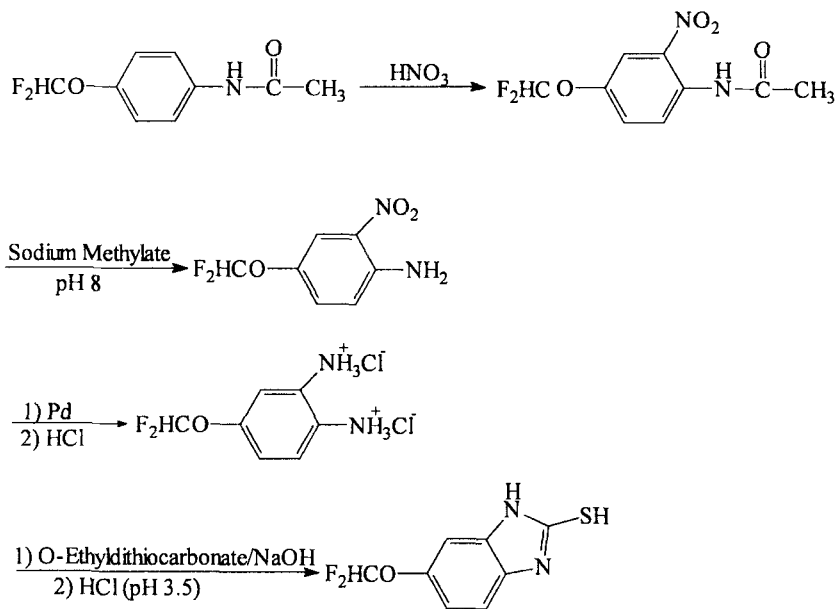
The route of synthesis of pantoprazole sodium, as described in US patent 4758579 (1988), is as follows. 2-chloromethyl-3,4 dimethoxypyridinium hydrochloride(I) is condensed with 5-difluoromethoxy-2-mercapto-benzimidazole(II) in ethanolic sodium hydroxide solution to yield 5-(difluoromethoxy)-2-(((3,4-dimethoxypyridine-2-yl) methyl) thio)-1*H*-benzimidazole(III). This compound is oxidized during reaction with *m*-chloroperbenzoic acid in methylene chloride, yielding pantoprazole base (IV). Further reaction with aqueous caustic soda solution gives pantoprazole sodium, which is then purified by crystallization from methanol. The various steps of this synthesis are illustrated in Scheme 1.

An alternate route of preparation for pantoprazole has been reported by Pan Li *et al* [4]. The compound was synthesized by refluxing 5-substituted phenylenediamine (I) with a pyridine derivative (II) in toluene to produce 5-(difluoromethoxy)-2-(((3,4-dimethoxypyridine-2-yl)methyl)thio)-1*H*-benimidazole(III). This reaction is followed by oxidation with *m*-chloroperbenzoic acid in chloroform to produce pantoprazole. The route of this synthesis is shown in Scheme 2.

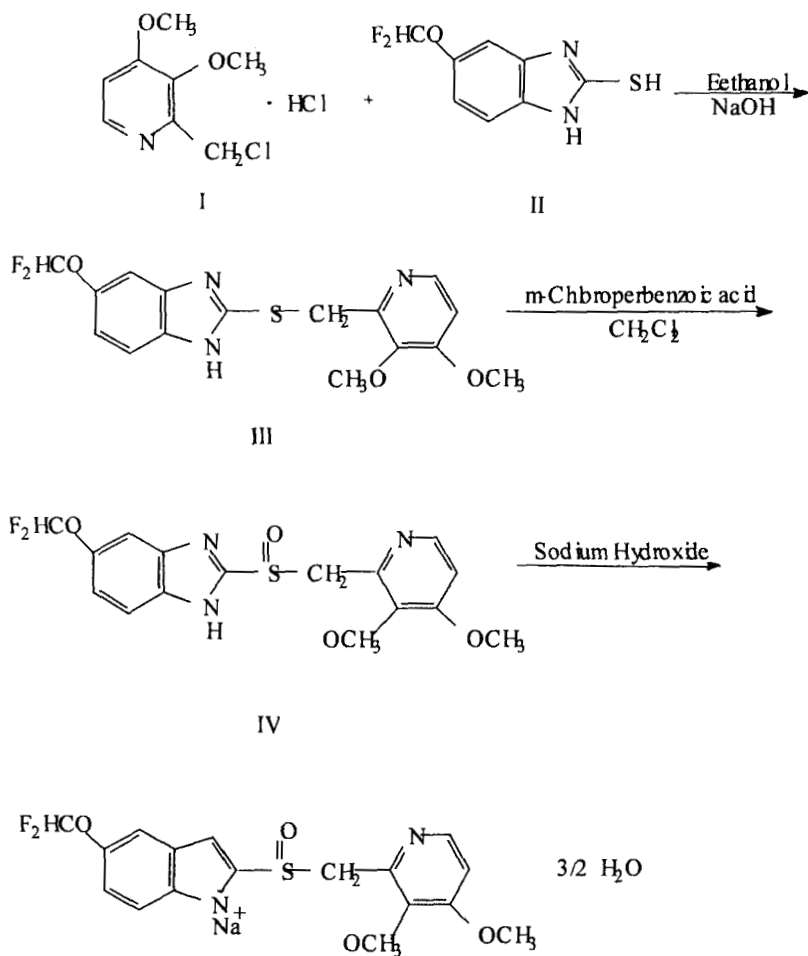


Scheme 1A. Preparation of 2-chloromethyl-3,4-dimethoxypyridinium hydrochloride.

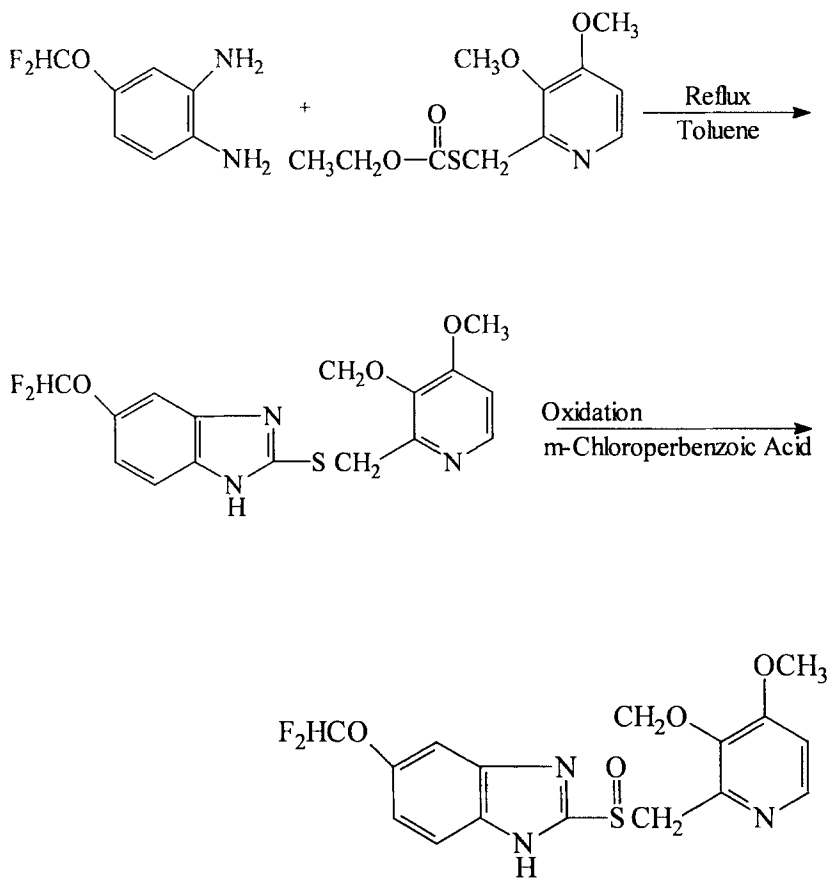




Scheme 1B. Preparation of 5-difluoromethoxy-2-mercapto-1-*H* benzimidazole

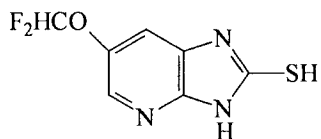


Scheme 1C. Preparation of pantoprazole sodium.

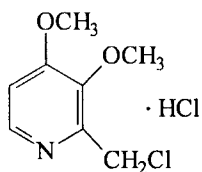
Scheme 2. Method of Pan Li *et al* for the preparation for pantoprazole.

## 2.1 Synthesis Impurities

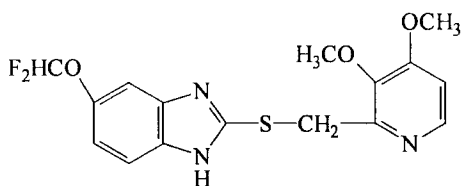
5-difluoromethoxy-2-mercapto-1*H* benzimidazole



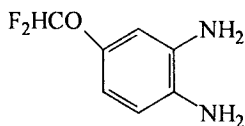
2-chloromethyl-3,4-dimethoxypyridine hydrochloride



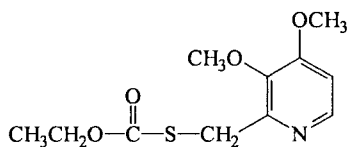
5-(difluoromethoxy)-2-(((3,4-dimethoxypyridine-2-yl)-methyl)thio)-1*H*-benzimidazole (the pantoprazole sulfide analogue)



5-difluoromethoxy phenyldiamine

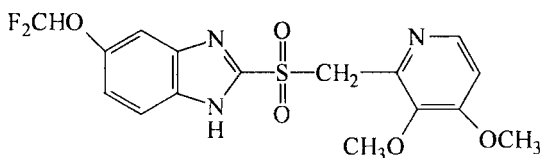


pyridine derivative

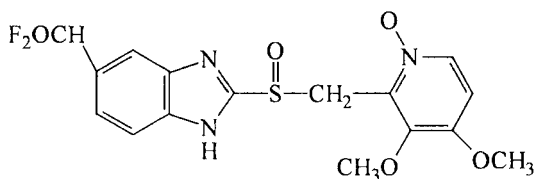


## 2.2 Degradation Products

Pantoprazole sulfone analogue (arising from an oxidation reaction)



Pantoprazole N-oxide (arising from an oxidation reaction)



## 3. Physical Properties [5]

### 3.1 Ionization Constants

It was reported that pantoprazole exhibits two dissociation constants,  $pK_{a1}$  of 3.92 and  $pK_{a2}$  of 8.19 [2].

### 3.2 Solubility Characteristics

The solubility of pantoprazole sodium has been studied in a variety of different solvents:

Solvent	Quantity Dissolved at 25°C (mg/mL)
Water	More than 1000
Methanol	More than 2000
Ethanol	More than 1000
Acetone	270
Chloroform	0.022
Dichloromethane	0.018
Diethyl ether	0.001
<i>n</i> -Hexane	0.001

Aqueous solutions of pantoprazole sodium are basic. The pH of a 1.0% w/v aqueous solution falls in the range of 9.5 to 10.0.

### 3.3 Partition Coefficients

The partition coefficient of pantoprazole sodium between *n*-octanol and water was determined at room temperature using a spectrophotometric procedure, and was found to be 1.3.

The pH dependence of the partition coefficient of aqueous solutions of pantoprazole was determined, and is shown in Figure 4. The results show that the partition coefficient decreases at elevated pH values. At low pH, the partition coefficient cannot be determined since pantoprazole is not stable below pH 6.

### 3.4 X-Ray Powder Diffraction Pattern

The X-ray powder diffraction pattern of pantoprazole sodium was obtained using a Philips diffractometer system (Model PW 105-81 goniometer and PW 1729 generation). The pattern was obtained using nickel filtered copper radiation ( $\lambda = 1.5405 \text{ \AA}$ ), and is shown in Figure 2. A full data summary is provided in Table 1.

### 3.5 Thermal Methods of analysis

#### 3.5.1 Melting Behavior

The melting point range of pantoprazole free base has been reported to be 139-140°C, and the substance melts with decomposition [2]. It has been noted that the sodium salt undergoes decomposition when heated beyond 130°C.

#### 3.5.2 Differential Scanning Calorimetry

The thermal behavior of pantoprazole sodium was examined by DSC, using a TA Instrument model 910S differential scanning calorimeter calibrated with indium. Pantoprazole sodium samples ranging from 5 to 10 mg were run at a heating rate of 5°C/min over a temperature range of 50°C to 179°C.

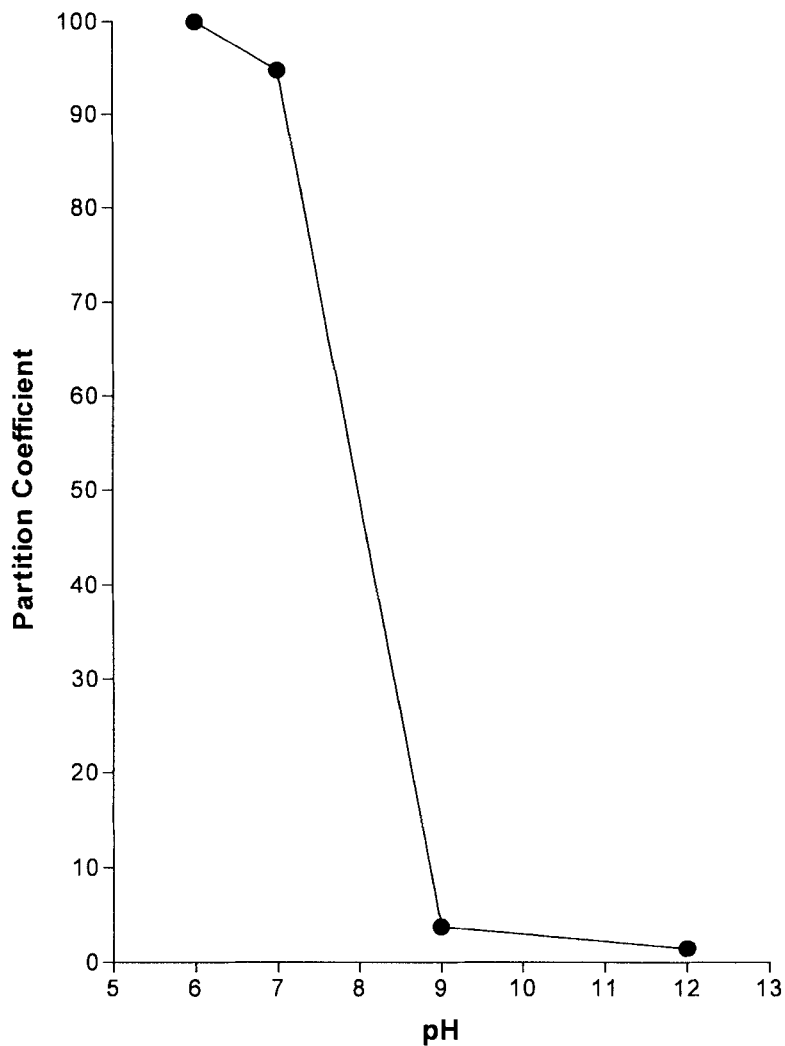


Figure 1. Partition coefficient of pantoprazole as a function of pH.

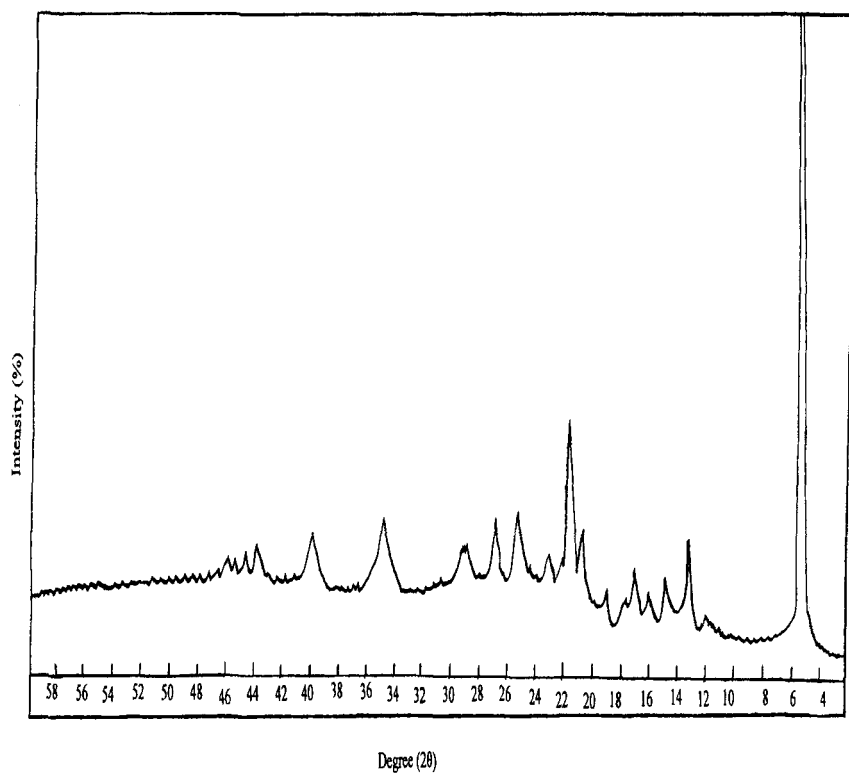


Figure 2. X-ray powder diffraction pattern of pantoprazole.



Table 1

Scattering Angles, Interplanar d-Spacings, and Relative Intensities in the X-Ray Powder Diffraction of Pantoprazole

Scattering Angle (deg. 2- $\theta$ )	d-Spacing (Å)	Relative Intensity (I/I <sub>o</sub> )
5.3	16.673	100.0
13.3	6.657	15.0
15.0	5.606	7.9
17.2	5.155	10.4
19.2	4.623	5.0
20.8	4.270	14.2
21.9	4.058	35.0
25.4	3.507	17.5
27.0	3.302	14.6
29.0	3.079	10.8
34.7	2.585	12.9
39.8	2.285	8.8
43.6	2.076	7.5

The DSC thermogram of pantoprazole sodium (shown in Figure 3) consisted of a single endothermic peak, assigned to the melting transition, and, having a peak maximum at 148°C. As is evident in Figure 3, the melting transition is accompanied by compound decomposition

### 3.5.3 Thermogravimetric Analysis

TG analysis of pantoprazole sodium was conducted obtained using a TA Instruments model 951 thermogravimetric analyzer system, calibrated using indium. The thermograms were carried out at a heating rate of 10°C/min, the sample size used ranged 5 to 10 mg, and the samples were heated over a temperature range of 50°C to 400°C.

The TG thermogram shown in Figure 4 for pantoprazole sodium shows a mass loss due to evolution of water equal to 3.1% at temperatures above the onset temperature of pantoprazole sodium (131°C). At higher temperatures, the compound starts to decompose, reaching about a 40% mass loss at temperature above 300°C.

## 3.6 Spectroscopy

### 3.6.1 UV/VIS Spectroscopy

The UV absorption spectrum of pantoprazole sodium was obtained using a Beckman model DU-650i UV/VIS spectrophotometer. The spectrum was scanned from 220 nm to 310 nm, using 1 cm quartz cells. A typical spectrum of pantoprazole sodium dissolved in 0.1 M NaOH is shown in Figure 5, where an absorbance maximum was observed at 295 nm.

The following UV absorbance maxima were obtained for pantoprazole sodium dissolved in different solvents, and the absorptivity parameter was calculated for solutions of 1% hydrated Pantoprazole.

Solvent	$\lambda$ max (nm)	A [1%,1-cm]
Water	287	326
0.1N NaOH	294	420
pH 9	294	417
pH 7	287	328
pH 6	288	315
Methanol	289	387
Ethanol	290	390
Chloroform	289	398

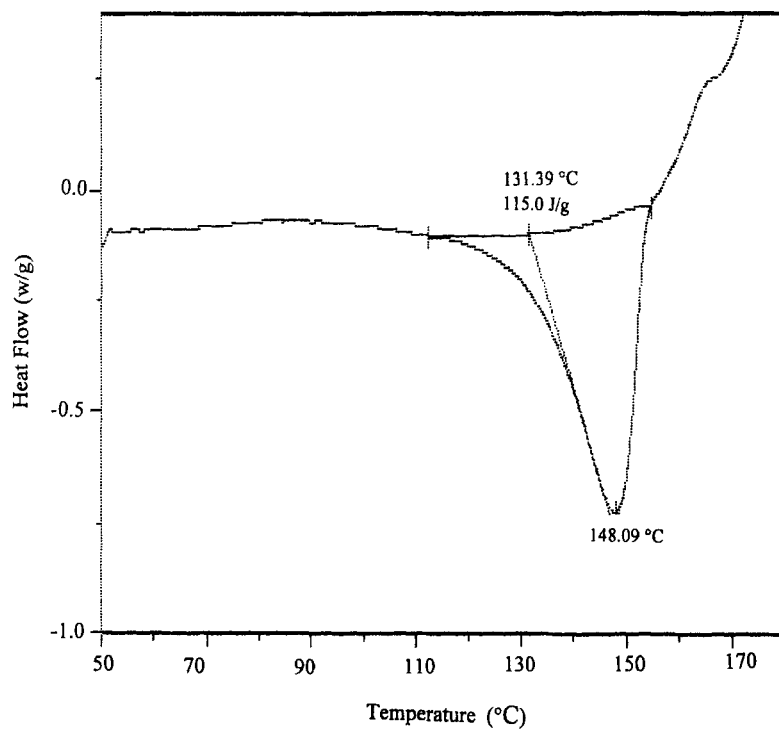


Figure 3. Differential scanning calorimetry thermogram of pantoprazole sodium.

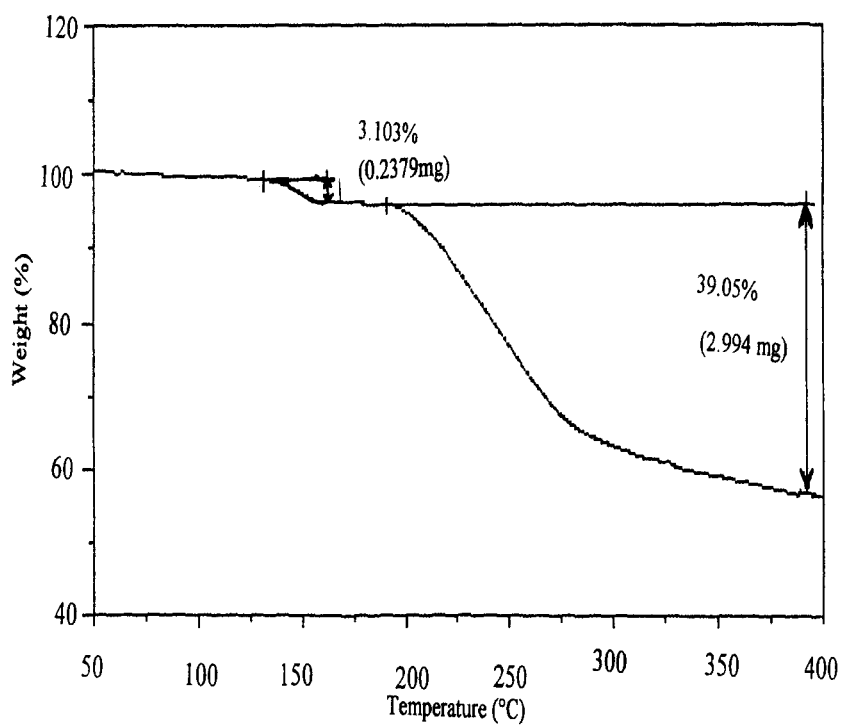


Figure 4. Thermogravimetric analysis of pantoprazole sodium.

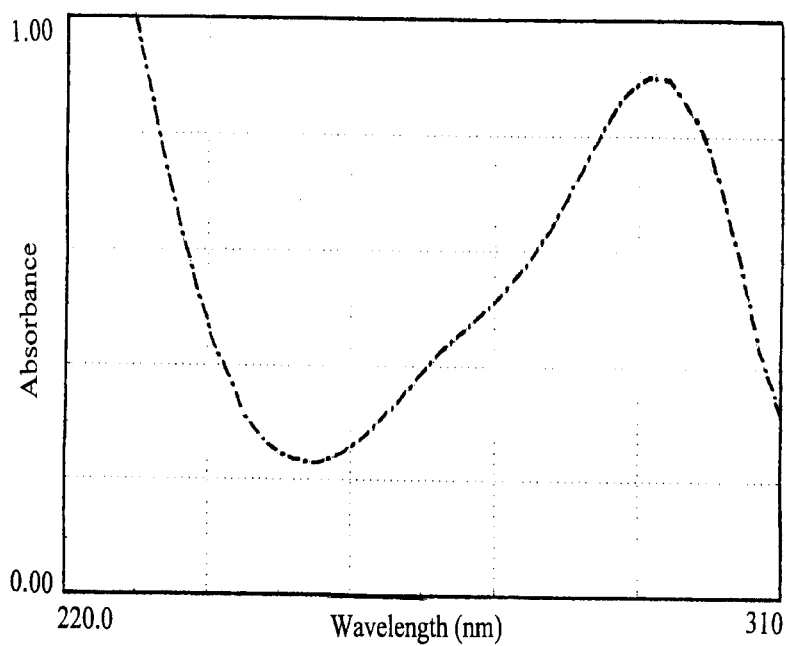


Figure 5. Ultraviolet absorption spectrum of pantoprazole sodium (concentration of 1 mg/100 mL in 0.1 M NaOH).

### 3.6.2 Vibrational Spectroscopy

The infrared spectrum of pantoprazole sodium was obtained in a KBr pellet (2% dispersion level) using a Perkin-Elmer 410 infrared spectrophotometer. The spectrum is shown in Figure 6, and the assignments for the major absorption bands are found in Table 2.

### 3.6.3 Nuclear Magnetic Resonance Spectrometry

#### 3.6.3.1 $^1\text{H}$ -NMR Spectrum

The one-dimensional  $^1\text{H}$ -NMR spectrum of pantoprazole sodium dissolved in DMSO was obtained using a Jeol 500 Lambda NMR spectrometer, and the resulting spectrum is shown in Figure 7. The assignments for the various resonance bands are found in Table 3.

#### 3.6.3.2 $^{13}\text{C}$ -NMR Spectrum

The one-dimensional  $^{13}\text{C}$ -NMR spectrum of pantoprazole sodium dissolved in DMSO was obtained using a Jeol 500 Lambda NMR spectrometer. The spectrum shown in Figure 8 was recorded at 24°C and internally referenced to tetramethylsilane. The assignments for the various resonance bands are found in Table 4.

### 3.7 Mass Spectrometry

The mass spectrum of pantoprazole sodium is shown in Figure 9, and the mass fragments with their assignments are shown in Table 5. The molecular weight of pantoprazole sodium was determined by using a Finnigan AQA LC/MS system (Thermoquest) operating in positive ionization mode (probe 4.00 kV, cone 200 V).

### 3.8 Electrochemistry

The electrochemical characteristics of pantoprazole sodium was studies using an EG&G model 264A polarographic analyzer stripping voltammeter in conjunction with a model 303 static mercury drop electrode. A differential pulse amplitude of 50 mV and a scan rate of 20 mV/sec were used.

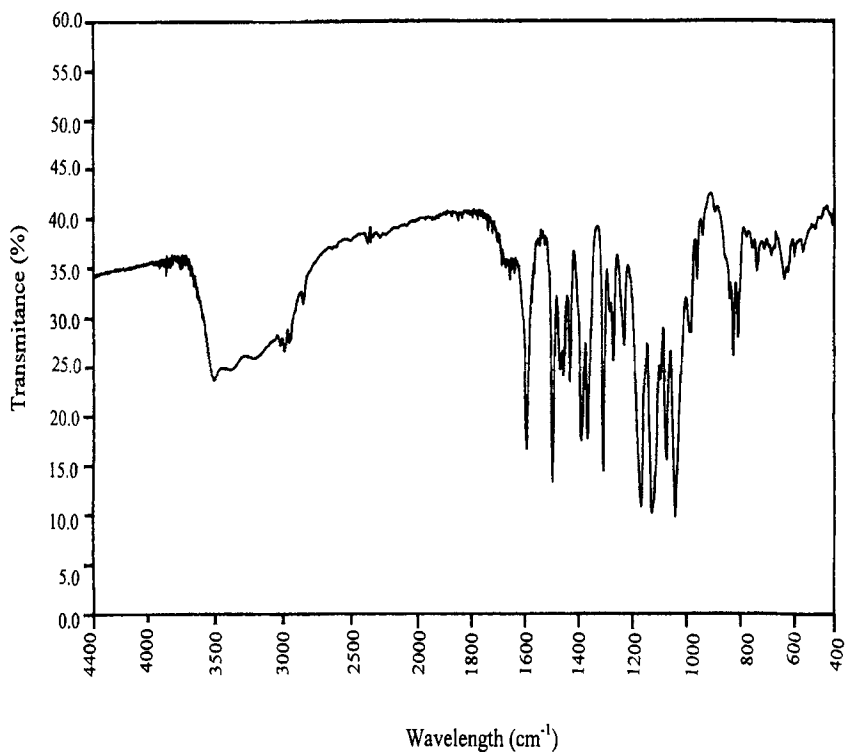


Figure 6. Infrared absorption spectrum of pantoprazole sodium.

Table 2

Assignments for the Infrared Absorption Bands of  
Pantoprazole Sodium

Energy (cm <sup>-1</sup> )	Assignment
3010	C-H aromatic stretching
2941 and 2835	C-H aliphatic stretching
1588	C=N stretching
1492, 1466, 1452 and 1428	C=C stretching in aromatic ring
1362 and 1384	C-H bending of CH <sub>2</sub> , CH <sub>3</sub>
1304	CF <sub>2</sub> stretching
1070	S=O stretching
805, 1027 and 1040	C-O of -OCH <sub>3</sub>



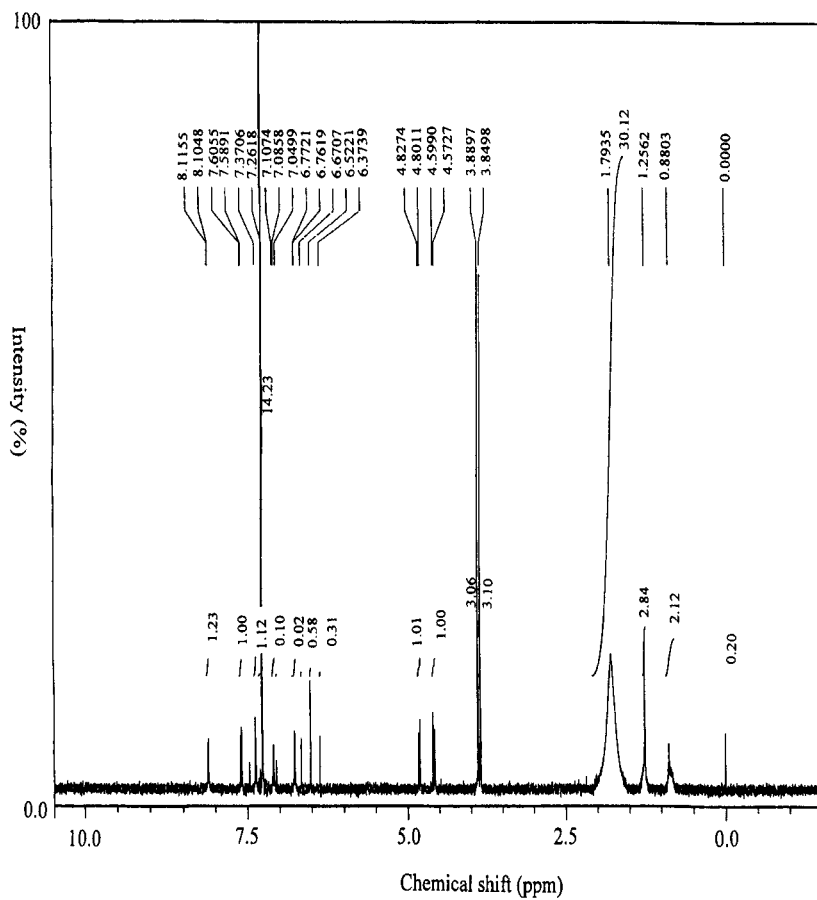
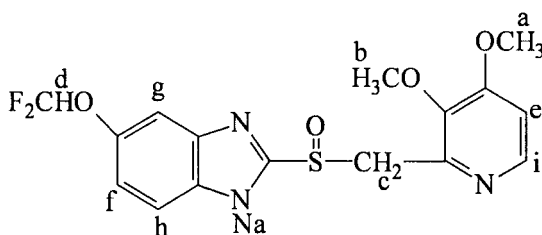


Figure 7. One-dimensional  $^1\text{H}$ -NMR spectrum of pantoprazole sodium.

Table 3

Assignments for the Resonance Bands in the  $^1\text{H}$ -NMR Spectrum of Pantoprazole Sodium



Chemical Shift (ppm)	Number of Protons (Multiplicity)	Assignment
3.76	3 (s)	a-OCH <sub>3</sub>
3.93	3 (s)	b-OCH <sub>3</sub>
4.50	2 (m)	c-CH <sub>2</sub>
6.75	1 (d)	d-CHO
6.90	1 (d)	e-CH
7.14	1 (dd)	f-CH
7.25	1 (s)	g-CH
7.40	1 (d)	h-CH
8.20	1 (d)	i-CH

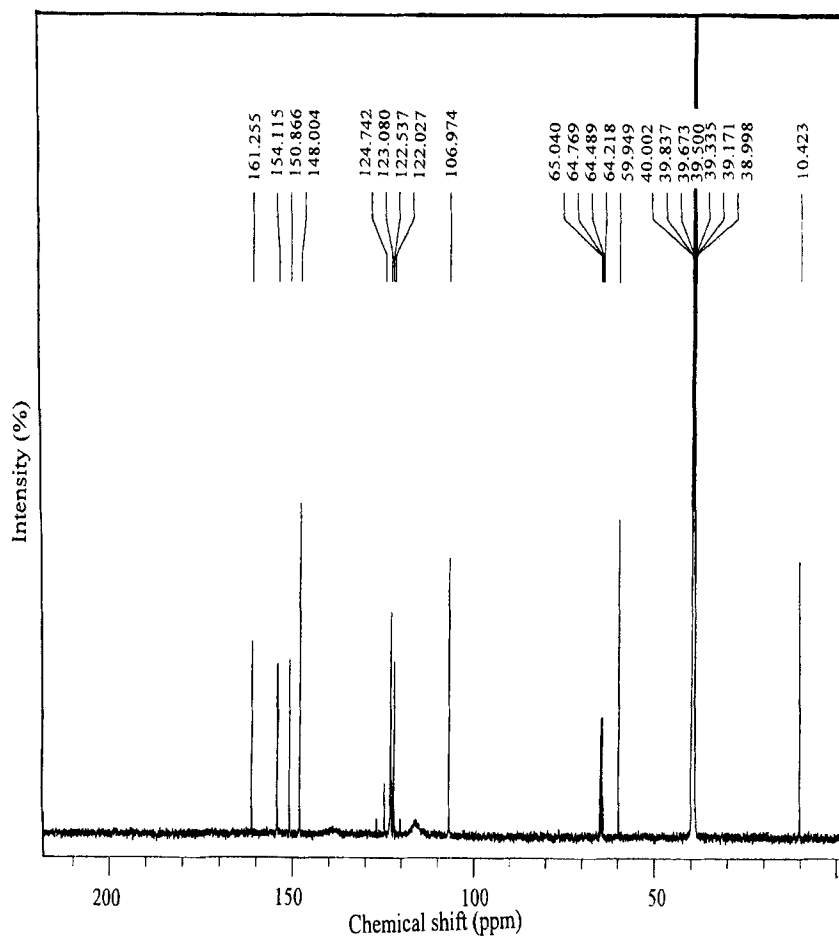
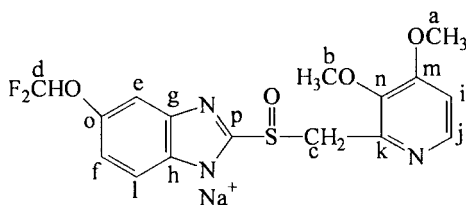


Figure 8. One-dimensional  $^{13}\text{C}$ -NMR spectrum of pantoprazole sodium.

Table 4

Assignments for the Resonance Bands in the  $^{13}\text{C}$ -NMR Spectrum of Pantoprazole Sodium



Chemical Shift (ppm)	Assignment
59.95	a, b
64.49	C
64.80	D
106.97	e, f
122.03	g, h
122.50	I
123.10	j, k
124.75	L
148.00	M
150.90	N
154.1	O
161.30	P

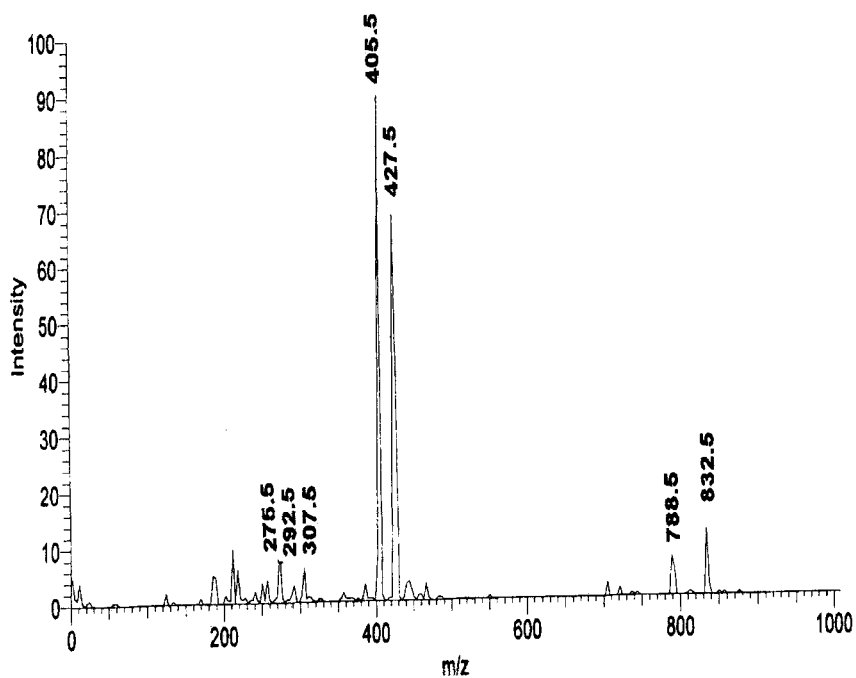
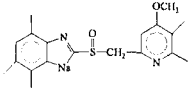
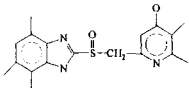
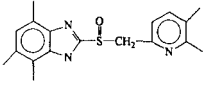


Figure 9. Mass spectrum of pantoprazole sodium.

Table 5

Assignments for the Fragment Ions in the Mass Spectrum of  
Pantoprazole Sodium

m/z	Assignment	Relative Intensity (%)
832.5	$(\text{Pantoprazole})_2\text{Na}_3$	12%
788.5	$[(\text{Pantoprazole})_2\text{Na}]^{+1}$	8%
427.5	$[\text{Pantoprazole Na}_2]^{+1}$	70%
405.5	$[\text{Pantoprazole Na}_2]^{+1}$	90%
307.5	$\text{C}_{14}\text{H}_{10}\text{N}_3\text{O}_2\text{SNa}/$ 	6%
292.5	$\text{C}_{13}\text{H}_7\text{N}_3\text{O}_2\text{SNa}/$ 	2%
275.5	$\text{C}_{13}\text{H}_7\text{N}_3\text{OSNa}/$ 	10%

Sample solutions of 10.0 mL containing 92  $\mu\text{g}$  pantoprazole in 0.1M KCl supporting electrolyte were deaerated with oxygen-free nitrogen. The differential pulse polarograms were recorded at  $25 \pm 1^\circ\text{C}$ , from 0 to  $-2.0\text{ V}$ , and using a scan rate of 20 mV/sec. The polarogram exhibited two reduction waves, corresponding to peaks at  $-1.17\text{ V}$  and  $-1.68\text{ V}$ . The direct current and differential pulse polarograms for pantoprazole sodium in 0.1M KCl are shown in Figures 10 and 11.

#### **4. Methods of Analysis**

##### **4.1 Identification**

Pantoprazole sodium may be identified as such on the basis of its characteristic infrared absorption spectrum (KBr pellet method), with the spectrum shown in Figure 6 serving as the reference.

##### **4.2 Titrimetric Analysis**

###### **4.2.1 Aqueous Titration**

200 mg of pantoprazole sodium is accurately weighed and dissolved in 50 mL of distilled water. The titration is performed using 0.1 M HCl acid as the titrant, and is conveniently carried out using a Mettler DL-67 potentiometric memo-titrator. Each milliliter of 0.1 M HCl is equivalent to 40.54 mg of pantoprazole sodium (as  $\text{C}_{16}\text{H}_{14}\text{F}_2\text{N}_3\text{O}_4\text{SNa}$ ).

###### **4.2.2 Non-aqueous Titration**

Pantoprazole sodium (200 mg) is dissolved in 50 mL of glacial acetic acid and titrated with 0.1 M  $\text{HClO}_4$ . The end point is detected potentiometrically using a Mettler DL-67 potentiometric memo-titrator. Each milliliter of 0.1 M  $\text{HClO}_4$  is equivalent to 40.54 mg of pantoprazole sodium (as  $\text{C}_{16}\text{H}_{14}\text{F}_2\text{N}_3\text{O}_4\text{SNa}$ ). It should be noted that pantoprazole degrades in the acidic media, but that the degradation does not affect the final results.

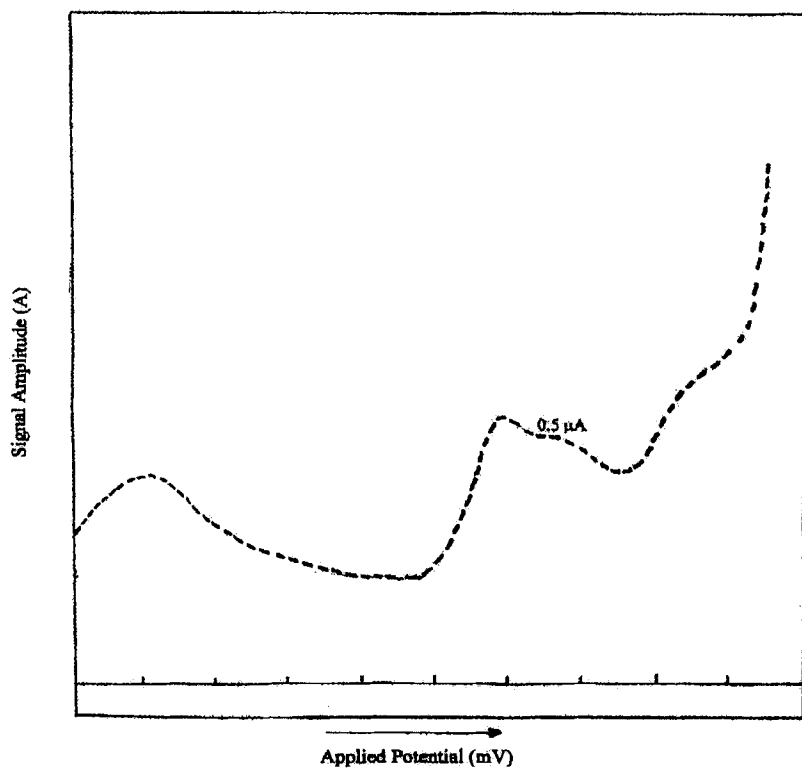


Figure 10. Direct current polarogram of pantoprazole sodium.



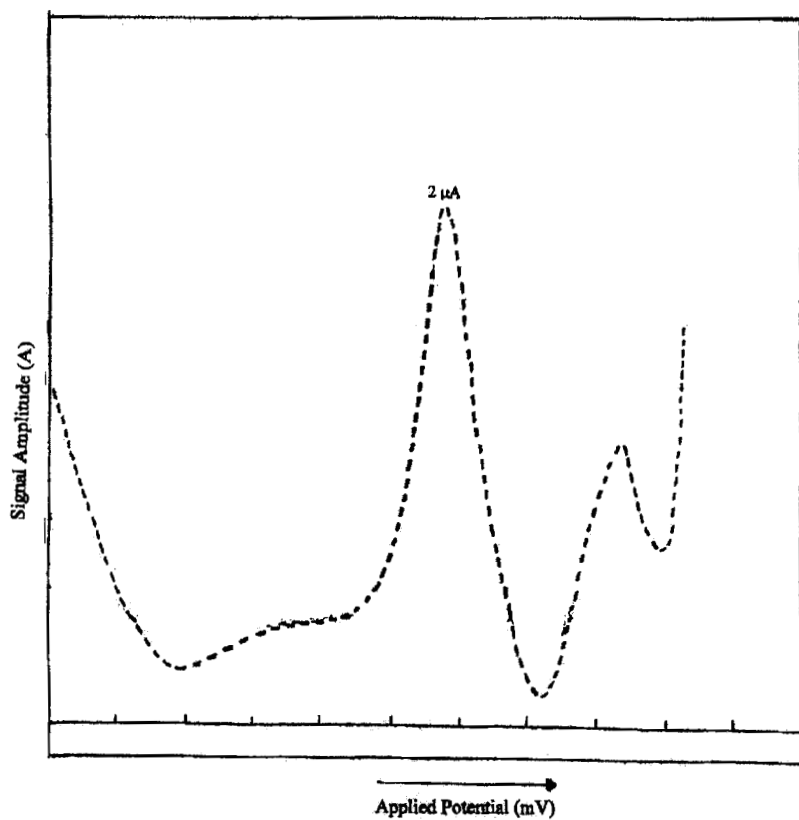


Figure 11. Differential pulse polarogram of pantoprazole sodium.

### 4.3 Spectroscopic Analysis

#### 4.3.1 Spectrophotometry

Pantoprazole sodium, in its bulk drug form or in tablet dosage forms, can be directly determined on the basis of its direct ultraviolet absorbance after being dissolved in 0.1 M NaOH.

The absorption of pantoprazole at 295 nm was used for the quantitative determination, and the method validated and used for the analysis of pantoprazole in its tablets. The results of validation study indicated that the method is linear over the range of 1.0 to 3.0 mg/mL ( $r = 0.9999$ ). The percent recovery and relative standard deviation were 99.3-101.5 ( $n=9$ ), and less than 1.0%, respectively. This method can be used for quality control and routine analysis [5].

#### 4.3.2 Colorimetry

Two colorimetric methods have been developed which were based on the charge transfer complexation reaction of pantoprazole sodium (acting as a  $n$ -donor) with either a  $\pi$ -acceptor (such as 2, 3-dichloro-5,6-dicyano-1,4-benzoquinone, or DDQ) or with a  $\sigma$ -acceptor (such as iodine).

Quantitation of the colored products was performed at a wavelength of 457 nm for the DDQ complex, and at wavelengths of 293 and 359 nm for the iodine complex. These methods can be used to determine pantoprazole in concentration ranges of 10-60  $\mu\text{g/mL}$  (DDQ complex), 17.7-141.6  $\mu\text{g/mL}$  (iodine complex), and 4.3-25.9  $\mu\text{g/mL}$  (Cu(II) ternary complex). The mean recoveries were found to be 99.51% (DDQ complex), and 98.97% and 99.84% (iodine complex). Relative standard deviations of 0.53% (DDQ complex), and 1.21% and 0.65%, (iodine complex) were found.

A third method was also developed based on formation of the ternary complex with eosin and Cu(II), with the colored product being quantified using its absorbance at 549 nm. A mean recovery of 99.46% was found, characterized by a relative standard deviation of 0.81%.

The three methods have been applied successfully to the analysis of the bulk drug or its pharmaceutical formulations with good accuracy and precision. These methods are recommended for quality control and routine analysis [6].

## 4.4 Chromatographic Methods of Analysis

### 4.4.1 Thin Layer Chromatography

It was reported by Ranger that planar chromatography (TLC) can be used for the quantitative analysis of pantoprazole during stability testing [16]. Silica gel was used as a stationary phase, and a 48:35:15:2 mixture of ethyl acetate, cyclohexane, methanol, and concentrated ammonia was used as the mobile phase. Detection was carried out at 295 nm.

### 4.4.2 High Performance Liquid Chromatography

A HPLC method has been developed to determine the assay value and chromatographic purity [5]. The method uses a Beckman system (Gold system software) equipped with a model 116 high-pressure programmable solvent module and a model 166 programmable detector module set at 290 nm was used for the analysis. The system was operated using a 20  $\mu$ L injection loop, and a Hypersil C<sub>8</sub>-column (250  $\times$  4.6 mm ID, 5  $\mu$ m particles). The mobile phase consisted of a 70:30 w/v mixture of buffer (0.02 M sodium dihydrogen orthophosphate and 0.003 M disodium hydrogen orthophosphate) and acetonitrile, adjusted to pH 6.0 with 10% orthophosphoric acid solution. The system was run at a flow rate of 2.0 mL/min.

Due to the high stability of pantoprazole sodium at high pH, the samples to be analyzed were dissolved in 0.1 M NaOH. The method was found to be specific for pantoprazole since it showed no interference from excipients in the formulation, and can separate the potential synthesis impurities and possible degradation products.

A typical chromatogram obtained using this method is shown in Figure 12, and the retention times ( $R_T$ ) and the relative retention time ( $R_{RT}$ ) for pantoprazole sodium and some of its related compounds are shown in Table 6. The calibration curve for the assay determination, obtained over a concentration range of 228-670  $\mu$ g/mL, was found to be linear with a correlation coefficient of 0.999. The recovery and relative standard deviation for various assays were 97.3-101.5 and 1.1, respectively. A calibration curve was also developed for pantoprazole sodium related compounds, covering a concentration range of 1 to 3  $\mu$ g/mL, and which was found to be linear with a correlation coefficient of more than 0.999. The limits of detection and limits of quantitation were calculated as 0.15  $\mu$ g/mL and 0.49  $\mu$ g/mL, respectively.

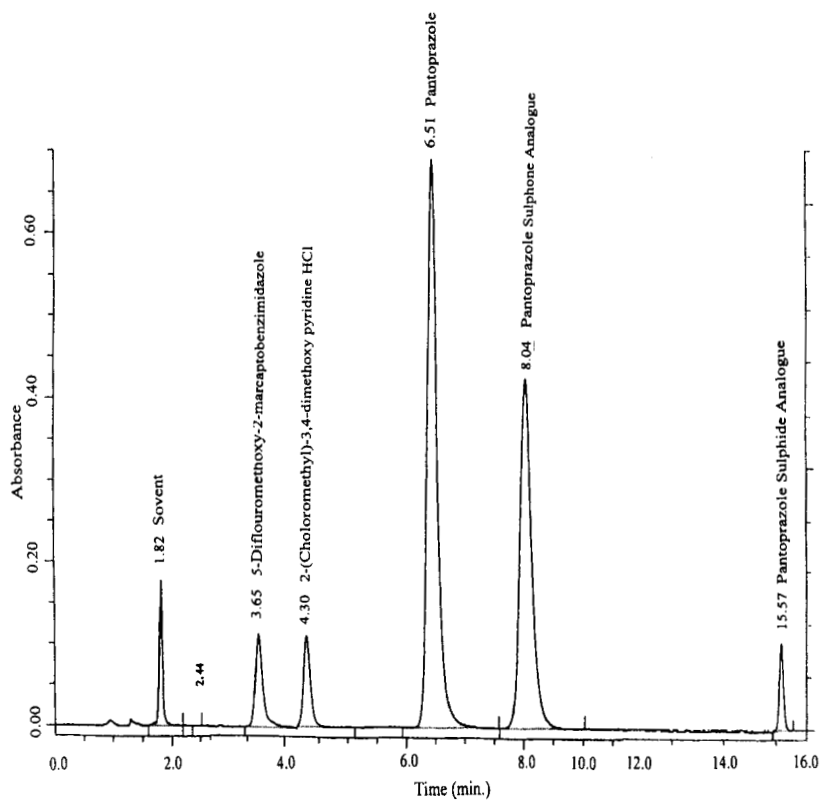


Figure 12. Typical HPLC chromatogram of pantoprazole sodium and its related substances.

Table 6

Retention Times and Relative Retention Times for  
Pantoprazole Sodium and its Related Compounds

Compound	Retention Time (min.)	Relative Retention Time (min.)
5-Difluoromethoxy-2-marcaptobenzimidazole	3.7	0.57
2-(Chloromethyl)-3,4-dimethoxy pyridine HCl	4.4	0.68
Pantoprazole Sodium	6.5	1.00
Pantoprazole Sulfone Analogue	8.0	1.26
Pantoprazole Sulfide Analogue	15.5	2.38

#### 4.4.3 Capillary Electrophoresis

Separation of the enantiomers of pantoprazole sodium was described by Kuhn *et al* [14]. Bovine serum albumin (BSA) was used as the chiral selector, and different experimental parameters were investigated to obtain good resolution between the enantiomers. Increasing the concentration of BSA improved the chiral resolution, but the sensitivity of the detection system was lowered. Using a buffer system having a pH around 7.4 and addition of 1-propanol caused an enhancement to the peak shape and the resolution. This method is suitable for routine analysis.

Svensson *et al* reported a non-aqueous capillary electrophoresis method for the analysis of pyridinyl-methyl-sulfinyl-benzimidazoles [15]. Different polar organic solvents were tested as background electrolytes, and *N*-methylformamide was found to have the best properties with respect to both electrophoretic behaviour and high solubility of the interested compounds. The method was found to be precise (1.8% RSD for normalized peak areas), with good linearity and a low detection limit.

#### 4.5 Determination in Body Fluids and Tissues

##### 4.5.1 Determination of Pantoprazole and its Metabolite in Serum and Plasma

Doyle *et al* have reported the determination of pantoprazole and its sulfone metabolite in serum and plasma using a direct HPLC method and a fully automated pre-column sample clean-up [7]. The method was optimised to obtain acceptable recovery. Linearity range, precision, and detection limits were determined, and the method was applied to define the pharmacokinetics of pantoprazole in dogs and humans.

Doyle *et al* also reported a direct injection HPLC method for the analysis of pantoprazole in biological samples [8]. The method was developed to determine pantoprazole and its sulfone metabolite, and was found to be accurate and reproducible.

Doyle *et al* [9] published an article describing two fully automated assays, one for zaprinost and the other for pantoprazole and its sulfone metabolite. Both assays were developed to support pharmacokinetics studies. Plasma or serum (20-200  $\mu$ L) was placed directly into an auto-sampler, and all subsequent manipulations were performed mechanically [9].

#### 4.5.2 Determination of Pantoprazole Enantiomers in Human Serum and Plasma

A direct, stereoselective, reversed-phase HPLC method was used for the determination of the enantiomers of pantoprazole in human serum [10]. The enantiomers were separated with high resolution on a cellulose-based chiral stationary phase (Chiralcel OJ-R), following online solid phase sample cleanup with a column-switching device. A mixture of acetonitrile and 50 mM sodium perchlorate was used as the mobile phase, and eluted at a flow rate of 0.5 mL/min. Pantoprazole enantiomers were detected using a UV detector operating at a wavelength of 290 nm. The calibration curve for each enantiomer was found to be linear over the range of 0.1 to 5.0 µg/mL. Under these conditions, the determination of pantoprazole enantiomers in human serum can be achieved with satisfactory selectivity, sensitivity, precision, and accuracy. The described procedure is very simple and rapid, since a labor-intensive procedure of sample preparation is not required. The method was applied to the analyses of the serum samples obtained from a volunteer who received an 80 mg oral dose of racemic pantoprazole. The samples showed the (+)/(-) isomer ratios ranged from 0.74 to 1.03 up to 6 hours after dosing, indicating that there is only a small difference in the concentration of (+) and (-) pantoprazole.

The enantiomers of pantoprazole were separated using HPLC at 40°C on Chiralcel OJ-R columns with 25% acetonitrile and 50 mM NaClO<sub>4</sub> (3:1 v/v) as the mobile phase [11]. Elution was performed at a flow rate of 0.5 mL/min, and detection was at 286 nm. Lichroprep PR-2 was used as a pre-column, and Lichrospher 100 RP-18 was used as a guard column.

The enantiomers of pantoprazole were also separated by Balmer *et al* using a chiral stationary phase [12]. The method is based on using a mixture of ethanol and hexane (1:4 v/v) as mobile phase, eluted at 1 mL/min, and Chiralpak AD (an amylose-based chiral material) as the stationary phase.

It also was reported by Lagerstroem *et al* that pantoprazole and its enantiomers can be separated by using normal-phase liquid chromatography, and detection by atmospheric pressure ionization tandem mass spectrometry [13].

## 5. Stability [5]

Pantoprazole sodium is stable under normal storage conditions, but the substance should be stored in tight containers and protected from light and humidity. The HPLC method described in a previous section has been used to test the stability of pantoprazole sodium under a variety of conditions that will be described in subsequent sections.

### 5.1 Solid-State Stability

Solid pantoprazole sodium was proven to be stable when stored for 3 months in open containers at 40°C and 75% relative humidity, and at 50°C and 75% relative humidity.

Pantoprazole sodium was also stable when stored at 65°C for 2 months. Although it showed discoloration at these conditions, no significant increase in impurities was obtained.

The stability data obtained during the course of these studies for pantoprazole and related impurities are shown in the following table:

Test Required	Initial	40°C / 75%RH	50°C / 75%RH	65°C
Assay	100.4%	100.1%	99.5%	99.4%
Total impurities	0.4%	0.5%	0.6%	0.6%
Water Content	5.0%	5.0%	5.0%	5.0%

### 5.2 pH Stability Profile

The pH stability profile for pantoprazole was studied at 25°C, and the percentage of original drug left after 24 hours of elapsed time was determined. The data are plotted in Figure 13, where it is evident that the stability of pantoprazole sodium was strongly dependent on the solution pH, and the compound was least stable at low pH. The highest stability of pantoprazole sodium can be achieved at pH higher than 5.5.



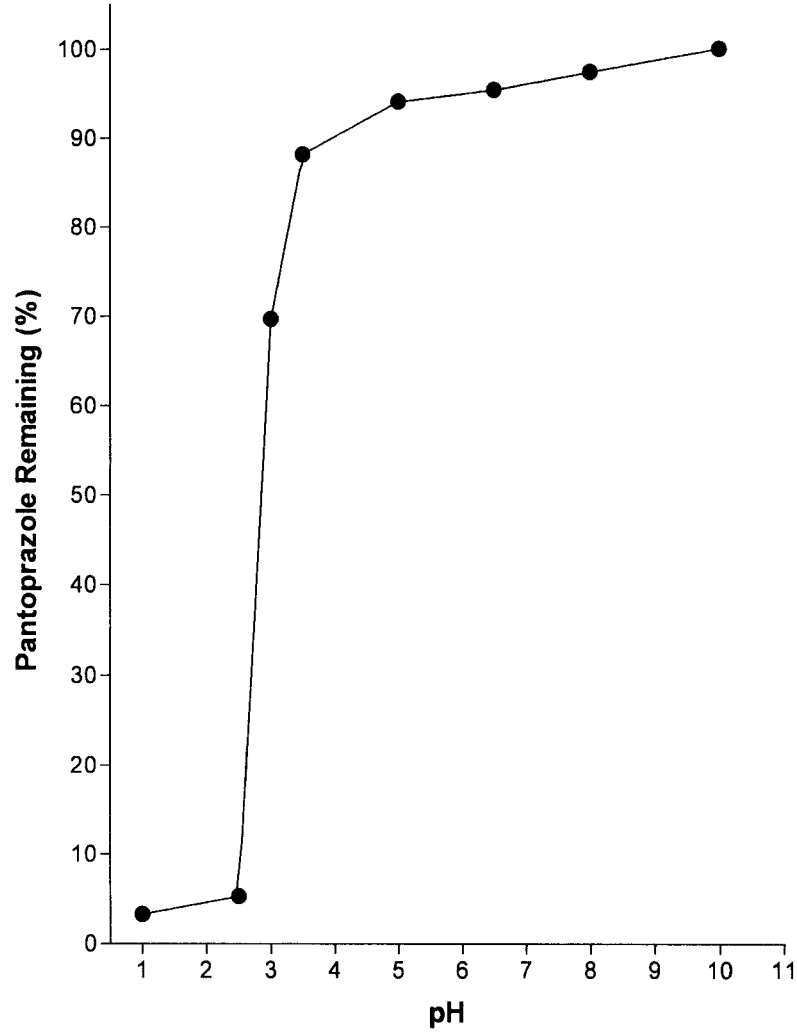


Figure 13. pH Stability profile of pantoprazole sodium at 25°C for 24 hours.

### 5.3 Drug-Excipient Interactions

Pantoprazole sodium was separately mixed in 1:1 ratios with sodium carbonate, mannitol, calcium stearate, colloidal anhydrous silica, povidone K90, crospovidone, and hydroxypropyl methylcellulose. The blends were stored at 40°C and 75% relative humidity, at 50°C and 75% relative humidity, and at 65°C for 30 days. No evidence for instability was noted, indicating that pantoprazole sodium is compatible with these common excipients.

### 5.4 Stability in the Presence of Various Salts

The stability of pantoprazole, omeprazole, and lansoprazole was studied chromatographically [17]. The three compounds were monitored using a HPLC system based on a Zorbax Eclipse XDB C<sub>8</sub>-column (5 µm; 150 cm × 4.6 mm i.d.), a mobile phase consisting of 700:300 v/v phosphate buffer: acetonitrile (with the pH adjusted to 7.0 with phosphoric acid), and detection at 280 nm. The method was used to study the effect of pH and various salts on the stability of the three compounds. The study showed that pantoprazole was the most stable compound and that lansoprazole was the least stable. The stabilities of the compounds in salt solutions were found to be in the following order:

phosphate buffer < trisodium citrate < citrate buffer ≤  
acetate buffer < citric acid ≤ monosodium citrate ≤ calcium  
carbonate < sodium bicarbonate < sodium chloride < water

Thus, the rate of degradation exhibited a direct relationship with pH and salt concentration.

## 6. Drug Metabolism and Pharmacokinetics

### 6.1 Adsorption

Pantoprazole is sensitive to degradation in the acidic medium of the stomach, so the drug is formulated in enteric-coated formulations. Pantoprazole is rapidly absorbed after oral administration, with peak plasma concentrations ( $C_{\max}$ ) of 1.1 to 3.1 (mean 2.1 mg/L) occurring at 2 to 4 (mean 2.7) hours ( $t_{\max}$ ) after ingestion of an enteric coated 40 mg tablet.

Concomitant intake of food has no influence on the bioavailability of pantoprazole, and any possible retardant effect of food on the rate of drug absorption is unlikely to be of clinical relevance, given the prolonged antisecretory action of pantoprazole [1].

Pantoprazole is subject to low first-pass hepatic extraction, as reflected in an estimated absolute oral bioavailability of 77%. On repeated oral administration, the pharmacokinetics of pantoprazole (20 and 40 mg once daily) are similar to those after single dose administration [1, 18]. The absolute bioavailability was 70% in patients with severe liver cirrhosis, and more than 90% in healthy elderly subjects [18].

## **6.2 Distribution**

Plasma protein binding of pantoprazole is high (approximately 98%), so therefore pantoprazole has a relatively low apparent volume of distribution (mean 0.16L/kg at steady state), suggesting limited tissue distribution [1,19,18].

## **6.3 Metabolism**

Pantoprazole undergoes extensive hepatic metabolism in humans via cytochrome P450 (CYP)-mediated oxidation, followed by sulfate conjugation [1]. The major metabolites of pantoprazole are shown in Figure 14.

The available data indicate that the metabolic disposition of pantoprazole is under the pharmacogenetic control of S-mephenytion 4'-hydroxylase (CYP2C19) [20]. This means that within a population, few individuals metabolize the compound slowly compared with the majority of the population. This genetic variant is rare among Caucasus 3%, although a higher proportion (approximately 15%) has been reported in people of Asian origin such as Japanese, Chinese, Caucasians, and Koreans.

The area under the curve of pantoprazole plasma concentration versus time (AUC) for a slow metabolizer is generally approximately 5 times higher than that for an average patient. Since pantoprazole is considered safe and well tolerated, and no dosage related adverse drug reactions have been identified, this finding seems to be of no clinical relevance.

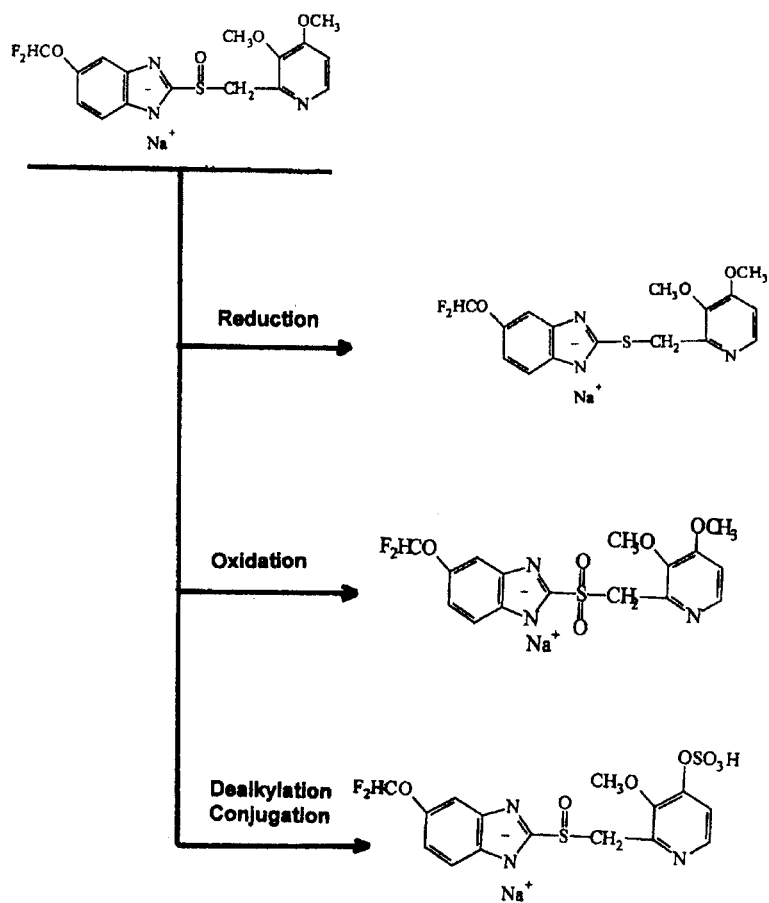


Figure 14. Principle metabolic pathways of pantoprazole in humans.

Pantoprazole must be completely and rapidly metabolized, since no parent compound is found in either feces or urine. Pantoprazole seems to be dependent on CYP3A and CYP2C19 for its metabolism [19].

#### **6.4 Elimination**

Elimination is predominantly renal, with about 80% of an oral dose being excreted as urinary metabolites. The remainder is excreted in the faeces and originates primarily from biliary secretion [1].

The elimination half life for pantoprazole in poor metabolizers was approximately 6 hours, as compared with 1.3 hours in normal metabolizers [19].

Plasma pantoprazole concentrations decline monophasically after oral administration, with a mean plasma terminal half-life ( $t_{1/2\beta}$ ) of 0.9 to 1.9. Despite the short  $t_{1/2\beta}$  of pantoprazole, inhibition of acid secretion, once accomplished, is long lasting, persisting after the drug has been cleared from the circulation. Thus, the plasma kinetics of pantoprazole have little bearing on its antisecretory action [1].

The pharmacokinetics of pantoprazole do not appear to be modified to any clinically relevant extent by renal impairment. Hemodialysis does not appear to significantly influence the pharmacokinetics of Pantoprazole or its main dealkylated conjugate in patients with renal disease or end stage renal failure [1, 21].

When pantoprazole was administered to patients with stable renal impairment undergoing hemodialysis the AUC and  $t_{1/2\beta}$  values were only 46% and 65%, respectively, of that observed in healthy volunteers. CL increased by 117%, and Vd was increased by 45%. It was not considered necessary to reduce the dose of pantoprazole in patients with renal impairment [22].

### **7. Pharmacology**

#### **7.1 Mechanism of Action**

The involvement of the proton pump ( $H^+$ ,  $K^+$ -ATPase) in the regulation of gastric acid secretion by the parietal (oxyntic) cell is well established.

As a weak base ( $pK_a = 3.9$ ), pantoprazole is highly ionized at low pH and readily accumulates in the highly acidic canalicular lumen of the stimulated parietal cell. In this acidic environment, pantoprazole is rapidly converted to the active species, a cationic cyclic sulfonamide, which binds covalently to cysteine residues on the luminal (acidic) surface of  $H^+$ ,  $K^+$ -ATPase to form a mixed disulphide, thereby causing irreversible inhibition of gastric proton pump function. As  $H^+$ ,  $K^+$ -ATPase represents the final step in the secretory process, inhibition of this enzyme suppresses gastric acid secretion regardless of the primary stimulus [1].

In comparison to omeprazole and lansoprazole, pantoprazole showed a much lower affinity to cytochrome P450 in vitro and it does not interact with the cytochrome P450 system in man. In the drug interaction studies conducted so far pantoprazole did not affect the pharmacokinetics or pharmacodynamics of antipyrimines diazepam, digoxin, a hormonal contraceptive, nifedipine, phenyntion, theophylline, and warfarin in man [23].

## 7.2 Toxicity

Doses up to 240 mg pantoprazole are well tolerated. It has no specific antidote and measures other than symptomatic treatment may be recommended [1].

## 8. Acknowledgment

The authors would like to thank Dr. Naji Najeeb and Mr. Izz Al-Deen Ghanem at the International Pharmaceutical Research Center for their participation in the mass spectrophotometry testing.

## 9. References

1. A. Fitlon and L. Wiseman, *Drugs*, **51**, 460 (1996).
2. S. Budavari, ed., *The Merck Index*, 12<sup>th</sup> edn., Merck & Co., Inc., Whitehouse Station, NJ (1996), p. 1205.
3. K. Parfitt, ed., *Martindale, The Extra Pharmacopeia*, 32<sup>nd</sup> edn., the Pharmaceutical Press, London, UK (1999), pp. 1207-1208.
4. M. Cheng, Q. Wang, and L. Pan, Faming Zhuanli Gongkai Shuomingshu, 1,102,411 (Cl. COID401/12), 10 May 1995; Appl. 948110, 342, 23 June 1994.
5. A.A. Badwan, L. Nabulsi, M. Al-Omari, N. Daraghme, and M. Ashour, Pantoprazole Sodium File, The Jordanian Pharmaceutical Manufacturing Company, P.O. Box 94, Naor 11710, Jordan.
6. A.A.M. Mustafa, *J. Pharm. Biomed. Anal.*, **22**, 45-58 (2000).
7. R. Huber, W. Mueller, M.C. Banks, S.J. Rogers, P.C. Norwood, and E. Doyle, *J. Chromatogr.*, **S29**, 389-401 (1990).
8. E. Doyle, R. Huber, V.S. and Picot, *Xenobiotica*, **22**, 765-774 (1992).
9. E. Doyle, R.D. McDowall, G.S. Murkitt, V.S. Picot, and S. Rogers, *J. Chromatogr.*, **S27**, 67-77 (1990).
10. M. Tanaka and H. Yamazaki, *Anal. Chem.*, **68**, 1513-1516 (1996).
11. M. Tanaka, H. Yamazaki, and H. Hakushi, *Chirality*, **7**, 612-615 (1995).
12. K. Balmer, B.A. Persson, and P.O. Lagerstrom, *J. Chromatogr. A*, **660**, 269-273 (1994).
13. H. Stenhoff, A. Blomquist, and P.O. Lagerstrom, *J. Chromatogr.*, **734**, 191-201 (1999).
14. D. Eberle, R.P. Hummel, and R. Kahn, *J. Chromatogr. A*, **759**, 185-192 (1997).

15. A. Tiveston, S. Folestod, V. Schonbacher, and K. Svensson, *Chromatographia*, **49**, S7-S11 (1999).
16. B. Renger, *J. Am. Off. Anal. Chem.*, **76**, 7-13 (1993).
17. A. Ekpe and T. Jacobsen, *Drug Dev. Indust. Pharm.*, **25**, 1057-1065 (1999).
18. R. Huber, M. Hartmann, H. Bliesath, R. Luhmann, and K. Zech, *Int. J. Clin. Pharm. Therap.*, **34** ( Suppl. 1), S7 (1996).
19. T. Anderson, *Clin. Pharmacokin.*, **31**, 9 (1996).
20. M. Tanaka, T. Ohkubo, K. Otani, A. Sozoki, S. Kaneko, K. Sugawara, Y. Ryokawa, H. Hakusui, S. Yamamori, and T. Ishizaki, *Clin. Pharmacol. Therap.*, **62**, 619 (1997).
21. M. Gladziwa and U. Klotz, *Clin. Pharmacokin.*, **27**, 393 (1994).
22. V.W. Steinijans, R. Huber, M. Hartmann, K. Zech, H. Bliesath, W. Wurst, and H.W. Radtke, *Int. J. Clin. Pharmacol. Therap.*, **32**, 385 (1994).
23. V. Klieun, J. Bahlmann, M. Hartmann, R. Huber, R. Luhmann, and W. Wurst, *Neph. Dial. Transplant.*, **13**, 1189 (1998).



This Page Intentionally Left Blank

# **SPIRONOLACTONE**

**Badraddin M.H. Al-Hadiya\*<sup>1</sup>, Fathalla Belal<sup>2</sup>,**

**Yousif A. Asiri<sup>1</sup>, and Othman A. Gubara<sup>1</sup>**

(1) Department of Clinical Pharmacy  
College of Pharmacy  
King Saud University,  
P.O. Box 2457  
Riyadh 11451  
Kingdom of Saudi Arabia

(2) Department of Pharmaceutical Chemistry  
College of Pharmacy  
King Saud University,  
P.O. Box 2457  
Riyadh 11451  
Kingdom of Saudi Arabia

## **Contents**

### **1. Description**

- 1.1 Nomenclature
  - 1.1.1 Systematic Chemical Names
  - 1.1.2 Nonproprietary Names
  - 1.1.3 Proprietary Names
- 1.2 Formulae
  - 1.2.1 Empirical Formula, Molecular Weight, CAS Number
  - 1.2.2 Structural Formula
- 1.3 Elemental Analysis
- 1.4 Appearance
- 1.5 Uses and Applications

### **2. Methods of Preparation**

- 2.1 Method (1)
- 2.2 Method (2)
- 2.3 Method (3)

### **3. Physical Properties**

- 3.1 Ionization Constants
- 3.2 Solubility Characteristics
- 3.3 Partition Coefficient
- 3.4 Specific Rotation
- 3.5 X-Ray Powder Diffraction
- 3.6 Thermal Methods of analysis
  - 3.6.1 Melting Behavior
  - 3.6.2 Differential Scanning Calorimetry
- 3.7 Spectroscopy
  - 3.7.1 UV/VIS Spectroscopy
  - 3.7.2 Vibrational Spectroscopy
  - 3.7.3 Nuclear Magnetic Resonance Spectrometry
    - 3.7.3.1  $^1\text{H}$ -NMR Spectrum
    - 3.7.3.2  $^{13}\text{C}$ -NMR Spectrum
- 3.8 Mass Spectrometry

**4. Methods of Analysis**

- 4.1 Identification
  - 4.1.1 Palladium Chloride Test
  - 4.1.2 Sulfuric Acid Test
  - 4.1.3 Lead Acetate Test
- 4.2 Compendial Tests
- 4.3 Spectroscopic Analysis
- 4.4. Polarography
- 4.5 Chromatographic Methods of Analysis
  - 4.5.1 Thin Layer Chromatography
  - 4.5.2 Gas Chromatography
  - 4.5.3 High Performance Liquid Chromatography
  - 4.5.4 Capillary Zone Electrophoresis
  - 4.5.5 Flow Injection Analysis
- 4.6 Thermal Analysis
- 4.7 Protein Binding Studies

**5. Clinical Applications**

- 5.1 Pharmacological Action
- 5.2 Mechanisms of Action

**6. Pharmacokinetic Profile**

- 6.1 Absorption
- 6.2 Distribution
- 6.3 Metabolism and Elimination

**7. Drug Interactions**

- 7.1 Drugs Increasing Serum Potassium Concentrations
- 7.2 Other Drugs
- 7.3 Precautions
  - 7.3.1 Carcinogenicity/ Tumorigenicity
  - 7.3.2 Pregnancy
  - 7.3.3 Breast-Feeding
  - 7.3.4 Pediatrics
  - 7.3.5 Geriatrics

**8. Toxicity and Adverse Effects**

8.1 Those More Frequently Occurring

8.2 Those Less Frequently Occurring

**9. Acknowledgement****10. References**

## 1. Description

### 1.1 Nomenclature [6]

#### 1.1.1 Systematic Chemical Names

(7 $\alpha$ ,17 $\alpha$ )-7-(acetylthio)-17-hydroxy-3-oxo-pregn-4-ene-21-carboxylic acid  $\gamma$ -lactone

17-hydroxy-7 $\alpha$ -mercapto-3-oxo-17 $\alpha$ -pregn-4-ene-21-carboxylic acid  $\gamma$ -lactone, acetate

3-(3-oxo-7 $\alpha$ -acetylthio-17 $\beta$ -hydroxy-4-androsten-17 $\alpha$ -yl) propionic acid  $\gamma$ -lactone

#### 1.1.2 Nonproprietary Names [7]

Generic: Spironolactone

Synonyms: Espironolactona

#### 1.1.3 Proprietary Names [9]

Aldactone, Aldopur, Altex, Diatensec, laractone, Sincomen, Spiretic, Spiroctan, Spirolang, Spirolone, Spirotone.

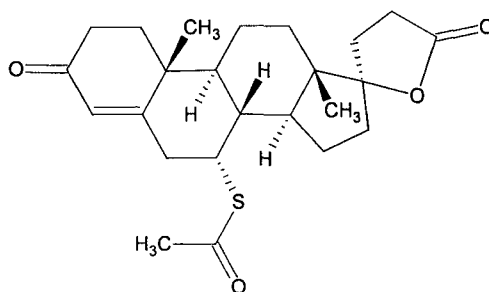
## 1.2 Formulae [8-12]

### 1.2.1 Empirical Formula, Molecular Weight, CAS Number

C<sub>24</sub>H<sub>32</sub>O<sub>4</sub>S [MW = 416.574]

CAS number = 52-01-7

### 1.2.2 Structural Formula



### 1.3 Elemental Analysis

The calculated elemental composition is as follows:

carbon:	69.20%
hydrogen:	7.74%
oxygen:	15.36%
sulfur:	7.70%

### 1.4 Appearance [9]

Spironolactone is a white or yellowish white crystalline powder that has a slight characteristic odor.

### 1.5 Uses and Applications [9]

The synthesis and subsequent widespread therapeutic use of spironolactone has been a logical consequence of the discovery of the most potent mineralocorticoid hormone in man, aldosterone. The latter compound was isolated in 1952 from dog and monkey adrenal venous blood [1], which also was shown to be present in human urine [2].

Soon after the discovery of aldosterone, it became apparent that its excessive production played an important role in the physiopathology of a variety of disorders, such as Cohn's syndrome, congestive heart failure, and nephritic syndrome [3]. It therefore seemed valuable to develop compounds with aldosterone-antagonist properties. This approach had its beginning in the work of Landau *et al* [4].

In 1957, Cella and Kagawa [5] reported about the preparation of two steroidal 17-spirolactones, which were capable of blocking the urinary sodium/potassium action of aldosterone and desoxycorticosterone-acetate in adrenalectomized rats. These compounds were closely related in structure to aldosterone and were assigned the code names SC 5233 and SC 8109, respectively. Structures of these three compounds are shown in Figure 1.

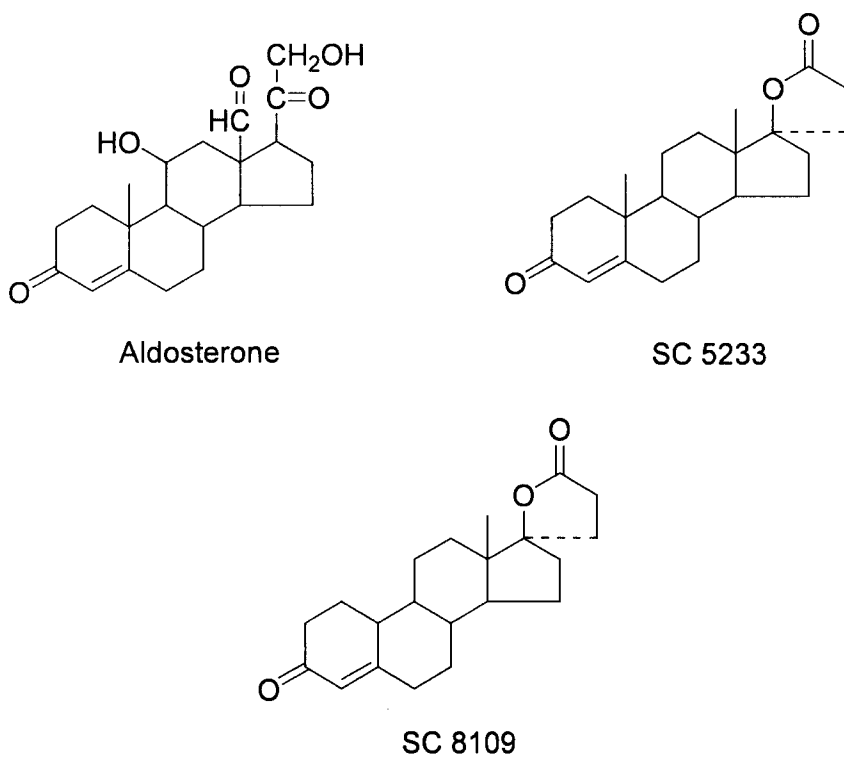


Figure 1. Structures of aldosterone, SC 5233, and SC 8109.



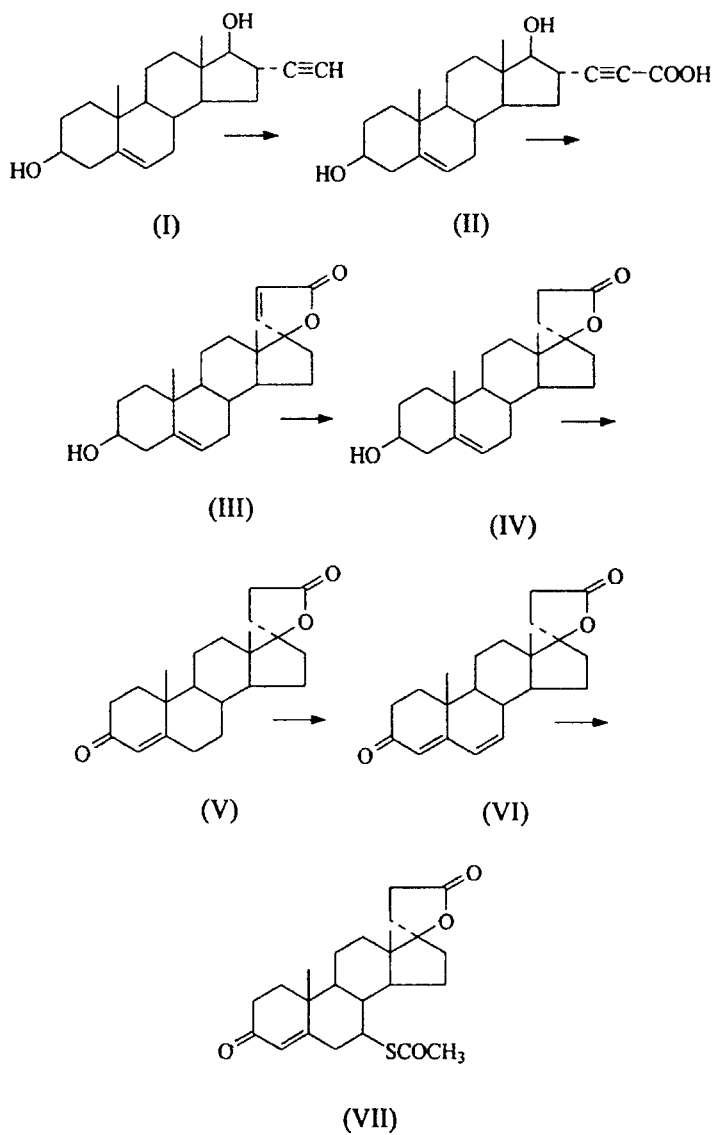
Spironolactone is a steroid with a structure resembling that of the natural adrenocortical hormone, aldosterone. It acts on the distal portion of the renal tubule as a competitive antagonist of aldosterone. It also acts as a potassium-sparing diuretic, increasing sodium and water excretion, and reducing potassium excretion. The substance is reported to have a slow onset of action (requiring 2-3 days for maximum effect), and a similarly slow diminishment of action (over 2-5 days on discontinuation). It is used for the treatment of refractory edema (associated with heart failure), cirrhosis of the liver (or the nephrotic syndrome), and in ascites associated with malignancy. It is frequently given with the thiazides, furosemide, and the similar diuretics. It has been also used for the treatment of essential hypertension.

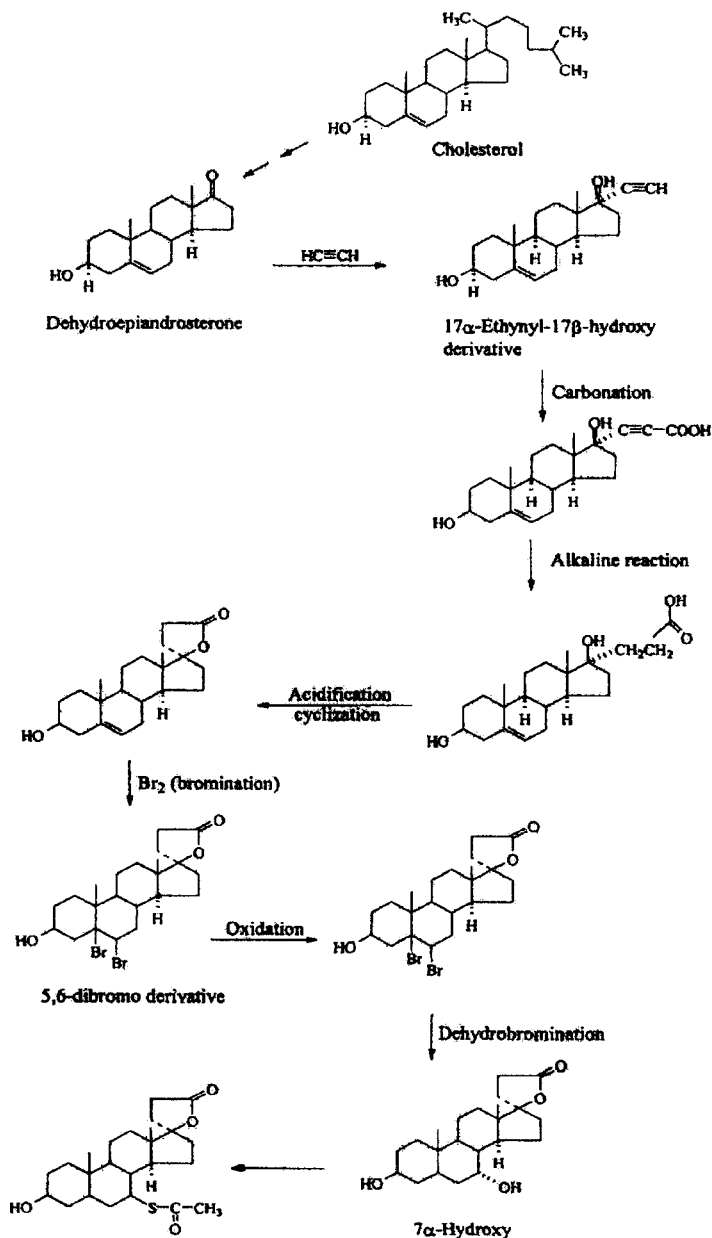
## **2. Methods of Preparation**

Three methods for the preparation of spironolactone have been reported, and the routes are illustrated in Schemes 1-3.

### **2.1 Method (1) [15]**

The first method for the preparation of spironolactone is outlined in Scheme 1. Carbonation of the Grignard reagent of 17 $\alpha$ -ethynyl-5-androstene-3 $\beta$ ,17 $\beta$ -diol (**I**) yielded an acetylenic acid (**II**). Selective reduction of the acetylenic bond was accomplished by catalytic hydrogenation over palladium on calcium carbonate, using dioxane and pyridine as solvents. Treatment of the product with mineral acid yielded the unsaturated lactone, 3-(3 $\beta$ , 17 $\beta$ -dihydroxy-5-androstene-17 $\alpha$ -yl)-propenoic acid lactone (**III**), which was easily reduced to the saturated lactone (**IV**) by hydrogen over palladium on charcoal. Oppenauer oxidation of the product afforded 3-(3-oxo-17 $\beta$ -hydroxy-4-androsten-17 $\alpha$ -yl) propionic acid lactone (**V**). Unsaturation at C<sub>6</sub> was then introduced by treatment with chloranil. Finally, the resulting 17-hydroxy-3-oxo-17 $\alpha$ -pregna-4,6-diene-21-carboxylic acid- $\gamma$ -lactone (**VI**) was reacted with thioacetic acid, yielding 17-hydroxy-7 $\alpha$ -mercapto-3-oxo-17 $\alpha$ -pregn-4-ene-21-carboxylic acid  $\gamma$ -lactone-7-acetate, spironolactone (**VII**) [13].

**Scheme 1**

**Scheme 2**

II

$\xrightarrow{\text{Cl-CH}_2\text{CH}_2\text{OCH}_2\text{CH}_2\text{O} / \text{lithium}}$

III

Pyridine . HBr  
 $\text{Br}_2 / \text{CrO}_3$   
 bromination, followed by  
 oxidation.

$\xleftarrow{\text{DHF/LiBr-Li}_2\text{CO}_3}$

IV  
 Androstadienone

Bromoketone derivative

ACSH thiol acetic acid will be added in 1,6 addition  
 to the double bond, acidic media will remove the  
 ethylene acetal (protecting group and  $\text{CrO}_3$  will  
 oxidize aldehydic group into  $\text{COOH}$  with  
 spontaneous cyclization.

I

## 2.2 Method (2) [14]

The second method of preparation (shown in Scheme 2) depends on treating dehydroepiandrosterone (prepared from cholesterol or sitosterol) with acetylene to form the  $17\alpha$ -ethynyl- $17\beta$ -hydroxy derivative, which is carbonated to the  $17\alpha$ -propionic acid. Reduction of the unsaturated acid in alkaline solution yields the saturated acid, which cyclizes to the lactone on acidification. Bromination to the 5,6-dibromo-compound, followed by oxidation of the hydroxyl group to the ketone, and then dehydrobromination to the  $7\alpha$ -hydroxyl derivative, produces spironolactone when esterified with thiolacetic acid.

## 2.3 Method (3) [15]

In the third method (illustrated in Scheme 3), spironolactone (**I**) was prepared from dehydroepiandrosterone (**II**). This starting material was treated with 3-chloropropionaldehyde ethylene acetal and lithium. The resulting acetal (**III**) was treated with a pyridine-HBr-Br<sub>2</sub> solution, followed by CrO<sub>3</sub> oxidation to give the bromo ketone. This compound was refluxed in dimethyl formamide containing LiBr-Li<sub>2</sub> CO<sub>3</sub> to give the androstadienone (**IV**). The addition of AcSH to **IV**, followed by CrO<sub>3</sub> oxidation, gave spironolactone in 23% overall yield.

## 3. Physical Properties

### 3.1 Ionization Constants

Spironolactone does not contain any potentially ionizable groups, and hence has no ionization constants.

### 3.2 Solubility Characteristics

The following solubility values have been reported for spironolactone in different solvents at room temperature (25°C) [10]:

Solvent	Solubility (mg/mL)
Water	0.028
Methanol	6.9
Ethanol	27.9
Chloroform	50.0
Heptane	0.24

### **3.3 Partition Coefficient**

Spironolactone is preferentially extracted from water into heptane. The partition coefficient has been reported as 3.5 at 25°C [10].

### **3.4 Specific Rotation**

The specific rotation of a 10 mg/mL solution of spironolactone in chloroform is between  $-33^\circ$  and  $-37^\circ$  [8].

### **3.5 X-Ray Powder Diffraction**

The X-ray powder diffraction pattern of spironolactone has been measured using a Philips PW-1710 diffractometer, equipped with a single crystal monochromator and using a copper  $K\alpha$  radiation. The pattern obtained is shown in Figure 2, and the scattering angles, interplanar d-spacings, and relative intensities are found in Table 1.

### **3.6 Thermal Methods of analysis**

#### **3.6.1 Melting Behavior**

The melting range of spironolactone is between 198 and 207°C, accompanied by decomposition. Occasionally materials may show preliminary melting at about 135°C, followed by re-solidification [8], and this behavior indicates the existence of another, metastable, crystal form.

#### **3.6.2 Differential Scanning Calorimetry**

The DSC thermogram of spironolactone was obtained using a Du Pont TA-9900 thermal analyzer system, interfaced to the Du Pont data collection system. The thermogram shown in Figure 3 was collected over a range of 50 to 250°C, using a heating rate of 10°C/minute. It was found that the compound melted at 210.5°C, with an enthalpy of fusion equal to 43.40 J/g.

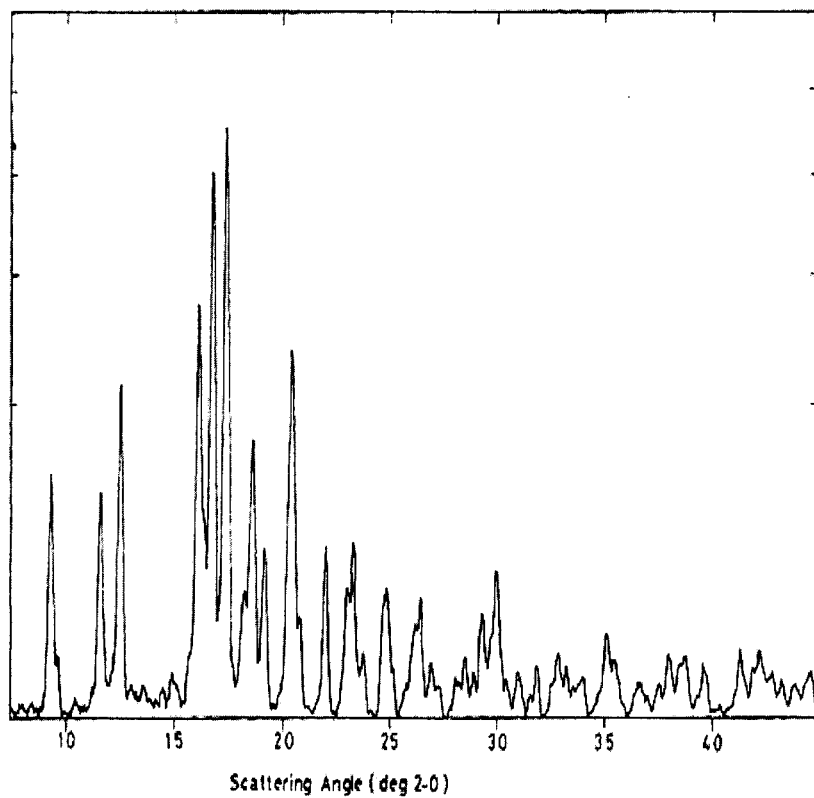


Figure 2. X-ray powder diffraction pattern of spironolactone.

Table 1  
Scattering Angles, Interplanar d-Spacings, and Relative  
Intensities in the X-Ray Powder Diffraction of Spironolactone

Scattering Angle (degrees 2- $\theta$ )	d-Spacing (Å)	Relative Intensity
9.124	9.5899	17.21
11.53	7.6683	14.63
12.419	7.1216	31.00
14.821	5.9721	0.56
16.021	5.5274	49.03
16.663	5.3160	84.45
17.30	5.1215	100.00
18.131	4.8887	4.55
18.520	4.7870	22.02
19.077	4.6485	8.43
20.357	4.3589	38.89
20.740	4.2793	2.91
21.945	4.0468	8.50
22.912	3.8782	4.85
23.224	3.8268	8.71
24.772	3.5911	4.74
26.893	3.3125	0.91
28.467	3.1328	0.94
29.949	2.9821	5.97
30.943	2.8875	0.57
31.826	2.8095	0.73
32.822	2.7264	1.16
33.963	2.6374	0.40
35.405	2.5332	0.93
36.577	2.4547	0.36
38.672	2.3264	1.11
39.544	2.2770	0.89
41.223	2.1881	1.36
44.487	2.0349	0.63
46.708	1.9431	0.29
60.71	1.5242	0.22



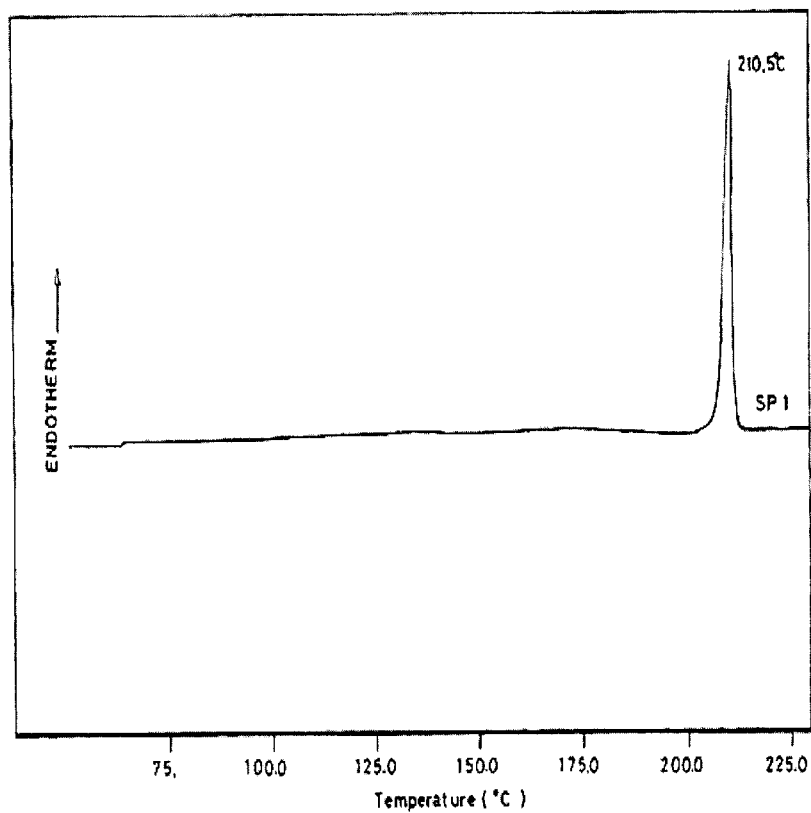


Figure 3. Differential scanning calorimetry thermogram pattern of spironolactone.

### 3.7 Spectroscopy

#### 3.7.1 UV/VIS Spectroscopy

UV absorption spectra of spironolactone were recorded using a Shimadzu UV-VIS spectrophotometer, model 1601 PC. Spectra were obtained in methanol, 0.1M HCl, and 0.1M NaOH, and these are shown in Figure 4. The values of  $A_{1\%,1\text{cm}}$ , and the molar absorptivity values at their corresponding  $\lambda_{\text{max}}$  are shown in the following table:

Solvent System	Wavelength Maximum (nm)	$A_{1\%,1\text{cm}}$	Molar Absorptivity ( $\text{L}\cdot\text{Mol}^{-1}\cdot\text{cm}^{-1}$ )
Methanol	237.8	458	19055
0.1M HCl	242.4	461	19180
0.1M NaOH	293.6	78	3245
	246.6	430	17890
	215.8	661	27500

#### 3.7.2 Vibrational Spectroscopy

The infrared absorption spectrum of spironolactone was obtained in a KBr pellet using a Perkin-Elmer infrared spectrophotometer. The principal absorption peaks of the spectrum shown in Figure 5 were noted at 1765, 1693, 1673, 1240, 1178, 1135, 1123 and 1193  $\text{cm}^{-1}$ .

#### 3.7.3 Nuclear Magnetic Resonance Spectrometry

The  $^1\text{H}$ -NMR and  $^{13}\text{C}$ -NMR spectra of spironolactone were obtained using a Jeol 400 MHz Eclipse FT-NMR Summit Spectrometer

##### 3.7.3.1 $^1\text{H}$ -NMR Spectrum

The full  $^1\text{H}$ -NMR spectrum of spironolactone in  $\text{CDCl}_3$  is shown in Figure 6, with various regions being expanded in Figures 7A through Figure 7H for easier viewing. Assignments for the resonance bands are given in Table 2.

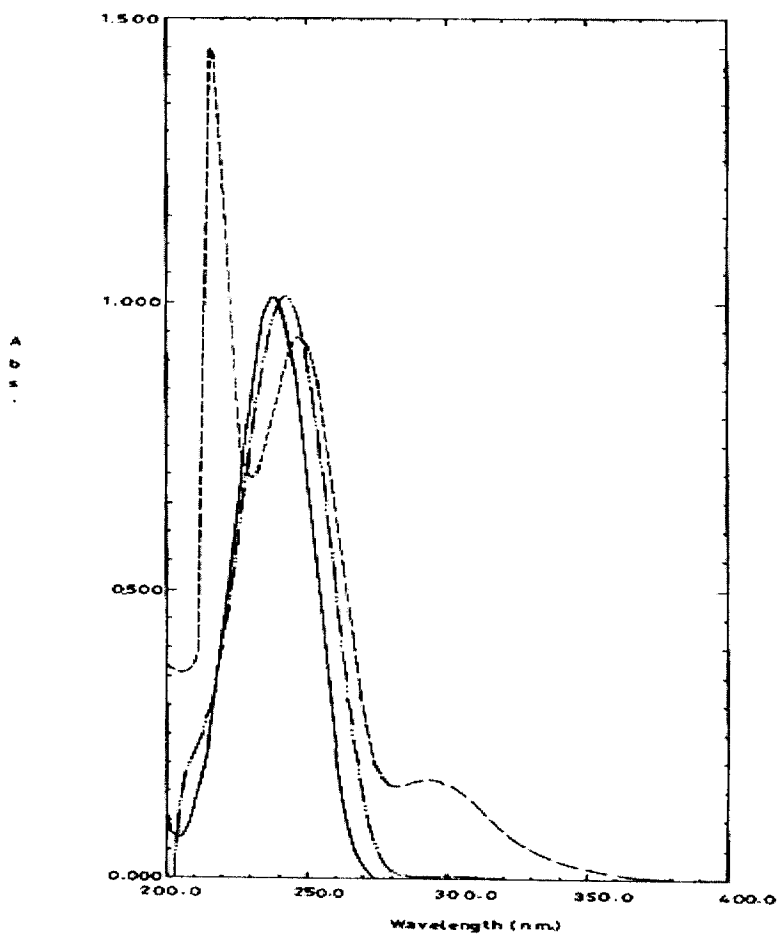


Figure 4. Ultraviolet absorption spectrum of spironolactone dissolved as 22 µg/mL in methanol (—), 0.1M HCl (- · - · -), and 0.1M NaOH (---).

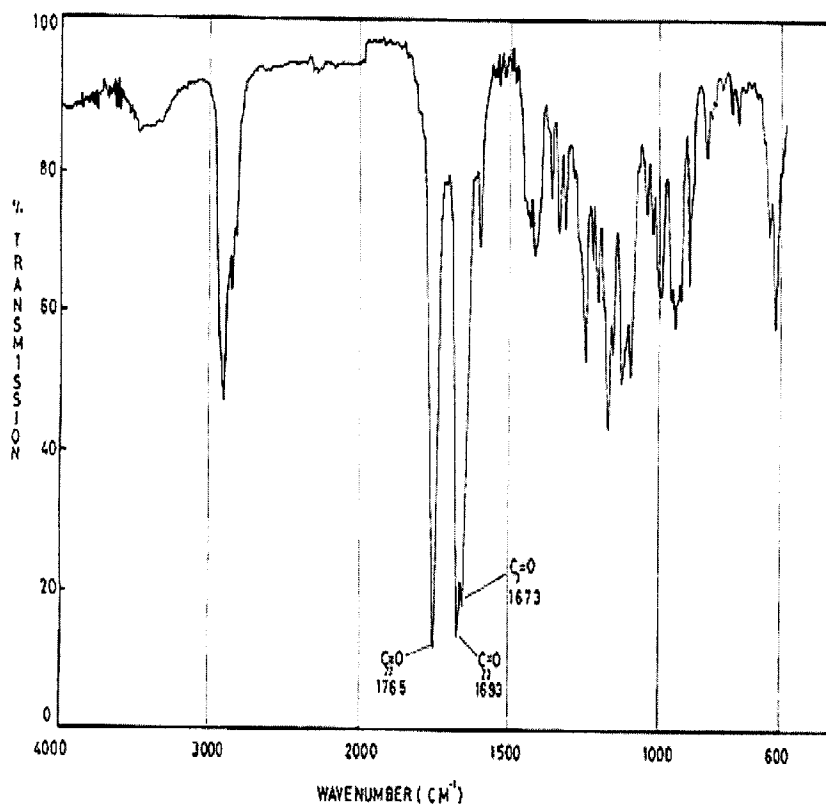


Figure 5. Infrared absorption spectrum of spironolactone.

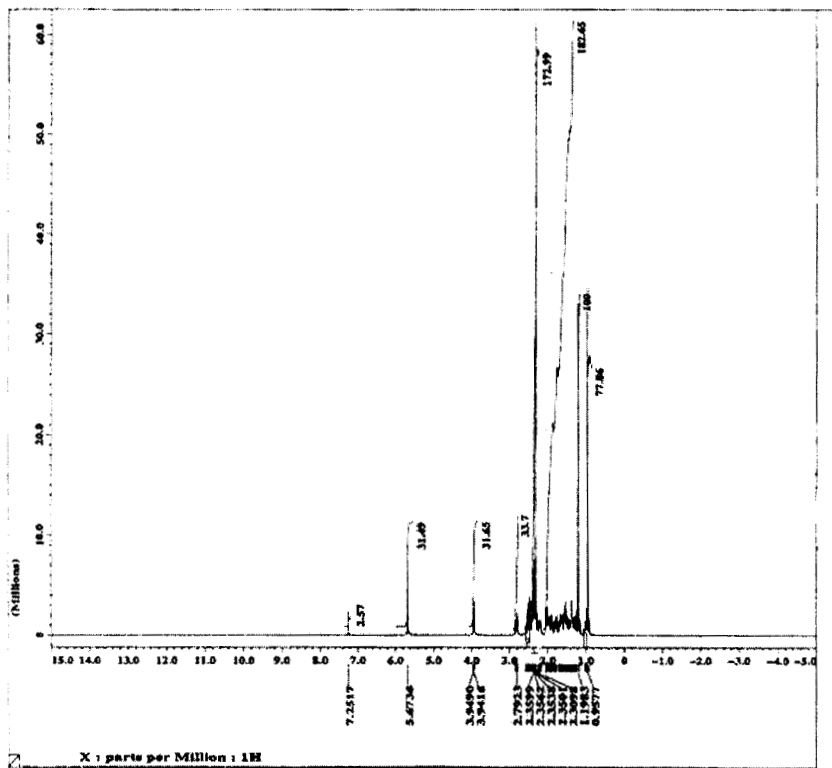
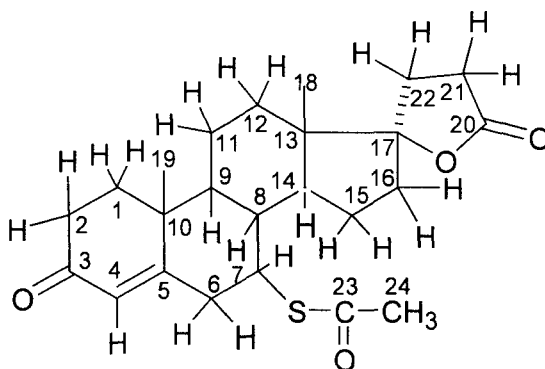


Figure 6. Complete  $^1\text{H}$ -NMR spectrum of spironolactone.

Table 2

Assignments for the Resonance Bands observed  
in the  $^1\text{H}$ -NMR Spectrum of Spironolactone



Chemical Shift (ppm)	Multiplicity	Number of Protons	Assignment
0.95	s	3	Protons of $\text{C}_{18}$ ( $-\text{CH}_3$ )
1.19	s	3	Protons of $\text{C}_{19}$ ( $-\text{CH}_3$ )
2.3	s	3	Protons of $\text{C}_{24}$ ( $-\text{CH}_3$ )
2.79	m	1	Methine proton at $\text{C}_8$
3.90	q	1	Methine Proton at $\text{C}_7$
5.67	s	1	Vinyl Proton at $\text{C}_4$
0.98; 1.04, 1.3, 1.55, and 2.35		10	Various other ring protons

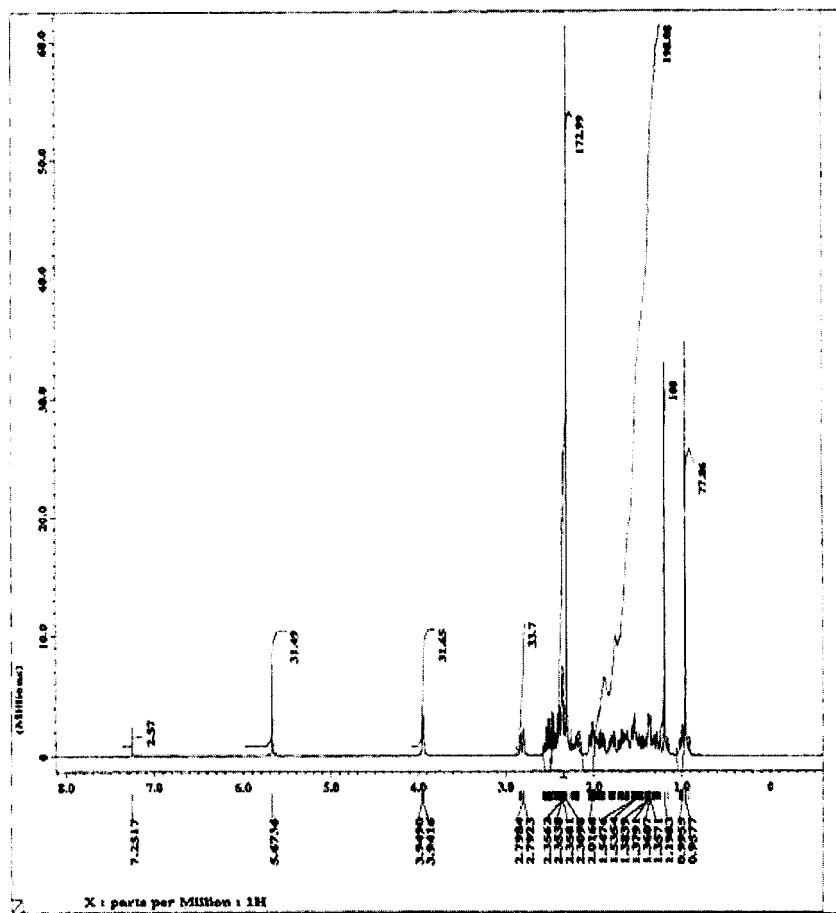


Figure 7A.  $^1\text{H}$ -NMR Spectrum of Spironolactone, 0.0 – 8.0 ppm.

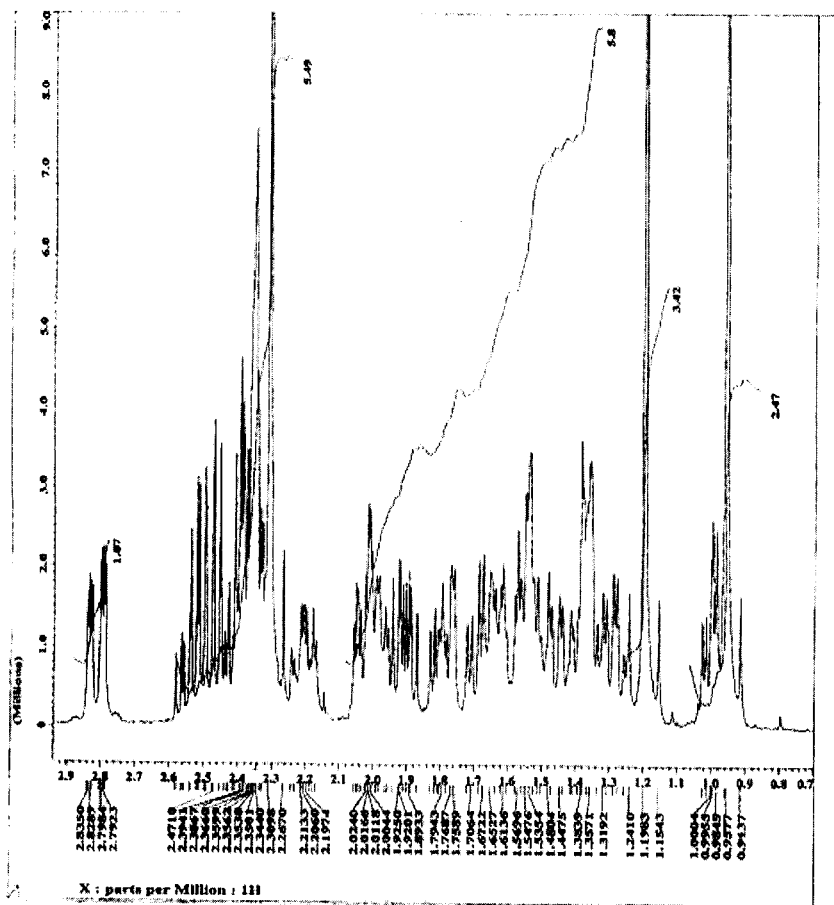


Figure 7B.  $^1\text{H}$ -NMR Spectrum of Spironolactone, 0.9 – 2.9 ppm.



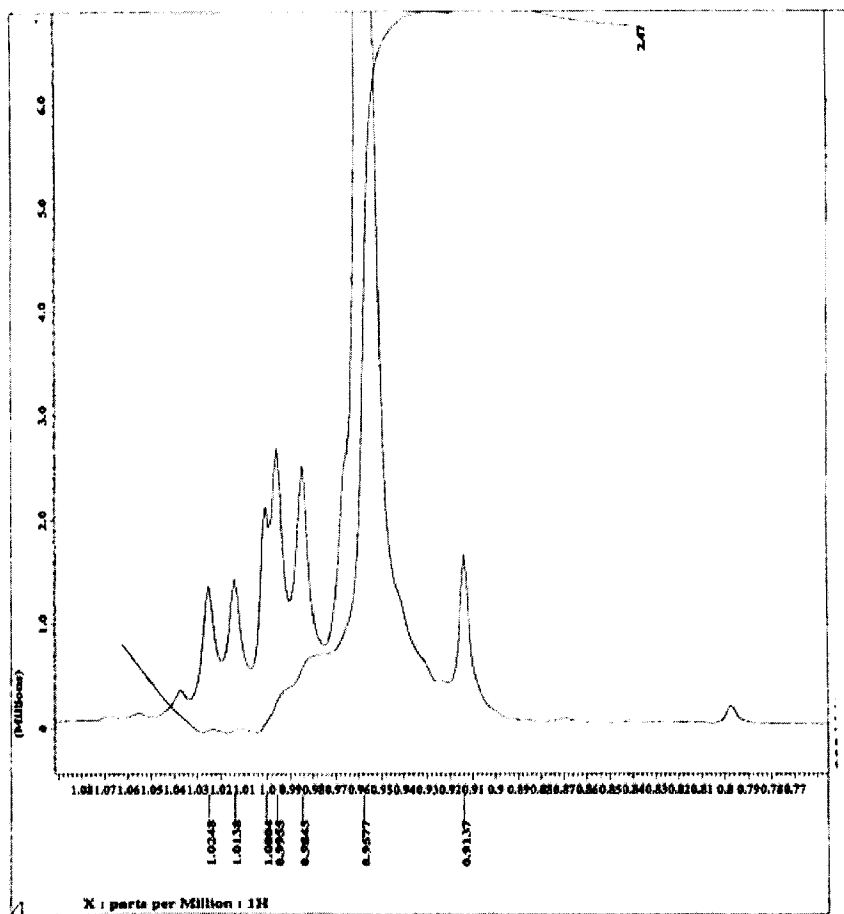


Figure 7C.  $^1\text{H}$ -NMR Spectrum of Spironolactone, 0.9 – 1.05 ppm.

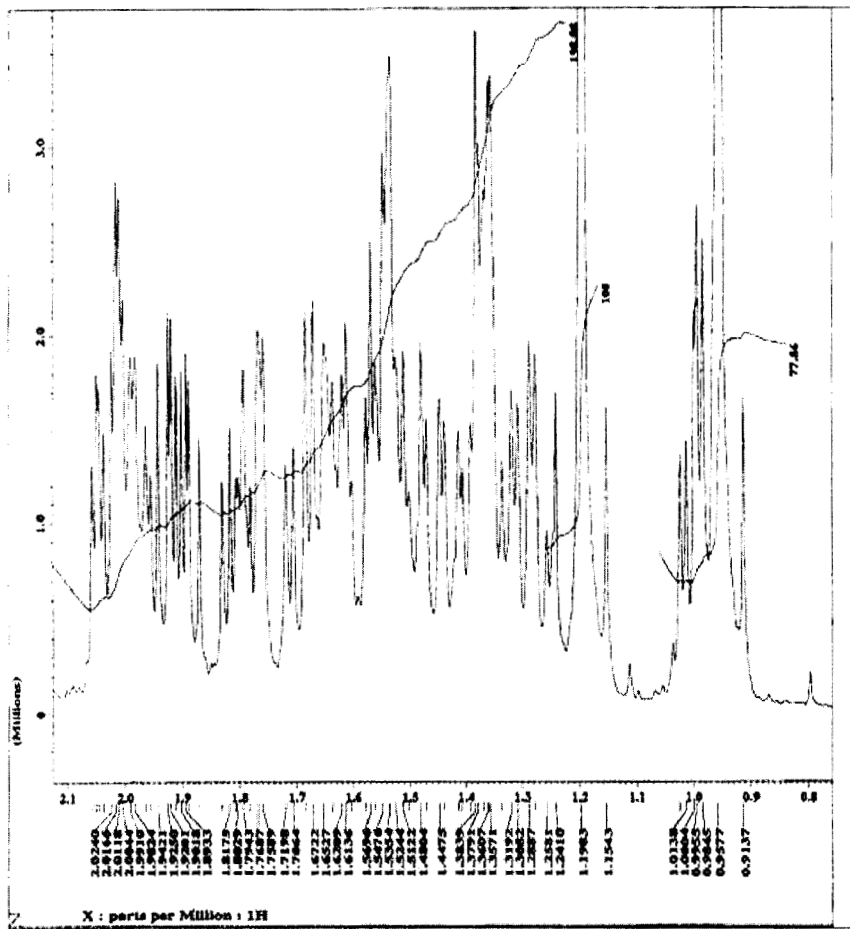


Figure 7D.  $^1\text{H}$ -NMR Spectrum of Spironolactone, 0.8 – 2.1 ppm.

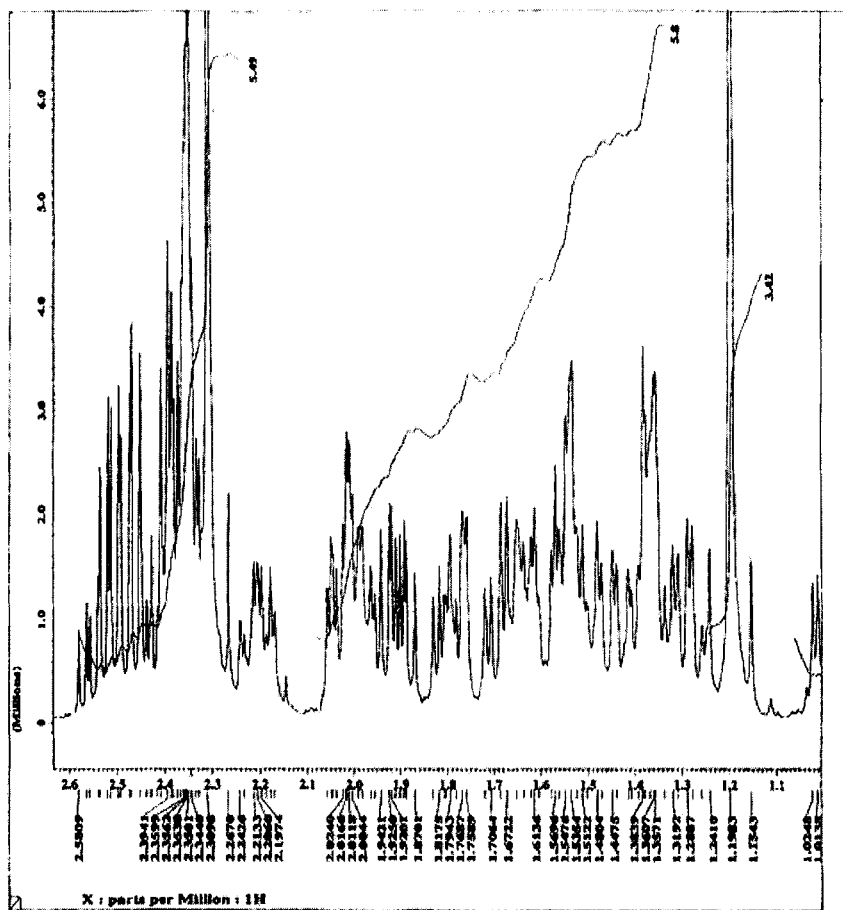


Figure 7E.  $^1\text{H}$ -NMR Spectrum of Spironolactone, 1.1 – 2.6 ppm.

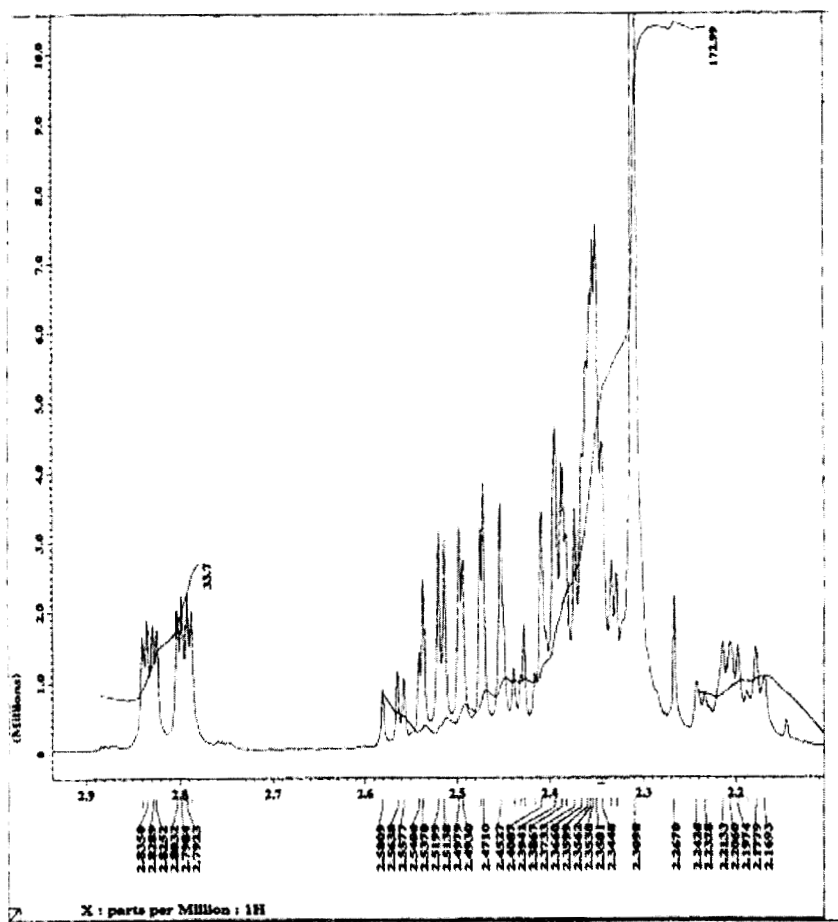


Figure 7F.  $^1\text{H}$ -NMR Spectrum of Spironolactone, 2.13 – 2.9 ppm.

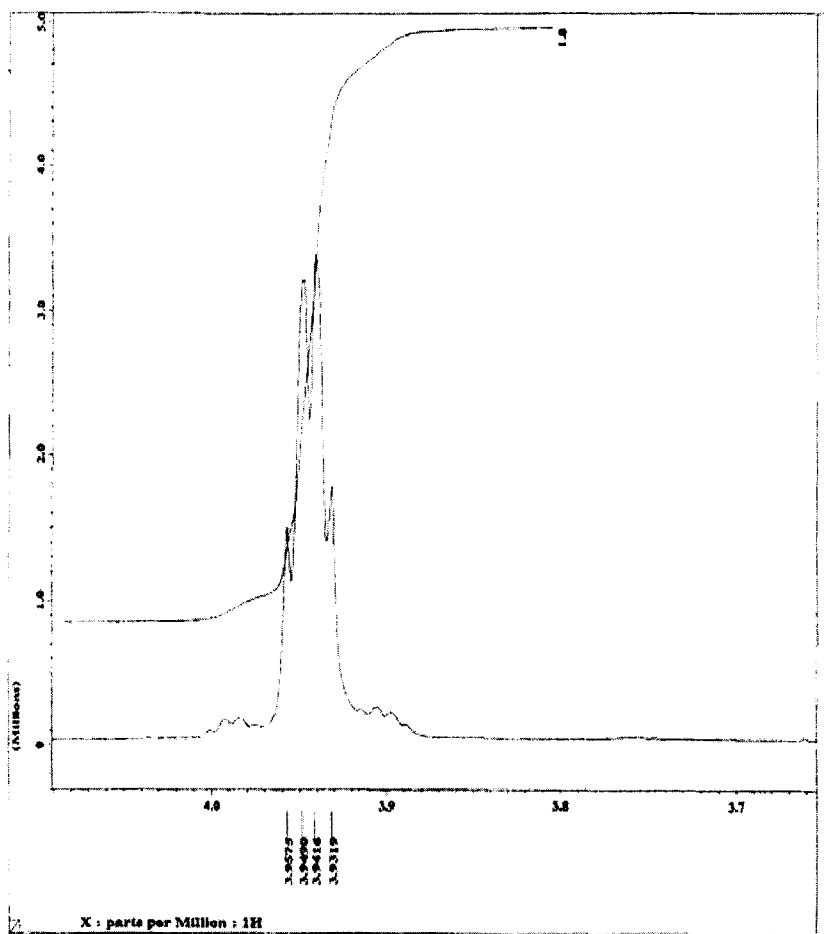


Figure 7G.  $^1\text{H}$ -NMR Spectrum of Spironolactone, 3.9 – 4.0 ppm.

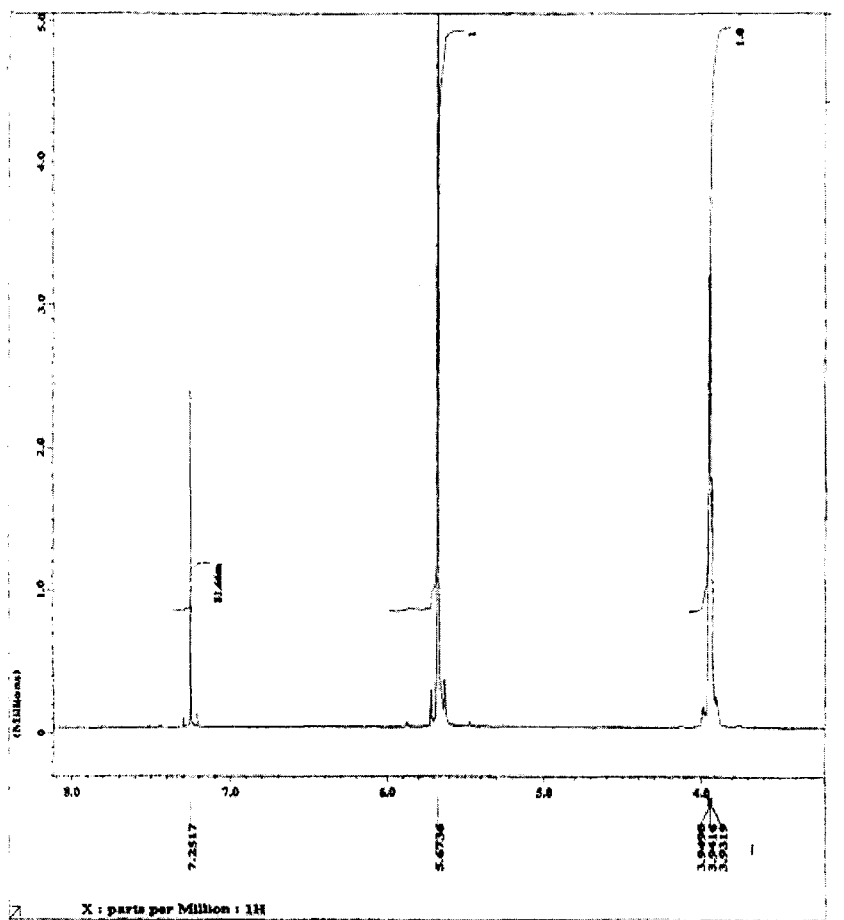


Figure 7H.  $^1\text{H}$ -NMR Spectrum of Spironolactone, 3.8 – 7.4 ppm.

### 3.7.3.2 $^{13}\text{C}$ -NMR Spectrum

The  $^{13}\text{C}$ -NMR spectrum of spironolactone was obtained in  $\text{CDCl}_3$ , and the spectra are shown in Figures 8 and 9. The assignments for the observed resonance bands are provided in Table 3.

## 3.8 Mass Spectrometry

The mass spectrum of spironolactone was obtained utilizing a Shimadzu PQ-5000 Mass Spectrometer, where the parent ion was collided with helium carrier gas. Figure 10 shows the detailed mass fragmentation pattern, where a base peak was noted at  $m/z = 341$ , along with a molecular ion peak at  $m/z = 416$ . The mass fragmentation pattern of the compound is detailed in Table 5. The peak that appeared at  $m/z = 267$  is due to loss of  $\text{CH}_3\text{CSO}$ ,  $\text{CO}_2$  and two  $\text{CH}_3$ , while the peak at  $m/z = 325$  is due to splitting of  $\text{CH}_3\text{CSO}$ ,  $\text{CH}_3$ , and  $\text{H}$  from spironolactone.

## 4. Methods of Analysis

### 4.1 Identification

#### 4.1.1 Palladium Chloride Test [7]

The reagent is prepared by dissolving 0.1 g of  $\text{PdCl}_2$  in 5 mL of 2M  $\text{HCl}$ , diluting to 100 mL with water, and then mixing with an equal volume of 2M  $\text{NaOH}$ . The reagent gives brown color with spironolactone.

#### 4.1.2 Sulfuric Acid Test [7]

Shake about 10 mg of spironolactone with 2 mL of 50% sulfuric acid, whereupon an orange solution with an intense yellowish green fluorescence is produced. Heat the solution gently, and the color becomes deep red with the evolution of  $\text{H}_2\text{S}$ . Add the solution to 10 mL of water, and a greenish yellow solution is produced which shows opalescence or a precipitate.

#### 4.1.3 Lead Acetate Test [11]

Add 100 mg of spironolactone to a mixture of 10 mL of water and 2 mL of 1N  $\text{NaOH}$ , boil for 3 minutes, and cool. Add 1 mL of glacial acetic acid and 1 mL of lead acetate solution; a brown to black precipitate of lead sulfide is produced.

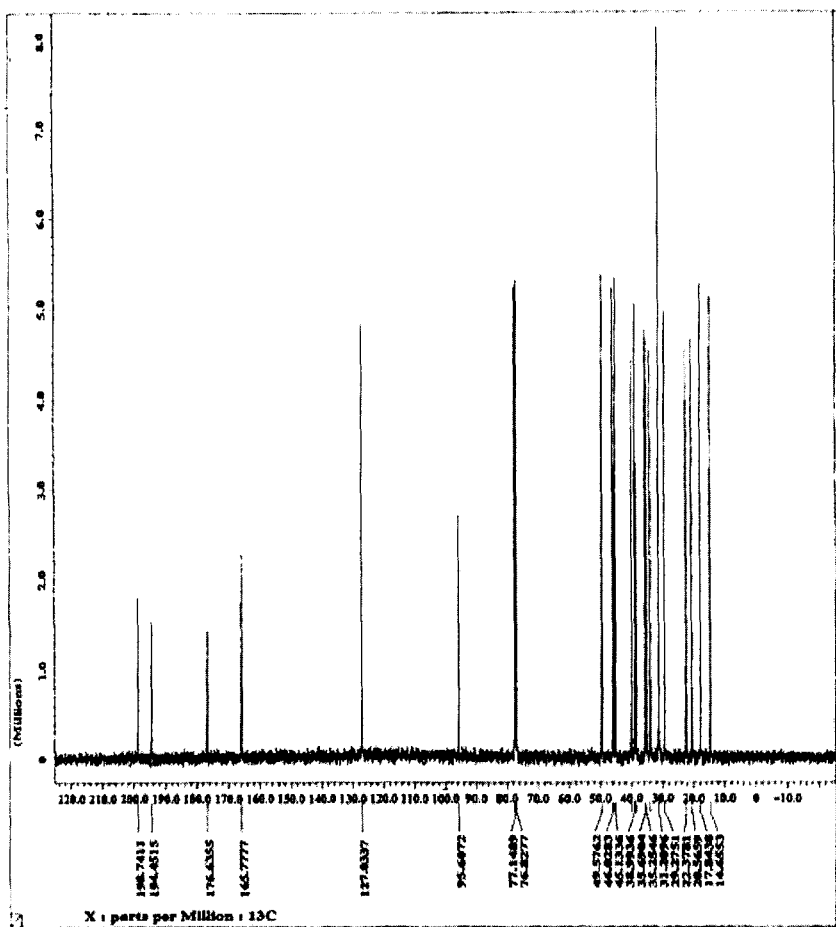
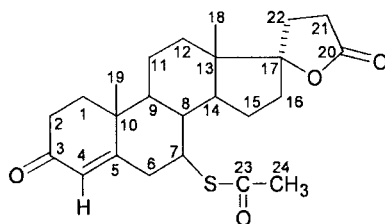


Figure 8. Full  $^{13}\text{C}$  nuclear magnetic resonance spectrum of Spironolactone.



Table 4

Assignments for the Resonance Bands observed in the  
 $^{13}\text{C}$ -NMR Spectrum of Spironolactone



Chemical shift (ppm)	Assignments	Chemical shift	Assignment
14.65	C <sub>18</sub>	45.13	C <sub>7</sub>
17.84	C <sub>19</sub>	45.51	C <sub>9</sub>
20.56	C <sub>16</sub>	46.03	C <sub>10</sub>
22.37	C <sub>15</sub>	49.57	C <sub>8</sub>
29.27	C <sub>24</sub>	38.99	C <sub>14</sub>
31.21	C <sub>6</sub>	77.14	C <sub>7</sub>
31.40	C <sub>11</sub>	95.61	C <sub>17</sub>
33.97	C <sub>12</sub>	127.03	C <sub>4</sub>
35.25	C <sub>21</sub>	165.77	C <sub>5</sub>
35.69	C <sub>22</sub>	176.63	C <sub>20</sub>
38.53	C <sub>2</sub>	194.45	C <sub>23</sub>
39.95	C <sub>13</sub>	198.74	C <sub>3</sub>

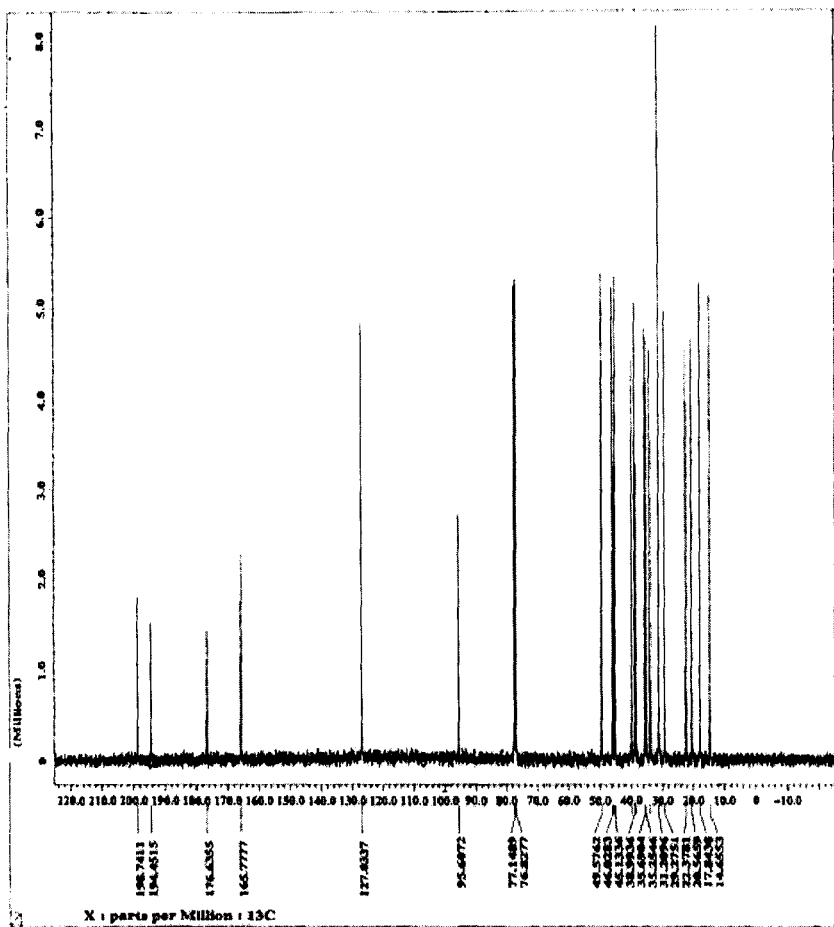


Figure 9. Expanded  $^{13}\text{C}$  nuclear magnetic resonance spectrum of Spironolactone.

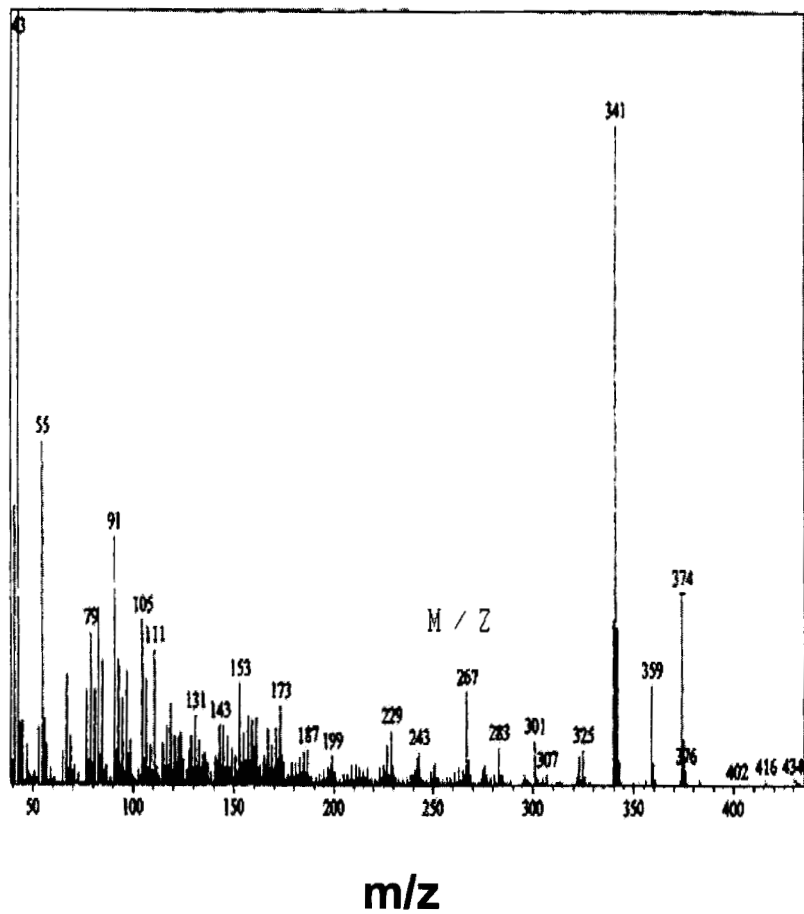


Figure 10. Mass spectrum of Spironolactone.

Table 4  
Mass Fragmentation pattern of Spironolactone

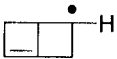
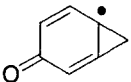
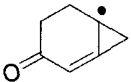
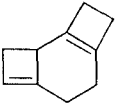
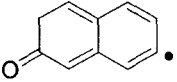
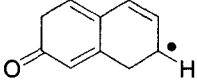
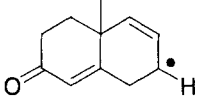
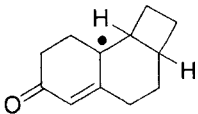
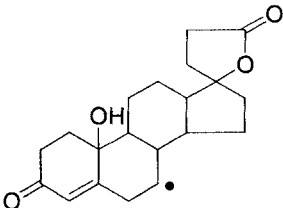
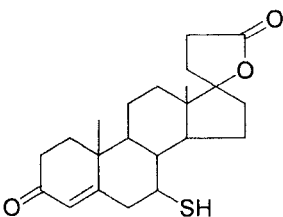
m/z	Relative intensity (%)	Fragment
43.10	100.00	$\text{CH}_3\text{-C}\equiv\text{O}^+$
55.10	44.44	$\text{CH}_2=\text{CH-C}\equiv\text{O}^+$
79.10	19.91	
105.10	21.58	
107.15	13.80	
131.20	9.15	
143.20	7.94	
145.20	7.93	

Table 4 (continued)

## Mass Fragmentation pattern of Spironolactone

161.20	8.92	
173.15	10.43	
341.25	85.47	
374.30	25.18	

## 4.2 Compendial Tests

Spironolactone is the subject of monographs in the United States Pharmacopoeia (USP), as well as in the European, Chinese, Poland, Japanese, and International Pharmacopoeias.

Both The European Pharmacopoeia [12] and the British Pharmacopoeia [11] describe a spectrophotometric method for spironolactone. The method is based on measurement of the absorbance of a 10  $\mu\text{g/mL}$  methanolic solution at 238 nm. The content is calculated taking 470 as the value of  $A_{1\%,1\text{cm}}$ .

The USP [8] recommends use of an HPLC method. The mobile phase is a 55:45 mixture of acetonitrile and aqueous 0.02M dibasic ammonium phosphate, eluted at a flow rate of 1 mL/min. The column is ODS (4 mm x 30 cm), and detection is on the basis of the UV absorbance at 254 nm.

## 4.3 Spectroscopic Analysis

A ratio-spectra, zero-crossing, derivative spectrophotometric method was described for the analysis of spironolactone in presence of hydrochlorothiazide [16]. After extracting the drugs from their tablets with 1:1 0.1 N HCl – methanol, the first derivative of the ratio of their absorption spectra to that of standard solution is computed at 270.7 and 269.9 nm.

Univariate and multivariate spectroscopy was applied to the analysis of spironolactone in presence of chlorthalidone [17]. Satisfactory results were obtained by partial least squares regression, with the calibration curve being linear over the range 2.92 – 14.6  $\mu\text{g/mL}$ . A kinetic-spectrophotometric method was described for the determination of spironolactone and canrenone in urine that also used a partial least-squares regression method [18]. After the compounds were extracted from urine, the spectra were recorded at 400 – 520 nm for 10 minutes at 30 second intervals. The relative error was less than 5%.

First-derivative spectroscopy was applied to the analysis of mixture of spironolactone and frusemide in combined dosage forms [19]. Calibration curves were linear up to 20  $\mu\text{g/mL}$ . The same mixture has been analyzed by extraction with methanol, and subsequent measurement in either 0.1 N HCl or in 0.1 N NaOH [20]. The relative standard deviation was in the

range of 1.4 – 7.8%, and recoveries were 98.6 – 99.9%.

Wahbi reported on the use of second-derivative spectroscopy for the determination of canrenone in spironolactone, and found that the method is stability-indicating for spironolactone [21]. First and second-derivative spectroscopy were also utilized for the simultaneous analysis of spironolactone in combination with either hydrochlorothiazide or frusemide [22]. The drugs are extracted with ethanol and analyzed through the use of the zero-crossing method. Nowakowska [23] analyzed mixtures of spironolactone and hydrochlorothiazide in tablets by measuring the absorbance of all species at 239 nm, and that of hydrochlorothiazide at 318 nm. The recoveries for spironolactone were found to be 97.9 to 101.8%, with a coefficient of variation of less than 0.1%.

Several calorimetric methods were reported for spironolactone using different derivatization reagents, such as thiosemicarbazide at 440 nm [24], 4-dinitrobenzene at 400 nm [25], isoniazide at 375 nm [26], acetic acid-acetic anhydride then  $\text{H}_2\text{SO}_4$  at 500 nm [27], 2,3,5-triphenyl-tetrazolium chloride and tetramethylammonium hydroxide at 480 nm [28]; sodium nitroprusside at 700 nm, and phosphotungstic acid at 410 nm [29].

Other spectrophotometric techniques have been reported for the analysis of spironolactone. Near infrared diffuse reflectance first-derivative spectroscopy was used for determination of spironolactone in pharmaceutical dosage forms [30]. Readings were taken at 15 nm intervals, and then 81 absorbance readings were input into a computer for principal component analysis.

Fourier-transform Raman and Fourier-transform infrared spectroscopic methods were adapted for the analysis of spironolactone and differentiation of its polymorphic forms [31, 32].

Neubert and Koch described a fluorimetric method for the determination of spironolactone metabolites in serum. The method used two extraction steps with dichloroethane at different pH values, followed by treatment with 65% sulfuric acid, and final measurement of the fluorescence at 436/525 nm [33].

#### 4.4. Polarography

Belal described a direct-current (DC) and differential pulse (DPP) polarographic method for spironolactone in dosage forms, using pH 10 Britton-Robinson buffer containing 40% methanol as a supporting electrolyte [34]. The current-concentration plot was found to be linear over the ranges of 0.005-1.0 mM (DC mode) and 0.0025-1.0 mM (DPP mode). A similar polarographic method based on the measurement of the cathodic current in 0.005 M H<sub>2</sub>SO<sub>4</sub>/methanol (1:1) was described [35].

#### 4.5 Chromatographic Methods of Analysis

##### 4.5.1 Thin Layer Chromatography

Three TLC systems have been described for the identification of spironolactone [36], all of which are based on the use of silica gel G as the adsorbent. Location of eluted spot was effected using either acidified iodoplatinate, or acidified potassium permanganate:

System A: chloroform–acetone (4:1):  $R_f = 66$

System B: ethyl acetate–methanol–strong ammonia solution (85:10:5):  
 $R_f = 79$

System C: ethyl acetate:  $R_f = 51$

Another TLC method involving also the use of silica gel G as an adsorbent, and a solvent system consisting of: benzene-ethyl acetate-methanol (73:25:2) [10]. The  $R_f$  value was 67, and detection was accomplished using phosphomolybdic acid at 80°C for 10 minutes.

##### 4.5.2 Gas Chromatography

Spironolactone is thermally stable, so therefore GC systems reported for its determination are relatively few. The reported methods are compiled in Table 5.



Table 5

## Gas Chromatographic Methods of Analysis of Spironolactone

Source	Column	Carrier gas	Flow rate	Temp.	Detection	Ref
Bulk drug	SE-30 column, containing 2.5% SE 30 on 800-100 mesh chromosorb G, 2 m x 4 mm internal diameter	Nitrogen	45 mL/min.	330°C	Flame ionization	[37]
Human Urine	HP-5 (0.33 $\mu$ m) Column 17 m x 0.2 mm i.d.	Helium	0.6-0.8 mL/min	Program-med	Mass spectrum	[38]
Human Urine	SE-30 column, packed with 1% SE 30 on diatomite CQ 80-100 mesh, 1.5 mx 4mm i.d.	Nitrogen	60 mL/min	230°C	Flame ionization	[39]
Human plasma	Glass column packed with 2% OV-1 on CQ 80-100 mesh (1.5 m x 4 mm i.d.)	Nitrogen	120 mL/min	250°C	Electron-Capture	[40]

#### **4.5.3 High Performance Liquid Chromatography**

HPLC is the most frequently used technique for the analysis of spironolactone as the bulk drug, in its dosage forms, or in biological fluids. The reported HPLC methods are summarized in Table 6.

#### **4.5.4 Capillary Zone Electrophoresis**

A CZE method has been described for the determination of spironolactone [59]. The analysis was conducted at pH 8, with UV detection (244 nm), at a constant voltage of 20 kV. The migration time was 11.9 minutes.

#### **4.5.5 Flow Injection Analysis**

A flow-injection method was reported for simultaneous determination of spironolactone and hydrochlorothiazide [60]. Samples are injected into a carrier stream of pH 5 acetate buffer, and spectra recorded from 220 – 350 nm at 1-second intervals and at an integration time of 0.4 seconds [60].

#### **4.6 Thermal Analysis**

Thermal analysis (TGA and DSC) of spironolactone and its ethanol, methanol, acetonitrile, ethyl acetate, and benzene solvates has been used to characterize the materials [61]. The analysis was carried out under dry nitrogen (50 mL/min), with the samples being contained in aluminum sample pans. Thermograms were obtained at a heating rate of 10°C/minute, with the final temperature being 230°C. Spironolactone and its methanol and ethanol solvates exhibited small exothermic transitions in addition to the anticipated endotherms.

#### **4.7 Protein Binding Studies**

Protein binding of spironolactone and canrenone was determined by both ultrafiltration (room temperature) [63] and equilibrium dialysis (overnight at 37°C) [64]. Both spironolactone and canrenone were extensively (>89%) bound to plasma proteins, and their blood-to-plasma concentration ratio was about 0.5, indicating that in blood these steroids were largely confined to plasma.

Table 6

## HPLC Methods for the Analysis of Spironolactone

Material	Column	Mobile Phase and (Flow Rate)	Detector	Ref
Human urine	Lichro-sphere 100 RP-18, 5 $\mu$ m	H <sub>2</sub> O / acetonitrile / H <sub>3</sub> PO <sub>4</sub> / triethylamine (530: 470: 0.65: 0.145 pH 3.3 or 800: 200: 0.38: 0.145 pH 6 (1 mL/min)	Diode array	[41]
Aqueous formulations and rat serum	4 $\mu$ m Nova-pak phenyl, 150x 3.9 mm i.d.	Aqueous 21.5% THF (1 mL/min)	250 nm	[42]
Human plasma	S5 ODS 2 Kontron columns 250 x 4.6 mm i.d.	Acetonitrile/ H <sub>3</sub> PO <sub>4</sub> (89:11) pH 3.4 (1 mL/min)	254 nm	[43]
Human urine	Hypersil ODS 30 $\mu$ m 125 x 4 mm	Aqueous Acetonitrile (1 mL/min)	238 nm	[44]
Urine	Spherisorb ODS2 C <sub>18</sub> , 5 $\mu$ m, 120 x 4.6 mm,i.d.	Aqueous 42 mM-SDS containing 4% propanol pH 4.5 with 10 mM phosphate buffer (1 mL/min)	254 nm	[45]

Table 6 (continued)

## HPLC Methods for the Analysis of Spironolactone

Material	Column	Mobile Phase and (Flow Rate)	Detector	Ref
Tablets	Spherisorb ODS 2, 5 $\mu$ m. 120 x 4.6 mm, i.d.	0.07M SDS containing 0.5% pentanol, pH 6.9 (1 mL/min)	254 nm	[46]
Urine	HP-Hypersil ODS, (25 cm x 4 mm)	Na H <sub>2</sub> PO <sub>4</sub> / propyl-ammonium chloride buffer pH 3 or acetate buffer pH 4 (1 mL/min)	230 nm	[47]
Dosage forms	Nucleosil C <sub>18</sub> , 10 $\mu$ m, 25 cm x 4 mm, i.d.	Methanol-acetonitrile-H <sub>2</sub> O-acetic acid (50: 40: 10: 1) or methanol- acetonitrile-H <sub>2</sub> O –triethylamine (550: 50:400:1) (1.5 mL/min)	254 nm; 280 nm	[48]
Stability study	i: Micro-bondapak C <sub>18</sub> , 30 cm x 3.9 mm, i.d.	63% methanol in 0.01M KH <sub>2</sub> PO <sub>4</sub> (2 mL/min)	238 nm;	[49]
	ii: Micro-bondapak phenyl, 30 cm x 3.9 mm	39% acetonitrile in 0.01M KH <sub>2</sub> PO <sub>4</sub> (1.2 mL/min)	254 nm	

Table 6 (continued)

## HPLC Methods for the Analysis of Spironolactone

Material	Column	Mobile Phase and (Flow Rate)	Detector	Ref
Biological fluids	Spherisorb S5 ODS 1, 5 $\mu$ m, 12.5 cm x 4.9 mm, i.d.	Aqueous 65% methanol adjusted to pH 3.4 with H <sub>3</sub> PO <sub>4</sub> (2 mL/min)	254 nm	[50]
Dosage form	Excalibar Spherisorb NH <sub>2</sub> , 5 $\mu$ m, 25 cm x 4.6 mm, i.d.	0.02 M NaH <sub>2</sub> PO <sub>4</sub> / methanol (3:2) (1.5 mL/min)	242 nm	[51]
Tablets	Apex Cyano RP 5 $\mu$ m, 15 cm x 4.6 mm, i.d.	Methanol - 0.1M NaH <sub>2</sub> PO <sub>4</sub> (9:11) (1 mL/min)	Amperometric	[52]
Plasma	Micro-Bondapak C <sub>18</sub> , 10 $\mu$ m	Water- methanol- acetonitrile (82: 65: 53) (6 mL/min)	254 nm	[53]
Dosage forms	Micro-bondapak NH <sub>2</sub>	Chloroform: methanol (9:11) (1 mL/min)	254 nm	[54]
Plasma	Radial pak C <sub>18</sub> , 5 $\mu$ m	65-100% methanol in water (gradient elution) (1 mL/min)	254 nm	[55]

Table 6 (continued)

## HPLC Methods for the Analysis of Spironolactone

Material	Column	Mobile Phase and (Flow Rate)	Detector	Ref
Tablets	Lichro-sorb RP, C <sub>18</sub> , 5 µm	Aqueous 50% acetonitrile (1 mL/min)	271 nm	[56]
Serum	Partisil, 5 µm, 150 x 4.6 mm, i.d.	Isopropyl ether-methanol (393:7) (2.2 mL/min)	240 nm	[57]
Plasma and urine	Spherisorb ODS 2, 125 x 4.6 mm, i.d.	Aqueous 65% methanol (1 mL/min)	285 nm	[58]

## **5. Clinical Applications**

### **5.1 Pharmacological Action**

Spironolactone competitively inhibits the physiologic effects of the adrenocortical hormone aldosterone on the distal tubules, thereby producing increased excretion of sodium chloride and water, and decreased excretion of potassium, ammonium, titratable acid, and phosphate. Spironolactone is a potassium-sparing diuretic that has diuretic activity only in the presence of aldosterone, and its effects are most pronounced in patients with aldosteronism. Spironolactone does not interfere with renal tubular transport mechanisms, and does not inhibit carbonic anhydrase.

Renal plasma flow and glomerular filtration rate are usually unaffected, but free water clearance may increase. Because most sodium is re-absorbed in the proximal renal tubules, spironolactone is relatively ineffective when administered alone. Concomitant administration of a diuretic which blocks re-absorption of sodium proximal to the distal portion of the nephron (such as a thiazide or loop diuretic) is required for maximum diuretic effects. When administered with other diuretics, spironolactone produces an additive or synergistic diuretic response and decreases potassium excretion caused by the other diuretic [65].

Spironolactone reportedly has hypotensive activity when given to hypertensive patients, by blocking the effect of aldosterone on arteriolar smooth muscle by altering the extracellular-intracellular sodium gradient.

Spironolactone exhibits antiandrogenic effects in males and females. It decreases testosterone biosynthesis by inhibiting steroid  $17\alpha$ -monooxygenase ( $17\alpha$ -hydroxylase) activity, possibly secondary to destruction of microsomal cytochrome P-450 in tissues with high steroid  $17\alpha$ -monooxygenase activity (testes, adrenals) [65].

### **5.2 Mechanisms of Action**

Spironolactone inhibits aldosterone effects by competing with aldosterone for intracellular mineralocorticoid receptors. When spironolactone (or its active metabolites) binds to these receptors, the complex fails to translocate into the nucleus and/ or bind to the nuclear chromatin. All of the subsequent phases of the effects of aldosterone are therefore inhibited,

clinically manifested as a natriuresis and potassium retaining action [66].

By competing with aldosterone for receptor sites, spironolactone is effective in reducing blood pressure, edema, and ascites in conditions of primary or secondary hyperaldosteronism. Spironolactone is also effective in managing essential hypertension, although aldosterone secretion may be within normal limits. The precise mechanism of hypotensive activity action has not been determined, but it has been suggested that the drug may act by blocking the effect of aldosterone on arteriolar smooth muscle or by altering the extracellular-intracellular sodium gradient [67].

Spironolactone induced a marked and statistically significant inhibitory effect on the cardiovascular reactivity to both the adrenergic and the rennin-angiotensin-aldosterone systems. This may play a major role in the vascular and antihypertensive properties of the drug [68].

The mechanism of antiandrogenic activity of spironolactone is complex, and appears to involve several effects of the drug. Hirsutism, an androgen-related increase in growth of facial and body hair, may occur in women with increased androgen production or with hypersensitivity of the hair follicle to androgenic stimulation [69]. The identification of the antiandrogenic activity of spironolactone has led to its use in the treatment of hirsutism. Spironolactone interferes with testosterone biosynthesis by reducing 17-hydroxylase activity, possibly secondary to destruction of microsomal cytochrome P-450 in tissues with high steroid 17 $\alpha$ -monooxygenase activity (*e.g.*, testes, adrenals), and thus lowers plasma testosterone levels [70].

It has also been shown that spironolactone inhibits the binding of dihydrotestosterone to cytosol protein receptor. The latter mechanism accounts for a direct anti-androgenic effect on target tissues (androgen receptor in human hair follicles) [70, 71]. Spironolactone-induced increases in serum estradiol concentration also may contribute to its anti-androgenic activity, although such increases may not occur consistently. Such increases appear to result from increased conversion of testosterone to estradiol. Spironolactone may have variable effects on serum 17-hydroxyprogesterone concentrations, possibly decreasing its production by inhibiting steroid 17 $\alpha$ -monooxygenase activity or decreasing its conversion (with resultant accumulation) to androstenedione by inhibiting cytochrome P450-dependent 17 $\alpha$ -hydroxyprogesterone aldolase (17, 20-



desmolase) activity. Serum progesterone concentrations may increase with the drug secondary to decreased hydroxylation (via steroid 17 $\alpha$ -monooxygenase) to 17-hydroxyprogesterone. In children compensatory increases in lutropin (luteinizing hormone) and follicle-stimulating hormone secretion can occur, probably secondary to the drug's anti-androgenic effects (*i.e.*, a feedback response to decreasing serum testosterone concentrations and/ or peripheral androgenic activity) [65].

## **6. Pharmacokinetic Profile**

### **6.1 Absorption**

Initial formulations of spironolactone were poorly absorbed from gastrointestinal tract because of less than optimal disintegration and dissolution [72]. In contrast to these early versions, newer preparations display enhanced absorption and oral bioavailability of 90% [73], resulting in a fall by a factor of four in the recommended oral dose of the medications [74].

Because of its low aqueous solubility, spironolactone has not been formulated for intravenous administration [72]. The oral absorption of spironolactone is improved by using micronized drug, or through the use of inclusion complexes of spironolactone with cyclodextrins.

Concomitant intake of food enhances drug absorption, most likely by increasing the degree of gastric dissolution, and decreasing the first-pass effect of spironolactone. The latter effect is possibly due to the secretion of bile acids in response to a meal serving that serves to enhance dissolution of the lipophilic compound [74].

Following a single oral dose of 100 mg of spironolactone, peak serum concentrations of the drug occur within 1-2 hours, and peak serum concentrations of its principal metabolites are attained within 2-4 hours [65,67,75-77]. When administered alone, spironolactone has a gradual onset of diuretic action, with the maximum effect being reached on the third day of therapy [65]. The delay in onset may result from the time required for adequate concentrations of the drug or its metabolites to accumulate [65]. When a thiazide diuretic is used concomitantly with spironolactone, diuresis usually occurs on the first day of therapy [65].

## 6.2 Distribution

Spironolactone and canrenone (a major metabolite of the drug) are both more than 90% bound to plasma proteins. Spironolactone or its metabolites may cross the placental barrier, and canrenone is distributed into breast milk [67,78,79].

## 6.3 Metabolism and Elimination

Spironolactone is rapidly and extensively metabolized in the body (particularly in liver) into a large number of metabolites (see Figure 10 for a metabolic map), with no unchanged drug appearing in the urine. It has been difficult to determine the half-life of the parent compound in humans. At least 17 metabolites have been isolated, of which 7 $\alpha$ -thiomethylspironolactone, 6 $\beta$ -hydroxy-7 $\alpha$ -thiomethylspironolactone, and canrenone, the principal metabolites, are the most pharmacologically active [65,80].

Canrenone is a dethioacetylated (non-sulfur containing) metabolite. This metabolite is thought to be primarily responsible for the drug's therapeutic effects. Approximately 25% to 30% of an administered dose is converted to canrenone, which accounts for one-tenth and one-fourth the anti-mineralocorticoid activity, after single and multiple doses, respectively [81,82].

7 $\alpha$ -thiomethylspironolactone is a sulfur-containing metabolite. This metabolite undergoes further metabolism to produce a sulfoxidized metabolite [75,76,81,82].

$\beta$ -hydroxy-7 $\alpha$ -thiomethylspironolactone is a sulfur-containing metabolite that undergoes further metabolism to produce a sulfoxidized metabolite [81,82].

It is uncertain to what extent the actions of spironolactone are dependant on the parent compound or its metabolites.

The elimination half-life of canrenone ranges from approximately 12 to 20 hours, depending upon the spironolactone dose administered [83]. Metabolites of spironolactone are primarily eliminated renally, with only minimal biliary excretion. Little to no parent drug is recoverable in the urine, reflecting the complete biotransformation of the compound [72,74,83].

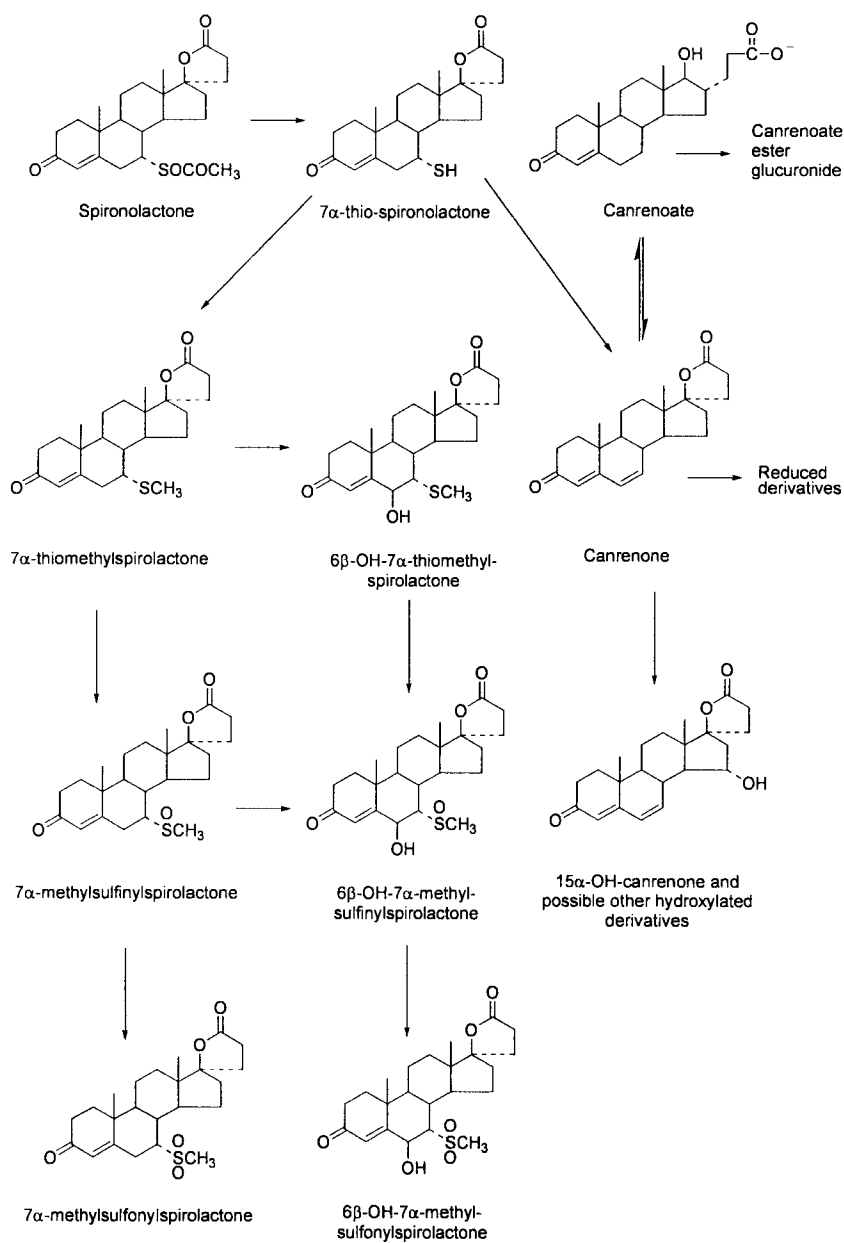


Figure 11. Metabolic pathway of spironolactone in humans.

## **7. Drug Interactions**

### **7.1 Drugs Increasing Serum Potassium Concentrations**

Spironolactone should not be used concurrently with another potassium-sparing agent (*e.g.*, amiloride, triamterene), or potassium-containing medications, or potassium supplements, or salt substitutes containing substantial amounts of potassium. Concomitant therapy with these drugs may increase the risk of hyperkalemia compared with spironolactone alone [65, 84].

Because indomethacin may increase serum potassium concentrations, indomethacin and spironolactone should be administered concomitantly with caution. Potassium-sparing diuretics should be used with caution, and serum potassium should be determined frequently in patients receiving an angiotensin-converting enzyme (ACE) inhibitor (*e.g.*, captopril). Concomitant administration with an ACE inhibitor may increase the risk of hyperkalemia. The dosage of spironolactone should be reduced, or the drug discontinued, as necessary. Patients with renal impairment may be at increased risk of hyperkalemia [65].

### **7.2 Other Drugs**

When used in conjunction with other diuretics or hypotensive agents, spironolactone may be additive with, or may potentiate, the action of these drugs. Therefore, dosage of these drugs, particularly ganglionic blocking agents, may need to be reduced by at least 50% when concomitant spironolactone therapy is instituted.

Spironolactone reportedly reduces vascular responsiveness to norepinephrine, so regional or general anesthesia should be used with caution in patients receiving spironolactone.

Aspirin has been shown to slightly reduce the natriuretic effect of spironolactone in healthy individuals, possibly by reducing active renal tubular secretion of canrenone, the active metabolite of spironolactone. However, the hypotensive effect of spironolactone and its effect on urinary potassium excretion in hypertensive patients is apparently not affected. Until more clinical data are available on this potential interaction, patients receiving both drugs should be monitored for signs and symptoms of decreased clinical response to spironolactone [65].

Concurrent use of lithium with spironolactone is not recommended, as the drug may provoke lithium toxicity by reducing renal clearance [84].

Spironolactone may increase the half-life of digoxin, so dosage reduction or increased dosing intervals of digoxin may be necessary, and careful monitoring is recommended.

### **7.3 Precautions [84]**

#### **7.3.1 Carcinogenicity/ Tumorigenicity**

Breast carcinoma has been reported in men and women taking spironolactone, but a direct causal relationship has not been established.

Spironolactone has been found to be tumorigenic in rats, mainly in endocrine organs and the liver. A statistically significant dose-related increase in benign adenomas of the thyroid and testes was found in male rats given spironolactone in doses up to 250 times the usual daily human dose of 2 mg/kg of body weight. In addition, a dose-related increase in proliferative liver changes was revealed in male rats. Hepatocytomegaly, hyperplastic nodules, and hepatocellular carcinoma were evident at the highest dosage level of 500 mg/kg. In female rats, a statistically significant increase in malignant mammary tumors was seen at the mid-dose level.

#### **7.3.2 Pregnancy**

Pregnant women should be advised to contact their physician before taking spironolactone, since routine use of diuretics during normal pregnancy is inappropriate and exposes the mother and her fetus to an unnecessary hazard. Diuretics do not prevent development of toxemia of pregnancy, and there is no satisfactory evidence that they are useful in the treatment of toxemia. Diuretics are indicated only in the treatment of edema due to pathologic causes, or as a short course of treatment in patients with severe hypervolemia.

Spironolactone may cross the placenta, however, problems in humans have not been documented.

### **7.3.3 Breast-Feeding**

Problems associated with spironolactone distribution into human breast milk have not been documented. However, canrenone (an active metabolite of spironolactone) is distributed into breast milk.

### **7.3.4 Pediatrics**

Studies performed to date have not demonstrated pediatric-specific problems that would limit the usefulness of potassium-sparing diuretics in children.

### **7.3.5 Geriatrics**

Although appropriate studies on the relationship of age to the effects of potassium-sparing diuretics have not been performed in the geriatric population, the elderly may be at an increased risk of developing hyperkalemia. In addition, elderly patients are more likely to have age-related renal function impairments, which may require caution in patients receiving potassium-sparing diuretics.

## **8. Toxicity and Adverse Effects**

The following side/ adverse effects have been selected on the basis of their potential clinical significance. Possible signs and symptoms were stated where appropriate [84].

### **8.1 Those More Frequently Occurring**

Hyperkalemia: May occur in up to 26% of patients receiving spironolactone, even when combined with thiazide diuretics. Irregular heartbeat is usually the earliest clinical indication of hyperkalemia, and is readily detected by ECG. Other signs and symptoms include confusion, nervousness, numbness or tingling in extremities (hands, feet, or lips), shortness of breath or difficult breathing, unusual tiredness or weakness, or weakness or heaviness of legs.

Gastrointestinal irritation: nausea or vomiting, stomach cramps and diarrhea.

## 8.2 Those Less Frequently Occurring

Effects related to dose and/or duration of therapy:

1. Antiandrogenic or endocrine effects. These include breast tenderness in females, deepening of voice in females, enlargement of breasts in males, inability to have or keep an erection, increased hair growth in females, irregular menstrual periods, and sweating.
2. Central nervous system effects, such as clumsiness or headache.

Effects not related to dose and/or duration of therapy:

1. Decreased sexual ability.
2. Dizziness.
3. Hyponatremia (drowsiness, dryness of mouth, increased thirst, lack of energy).

Effects rarely occurring:

1. Allergic reaction or anaphylaxis (shortness of breath, skin rash or itching).
2. Agranulocytosis (fever or chills, cough or hoarseness, lower back or side pain, painful or difficult urination).

## 9. Acknowledgement

The authors sincerely and appreciably thank Professor A.A.Al-Badr for his valuable suggestions, support, and advice throughout the work, and for his review of this publication. The authors also wish to express their gratitude to Professor H.A. El-Obeid for his valuable technical help, and Mr. Tanvir A. Butt (Department of Pharmaceutical Chemistry, College of Pharmacy, King Saud University, Riyadh, Saudi Arabia) for his helpful assistance in typing this manuscript.

## 10. **References**

1. S.A. Simpson, J.F. Tait, and J.E. Bush, *Lancet*, **2**, 226 (1952).
2. J.A. Leutscher, R. Neher, and A. Wetlstein, *Experientia*, **10**, 456 (1954).
3. G.W. Liddle, *Arch. Intern. Med.*, **102**, 998 (1958).
4. R.L. Landau, D.M. Bergenstal, K. Lugibhl, and M.E. Kascht, *J. Clin. Endocrinol. Metab.*, **15**, 1194 (1955).
5. J.A. Cella and C.M. Kagawa, *J. Am. Chem. Soc.*, **79**, 4808 (1957).
6. S.Budavari, ed., *The Merck Index*, 12<sup>th</sup> edn., Merck and Co., NJ (1996).
7. *Clarke's Isolation and Identification of Drugs*, 2<sup>nd</sup> edn., A.C. Moffat, ed., The Pharmaceutical Press, London (1986) p.973.
8. *The United States Pharmacopoeia XXIV*, The United States Pharmaceutical Convention, Rockville, MD (2000) p.1546.
9. *Martindale, The Complete Drug Reference*, 32<sup>nd</sup> edn., K. Parfitt, ed., World Color Book Services, Taunton, Massachusetts (1999) p.946.
10. J.L. Sutter and P.K.E. Lau, "Spironolactone", in *Analytical Profile of Drug Substances*, volume 4, K. Florey, ed., Academic Press, New York (1975) pp. 431-451.
11. *The British Pharmacopoeia*, Her Majesty's Stationary Office, London (1993) p.627, 1111.
12. *The European Pharmacopoeia*, Council of Europe, Strasburg, France (1998) p. 1538.
13. J.A. Cola, E.A. Brown, and R.R. Burtner, *J. Org. Chem.*, **24**, 1109 (1959).



14. ***Remington's: The Science and Practice of Pharmacy***, 19<sup>th</sup> edn. Volume II, K.G. Alfonso, ed.; Mack Publishing Co., Pennsylvania (1995) p.1048.
15. G. Anner and H. Wehrli (*Ciba-Geigy, A.-G.*), German Offen 2, 625, 723 (cl.C07J21/ 00), Dec.1976; Swiss Appl. 75/7, 696, 13 Jun. 1975; pp. 37.
16. N. Eak, *Anal. Lett*, **32**, 1371 (1999).
17. M.L. Luis, J.M. Garcia, F. Jimenez, A.I. Jimenez, and J.J. Arias, *J. Assoc. Off. Anal. Chem.*, **82**, 1054 (1999).
18. E. Martin, A.I. Jimenez, O. Hernandez, F. Jimenez, and J.J. Arias, *Talanta*, **49**, 143 (1999).
19. S. Ganwal and P. Trivedi, *Indian Drugs*, **35**, 412 (1998).
20. S.V. Erram and H.P. Tipnis, *Indian Drugs*, **30**, 555 (1993).
21. A.A.M. Wahbi, S.M. Mahrous, Y.A. Beltagy, A.S. Issa, and H. Lymona, *Spectrosc. Lett.*, **25**, 721 (1992).
22. H. Salem, M. El-MaamLi, M. El-Sadek, and A.A. Kheir, *Spectrosc. Lett.*, **24**, 451 (1991).
23. Z. Nowakowska, *Farm. Pol.*, **45**, 454 (1989).
24. D.M. Shingbal, *Indian Drugs*, **24**, 450 (1987).
25. D.M. Shingbal and V.R. Rao, *Indian Drugs*, **23**, 232 (1986).
26. D.M. Shingbal and J.S. Prabhudesai, *Indian Drugs*, **21**, 306 (1984).
27. D.M. Shingbal and U.G. Barad, *Indian Drugs*, **22**, 163 (1984).
28. V. Nevrekar, *Indian Drugs*, **21**, 349 (1984).
29. C.S.P. Sastry, T.N.V. Prasad, and V. Rao, *Indian J. Pharm. Sci.*, **45**, 190 (1985).
30. Y.L. Ren, W. Li, J.M. Shen, R.X. Ren, C. Hui, L. Zhang, and D.H.

- Jin, *Fenxi Kexue. Xuebao.*, **13**, 281 (1997).
31. G.A. Neville, H.D. Beckstead, and H.F. Shurvell, *J. Pharm. Sci.*, **81**, 1141 (1992).
32. H.D. Beckstead, G.A. Neville, and H.F. Shurvell, *Fresenius J. Anal. Chem.*, **345**, 727 (1993).
33. P. Neubert and K. Koch, *J. Pharm. Sci.*, **66**, 1131 (1977).
34. F. Belal, *Mikrochim. Acta.*, **107**, 11 (1992).
35. A.P. Arzamatshev, N.B. Grigoryev, S.K. Ordabayeva, A.P. Ryzhenkova, Y.V. Degterev, and T.P. Arystanova, *Khim. Farm. Zh.*, **28**, 60 (1994).
36. A.H. Stead, R. Gill, T. Wright, J.P. Gibbs, and A.C. Moffat, *Analyst*, **107**, 1106 (1982).
37. R.E. Ardrey, A.C. Moffat, *J. Chromatogr.*, **220**, 195 (1981).
38. Y.W. Li, J. Li, and T.H. Zhou, *Chin. Chem. Lett.*, **2**, 19 (1991).
39. T. Feher, L. Bodrogi, and A. Varadi, *J. Chromatogr.*, **123**, 460 (1976).
40. J. Chamberlain, *J. Chromatogr.*, **55**, 249 (1971).
41. H.J. Guchelaar, L. Chandi, O. Schouten, and W.A. van-den-Brand, *Fresenius J. Anal. Chem.*, **363**, 700 (1999).
42. M.A. Kaukonen, P. Vuorela, H. Vuorela, and J.P. Mannerman, *J. Chromatogr.*, **797**, 271 (1998).
43. A. Jankowski, A. Skorek-Jankowska, and H. Lamparczyk, *J. Pharm. Biomed. Anal.*, **14**, 1359 (1996).
44. R. Herraiez-Hernandez, E. Soriano-Vega, and P. Campins-Falco, *J. Chromatogr. B*, **658**, 303 (1994).

45. E. Bonet-Domingo, J.R. Torres-Lapasio, M.J. Medina-Hernandez, and M.C. Garcia-Alvarez-Coque, *Anal. Chim. Acta.*, **287**, 201 (1994).
46. E. Bonet-Domingo, M.J. Medina-Hernandez, and M.C. Garcia-Alvarezcoque, *J. Pharm. Biomed. Anal.*, **11**, 711 (1993).
47. R. Harraez-Hernandez, P. Campins-Falco, and A. Sevillano-Cabeza, *J. Liq. Chromatogr.*, **15**, 2205 (1992).
48. K.T. Sane, A.J. Vaidya, J.K. Ghadge, A.B. Jani, and S.K. Kotwal, *Indian Drugs*, **29**, 232 (1992).
49. Y. Parmas, V.D. Gupta, and T. Zerai, *Drug Dev. Ind. Pharm.*, **17**, 747 (1991).
50. F.I. Varin, Y.U. the-Minh, F. Benoit, J.P. Villeneuve, and Y. Theoret, *J. Chromatogr. B.*, **112**, 57 (1992).
51. C.D. Gaitonde and P.P. Jayade, *Indian Drugs*, **28**, 242 (1991).
52. W.J. Bachman and J.T. Stewart, *J. Chromatogr. Sci.*, **28**, 123 (1990).
53. L.S. Jackson and J.E.H. Stagord, *J. Chromatogr. B.*, **72**, 377 (1988).
54. T.N.V. Prasad, E.V. Rao, C.S.P. Satrey, and G.R. Rao, *Indian Drugs*, **24**, 346 (1987).
55. J.H. Sherry, J.P. O'Donnell, and Colby H.D, *J. Chromatogr. B.*, **47**, 183 (1986).
56. F. De-Croo, W. van-den-Bossche, and P. De-Moerloose, *J. Chromatogr.*, **329**, 422 (1985).
57. J.W.P.M. Drediek, W.A.J.J. Hermems, and F.W.H.M. Merkus, *J. Chromatogr. B.*, **42**, 279 (1985).
58. W. Krause, R.J. Karras, and U. Jakbos, *J. Chromatogr. B.*, **28**, 191 (1983).

59. E. Gonzalez and J.J. Laserna, *Electrophoresis*, **15**, 240 (1994).
60. E. Martin, O. Hernandez, J.J. Arias, and A.I. Jimenet, *Microchem. J.*, **56**, 207 (1997).
61. A.G. Neville, H.D. Beckstead, and J.D. Cooney, *Fresenius J. Anal. Chem.*, **349**, 746 (1994).
62. E.S. Vesell, *Ann. Rev. Pharmacol.*, **14**, 249 (1974).
63. Y.W. Chien, H.J. Lambert, and A. Karim, *J. Pharm. Sci.*, **63**, 1877 (1974).
64. N.D. Lee and V.J. Pileggi, *Clin. Chem.*, **17**, 166 (1973).
65. **American Hospital Formulary Services (AHFS) Drug Information**, American Society of Health-System Pharmacists, Inc., Bethesda MD (1996) p. 1931.
66. J.D. Horisberger and G. Giebisch, *Renal Physiol.*, **10**, 198 (1987).
67. **Product Information: Aldactone®**, **Spironolactone**, G.D. Searle & Co., Chicago, IL, 1999.
68. D. Schohn, H.A. Jahn, and B.C. Pelletier, *Am. J. Cardiol.*, **71**, 40A (1993).
69. A.A.A. Ismail, D.W. Davidson, A.R. Souka, et al., *J. Clin. Endocrinol. Metab.*, **39**, 81 (1974).
70. D.L. Loriaux, R. Menard, A. Taylor, et al., *Ann. Intern. Med.*, **85**, 630 (1976).
71. A. Boisselle and R.R. Tremblay, *Fertil. Steril.*, **32**, 276 (1979).
72. C.R. Shackelton, N.L.M. Wong, and R.A.L. Sutton, "Distal (potassium-sparing) diuretics", in **Diuretics, Physiology, Pharmacology, and Clinical Use**, J.H. Dirks and R.A.L. Sutton, eds., WB Saunders, Philadelphia (1986) pp. 117-134.
73. T. Dyckner and P.O. Wester, *Acta Med. Scand.*, **707** (suppl), 79 (1986).

74. I.M. Weiner, "General Pharmacological Aspects of Diuretics", in ***Diuretics, Physiology, Pharmacology, and Clinical Use***, J.H. Dirks and R.A.L. Sutton, eds., WB Saunders, Philadelphia (1986) pp. 3-28.
75. J.W.P.M. Overdiek, W.A.J.J. Hermens, and F.W.H.M. Merkus, *Clin. Pharmacol. Therap.*, **38**, 468 (1985).
76. P. Gardiner, K. Schrode, D. Quinlad, et al, *J. Clin. Pharmacol.*, **29**, 342 (1989).
77. J.W.P.M Overdiek and F.W.H.M. Merkus, *Clin. Pharmacol. Therap.*, **40**, 531 (1986).
78. P.C. Ho, D.W.A. Bourne, E.J. Triggs, et al, *Eur. J. Clin. Pharmacol.*, **27**, 435 (1984).
79. A. Karim, J. Zagarella, J. Hribar, et al, *Clin. Pharmacol. Therap.*, **19**, 158 (1976).
80. ***Review on the Pharmacokinetics and Biopharmaceutics of Spironolactone in Man***, J.W.P.M. Overdiek and F.W.H.M. Merkus, eds., (1987) pp. 15-40.
81. J.W.P.M. Overdiek and F.W.H.M. Merkus, *Rev. Drug Metabol. Drug Interact.*, **5**, 273 (1987).
82. L.B. La Cagnin and H.D. Colby, *Biochem. Pharmacol.*, **36**, 3439 (1987).
83. W. Sadee, M. Dagcioglu, and R. Schroder, *J. Pharmacol. Exp. Therap.*, **185**, 686 (1973).
84. ***Drug Information for the Health Care Professionals***, volume 1, 19<sup>th</sup> edn., United States Pharmacopoeial Convention Drug Information, Rockville, MD (1999) p. 1267.

## CUMULATIVE INDEX

Bold numerals refer to volume numbers.

- Acebutolol, **19**, 1  
Acetaminophen, **3**, 1; **14**, 551  
Acetazolamide, **22**, 1  
Acetohexamide, **1**, 1; **2**, 573; **21**, 1  
Adenosine, **25**, 1  
Allopurinol, **7**, 1  
Amantadine, **12**, 1  
Amikacin sulfate, **12**, 37  
Amiloride hydrochloride, **15**, 1  
Aminobenzoic acid, **22**, 33  
Aminogluthethimide, **15**, 35  
Aminophylline, **11**, 1  
Aminosalicylic acid, **10**, 1  
Amiodarone, **20**, 1  
Amitriptyline hydrochloride, **3**, 127  
Amobarbital, **19**, 27  
Amodiaquine hydrochloride, **21**, 43  
Amoxicillin, **7**, 19; **23**, 1  
Amphotericin B, **6**, 1; **7**, 502  
Ampicillin, **2**, 1; **4**, 518  
Apomorphine hydrochloride, **20**, 121  
Arginine, **27**, 1  
Ascorbic acid, **11**, 45  
Aspartame, **29**, 7  
Aspirin, **8**, 1  
Astemizole, **20**, 173  
Atenolol, **13**, 1  
Atropine, **14**, 325  
Azathioprine, **10**, 29  
Azintamide, **18**, 1  
Aztreonam, **17**, 1  
Bacitracin, **9**, 1  
Baclofen, **14**, 527  
Bendroflumethiazide, **5**, 1; **6**, 597  
Benperidol, **14**, 245  
Benzocaine, **12**, 73  
Benzoic acid, **26**, 1  
Benzyl benzoate, **10**, 55  
Betamethasone dipropionate, **6**, 43  
Bretylium tosylate, **9**, 71  
Brinzolamide, **26**, 47  
Bromazepam, **16**, 1  
Bromocriptine methanesulfonate, **8**, 47  
Bumetanide, **22**, 107  
Bupivacaine, **19**, 59  
Busulphan, **16**, 53  
Caffeine, **15**, 71  
Calcitriol, **8**, 83  
Camphor, **13**, 27  
Captopril, **11**, 79  
Carbamazepine, **9**, 87  
Carbenoxolone sodium, **24**, 1  
Cefaclor, **9**, 107  
Cefamandole nafate, **9**, 125; **10**, 729  
Cefazolin, **4**, 1  
Cefixime, **25**, 39  
Cefotaxime, **11**, 139  
Cefoxitin sodium, **11**, 169  
Ceftazidime, **19**, 95  
Cefuroxime sodium, **20**, 209  
Celiprolol hydrochloride, **20**, 237  
Cephalexin, **4**, 21  
Cephalothin sodium, **1**, 319  
Cephradine, **5**, 21

- Chloral hydrate, **2**, 85  
Chlorambucil, **16**, 85  
Chloramphenicol, **4**, 47; **15**, 701  
Chlordiazepoxide, **1**, 15  
Chlordiazepoxide hydrochloride, **1**, 39; **4**, 518  
Chloropheniramine maleate, **7**, 43  
Chloroquine, **13**, 95  
Chloroquine phosphate, **5**, 61  
Chlorothiazide, **18**, 33  
Chlorpromazine, **26**, 97  
Chlorprothixene, **2**, 63  
Chlortetracycline hydrochloride, **8**, 101  
Chlorthalidone, **14**, 1  
Chlorzoxazone, **16**, 119  
Cholecalciferol, **13**, 655  
Cimetidine, **13**, 127; **17**, 797  
Cisplatin, **14**, 77; **15**, 796  
Citric Acid, **28**, 1  
Clarithromycin, **24**, 45  
Clidinium bromide, **2**, 145  
Clindamycin hydrochloride, **10**, 75  
Clioquinol, **18**, 57  
Clofazimine, **18**, 91; **21**, 75  
Clomiphene citrate, **25**, 85  
Clonazepam, **6**, 61  
Clonfibrate, **11**, 197  
Clonidine hydrochloride, **21**, 109  
Clorazepate dipotassium, **4**, 91  
Clotrimazole, **11**, 225  
Cloxacillin sodium, **4**, 113  
Clozapine, **22**, 145  
Cocaine hydrochloride, **15**, 151  
Codeine phosphate, **10**, 93  
Colchicine, **10**, 139  
Cortisone acetate, **26**, 167  
Crospovidone, **24**, 87  
Cyanocobalamin, **10**, 183  
Cyclandelate, **21**, 149  
Cyclizine, **6**, 83; **7**, 502  
Cyclobenzaprine hydrochloride, **17**, 41  
Cycloserine, **1**, 53; **18**, 567  
Cyclosporine, **16**, 145  
Cyclothiazide, **1**, 65  
Cypripheptadine, **9**, 155  
Dapsone, **5**, 87  
Dexamethasone, **2**, 163; **4**, 519  
Diatrizoic acid, **4**, 137; **5**, 556  
Diazepam, **1**, 79; **4**, 518  
Dibenzepin hydrochloride, **9**, 181  
Dibucaine, **12**, 105  
Dibucaine hydrochloride, **12**, 105  
Diclofenac sodium, **19**, 123  
Didanosine, **22**, 185  
Diethylstilbestrol, **19**, 145  
Diflunisal, **14**, 491  
Digitoxin, **3**, 149; **9**, 207  
Dihydroergotoxine methanesulfonate, **7**, 81  
Diloxanide furoate, **26**, 247  
Diltiazem hydrochloride, **23**, 53  
Dioctyl sodium sulfosuccinate, **2**, 199; **12**, 713  
Diosgenin, **23**, 101  
Diperodon, **6**, 99  
Diphenhydramine hydrochloride, **3**, 173  
Diphenoxylate hydrochloride, **7**, 149  
Dipivefrin hydrochloride, **22**, 229  
Disopyramide phosphate, **13**, 183  
Disulfiram, **4**, 168  
Dobutamine hydrochloride, **8**, 139  
Dopamine hydrochloride, **11**, 257  
Dorzolamide hydrochloride, **26**, 283; **27**, 377  
Doxorubicine, **9**, 245  
Droperidol, **7**, 171  
Echothiophate iodide, **3**, 233  
Econazole nitrate, **23**, 127  
Edetic Acid (EDTA), **29**, 57

- Emetine hydrochloride, **10**, 289  
Enalapril maleate, **16**, 207  
Ephedrine hydrochloride, **15**, 233  
Epinephrine, **7**, 193  
Ergonovine maleate, **11**, 273  
Ergotamine tartrate, **6**, 113  
Erthromycin, **8**, 159  
Erthromycin estolate, **1**, 101; **2**, 573  
Estradiol, **15**, 283  
Estradiol valerate, **4**, 192  
Estrone, **12**, 135  
Ethambutol hydrochloride, **7**, 231  
Ethynodiol diacetate, **3**, 253  
Etodolac, **29**, 105  
Etomidate, **12**, 191  
Etoposide, **18**, 121  
Eugenol, **29**, 149  
Fenopropfen calcium, **6**, 161  
Fenoterol hydrobromide, **27**, 33  
Flavoxate hydrochloride, **28**, 77  
Flecainide, **21**, 169  
Fluconazole, **27**, 67  
Flucytosine, **5**, 115  
Fludrocortisone acetate, **3**, 281  
Flufenamic acid, **11**, 313  
Fluorouracil, **2**, 221; **18**, 599  
Fluoxetine, **19**, 193  
Fluoxymesterone, **7**, 251  
Fluphenazine decanoate, **9**, 275; **10**, 730  
Fluphenazine enanthate, **2**, 245; **4**, 524  
Fluphenazine hydrochloride, **2**, 263; **4**, 519  
Flurazepam hydrochloride, **3**, 307  
Flutamide, **27**, 115  
Fluvoxamine maleate, **24**, 165  
Folic acid, **19**, 221  
Furosemide, **18**, 153  
Gadoteridol, **24**, 209  
Gentamicin sulfate, **9**, 295; **10**, 731  
Glafenine, **21**, 197  
Glibenclamide, **10**, 337  
Gluthethimide, **5**, 139  
Gramicidin, **8**, 179  
Griseofulvin, **8**, 219; **9**, 583  
Guaifenesin, **25**, 121  
Guanabenz acetate, **15**, 319  
Guar gum, **24**, 243  
Halcinonide, **8**, 251  
Haloperidol, **9**, 341  
Halothane, **1**, 119; **2**, 573; **14**, 597  
Heparin sodium, **12**, 215  
Heroin, **10**, 357  
Hexestrol, **11**, 347  
Hexetidine, **7**, 277  
Histamine, **27**, 159  
Homatropine hydrobromide, **16**, 245  
Hydralazine hydrochloride, **8**, 283  
Hydrochlorothiazide, **10**, 405  
Hydrocortisone, **12**, 277  
Hydroflumethazide, **7**, 297  
Hydroxyprogesterone caproate, **4**, 209  
Hydroxyzine dihydrochloride, **7**, 319  
Hyoscyamine, **23**, 155  
Ibuprofen, **27**, 265  
Imipramine hydrochloride, **14**, 37  
Imipenem, **17**, 73  
Indapamide, **23**, 233  
Indinavar sulfate, **26**, 319  
Indomethacin, **13**, 211  
Iodamide, **15**, 337  
Iodipamide, **2**, 333  
Iodoxamic acid, **20**, 303  
Iopamidol, **17**, 115  
Iopanoic acid, **14**, 181  
Iproniazid phosphate, **20**, 337  
Isocarboxazid, **2**, 295  
Isoniazide, **6**, 183  
Isopropamide, **2**, 315; **12**, 721  
Isoproterenol, **14**, 391



- Isosorbide dinitrate, **4**, 225; **5**, 556  
Isosuprine hydrochloride, **26**, 359  
Ivermectin, **17**, 155  
Kanamycin sulfate, **6**, 259  
Ketamine, **6**, 297  
Ketoprofen, **10**, 443  
Ketotifen, **13**, 239  
Khellin, **9**, 371  
Lactic acid, **22**, 263  
Lactose, anhydrous, **20**, 369  
Lansoprazole, **28**, 117  
Leucovorin calcium, **8**, 315  
Levallorphan tartrate, **2**, 339  
Levarterenol bitartrate, **1**, 149;  
    **2**, 573; **11**, 555  
Levodopa, **5**, 189  
Levothyroxine sodium, **5**, 225  
Lidocaine, **14**, 207; **15**, 761  
Lidocaine hydrochloride, **14**, 207;  
    **15**, 761  
Lincomycin, **23**, 275  
Lisinopril, **21**, 233  
Lithium carbonate, **15**, 367  
Lobeline hydrochloride, **19**, 261  
Lomefloxacin, **23**, 327  
Lomustine, **19**, 315  
Loperamide hydrochloride, **19**, 341  
Lorazepam, **9**, 397  
Lovastatin, **21**, 277  
Mafenide acetate, **24**, 277  
Malic Acid, **28**, 153  
Maltodextrin, **24**, 307  
Mandelic Acid, **29**, 179  
Maprotiline hydrochloride, **15**, 393  
Mebendazole, **16**, 291  
Mebeverine hydrochloride, **25**, 165  
Mefloquine hydrochloride, **14**, 157  
Melfalan, **13**, 265  
Meperidine hydrochloride, **1**, 175  
Meprobamate, **1**, 207; **4**, 520;  
    **11**, 587  
Mercaptopurine, **7**, 343  
Mesalamine, **25**, 209; **27**, 379  
Mestranol, **11**, 375  
Metformin hydrochloride, **25**, 243  
Methadone hydrochloride, **3**, 365; **4**,  
    520; **9**, 601  
Methaqualone, **4**, 245  
Methimazole, **8**, 351  
Methixen hydrochloride, **22**, 317  
Methocarbamol, **23**, 377  
Methotrexate, **5**, 283  
Methoxamine hydrochloride, **20**, 399  
Methoxsalen, **9**, 427  
Methylclothiazide, **5**, 307  
Methylphenidate hydrochloride, **10**,  
    473  
Methyprylon, **2**, 363  
Metipranolol, **19**, 367  
Metoclopramide hydrochloride, **16**,  
    327  
Metoprolol tartrate, **12**, 325  
Metronidazole, **5**, 327  
Mexiletine hydrochloride, **20**, 433  
Minocycline, **6**, 323  
Minoxidil, **17**, 185  
Mitomycin C, **16**, 361  
Mitoxanthrone hydrochloride, **17**, 221  
Morphine, **17**, 259  
Moxalactam disodium, **13**, 305  
Nabilone, **10**, 499  
Nadolol, **9**, 455; **10**, 732  
Nalidixic acid, **8**, 371  
Nalmefene hydrochloride, **24**, 351  
Nalorphine hydrobromide, **18**, 195  
Naloxone hydrochloride, **14**, 453  
Naphazoline hydrochloride, **21**, 307  
Naproxen, **21**, 345  
Natamycin, **10**, 513; **23**, 405  
Neomycin, **8**, 399  
Neostigmine, **16**, 403  
Nicotinamide, **20**, 475

- Nifedipine, **18**, 221  
Nimesulide, **28**, 197  
Nitrazepam, **9**, 487  
Nitrofurantoin, **5**, 345  
Nitroglycerin, **9**, 519  
Nizatidine, **19**, 397  
Norethindrone, **4**, 268  
Norfloxacin, **20**, 557  
Norgestrel, **4**, 294  
Nortriptyline hydrochloride, **1**, 233;  
    **2**, 573  
Noscapine, **11**, 407  
Nystatin, **6**, 341  
Ondansetron hydrochloride, **27**, 301  
Oxamniquine, **20**, 601  
Oxazepam, **3**, 441  
Oxyphenbutazone, **13**, 333  
Oxytocin, **10**, 563  
Pantoprazole, **29**, 213  
Papaverine hydrochloride, **17**, 367  
Penicillamine, **10**, 601  
Penicillin-G, benzothine, **11**, 463  
Penicillin-G, potassium, **15**, 427  
Penicillin-V, **1**, 249; **17**, 677  
Pentazocine, **13**, 361  
Pentoxifylline, **25**, 295  
Pergolide Mesylate, **21**, 375  
Phenazopyridine hydrochloride, **3**,  
    465  
Phenelzine sulfate, **2**, 383  
Phenformin hydrochloride, **4**, 319;  
    **5**, 429  
Phenobarbital, **7**, 359  
Phenolphthalein, **20**, 627  
Phenoxymethyl penicillin potassium,  
    **1**, 249  
Phenylbutazone, **11**, 483  
Phenylephrine hydrochloride, **3**, 483  
Phenylpropanolamine hydrochloride,  
    **12**, 357; **13**, 767  
Phenytoloin, **13**, 417  
Physostigmine salicylate, **18**, 289  
Phytonadione, **17**, 449  
Pilocarpine, **12**, 385  
Piperazine estrone sulfate, **5**, 375  
Pirenzepine dihydrochloride, **16**, 445  
Piroxicam, **15**, 509  
Polythiazide, **20**, 665  
Polyvinyl alcohol, **24**, 397  
Polyvinylpyrrolidone, **22**, 555  
Povidone, **22**, 555  
Povidone-Iodine, **25**, 341  
Pralidoxine chloride, **17**, 533  
Praziquantel, **25**, 463  
Prazosin hydrochloride, **18**, 351  
Prednisolone, **21**, 415  
Primidone, **2**, 409; **17**, 749  
Probenecid, **10**, 639  
Procainamide hydrochloride, **4**, 333;  
    **28**, 251  
Procaine hydrochloride, **26**, 395  
Procarbazine hydrochloride, **5**, 403  
Promethazine hydrochloride, **5**, 429  
Proparacaine hydrochloride, **6**, 423  
Propiomazine hydrochloride, **2**, 439  
Propoxyphene hydrochloride, **1**, 301;  
    **4**, 520 ; **6**, 598  
Propylthiouracil, **6**, 457  
Pseudoephedrine hydrochloride, **8**,  
    489  
Pyrazinamide, **12**, 433  
Pyridoxine hydrochloride, **13**, 447  
Pyrimethamine, **12**, 463  
Quinidine sulfate, **12**, 483  
Quinine hydrochloride, **12**, 547  
Ranitidine, **15**, 533  
Reserpine, **4**, 384; **5**, 557; **13**, 737  
Riboflavin, **19**, 429  
Rifampin, **5**, 467  
Rutin, **12**, 623  
Saccharin, **13**, 487  
Salbutamol, **10**, 665

- Salicylamide, **13**, 521  
Salicylic acid, **23**, 427  
Scopolamine hydrobromide, **19**, 477  
Secobarbital sodium, **1**, 343  
Sertraline hydrochloride, **24**, 443  
Sildenafil citrate, **27**, 339  
Silver sulfadiazine, **13**, 553  
Simvastatin, **22**, 359  
Sodium nitroprusside, **6**, 487; **15**, 781  
Solasodine, **24**, 487  
Sorbitol, **26**, 459  
Sotalol, **21**, 501  
Spironolactone, **4**, 431; **29**, 261  
Starch, **24**, 523  
Streptomycin, **16**, 507  
Strychnine, **15**, 563  
Succinylcholine chloride, **10**, 691  
Sulfacetamide, **23**, 477  
Sulfadiazine, **11**, 523  
Sulfadoxine, **17**, 571  
Sulfamethazine, **7**, 401  
Sulfamethoxazole, **2**, 467; **4**, 521  
Sulfasalazine, **5**, 515  
Sulfathiazole, **22**, 389  
Sulfisoxazole, **2**, 487  
Sulfoxone sodium, **19**, 553  
Sulindac, **13**, 573  
Sulphamerazine, **6**, 515  
Sulpiride, **17**, 607  
Talc, **23**, 517  
Teniposide, **19**, 575  
Tenoxicam, **22**, 431  
Terazosin, **20**, 693  
Terbutaline sulfate, **19**, 601  
Terfenadine, **19**, 627  
Terpin hydrate, **14**, 273  
Testolactone, **5**, 533  
Testosterone enanthate, **4**, 452  
Tetracaine hydrochloride, **18**, 379  
Tetracycline hydrochloride, **13**, 597  
Theophylline, **4**, 466  
Thiabendazole, **16**, 611  
Thiamine hydrochloride, **18**, 413  
Thiamphenicol, **22**, 461  
Thiopental sodium, **21**, 535  
Thioridazine, **18**, 459  
Thioridazine hydrochloride, **18**, 459  
Thiostrepton, **7**, 423  
Thiothixene, **18**, 527  
Ticlopidine hydrochloride, **21**, 573  
Timolol maleate, **16**, 641  
Titanium dioxide, **21**, 659  
Tobramycin, **24**, 579  
 $\alpha$ -Tocopheryl acetate, **3**, 111  
Tolazamide, **22**, 489  
Tolbutamide, **3**, 513; **5**, 557;  
**13**, 719  
Tolnaftate, **23**, 549  
Tranlycypromine sulfate, **25**, 501  
Trazodone hydrochloride, **16**, 693  
Triamcinolone, **1**, 367; **2**, 571;  
**4**, 521; **11**, 593  
Triamcinolone acetoneide, **1**, 397; **2**,  
571; **4**, 521; **7**, 501; **11**, 615  
Triamcinolone diacetate, **1**, 423;  
**11**, 651  
Triamcinolone hexacetoneide, **6**, 579  
Triamterene, **23**, 579  
Triclobisonium chloride, **2**, 507  
Trifluoperazine hydrochloride, **9**, 543  
Triflupromazine hydrochloride, **2**,  
523; **4**, 521; **5**, 557  
Trimethaphan camsylate, **3**, 545  
Trimethobenzamide hydrochloride, **2**,  
551  
Trimethoprim, **7**, 445  
Trimipramine maleate, **12**, 683  
Trioxsalen, **10**, 705  
Tripeleennamine hydrochloride, **14**,  
107  
Triprolidine hydrochloride, **8**, 509  
Tropicamide, **3**, 565

Tubocurarine chloride, **7**, 477  
Tybamate, **4**, 494  
Valproate sodium, **8**, 529  
Valproic acid, **8**, 529  
Verapamil, **17**, 643  
Vidarabine, **15**, 647  
Vinblastine sulfate, **1**, 443; **21**, 611  
Vincristine sulfate, **1**, 463; **22**, 517  
Vitamin D3, **13**, 655  
Warfarin, **14**, 423  
Xylometazoline hydrochloride, **14**,  
135  
Yohimbine, **16**, 731  
Zidovudine, **20**, 729  
Zileuton, **25**, 535  
Zomepirac sodium, **15**, 673

ISBN 0-12-260829-1



9 780122 608292

90038